

Design of trace analytical methods based on capillary gas chromatography : selected applications in industrial process and emission monitoring

Citation for published version (APA):

Pham Tuan, H. (1998). *Design of trace analytical methods based on capillary gas chromatography : selected applications in industrial process and emission monitoring*. [Phd Thesis 1 (Research TU/e / Graduation TU/e), Chemical Engineering and Chemistry]. Technische Universiteit Eindhoven. <https://doi.org/10.6100/IR507393>

DOI:

[10.6100/IR507393](https://doi.org/10.6100/IR507393)

Document status and date:

Published: 01/01/1998

Document Version:

Publisher's PDF, also known as Version of Record (includes final page, issue and volume numbers)

Please check the document version of this publication:

- A submitted manuscript is the version of the article upon submission and before peer-review. There can be important differences between the submitted version and the official published version of record. People interested in the research are advised to contact the author for the final version of the publication, or visit the DOI to the publisher's website.
- The final author version and the galley proof are versions of the publication after peer review.
- The final published version features the final layout of the paper including the volume, issue and page numbers.

[Link to publication](#)

General rights

Copyright and moral rights for the publications made accessible in the public portal are retained by the authors and/or other copyright owners and it is a condition of accessing publications that users recognise and abide by the legal requirements associated with these rights.

- Users may download and print one copy of any publication from the public portal for the purpose of private study or research.
- You may not further distribute the material or use it for any profit-making activity or commercial gain
- You may freely distribute the URL identifying the publication in the public portal.

If the publication is distributed under the terms of Article 25fa of the Dutch Copyright Act, indicated by the "Taverne" license above, please follow below link for the End User Agreement:

www.tue.nl/taverne

Take down policy

If you believe that this document breaches copyright please contact us at:

openaccess@tue.nl

providing details and we will investigate your claim.

**Design of Trace Analytical Methods
Based on
Capillary Gas Chromatography:**

**Selected Applications in
Industrial Process and Emission Monitoring**

Phạm Tuấn Hải

**DESIGN OF TRACE ANALYTICAL METHODS
BASED ON
CAPILLARY GAS CHROMATOGRAPHY:**

**SELECTED APPLICATIONS IN INDUSTRIAL PROCESS AND
EMISSION MONITORING**

PROEFSCHRIFT

ter verkrijging van de graad van doctor aan de
Technische Universiteit Eindhoven, op gezag van
de Rector Magnificus, prof.dr. M. Rem,
voor een commissie aangewezen door het College
voor Promoties in het openbaar te verdedigen op
dinsdag 17 maart 1998 om 16.00 uur

door

Hai PHAM TUAN

geboren te Hanoi, Vietnam

Dit proefschrift is goedgekeurd door de promotoren:

Prof.dr.ir. C.A.M.G. Cramers

en

Prof.dr. P.J.F. Sandra

Copromotor: Dr.ir. J.G.M. Janssen

Kính tặng Bố Mẹ và Chị Hà
aan mijn ouders en mijn zus

The research project described in this thesis and thesis printing were supported by:

 **CHROMPACK**

Chrompack International B.V., R&D Department, PO Box 8033, 4330 EA Middelburg, The Netherlands,


Gasunie

Nederlandse Gasunie N.V., Gasunie Research, PO Box 19, 9700 MA Groningen, The Netherlands, and

 **Technology**

ICI Technology, PO Box 8, The Heath, Runcorn, Cheshire, WA7 4QD, United Kingdom.

CIP-DATA LIBRARY TECHNISCHE UNIVERSITEIT EINDHOVEN

Hai, PHAM TUAN

Design of trace analytical methods based on capillary gas chromatography: selected applications in industrial process and emission monitoring / by Pham Tuan Hai. – Eindhoven: Technische Universiteit Eindhoven, 1998. Proefschrift.

ISBN 90-386-0718-0

NUGI 813

Trefw.: gaschromatografie / sporenanalyse

Subject headings: capillary gas chromatography / trace analysis

CONTENTS

GENERAL INTRODUCTION AND SCOPE	1
PART 1: SULFUR ANALYSIS IN NATURAL GAS	9
Chapter 1: Determination of Sulfur Components in Natural Gas:	
A Literature Survey	11
1.1. Introduction	12
1.2. Trace Enrichment of Sulfur Components	15
1.3. Chromatographic Separation	20
1.3.1. Packed-Column Systems	21
1.3.2. Capillary-Column Systems	24
1.4. Detection systems for GC-based Sulfur Analysis	29
1.4.1. Improvements in Flame Photometric Detection	30
1.4.2. Improvements in Sulfur Chemiluminescence Detection	37
1.4.3. Mass Spectrometric Detection of Sulfur Compounds	37
1.4.4. Other Detection Systems for Sulfur Analysis	40
1.5. Calibration	41
1.5.1. Methods for Preparing Standard Mixtures in Natural Gas Analysis	42
1.5.2. Calibration Mixtures for Sulfur Components	44
1.6. Conclusions	51
References	51
Chapter 2: Detectors for Sulfur Analysis	55
2.1. Introduction	56
2.2. Detailed Procedures for the Evaluatory Studies	57
2.3. Experimental	59
2.4. Optimization of the Experimental Conditions	61
2.5. Results and Discussions	62
2.5.1. Sulfur Chemiluminescence Detector	61
2.5.2. Flame Photometric Detector	69
2.5.3. Mass Spectrometric Detector	71
2.5.4. Thermal Conductivity Detector	72
2.5.5. Pulsed-Flame Photometric Detector	74
2.5.6. Atomic Emission Detector	80
2.5.7. Comparison of the Various Detectors Evaluated	82

2.5.8. Other Possible Detection Techniques Not Included in the Evaluatory Study	83
2.6. Conclusions	84
Chapter 3: Design Considerations of a GC Method for Sulfur Determination	85
3.1. Introduction	86
3.1.1. Injection Volume	86
3.1.2. Required Quality of Pre-Separation	87
3.1.3. Selective Enrichment	88
3.1.4. Requirements for the Chromatographic Separation	89
3.1.5. Problem Definition for the Calibration	90
3.2. Experimental	91
3.3. Results and Discussions	92
3.3.1. Selective Enrichment of Sulfur Components from Natural Gas	92
3.3.2. Columns for Sulfur Analysis	98
3.3.3. Calibration Techniques	103
3.4. Conclusions	113
Chapter 4: Newly Designed Procedure for Determination of Sulfur Components in Natural Gas	115
4.1. Introduction	116
4.2. Experimental	116
4.3. Results and Discussion	118
4.4. Conclusions	128
 PART 2: EMISSION MONITORING USING A PORTABLE GAS CHROMATOGRAPH	 131
Chapter 5: Gas Chromatography in Process and Emission Monitoring	133
5.1. Introduction	134
5.2. Process Gas Chromatographs	137
5.3. Transportable Gas Chromatographic Systems	140
5.4. Portable Gas Chromatographs	141
5.5. Conclusions	150
References	151
Chapter 6: Analysis of Vent Stack Gases Using a Portable Micro Gas Chromatograph	155
6.1. Introduction	156

6.2. Micro GC Evaluation and Optimization	157
6.3. Field Trial	170
6.4. Conclusions	175
References	177
Chapter 7: Sample Enrichment by Equilibrium (Ab)sorption in Open Tubular Traps. Fundamental Aspects	179
7.1. Introduction	180
7.2. Theory	181
7.2.1. Equilibrium (Ab)sorption Procedure	182
7.2.2. Prediction of Enrichment Factors	183
7.2.3. Effect of Pressure Drop	185
7.2.4. "Vacuum Enrichment" Considerations	186
7.2.5. Sampling Flow Rate	188
7.2.6. Requirements for the Open Tubular Trapping Column	186
7.3. Experiments	191
7.3.1. Experimental Set-up	191
7.3.2. Results and Discussion	192
7.4. Conclusions	195
References	195
Chapter 8: VOC Analysis by Coupling the Equilibrium (Ab)sorption Enrichment Device to a Portable Micro GC	197
8.1. Introduction	198
8.2. On-line Coupling to the Micro GC	198
8.2.1. Experimental Set-up	198
8.2.2. Sampling and Desorption Procedure	201
8.2.3. Results and Discussion	201
8.3. Application in VOC Analysis	207
8.3.1. Enrichment at Ambient Temperature	207
8.3.2. Enrichments at Elevated Temperatures	210
8.3.3. Displacement Effects	215
8.4. Conclusions	216
Appendix: Prediction and Optimization of Separation on the Micro GC	219
SUMMARY	233
SAMENVATTING	240
ACKNOWLEDGEMENT	244
CURICULUM VITAE	245
LIST OF PUBLICATIONS	246

GENERAL INTRODUCTION AND SCOPE

Chromatography, since its discovery in 1906 by a Russian botanist Michael Tswett [1], has become one of the most frequently used techniques in analytical chemistry. In the family of chromatography-based techniques, gas chromatography (GC), first described by Martin and James in 1952 [2], has definitely an unsurpassed role in the separation of mixtures of not only gases but also of volatile liquids and solids. The introduction of open-tubular capillary columns in GC by Golay in 1958 [3] marked a turning point in the development of gas chromatographs. The revolution has not, however, really started until the end of the 70's, when Dandeneau and Zerenner introduced fused-silica columns [4]. The remarkably high plate numbers together with high flexibility and strength are the main advantages of the fused-silica open-tubular capillary columns over their packed counterparts. Owing to the excellent inertness and homogeneity of the stationary phase film coated on the inner column wall, capillary columns have shown a very reliable performance. Moreover, the fact that capillary columns are available with a wide range of polarities and film-thicknesses of the stationary phase film, has added the conclusive plus for the definitive wide acceptance and almost exclusive use of (fused-silica) capillary columns.

The tremendous progress in column technology, along with the immense development in sample pretreatment and detection techniques has pushed GC a giant step forward in all aspects: sensitivity, selectivity, precision and accuracy, linear dynamic range and number of components amenable to GC. Many analytical problems in environmental sciences, medicine, biology and chemical industry have relied on GC in finding proper solutions. In the special case of environmental monitoring and industrial process control, the GC technique is by far the most widely used and valuable method.

A GC method for quantitation purposes for use in an analytical laboratory consists of a number of steps. In such a procedure the following five basic steps can be distinguished:

1. Collection of representative samples, their storage and transportation from the site to the laboratory,

2. Preliminary treatment of the samples in order to make them amenable to the analytical method,
3. Separation of the components of interest from the matrix and from each other on suitable column(s),
4. Detection and measurement of the component signals using proper detectors(s),
5. Interpretation of the collected analytical data.

Among the five steps listed above, the sample collection and the pretreatment process, steps number 1 and 2, are unarguably the most vulnerable steps. These steps are prone to errors and are generally time consuming. The situation is much better with other steps. For example the breathtaking progress in computer science has reduced the time required for data collection and interpretation from days to minutes or seconds. Numerous innovations in all parts of GC instrumentation from injector to detector have allowed a sample to be analyzed in minutes instead of hours. On-line systems and automation have resulted in analyses in which there is no more need for the human operator to interact with the system from the time the sample is injected till the chromatogram is completed and shown on the computer display. Possible "humanly" enforced errors thus have been minimized.

The sample preparation process, however, is a notable exception from the revolutionary process of automation. Despite clear progress in this step of the analysis, a great deal of manual labor is still involved. This is best illustrated by looking to the analysis of gas samples. An operator still has to walk to the sampling point, take a sample in a sample bag or on an adsorption tube, carefully store the sample in a temperature controlled device and get it back to the laboratory as quickly as possible. There the sample in the best instances can be directly injected into the GC. Errors are clearly possible due to the loss of sample caused by a number of reasons, *e.g.* leakage, evaporation, decomposition and/or adsorption. This clearly indicates that we can improve the integrity of the analysis if we can bring the analytical instrument to the sampling site and even better, hook the instrument on-line to the sampling point.

A GC connected on-line to the sampling point is called a process gas chromatograph (PGC) [5,6]. The PGC represents one extreme of a wide spectrum of GC-based instruments that offer analytical solutions for industrial applications. On the opposite end of this spectrum stand the sophisticated analytical systems con-

sisting of conventional GCs equipped with a high performance sample introduction device and a sensitive, selective detector for use in the laboratory. Somewhere in between these extremes there are the transportable and portable GC systems. The former will be more or less a complete conventional laboratory GC on some means of a moving platform [7-9]. Much smaller, mostly micro-machined GC instruments represent the latter class [10-12]. The moving laboratory still maintains some of the flexibility and sensitivity inherent to a sophisticated GC system while at the same time providing nearly on-site analysis. The sample, however, still has to be brought from the sampling point to the moving platform. This "walking" distance can be eliminated when using a portable micro GC, which can really be brought directly to the sampling points. These instruments trade off some of their sensitivity and flexibility for a higher ruggedness and superb portability. With the above in mind, it is easy to understand that for the application of GC in chemical industry, all types of instrumentation have been used, depending on the specifications of the analytical problem at hand.

Once the platform of an analytical system has been chosen, sensitivity and selectivity become the most important characteristics for its overall performance. Depending on the level of sensitivity and selectivity desired and the complexity of the sample matrix, attention must be paid to the optimization of some or all parts of a GC system: injector, column, and detector. By choosing the proper column dimensions and polarity, the components of interest will be at least in some degree separated from the interfering contaminants present in the matrix. With the use of one or more dedicated selective detectors we exhaust the ability of a simple conventional GC system. Improvements in detectors, although tremendous, cannot, however, catch up with ever growing demands on sensitivity and selectivity in trace analysis. In case the target components are present at extremely low concentrations and/or the interfering components are present in very large amounts, the GC system used will not be able to detect the components of interest and/or give false signals. In such instances we have no choice but look for an improved, and often more laborious sample preparation or enrichment procedure.

The purpose of elaborating a sample preconcentration step is two-fold: to introduce larger amounts of target components and/or to eliminate as much as possible the interfering matrix. For laboratory GC systems there is a large variety of

sample preparation techniques which have been thoroughly developed and that are, at least in principle, suitable for on-line coupling. A relatively straightforward approach to introduce larger amounts of the target components is using a nowadays fully developed large volume injection technique [13], based on either the on-column [14] or the temperature programmed vaporizing principle [15]. The latter injector has become more or less a norm for conventional GCs in recent years. Moreover, the temperature programmed vaporizer can be conveniently used as a selective preconcentration device based on the principle of adsorption/thermal desorption. With such a set-up both goals mentioned above, selectivity and larger volumes, can be achieved simultaneously.

While laboratory GC systems enjoy a high flexibility in choosing a suitable preconcentration device, their portable counterpart is extremely difficult to combine with such an instrument. As a trade off for high ruggedness and portability, portable GC systems generally have a relatively poor sensitivity that leads to an even more pronounced need for a preconcentrator. In portable micro GCs, being applications of high-speed narrow-bore capillary GC technology, the demand of narrow input bandwidths, however, is a serious obstacle for direct coupling to any of the well-known enrichment techniques. To overcome this limitation a novel preconcentration technique - sample enrichment by equilibrium absorption - has been developed. The theoretical backgrounds and applications of this method are treated in this thesis.

Trace analysis of organic micropollutants in the atmosphere and process control in chemical industry are typical examples of the most pressing problems that analytical chemists have to face today. The need for more sensitive, more accurate and faster analytical methods suited for environmental emission monitoring is presented everyday due to the ever more stringent regulations imposed by national and international environmental institutions. Similar demands apply for process control as well, due to the need of the chemical industry to improve the quality of their products and the efficiency of their production processes. In order to meet these requirements, new analytical procedures have to be developed involving the development and evaluation of instrumentation for laboratory use as well as for use in field applications. While complex and dedicated analytical instruments used "in-door" in the laboratory excel in sensitivity, accuracy and adaptability, field-portable equipment has its advantages in terms of ruggedness and real-time on-the-spot response. As an illustration for the developments in

this field, two analytical problems have been addressed in this thesis. The first is the determination of trace levels of sulfur components in natural gas. The analysis of volatile organic compounds in process emission control and environmental monitoring is the second. Due to the differences in instrumentation and required developments involved, each of the problems mentioned above is addressed in a separate part of this thesis.

Part One of the thesis is dedicated to the problem of determining extremely low concentrations of sulfur components in natural gas. The main aim of the study is to develop a gas chromatography based analytical procedure for laboratory use. The driving force behind the research work is the need of accurate monitoring the sulfur contents in order to protect vulnerable catalytic processes that use natural gas as a starting material. Moreover, sulfur in natural gas is more and more becoming an environmental issue. The stringent requirements in terms of detection limits (micrograms of sulfur per cubic meter) for the individual sulfur components in the complex and interfering natural gas matrix resulted in the need of improvements in all three essential steps of the analytical procedure: sample pretreatment, chromatographic separation and target compound detection. An overview, given in Chapter 1, provides information on state-of-the-art equipment and recent developments relevant to all three steps of the sulfur analysis. Further experimental work described in subsequent chapters was based on this literature study. Every step involved in the complete process of sulfur analysis has been carefully evaluated. Evaluatory studies are described in the chapters 2 and 3. Due to the important role that the detector plays in the overall performance of the instrumental set-up, the detectors, selective as well as universal, are evaluated in a separate chapter, Chapter 2. Chapter 3 describes jointly the optimization of other fundamental steps integrating in the GC-based analytical procedure designed for the determination of sulfur components in natural gas. The topics treated in this chapter are: *i/* adsorbents for selective sample pretreatment using a temperature programmed vaporizer device; *ii/* capillary columns; and *iii/* calibration systems. After careful optimization, the various components are combined which finally resulted in the instrument set-up described in chapter 4. The newly proposed procedure was evaluated in terms of sensitivity, selectivity, accuracy and precision. The system is applied for analysis of real natural gas samples.

As opposed to the development of an analytical procedure for industrial trace analysis for use in the laboratory as described in Part One, **Part Two** is dedicated to analytical systems for field applications. These field-portable GC instruments are dramatically different from their laboratory counterparts in design as well as performance. Real-time on-the-spot analytical results are more and more demanded in process control and in emission and environmental pollution monitoring. To achieve a high degree of portability and ruggedness, some instrument sensitivity and selectivity must be sacrificed. Most of these instruments are specially constructed for specifically predetermined analytical tasks. Chapter 5 gives a quick introduction into the developments and use of various (trans)portable and on-line GC systems. In Chapter 6, vent stack gas monitoring using a dedicated field-portable micro gas chromatograph (micro-GC) is described. To improve the sensitivity and make the portable GC instrument suitable for environmental applications, a novel preconcentration technique - equilibrium (ab)sorption enrichment - is developed for on-line coupling to portable GC instruments. With this new technique the requirements for an extremely narrow input bandwidth imposed by the use of narrow-bore columns can be met. Incorporation of this preconcentration device in a field-portable gas chromatograph can result in an improvement of detection limits from the part-per-million level to the part-per-billion range. The theoretical principles of this technique are described in Chapter 7. Its application in the analysis of volatile organic compounds in environmental air samples is treated in Chapter 8.

To aid the operator in transferring methods from the laboratory to the field, part 2 also contains an appendix, where a mathematical method for predicting the optimal chromatographic settings of a portable micro GC is described.

All aspects of the entire study are summarized in the last part of the thesis. Several suggestions for future studies are given.

REFERENCES

1. V. G. Berezkin, *Chem. Revs.*, 89 (1989) 277.
2. A.T. James and A. J. P. Martin, *Biochem. J.*, 50 (1952) 679.
3. M. J. E. Golay, in "Gas Chromatography", V. J. Coates *et al.* (Eds.), Academic Press, New York, 1958.
4. R. D. Dandeneau and E. H. Zerenner, *J. High Resolut. Chromatogr. Chromatogr. Comm.*, 2 (1979), 351.
5. R. Annino, *Am. Lab.*, 21 (1989) 60-67.

6. R. Villalobos and R. Annino, *Analysis Instrum.*, 21 (1985) 73.
7. G. Matz, W. Schröder, and T. Ollesch, *J. Chromatogr. A*, 750 (1996) 151-153.
8. A. C. Lewis and K. D. Bartle, *Proc. 19th Int. Symp. Capillary Chromatogr. Electrophoresis*, Wintergreen, Virginia, USA, May 18-22, 1997, p. 394-395.
9. W. H. McClennen and H. Meuzelaar, *Proc. 19th Int. Symp. Capillary Chromatogr. Electrophoresis*, Wintergreen, Virginia, USA, May 18-22, 1997, p. 136-137.
10. S. C. Terry, J. H. Jerman, and J. B. Angell, *IEEE Trans. Electrom. Devices*, ED-26 (1979) 1880.
11. M. W. Bruns, *Proc. 1992 Int. Conf. Ind. Electronics, Control, Instrum. Automation*, Volume 3, New York: IEEE, 1992, p. 1640-1644.
12. H. Pham Tuan, H.-G. Janssen, C. A. Cramers, P. Mussche, J. Lips and N. Wilson, *Proc. 18th Int. Symp. Capillary Chromatogr. Electrophoresis*, Riva del Garda, Italy, May 20-24, 1996, p. 2213.
13. H. G. J. Mol., H.-G. Janssen, C. A. Cramers, J. J. Vreuls, and U. A. Th. Brinkman, *J. Chromatogr. A*, 703 (1995) 277-307.
14. K. Grob, *On-line coupled LC-GC*, Hüthig, Heidelberg, 1991.
15. W. Vogt, K. Jacob and H. W. Obwexer, *J. Chromatogr.*, 174 (1979) 437.

Part 1

SULFUR ANALYSIS IN NATURAL GAS

Chapter 1

DETERMINATION OF SULFUR COMPONENTS IN NATURAL GAS: A LITERATURE SURVEY¹

ABSTRACT

More stringent environmental regulations as well as higher demands presently being imposed on the sulfur content of natural gas feed-stocks for chemical processes necessitate the development of new analytical procedures for sulfur determination in natural gas. Only analytical procedures based on gas chromatography can meet the sensitivity and accuracy requirements dictated by environmental regulation institutions and modern chemical industry. The complexity of the natural gas matrix as well as the extremely low concentration levels at which the sulfur species occur make the development of these analytical methods a true challenge. In this review the three steps common for analytical methods for trace analysis in complex matrices, i.e. pretreatment, chromatographic separation, and detection, are discussed in detail. Possible methods for calibration of the system are discussed in the final section.

Various techniques to determine sulfur in natural gas are described. Depending on the application, the most suitable system has to be selected. For example, for on-line application in a hazardous area a simple and rugged system is required, i.e. a simple gas chromatograph with a flame photometric detector, while for laboratory application a more complex instrument including preconcentration, column switching and more exotic detection systems could be more suitable. Therefore it is crucial to define the requirements of the instrument in an early stage and use the information in this literature survey to develop/select a dedicated instrument/procedure for the analytical problem at hand.

¹ Published as "Determination of Sulfur Components in Natural Gas: A Review" by H. Pham Tuan, H.-G. Janssen, C. A. Cramers, A. L. C. Smit, and E. M. van Loo, *J. High Resolut. Chromatogr.*, 17 (1994) 373.

1.1. INTRODUCTION

Natural gas is a well-established contributor to the world's energy needs. At this moment the use of natural gas comprises over 20% of the total energy consumed worldwide. Furthermore, natural gas is also an important starting material in a number of large-scale production processes in chemical industry. The presence of sulfur components in natural gas constitutes a source of concern because of the corrosive nature of these components as well as their potential hazards for human health and for the natural environment. Additionally, if natural gas is used as a reagent in chemical processes, sulfur species present in the gas may adversely affect the performance and lifetime of catalysts involved in the reaction.

For the reasons outlined above, the accurate determination of sulfur components in natural gas is of utmost importance. The group of components that should be analyzed includes hydrogen sulfide (H_2S), carbonyl sulfide (COS), the C_1 to C_4 mercaptans, lower sulfides and odorants, such as for example tetrahydrothiophene (THT), added to the gas to impart a characteristic smell for safety purposes. The concentrations of these components differ, depending on the origin of the gas. In general, the concentrations of sulfur components in natural gas for domestic and industrial use range typically from a few to several tens of parts per million on a volume basis. An exception is H_2S that can be present at concentration levels up to 1% [1].

Standardized methods for the determination of sulfur species in natural gas have been published by the International Organization for Standardization (ISO). They can be classified as either conventional techniques (Wickbold, Lingener) or modern instrumental techniques (GC). ISO standard 4260 describes the Wickbold combustion method, a method for the determination of the total-sulfur content of natural- and other gases. In the Wickbold method the natural gas sample is supplied to the burner of an oxy-hydrogen flame, where the sulfur compounds are burnt with a considerable excess of oxygen. The resulting sulfur oxides are converted into sulfuric acid by absorption in a hydrogen peroxide solution. Depending on the sulfur content of the sample, the sulfate ions in the absorption solution are determined by colorimetric, nephelometric, turbidimetric or conductometric titrations. More recently, ISO standard 6326-5 was published. This standard procedure describes the use of the Lingener combustion method. In the Lingener method a given volume of natural gas is burnt with air at atmos-

pheric pressure in an enclosed combustion apparatus. The resulting sulfur oxides are oxidized into sulfuric acid by absorption in a hydrogen peroxide solution and afterwards titrated with a barium chloride solution. The total sulfur content, which can be determined with this measurement method, is from 10 to 1000 milligrams of sulfur per cubic meter (mg S/m^3) [2].

As opposed to the Lingener and the Wickbold method, which both measure the total sulfur content, ISO method 6326-3 describes a potentiometric method for sulfur determination that only responds to H_2S , COS and mercaptans. In this method H_2S and mercaptans are absorbed in a 40% (m/m) potassium hydroxide solution; COS is absorbed downstream in a 5% (m/m) alcoholic mono ethanola mine solution and afterwards titration of the absorbed H_2S , mercaptans and COS is performed with a AgNO_3 solution. The concentration range of sulfur compounds which can be determined with this measurement method is 1-10 mg S/m^3 for H_2S , 1-20 mg S/m^3 for mercaptans and 1-30 mg S/m^3 for COS [2].

Apart from one common advantage, *i.e.* no calibration procedure is needed because the three methods described above are absolute measurement techniques, they also suffer from a number of common disadvantages. The measurements are time-consuming, complex and are, due to the complexity of the experimental steps involved, difficult to automate. Moreover, the accuracy and the detection limits of especially the Lingener method do not meet the required limits. It is evident that because the methods measure the *total* sulfur content (ISO 4260 and ISO 6326-5) or the concentration of different *classes* of sulfur compounds (ISO 6326-3), no information on the concentrations of the *individual* sulfur species is obtained. This disadvantage can be overcome by using GC-based methods for sulfur determination. The ISO standards 6326-2 and 6326-4 describe gas chromatographic methods for separation and detection of individual sulfur components in natural gas. In ISO 6326-2 H_2S , C_1 to C_4 mercaptans and THT are separated on a gas chromatographic system equipped with a separation column containing 30% (m/m) Silicone oil and 30% (m/m) Dinonylphthalate on Chromosorb W. The sulfur compounds are subsequently detected with an electrochemical cell, in which they are oxidized by a chromium oxide solution and at the same time the potential difference over the platinum electrodes is measured. The ISO 6326-2 method suffers from two serious disadvantages. Firstly, it is not applicable for the determination of COS. Furthermore, the chromatographic conditions specified in the method only enable H_2S and methylmercaptan (MeSH) to be determined if the ratio of the concentration of the

former to that of the latter is less than 10. The same applies for the quantification of two mercaptans eluted consecutively.

A few of the major limitations of the ISO 6326-2 method were eliminated in ISO 6326-4. The chromatographic separation of the sulfur components was optimized, resulting in a system that enabled quantification of all major sulfur species in natural gas samples. The components are separated using a temperature programmed 1.2 m \times 2 mm column packed with styrene/divinylbenzene porous polymer beads (80-100 mesh) and measured with a sulfur-selective flame photometric detector (FPD). The detection limit is approximately 0.1 mg S/m³, which is comparable to the detection limits obtainable by the ISO standard method 6326-2.

The ISO methods 6326-2 and 6326-4 yield the concentrations of the *individual* sulfur components in the gas. The *total* sulfur concentration can then be obtained by summing the equivalent sulfur-weights of the individual components. The chromatographic separation procedure incorporated in ISO 6326-4 provides sufficient separation of all sulfur components. Unfortunately, however, it still has a number of problems, most of which originate from the use of flame photometric detection. The selectivity of the flame photometric detector (FPD) is limited and although fairly selective, this detector still responds to high concentrations of non-sulfur components. Moreover, high concentrations of hydrocarbons coeluting with a sulfur-containing component can quench the sulfur signal. Finally, the response of the FPD is inherently non-linear and often also compound dependent. For these reasons, the concentration of the sulfur species to be determined are limited to the range of 0.1-30 mg S/m³.

For most present applications, the detection limits and the reliability of the analytical results achievable by GC with FPD detection are within the desired range. More stringent environmental regulations as well as higher demands currently being posed on the purity of natural feed-stocks for chemical processes, however, force analytical chemists to develop new analytical methods that allow the accurate and reliable determination of sulfur in natural gas at concentrations well below the limits currently achievable. The complexity of the natural gas matrix and the extremely low detection limits required render this task extremely challenging. Analytical methods for analyses at trace levels in complex and interfering matrices often require the use of selective preconcentration/enrichment techniques. Only if this step and the subsequent separation and detec-

tion are fully optimized, it is possible to meet the required sensitivity limits with an acceptable level of reliability. In the vast majority of applications, the demands posed on each of these three steps is determined by the performance of the other two. If, for example, a universal detector is employed, the requirements imposed on the sample pretreatment and separation are much more stringent than in the case of the use of a truly specific detector.

In subsequent sections of this review, each of the three steps of the analytical procedure for the quantification of low concentrations of sulfur components in natural gas, *i.e.* sample pretreatment, separation and detection, will be discussed in detail. Up till now, virtually no attention has been paid in literature to the use of preconcentration techniques in natural gas analysis. On the other hand, various methods for preconcentration of sulfur in samples of environmental or medical origin have been published. In general, the principles of these methods are also applicable for trace analysis of sulfur in natural gas. Irrespective of the matrix, the strong tendency of sulfur components to adsorb on various types of surfaces seriously complicates preconcentration and analysis of these compounds. In literature, both packed and open-tubular columns have been employed for the separation of sulfur species in a wide variety of samples. In a section devoted to the chromatographic separation of sulfur components, the merits of each of these two approaches will be compared. The selection of the detection device is of crucial importance for the performance of the combined set-up. Various detectors will be considered in a separate section. As opposed to the three standardized absolute methods for sulfur determination described earlier, GC-based techniques are relative methods and hence require calibration. Procedures for calibration will be treated in detail in the last section. Again, the adsorptive nature constitutes a serious source of concern in preparation and storage of sulfur calibration mixtures.

1.2. TRACE ENRICHMENT OF SULFUR COMPONENTS

The determination of trace components in a complex matrix often requires selective enrichment of the components of interest prior to transfer of the sample into the chromatographic system. In this step the target compounds are selectively retained on for example a solid adsorbent or a cold trap while at the same time the interfering main components are eliminated. For the particular case of

sulfur determination in natural gas this means a material is required that selectively adsorbs sulfur-containing species without adsorbing hydrocarbons.

Up till now, no preconcentration techniques have been developed for the GC determination of sulfur components in natural gas. Several preconcentration methods, however, were described for determination of these compounds in ambient air. Due to the low concentrations of sulfur components in air a preconcentration step prior to analysis is virtually always required.

Early work in this field, without connection to a GC separation [3,4], often reports collection methods for individual sulfur compounds from an atmospheric matrix by wet chemical techniques or by using impregnated filters with subsequent spectrophotometric analysis. West and Gaeke [5] developed a nowadays traditional wet chemical technique for atmospheric sulfur dioxide (SO₂) measurements. This method uses a bubbler trapping system containing a tetrachloromercurate (II) (HgCl₂ + 2NaCl) solution. The analysis is spectrophotometric involving the dye pararosaniline. The West - Gaeke procedure has been successfully used to measure concentrations as low as 5 parts-per-billion (ppb)². Axelrod *et al.* [4] used an alternative to the bubbler sampling method, *i.e.* the use of an impregnated filter containing the same solution, and were able to determine SO₂ in concentrations down to 0.05 ppb. Similarly, H₂S [3] was extracted from air by reaction with an AgNO₃ impregnated filter. The resulting Ag₂S was dissolved in a NaCN solution and analyzed fluorimetrically by using a very dilute fluorescing mercuric acetate. A detection limit of 5 parts-per-trillion (ppt) was reported. In both experiments very high collection efficiencies were achieved: 92-95%.

For determination of H₂S and other organosulfur compounds in air Braman *et al.* [6] used preconcentration of the components in a trap filled with gold coated glass beads. Sulfur compounds were removed by heating the trap (500-600°C for 5 min) and were subsequently separated on a short liquid nitrogen cooled U-trap column, and detected by means of a flame photometric detector (FPD). These authors reported detection limits of approximately 0.01 ng or 0.1 ppt for 100 L sample. Collection efficiencies of several metal-foils for a larger group of atmospheric sulfur gases were examined by Kagel and Farwell [7]. Here the

² For gaseous samples the unit part-per-million (ppm) is defined as 10⁻⁶ mol/mol, this in contrast to the situation in liquids where one ppm is usually defined as one mg/L. This can lead to confusion as some authors incorrectly apply the liquid definition of ppm to gases.

compounds were released by flash desorption and determined by an FPD. These authors found Pd and Pt foils to be the best for the preconcentration of the gases of interest. The collection efficiencies ranged from 13% for COS on Pt-foil to 45% for H₂S on Pd-foil. The sulfur gas detectability of this metal foil collection / flash vaporization / flame photometric detection (MC/FV/FPD) approach was less than 50 ppt. A similar method of desorption and detection (FV/FPD) was employed by Farwell *et al.* [8]. SO₂ was collected in a glass fiber filter after complete thermal conversion of the reduced sulfur gases to SO₂ in a quartz tube held at a furnace temperature of 1050°C. The recoveries here were 100%. No detection limits were reported. Also no information on the applicability of this approach for the isolation of other sulfur species is available.

The largest group of collection materials used for preconcentrating sulfur components are the solid adsorbents, which were used both at ambient as well as at sub-ambient temperature (cryogenic trapping). An attractive aspect of the use of solid adsorbents is their capability to be directly coupled to a GC system. An effective solid adsorbent should fulfill the following criteria: *i/* high breakthrough volume³. This means a high capacity for the compounds of interest but as low as possible for other interfering components; *iii/* easy to desorb.

Black *et al.* [9] tried to collect SO₂ and H₂S in glass tubes packed with several non-polar adsorbents such as Tenax GC, Carbopak B, Porapak Q or P, Chromosorb 102, Mol. Sieve 5A and Mol. Sieve 13X. They found Molecular Sieve 5A to be the best solid adsorbent for these sulfur gases at ambient temperature (25°C). All tubes were conditioned prior to use by heating at a high temperature (200-250°C for 10-12 hours) under nitrogen. This conditioning step was required for obtaining quantitative recoveries and sharp desorption profiles. The selected Molecular Sieve material showed the highest breakthrough volume (*ca.* 25 L/g) and released the adsorbed components almost completely during the thermal desorption process (1 minute at 258°C). The recoveries were 83-87% for SO₂ and 75-82% for H₂S. The GC analysis was carried out on a Teflon column packed with Supelpak S. Detection using an FPD yielded detection limits in the ppb range for both gases. For the specific purpose of sulfur determination in natural gas the applicability of the non-polar adsorbents such as those studied by

³ Breakthrough volume, defined as the volume of gas that can be passed through an adsorbent before the investigated compound begins to be eluted.

Black *et al.* appears to be limited as these materials are most likely not capable of selectively isolating sulfur species from a large excess of hydrocarbons.

For the simultaneous collection of a larger group of sulfur compounds in air (COS, H₂S, MeSH, CS₂, dimethyl sulfide (DMS) and dimethyl disulfide (DMDS)) Steudler *et al.* [10] used a combination of two solid adsorbents: Molecular Sieve 5A for SO₂ and H₂S and Tenax GC for the others. The specially designed adsorption tubes showed a very high affinity for the sulfur compounds tested and yielded acceptable recoveries, varying from 50% for DMDS to 75% for COS. The recovery efficiencies were found to be a function of the desorption temperature, time and the helium gas flow rate during desorption. Because of the long time required for thermal desorption, it was necessary to cryogenically focus the desorbed sulfur gases in a Teflon loop cooled by liquid nitrogen before injection onto the GC column. The detection limits achieved were 8.8-20 pg S depending on the various sulfur gases (FPD). An interesting observation was that the recoveries appeared to be constant for each sulfur gas within the humidity range studied (30-95%). Again the application of a very strong non-selective adsorbent such as Mol. Sieve 5A precludes the use of this set-up for selective enrichment of sulfur components from natural gas.

In contrast to the results published by Steudler, Przyjazny [11] in his comparative study of several porous polymers: Chromosorb 102, XAD-2, XAD-4, XAD-7, Tenax GC concluded that Tenax GC is a poor adsorbent for organosulfur compounds (mercaptans, sulfides, disulfides, thiophenes). XAD-4, with its extremely large specific surface area (850 m²/g) was found to have the highest sorption capacity. Unfortunately, the long time necessary for complete thermal desorption makes the following GC analysis more difficult unless a cryogenic focusing step is employed. For samples consisting of high-boiling components only, Tenax GC may be the adsorbent of choice, because of its high thermal stability and relatively low breakthrough volumes. These characteristics would allow the sample components to be desorbed more rapidly from Tenax than from other sorbents. Also the sorption of MeSH and DMS on the carbon molecular sieve Carbosphere was investigated. The breakthrough volumes determined were *ca.* 2900 L/g for both sulfur compounds. Hence, this sorbent can be used for preconcentration of MeSH and DMS from samples containing extremely low levels of these contaminants. However, thermal desorption from Carbosphere is very difficult due to strong retention of the different sulfur derivatives.

Tangerman *et al.* [12] and also Przyjazny [11] studied the sorption capacities of Tenax GC towards highly volatile sulfur compounds, when using lower adsorption temperatures. With the goal of measuring volatile sulfur compounds in human breath Tangerman found that the capacity of the Tenax trap tubes is increased to a large extent by keeping the trap tubes in dry ice (-70°C) or in liquid nitrogen (-196°C). This was especially the case for H_2S adsorption. The minimum amount of sulfur gases that could be detected by gas chromatography employing a glass column packed with 20% SE-30 on Chromosorb P and an FPD was approximately 0.2 ng/L (0.1 ppb). The same technique: cryogenic Tenax trapping (liquid nitrogen -196°C), thermal desorption (200°C) / GC / FPD was later used by the same author [13] to determine simultaneously a large group of volatile sulfur gases: H_2S , COS, CS_2 , mercaptans, sulfides, disulfides in ambient air. To prevent build-up of water in the Tenax tube at these low temperatures, the water was pre-trapped by passing the gas through a desiccant (calcium chloride) which was found not to adsorb any of the sulfur-containing volatiles [13]. The experimental recoveries were relatively high (around 92%) and the author could detect volatile sulfur gases in air at the ppt level, although no concrete detection limits were quoted. Problems were only found in the determination of SO_2 . Preconcentration of this component onto Tenax at -196°C followed by GC analysis resulted in a complete loss of this component. Probably, in spite of the use of calcium chloride drying tubes, traces of water react with SO_2 in the Tenax tube or in the GC column, thereby preventing its detection.

Later, when analyzing low-boiling organic sulfur compounds (MeSH, DMDS, CS_2) in anoxic lake-water, Henatsch *et al.* [14] used cryoadsorption on Tenax tubes followed by analysis on a UCON coated glass capillary column and FPD detection. Due to the sensitivity differences of the FPD for the individual sulfur compounds different detection limits were found, CS_2 was detectable with a lowest limit of 5 ng/L. The detection limits of MeSH and DMDS were around 50 ng/L. One of the features of this process is that the disturbance of the procedure by excessive amounts of methane also present in the anoxic sample was avoided by using solid carbon dioxide rather than liquid nitrogen to cool the cryotrap. A schematic representation of the instrumentation developed by Henatsch and Jüttner is shown in Figure 1.1. The water-trap (part D in Figure 1.1) was constructed by using two 1-ml pipette tips connected end-to-end by silicone tubing. This trap was introduced into the gas line and cooled with solid

carbon dioxide. It was shown that the sulfur compounds were not retained in this trap.

Several experiments of cryogenic absorption of sulfur gases on unpacked sorption tubes were also described. In these cases, liquid argon [15], nitrogen [16], or oxygen [17] were used to cool the deactivated Pyrex glass or Teflon trap tubes. Hot water ensured desorption into the chromatographic system. Flame photometric detectors or even mass spectrometers were used to detect the sulfur gases tested at sub-ppb concentrations.

From the literature study described above, it is clear that several materials are capable of adsorbing sulfur species with large breakthrough volumes. Whether these materials provide sufficient sulfur-to-hydrocarbon selectivity yet remains to be established.

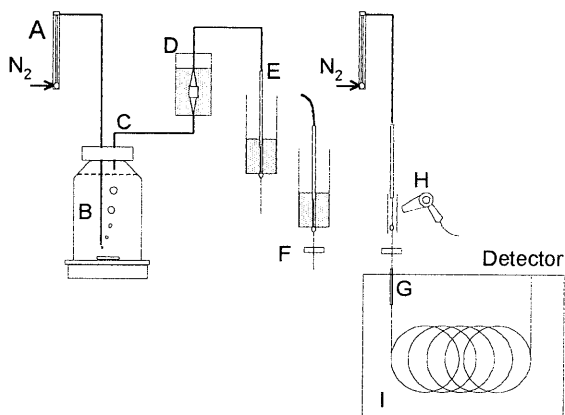


Figure 1.1: Cryotrapping system for the preconcentration of volatile organic sulfur. A - Rotameter for regulation of the nitrogen gas flow, B - Injection needle, C - Exit needle, D - Water trap, E - Cryotrap, F - Cryotrap connected to the GC system, G - Thermal transfer of the compounds onto the capillary column by rapid heating of the cryotrap with a heating gun (H). For the transfer, the GC oven was cooled to 0°C. PTEF tubes were fixed to the individual parts of the arrangements with silicone tubing. Reprinted with permission granted by Elsevier Science Publishers BV from *J. Chromatogr.*, 445 (1988) 95 by J.J. Henatsch and F. Jüttner.

1.3. CHROMATOGRAPHIC SEPARATION

The second step in GC-based analytical procedures for the determination of sulfur components in natural gas is the separation of the individual sulfur components. The separation efficiency required depends on both the performance of the selective enrichment step as well as on the selectivity of the detector. If non-sulfur-containing species are removed quantitatively in the sample pretreatment step, a separation of the individual sulfur components solely is sufficient. The same holds for the case that a truly selective, quenching-free detector is em-

ployed. In more realistic cases where both the sample pretreatment and the detection step are not 100% selective, separation of only the individual sulfur species is no longer adequate. Now all sulfur peaks should not only be separated from each other but also from all other components that might perturb measurements. For a successful and complete separation of a mixture covering such a wide range in boiling points as sulfur compounds in natural gas, it is very important to have a suitable column or system of columns for separation. If the separation performance is found to be insufficient due to poor resolution or to a too long analysis time, combination of two or more columns with or without switching valves could be an alternative. Details of these approaches and an overview of advantages and/or disadvantages of the individual techniques will be reviewed subsequently.

1.3.1. Packed-Column Systems

One of the advantages of packed columns over capillary columns is the high sample capacity of packed systems, which make it possible to inject large sample volumes. On the other hand, however, packed columns generally suffer from a low resolving power. For sulfur analysis this means that only a limited number of sulfur gases can be simultaneously separated on one single column. Moreover, there is a serious risk of adsorption losses on the column due to the adsorptive nature of sulfur components on the one hand, and the limited inertness of packed columns on the other hand. As column materials, Teflon or properly deactivated glass are usually the materials of choice due to the activity of volatile sulfur compounds and their strong tendency to adsorb onto glass and/or metal surfaces. This can cause peak tailing and sometimes complete losses of trace sample components. Thus, it is essential to deactivate the glass and metal surfaces of a chromatographic system or to use only Teflon columns and connections to minimize both peak tailing and losses incurred by irreversible adsorption of low concentrations of sulfur-containing compounds.

In the ISO methods for the GC determination of individual sulfur components in natural gas packed GC columns are used exclusively. ISO method 6326-2 uses a glass or Teflon column packed with two stationary phases. The first two thirds of the column is packed with 40% silicone oil DC 200 on Chromosorb W and the last one third is packed with 40% dinonylphthalate on the same support. The separation strength of this column is limited. Accurate quantification of for

example H_2S and MeSH is only possible if the ratio of the concentrations of these components is below approximately 10. ISO method 6326-4 is based on the use of a glass or Teflon column packed with 80-100 mesh polystyrene/divinylbenzene porous polymer beads. With this column a good resolution between the components of interest is achieved. Various chromatographic columns optimized for the separation of sulfur containing components have been described in literature. A short overview of these systems is presented below.

Stevens [18] described the use of a 36-foot Teflon column packed with Teflon powder coated with 1% polyphenyl ether and orthophosphoric acid and succeeded in analyzing H_2S , SO_2 and mercaptans at the ppb level using a GC system equipped with an FPD. Following this example Bruner *et al.* [19] also used a small amount of orthophosphoric acid (0.5%) mixed with 0.3% Dextsil 300 as a non-polar, low-bleeding liquid phase. Now, however, Graphon, a type of graphitized carbon black was used as solid support for packing a 1.25 m \times 3 mm i.d. Teflon column. Orthophosphoric acid increased the retention time of H_2S and SO_2 , which only have a weak interaction with the pure Graphon surface, while the Dextsil 300 reduces the surface area of the adsorbent. In this way the retention times of the compounds under examination are compressed into a smaller elution window. With such a column, operated isothermally at 40°C, H_2S and SO_2 could be detected on an FPD at minimal detectable concentrations of 20 and 10 ppb, respectively.

Later, H_2S and COS were detected in a mixture of hydrocarbons and inorganic gases (CO , CO_2 , N_2 and O_2) by Suier and Hill [20]. These authors used the observation from the work by de Souza *et al.* [21] that a column packed with acetone-washed Porapak QS gave a good separation of H_2S and COS and from the work by Burgett [22], that COS , H_2S and SO_2 could be determined in the sub-ppm range using a column packed with acetone-washed Porapak coated with 0.5% H_3PO_4 . In their own experimental work, Suier and Hill used a Teflon-coated stainless steel column packed with Porapak QS to separate a slightly more complex mixture and improved this procedure by adding a short (3 feet) pre-column packed with Porapak R to achieve adequate separation of H_2S and SO_2 from interfering water. Separation between the COS and the water peak was improved by temperature programming the column at a slow rate, *i.e.* sub-ambient initial temperature -65°C (3 min) to 10°C at 30°C/min, then to 92°C at 5°C/min, then at 30°C/min to 170°C, allowing the COS to elute before the elution of the water began. A thermal conductivity detector (TCD) was used but

no detection limits were quoted. The separation was relatively slow. The total analysis time was 45 minutes.

All columns described above could separate only a limited mixture of sulfur compounds. Tailing was frequently observed when trying to detect other components. De Souza [23] tried to resolve this problem by using a special packing material: Supelpak-S, *i.e.* acetone-washed Porapak QS. This author reported a number of advantages of a column packed with this material: *i/* water (present in many fuel gases and also in natural gas) and other highly polar molecules are quickly eluted from the column and do not interfere with the separation of the sulfur gases; *ii/* a very short-length (only 48 cm effective length) is required, hence, low inlet pressures are employed; *iii/* the column has a high resolving power; *iv/* the column can be temperature programmed to as high as 230°C; *v/* no liquid phase is used because the porous nature of the bead packing serves the function of both the liquid phase and the solid support, hence, column bleeding is low; *vi/* symmetrical peak shape for SO₂; and *vii/* the column can separate H₂S from COS and all other sulfur gases tested. Typical chromatograms obtained with and without pretreatment of Porapak QS are shown in Figure 1.2.

For the separation of individual sulfur gases in several different matrices, *e.g.* CO₂, ambient air, fresh lake water *etc.*, using a single packed column set-up a number of other packing materials were investigated: Porapak QS coated with 5% silicone oil QF-1 or Chromosorb G + 5% polyphenyl ether [24], silica gel or Porapak R without liquid phase [25], acid-washed Porapak Q [26], Chromosorb

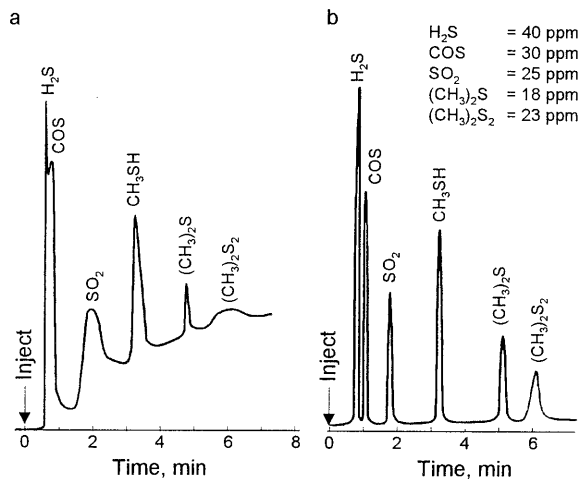


Figure 1.2: Typical chromatograms obtained without (a) and with (b) acetone washing of Porapak QS. GC conditions: carrier gas He 30 mL/min; sample volume 2 mL; FPD temperature 115°C; detector gases hydrogen 155 mL/min, oxygen 15 mL/min and air 50 mL/min; temperature program: 30°C (1 min) to 210°C (4 min) at 30°C/min. Reprinted with permission granted by Preston Publication, A Division of Preston Industries, Inc. from *J. Chromatogr. Sci.*, 22 (1986) 470 by T.L.C de Souza.

W AW DMCS coated with 15% SF-96 and 6% OV-225 [27], Chromosil 310 [28], Chromosorb G coated with Triton X-305 [29], Tenax GC [30], Diatomite CQ coated with 30% Triton X-305 [31], Chromosorb W ASTM with 15% OV-17 [32]. The detection limits range from ppm to ppb and sub-ppb level depending on the detector employed.

In most cases the column material used for sulfur separations was Teflon and/or Teflon coated aluminum or deactivated glass. It is generally stated that the use of bare metal or glass has to be avoided because of the strong tendency of active sulfur compounds to adsorb onto metal and glass surfaces. A notable exception in this respect is Pearson [24], who concluded contrarily and rejected Teflon in favor of stainless steel when he tried to determine C₁-C₄ mercaptans and sulfides in natural gas. According to Pearson, stainless steel columns and connections are much more robust and cause fewer problems with absorption than Teflon. Pearson could detect 0.1 ppm of tertiary butyl mercaptan and concluded that this technique is specific for sulfur compounds.

1.3.2. Capillary-Column Systems

Although several types of packed columns have been used in the gas chromatographic measurements of various sulfur-containing gases at concentrations down to approximately 5 ppm, packed columns are plagued with several disadvantages: *i/* large surface areas and concomitant adsorption losses; *ii/* a gradual approach to equilibration and the corresponding need to perform a number of "conditioning" injections both before and during the working period in order to obtain stable responses; *iii/* inadequate resolution for certain important compounds in mixtures of sulfur-containing gases (*e.g.* H₂S and COS); *iv/* relatively high pressure drops due to the long column length and the low permeability; and *v/* considerable potential for hydrocarbon quenching of the FPD's response due to inadequate peak resolution between the sulfur compounds and other organic constituents of the samples. Because of these inherent limitations of packed columns, glass capillary wall-coated open-tubular (WCOT) columns were investigated for their potential utility in the GC determination of sulfur-containing gases. Although glass columns are clearly more inert than packed columns they can still exhibit a substantial amount of residual surface activity. Various methods for deactivation of glass surfaces have been reported. Blomberg [33] used glass capillary columns deactivated by a thin layer of non-extractable Carbowax

20M coated with SF-96 to analyze the gas phase of fresh tobacco smoke. The detection limit, achieved with FPD, was 40 pg of sulfur. In capillary columns, the retention times of inorganic sulfur gases such as H₂S and COS are reduced dramatically, hence, cryogenic temperature programming is often necessary [33]. Farwell *et al.* [17] evaluated the deactivation of borosilicate glass WCOT columns with several materials such as SE-30, Carbowax 20M, OV-17, OV-101 and SE-54. These authors found that the first three reagents caused broadening and tailing of the sulfur gases under investigation. Only the two latter reagents showed sufficient efficiency for high-resolution separations (Figure 1.3). For some other components, the results achieved by capillary chromatography were found to be unsatisfactory. For example, SO₂ always produced broad, tailing peaks on a variety of glass and fused-silica open-tubular (FSOT) capillary columns. Depending upon the particular column and/or temperature program, MeSH also yielded a distorted, unsymmetrical peak with either a leading or tailing edge. These problems are caused not only by residual active surface sites of capillary columns but could also be caused by carrier gas impurities, such as water, as Barinaga and Farwell reported in a later publication [34], in which they also suggested a procedure to minimize these water effects by adding a dryer cartridge packed with 5Å Molecular Sieve between the carrier gas purifier and the injection valve.

Although the use of glass and FSOT capillary columns provides a greater inertness, better peak shapes, lower detection limits, and little or no memory effects, capillary columns also suffer from certain

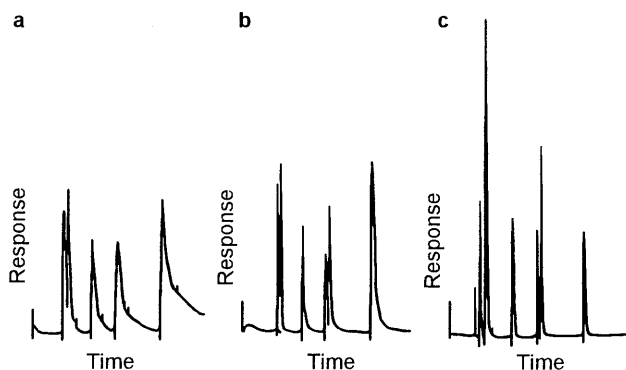


Figure 1.3: Influence of pretreatment of chromatographic packing materials on the sulfur elution pattern. Chromatograms obtained with undeactivated (a), SE-30 WCOT (b), and OV-101 WCOT (c) capillary columns, respectively. Elution order: H₂S, COS, MeSH, DMS, CS₂, and DMDS. Chromatographic conditions: $u = 20.4$ cm/sec of helium, oven programmed from -70°C to 150°C at 16°C/min. Reprinted with permission from *Anal. Chem.*, 51(6) (1979) 609 by S.O. Farwell, S.J. Gluck, W.L. Barnesberger, T.M. Schutte, and D.F. Adams. Copyright 1979 American Chemical Society.

disadvantages. One of those disadvantages is that the volumetric flow rate of the preconcentration device may be incompatible with that of the capillary column. For example, the 0.5 to 2 mL/min carrier gas flow for capillary columns is not compatible with the common desorption flow rate of many solid adsorbent traps. Capillary cryofocusing and cryotrapping techniques are not effective for poorly retained, low k' solutes like H_2S , COS and SO_2 that can break through the capillary cryotrapping or cryofocusing region. Also in the case of atmospheric sampling, microgram amounts of CO_2 and/or water collected in the preconcentration device can occlude the capillary cryofocusing and cryotrapping region. This causes incomplete analyte transfer and overpressurization of the column upon injection resulting in losses of analytes due to the back-flush of the loop contents into the upstream system and consequent exposure to active surface sites. Another disadvantage of capillary columns is the extreme demands placed on the dead volume and the actual transducing region of the detectors. A third disadvantage is the low initial oven temperatures, -50° to -70°C , required to obtain baseline separation between the unretained peak (CO_2) and the early eluting compounds H_2S , COS and SO_2 on thin film non-polar columns. The necessary sub-ambient initial oven temperature can only be produced by costly and logistically inconvenient cryogenics, such as liquid nitrogen. To overcome these disadvantages and to achieve baseline separation of sulfur gases at ambient temperatures as well as to increase sample throughput by decreasing the elution times, Barinaga and Farwell [35] explored the use of wide-bore, thick-film FSOT columns and "phase tuning" to optimize selectivity. Wide-bore, 0.5 mm i.d. FSOT columns have been recommended for certain separations because of their higher sample capacity and shorter analysis times at higher carrier gas flow rates compared to narrow-bore columns. Likewise, stationary phase films of greater thickness (1 to 8 μm) have been used in special situations for their greater capacity and, as a consequence, greater retention of very volatile compounds. A thick film non-polar column connected to a short length of a more polar column was used to eliminate the necessity of sub-ambient initial oven temperatures while maintaining baseline separation of the commonly occurring sulfur gases. The best results were obtained using column system consisting of a 30 m \times 0.53 mm \times 5 μm DB-1 coupled to a 3 m \times 0.53 mm \times 1 μm DB WAX. This column combination, equipped with a modified FPD [35] to decrease the dead volume and improve the streamlining, and operated in the temperature programmed mode: initial temperature: 30°C (1.2 min) to 140°C at $30^\circ\text{C}/\text{min}$ can achieve baseline separation of all seven sulfur gases H_2S , COS , SO_2 , MeSH ,

DMS, CS₂, DMDS and CO₂ within a total elution time of less than 5 minutes (Figure 1.4).

Porous-layer open-tubular (PLOT) columns with PoraPLOT Q deposited on the column wall have become commercially available. Jacobsson *et al.* [36] found that PLOT columns can take advantage of both the selectivity of the solid adsorbent material deposited as a thin layer on the wall and of the large plate numbers that are generated by capillary columns. Moreover, the use of PLOT columns was found to be highly compatible with mass spectrometry. Jacobsson succeeded in determining H₂S in liquid and solid samples at sub-pg levels. Similarly, Gaines *et al.* [37] evaluated the PoraPLOT U FSOT

column for determination of the seven common sulfur gases listed above. With a temperature program of: 80°C (2 min) to 180°C at 30°C/min in combination with an FPD and a sulfur chemiluminescence detector (SCD), they achieved detection limits in the pg - ng S range for the individual sulfur compounds. However, H₂S was very reactive towards the stationary phase and SO₂ showed some chemical derivatization on the column (Table 1.1 and Figure 1.5). Therefore, the PoraPLOT U column is not useful for low ppb/ppt analysis of H₂S and SO₂. Nevertheless, it is suitable for the determination of COS, CS₂, DMDS, and DMS at concentrations down to the ppt range, while H₂S and SO₂ can be successfully analyzed on this column at higher ppb/ppm concentrations.

For the analysis of odorants and natural gas sulfur compounds Russo and Maghini [38] used a fused-silica capillary column: 50 m × 0.2 mm × 0.3 μm (crosslinked methyl silicone film). To perform the specific analysis, two different runs had to be performed. A temperature-programmed analysis (35°C (10 min) to 250°C at 7°C/min) was used for the analysis of mercaptans and sulfides, while

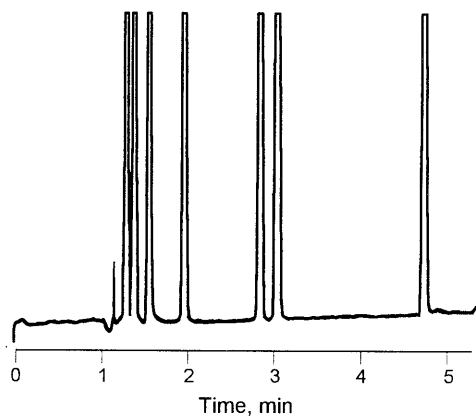


Figure 1.4: Chromatogram of cryogenically collected sulfur gases obtained at ambient initial oven temperature. Mixed phase column: 30 m × 0.53 mm × 5 μm DB-1 column coupled to 3 m × 0.53 mm × 1 μm DB WAX. Elution order: air, CO₂, H₂S, COS, SO₂, MeSH, DMS, CS₂, and DMDS. Reprinted with permission granted by Hüthig GmbH from *J. High Resolut. Chromatogr. Chromatogr. Commun.*, 10 (1987) 538 by C.J. Barinaga and S.O. Farwell.

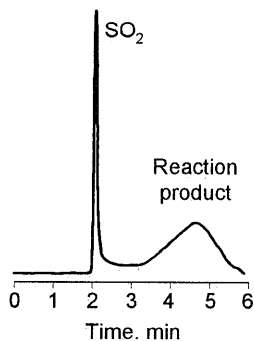


Figure 1.5: Reaction of sulfur dioxide on the PoraPLOT column. Detector: sulfur chemiluminescence. Reprinted with permission granted by Hüthig GmbH from *J. High Resolut. Chromatogr.*, 11 (1990) 585 by K.K. Gaines, W.H. Chatham, and S.O. Farwell.

Table 1.1: Detection limits for sulfur species on the poraPLOT U column. Detectors: FPD and SCD. Column length 12.5 m. Reproduced with permission granted by Hüthig GmbH from *J. High Resolut. Chromatogr.*, 11 (1990) 585 by K.K. Gaines, W.H. Chatham, and S.O. Farwell.

Component	Detection limits (pg)	
	FPD	SCD
COS	30	5
CS ₂	110	20
DMDS	660	30
DMS	160	30
H ₂ S	2000	760
MeSH	850	190
SO ₂	850	270

H₂S and COS were analyzed isothermally at -15°C. Highly purified helium was used as carrier gas.

Monks [39], on the other hand, achieved complete determination of sulfur components in natural gas by using a multi-packed-column system operated isothermally at 115°C. A schematic representation of this system is shown in Figure 1.6. Separation of sulfur compounds from hydrocarbons is achieved on a main column with a length of 1 m. This column is packed with acetone-washed Porapak PS. The bypass column, which is 2 m long packed with acetone-washed Porapak QS, is used to selectively isolate some of the sulfur components during the analysis. A 0.25 m buffer column packed with acetone-washed Porapak QS is placed immediately before the detector to damp pressure surges caused by valve switching. A compromise that had to be made with this system involves the separation of tertiary butyl mercaptan (*t*-BuSH) from methyl ethyl sulfide (MeEtS), an indigenous component of natural gas. In order to keep the analysis time as short as possible, these components elute together at about 5.3 min. The total analysis time is 15 min. The detection limits vary between 0.05 and 70 ppm.

Obbens *et al.* [40] reported another alternative for the GC analysis of sulfur components in natural gas with a combination of packed and capillary columns installed in two independently, thermostatically controlled, heated compartments. Separation of H₂S and SO₂ was performed on an acetone-washed Porapak QS

packed column loaded with 0.5% H_3PO_4 to increase inertness and to prevent tailing of H_2S . The separation of THT and other sulfur compounds was achieved on a very thick-film 50% phenyl-methyl silicone phase on a FSOT capillary column. The last two techniques described above have employed an FPD for detection of the eluted sulfur compounds.

From the literature survey presented in this chapter it can be concluded that future research in the area of sulfur separation for natural gas analysis should be directed towards the development of separation systems that enable both a separation of the individual sulfur peaks and, more importantly, separation of sulfur peaks and interfering hydrocarbons. To date, no such system is available.

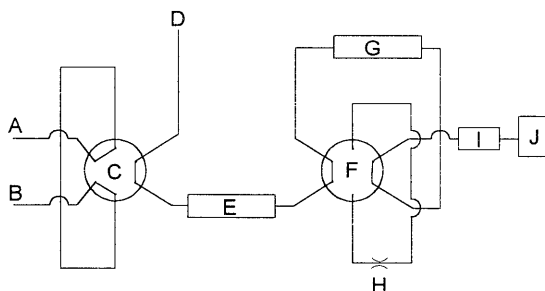


Figure 1.6: Schematic diagram of valve and column layout designed by Monks. A - sample in, B - sample gas out, C - six-port sampling valve, D - carrier gas in, E - analytical column, F - six-port valve, G - bypass column, H - bypass needle valve, I - buffer column, J - detector. Reprinted with permission granted by Elsevier Science Publishers BV from *Proceedings of the Congress of "Gas Quality – Specification and Measurement of Physical and Chemical Properties of Natural Gas"*, Groningen, the Netherlands, 22–25 April 1986, Elsevier, Amsterdam, the Netherlands, 1986, p. 641 by Monks.

1.4. DETECTION SYSTEMS FOR GC-BASED SULFUR ANALYSIS

One of the major advantages of gas chromatography is the availability of a large number of sensitive universal as well as selective detectors. The combination of the excellent separation capability of (capillary) GC with sensitive selective detection enables the measurement of low concentrations of different components in sample matrices of ever increasing complexity. Selective detectors are becoming increasingly popular in recent years. Not only for the fact that they partially eliminate the need for laborious and time-consuming methods for sample preparation, the use of a selective detection device also reduces the risk of false-positive identifications. It is evident that also the separation itself is simplified if selective detectors are employed. Selective detection enables target compounds

to be measured while other coeluting compounds are not sensed. Important universal detectors are the flame ionization detector (FID) and the thermal conductivity detector (TCD). As these detectors respond to virtually all components amenable to GC, high demands are posed on sample preparation and separation.

For non-hydrocarbon compounds containing for example sulfur, nitrogen or phosphorous, a wide range of selective detectors is available. For the selective detection of sulfur this includes the flame photometric detector (FPD), the sulfur chemiluminescence detector (SCD), atomic emission detector (AED), photo ionization detector (PID), electron capture detector (ECD), mass spectrometric (MS) detection devices and detection techniques based on electrochemical principles such as the Hall electrolytic conductivity detector (HEICD) and coulometric detection devices. The basic principles of the various detection systems for GC as well as the hardware requirements are the subject of a series of books and review articles [41-44]. An excellent review article of potential gas chromatographic sulfur-sensitive detectors in environmental analysis has been published by Wardencki and Zygmunt in 1991 [45]. In the present review only improvements that have been achieved after this date will be discussed. In spite of the fact that most of the sulfur selective detectors are already available for many years, considerable improvements in the performance of especially the FPD and the SCD have been achieved in the last three years.

1.4.1. Improvements in Flame Photometric Detection

The FPD is nowadays the most widely used sulfur-selective detector for GC. Present-day systems are mostly based on the work of Brody and Chaney [46] published some 30 years ago. The FPD is basically a flame emission photometer. Sulfur compounds, burnt in a hydrogen-rich flame, produce S_2^* which emits radiation near 400 nm. This radiation is monitored by a photomultiplier tube. Although the role of S_2^* as a main emitter in FPD has not been totally unambiguous [47], the S_2^*/S_2 mechanism is now widely accepted and used to explain the square root dependence of the detector response towards the concentration of sulfur compounds tested. Although rather sensitive, the FPD suffers from a number of inherent problems such as non-linear response; dependence of the response factor on molecular structure; and quenching by hydrocarbons and other species coeluting with the sulfur compounds.

The most serious problem in the practical application of the FPD is the quenching effect. Although the exact cause of quenching remains yet to be established, it appears that both the change in the flame temperature as well as in the flame chemistry that occur when large amounts of hydrocarbons are introduced in the flame play a role. Various instrumental changes to reduce the susceptibility of the FPD for quenching have been proposed in literature. Patterson *et al.* [48] developed the dual flame photometric detector. In this detector components eluting from the GC column are burnt in a hydrogen rich first flame. In a second flame S_2^* species emit light which is then measured on the photomultiplier tube. As all components are burnt in the first flame, the flame chemistry of the second flame is much less affected by coelution of sulfur and non-sulfur containing components. As a result of this the dual-flame mode FPD resists quenching and is more truly quadratic in response. Unfortunately, however, the sensitivity of the dual flame FPD is only approximately 10% to 20% of that of the single flame version [49]. Moreover, dual flame operation enhances hydrocarbon response. The selectivity of sulfur *versus* carbon of the dual flame FPD is only 10^3 to 10^4 as opposed to a selectivity of 10^5 to 10^6 for the single flame FPD [50]. Because the poor selectivity of the dual flame FPD (DFPD) the analysis of individual sulfur compounds in a complex hydrocarbon mixture is complicated by the simultaneous hydrocarbon response. A method to overcome this difficulty has been published by Baig *et al.* [50]. In the method designed by these authors the effluent of the column is split into two streams. One stream is fed to the DFPD, the second to an FID. Next, the FID signal is subtracted from the DFPD signal which results in a simplified chromatogram as the hydrocarbon response is eliminated.

A fully chromatographic approach for eliminating quenching of the FPD was described by Efer *et al.* [51]. These authors used the series-coupled system of two capillary columns with different polarities to achieve selectivity tuning. By varying the mid-point pressure settings, controlled overlap of sulfur-containing and sulfur free components could be obtained resulting in quenching free chromatograms or at least chromatograms that contain quenching free regions. Efer also applied this set-up for detailed studies of the magnitude of the quenching effect. When studying the degree of quenching of ethylthiophene by nonane, it was found that a ten-fold excess of the quenching compound was required to obtain a significant signal reduction. The relationship between signal reduction and the concentration of the quenching component was found to be non-linear.

Similar studies by Liu *et al.* [52] revealed that the decrease of the sulfur signal caused by flame hydrocarbons is strongly dependent on the oxygen-to-hydrogen (O/H) ratio in the flame and, under certain conditions, also on the sulfur-to-carbon (S/C) ratio of the sample. Higher O/H ratios decrease the quenching effects as well as the dependence of this quenching on the S/C ratio in the sample. The detection limit of the FPD is about 10^{-11} g S/sec, which provides

mass detection limits in the sub-nanogram range.

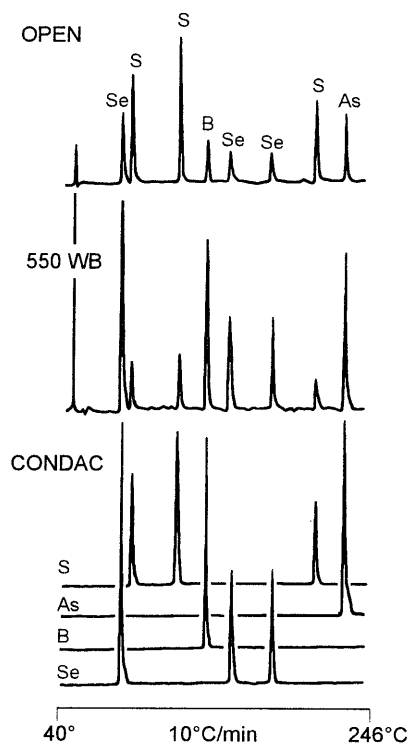


Figure 1.7: Flame photometric detection of various elements using differential operation and CONDAC algorithm. Two-channel and CONDAC chromatograms of (in order of elution) 14 ng dimethyldiselenide, 1.0 ng diethyl disulfide, 1.6 ng di-*tert*-butyldisulfide, 100 ng *o*-carborane, 20 ng methylbenzselenazole, 15 ng diphenylselenide, 1.0 ng thianthrene and 10 ng triphenylarsine. Reprinted with permission granted by Elsevier Science Publishers BV from *J. Chromatogr.*, 606 (1992) 73 by W.A. Aue, X.-Y. Sun, and B. Miller.

Apart from quenching also the limited linearity and selectivity of the FPD can hamper its use in practical applications. A series of other papers have been published in literature in which important methods for improving the linearity and the selectivity are described. A numbers of authors [53-55] proposed the use of dopants such as SO_2 or CS_2 to linearize the detector output. The difficulty with this procedure is that the dynamic range is reduced and the linear output is dependent on the dopant and the solute. Sevcik and Phuong Thao [56] have evaluated the selectivity of the FPD and suggested that the unsuitable geometry of the interference filters resulted in interference from hydrocarbons and heteroatoms. They found that the selectivity of the detector improved with respect to hydrocarbon and heteroatom interference when the flame output was collimated. Aue *et al.* [57] improved the sulfur selectivity by about one to three orders of magni-

tude by using a dual-channel FPD, which annulled the response of carbon or other elements by differential operation; or by having the CONDAC ("conditional access" or "conditional acceptance") algorithm deny unwanted elements access to the chromatogram [57]. The two-channel and CONDAC chromatograms of the compounds under investigations are shown in Figure 1.7. In their own experiments Aue *et al.* preferred to use the FPD "open", *i.e.* free of spectral discrimination beyond the response profile of the photomultiplier tube.

An approach to obtain a truly linear relationship between the FPD output signal and the sulfur concentration was published by Aue and Sun [58]. Experimental work by these authors confirmed that although the luminescence from sulfur compounds in the FPD is dominated by the S₂ main-system bands (of approx. quadratic response), it also contains a linear emitter with a "spectrum" in the 600 to 850 nm region. Up till now in the spectra of conventional quadratic emissions (Figure 1.8) no emission beyond 520 nm had been measured. For that reason the linear sulfur emission had remained hidden for so long. In the 600-850 nm region the sulfur chemiluminescence is a first-order process and varies, if at all, by a factor of less than two in elemental response (sulfur equivalency) among several structurally diverse compounds. A linear response was measured for a band at *ca.* 750 nm (where the spectrum has its global maximum) as well as for the wider 600 to 850 nm range (with a long-pass filter). The detection limit measured in the "linear" sulfur mode is 2×10^{-13} mol S/sec and its linear range spans four orders of magnitude. The detection limit could be improved further by using capillary columns and temperature programmed operation. The authors [59] believe that the emitter of this spectrum is HSO (²A' - ²A" electron transition) [60]. The HSO 0,1 band shows up clearly at 749 nm. The 0,0 and 1,1 bands occur at 696 and 711 nm. The 2,0; 1,0 and 0,2 bands at 634, 663 and 809 nm appear to be present as well (Figure 1.9). Some other advantages of the linear FPD have been emphasized: *i/* the response of hydrocarbons is generally negative, thereby providing a quantitative distinction between compounds that contain sulfur and those that contain only carbon and hydrogen; *ii/* only a minor dependence of the response of sulfur on the compound structure; *iii/* preliminary experiments indicate that the linear sulfur mode suffers significantly less from quenching by co-eluting hydrocarbons than does the quadratic mode. Overall, the new linear mode appears to be superior over the conventional quadratic one, and it appears competitive with other methodologies of organosulfur detection. On the other hand the authors have also emphasised that the range of compounds tested in this

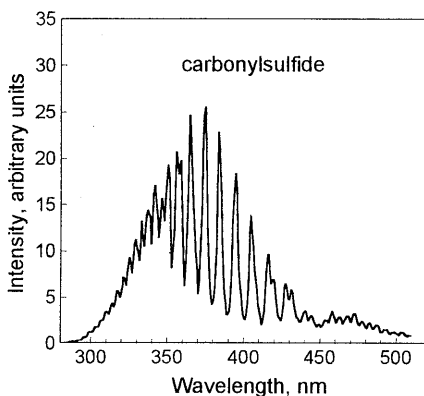


Figure 1.8: S_2 luminescence (obtained from continuous introduction of COS) measured with an FPD in the "quadratic mode". Conditions: hydrogen 50 mL/min, air 40 mL/min, bandpass ca. 6.7 nm. Reprinted with permission granted by Elsevier Science Publisher BV from *J. Chromatogr.*, 633 (1993) 151 by W.A. Aue and X.-Y. Sun.

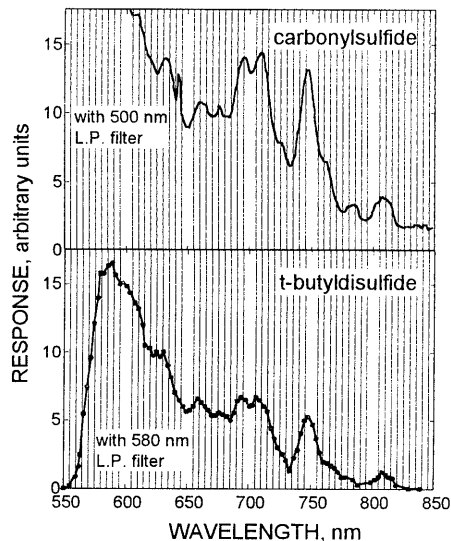


Figure 1.9: Comparison of sulfur spectra measured with an FPD in the "quadratic" and "linear" mode. Luminescence obtained by continuous introduction of COS (above) and repeated injection of tert-butylidysulfide (below) in the "linear mode". Conditions: hydrogen 500 mL/min, air 40 mL/min. Bandpass ca. 6.7 nm: 500-nm (above) and 580-nm (below) longpass (L.P.) filters are used for order sorting. Reprinted with permission granted by Elsevier Science Publisher BV from *J. Chromatogr.*, 633 (1993) 151 by W.A. Aue and X.-Y. Sun.

study is limited (only seven) and that the present conclusion should remain open to future re-evaluation.

Driscoll and Berger [61] developed an FPD that employs rare-earth glass filters, improving the sensitivity by eliminating angular dependence, which occurs with interference filters. At the same time, the detector sensitivity is improved by a factor of 2-3 owing to simultaneous detection of the various S_2^* emission lines.

A very interesting and highly promising development in the field of flame photometric detection was published by Cheskis *et al.* [62] in 1993. Cheskis described a novel gas chromatographic detector based on the flame photometric principle: the Pulsed - Flame Photometer. The pulsed-flame photometric detector (PFPD) is based on a flame source and a combustible gas flow rate that cannot

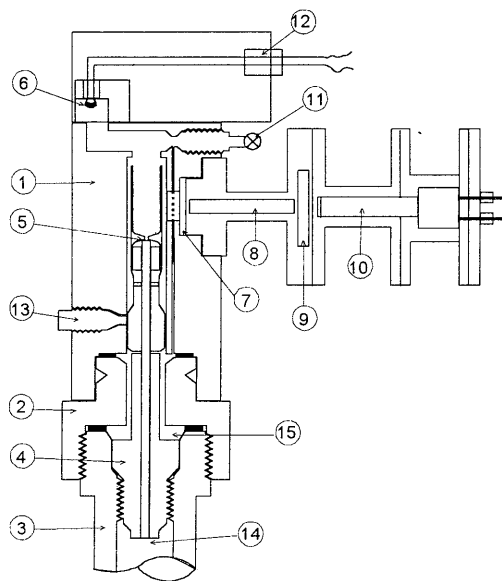


Figure 1.10: Schematic diagram of the pulsed FPD. The optical detection system is not drawn to scale. (1) main structure, (2) GC adapter, (3) GC-FID mount, (4) combustion cell holder, (5) quartz combustor, (6) igniter, (7) window, (8) quartz rod light guide, (9) color glass filter, (10) photomultiplier, (11) auxiliary screw valve, (12) ingniter and heater electrical feedthroughs, (13) external material sampling inlet, (14) hydrogen inlet, (15) air inlet. Reprinted with permission from *Anal. Chem.*, 65 (1993) 539 by S. Cheskis, E. Altar and A. Amirav. Copyright 1993 American Chemical Society.

sustain continuous-flame operation. Thus, the ignited flame propagates back to the combustible gas mixture source and is self-terminated after the combustible gas mixture is burnt. The continuous gas flow creates additional ignitions in a periodic fashion. A schematic diagram of the PFPD is shown in Figure 1.10.

The main feature that characterizes the PFPD is the pulsed-nature of the emitted light. Time domain information is added to the heteroatom specific emission with time dependent emission being observed (e.g. Figure 1.11). The main advantages of the PFPD include improved detection sensitivity for S and P, much higher selectivity against hydrocarbon molecules, lower gas consumption, reduced emission quenching, additional temporal information, and the ability to detect selectively other heteroatoms such as nitrogen or the simultaneous detection of S and C. The minimum

detection levels achieved are 2×10^{-13} g S/sec, 1×10^{-14} g P/sec, 5×10^{-12} g N/sec, and 6×10^{-11} g C/sec. The sulfur concentration dependence of the PFPD is quadratic and its response is independent of the structure of the sulfur-containing molecules (linear factor $n = 2.00 \pm 0.03$). A comparison between the commercial double-flame photometer and the pulsed FPD is shown in Figure 1.12.

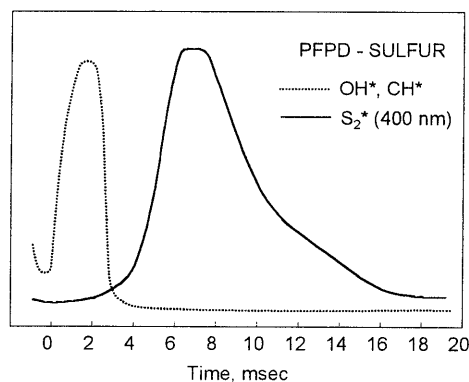


Figure 1.11: Time dependence of sulfur and carbon emission measured with a pulsed-FPD. PFPD emission time dependence of sulfur (S_2^*) (solid line) is obtained at 395 nm through a monochromator and that of OH is obtained at 312 nm (dashed line) which is identical to that of hydrocarbon emission such as from CH^* or C_2^* . Detector temperature was 150°C and very hydrogen-rich flame conditions were used. Tetrahydrothiophene was introduced as the source of sulfur. The combustion cell length was 10 cm. The viewing window is 5 mm in diameter and is centered on the combustor. Reprinted with permission from *Anal. Chem.*, 65 (1993) 539 by S. Cheskis, E. Altar and A. Amirav. Copyright 1993 American Chemical Society.

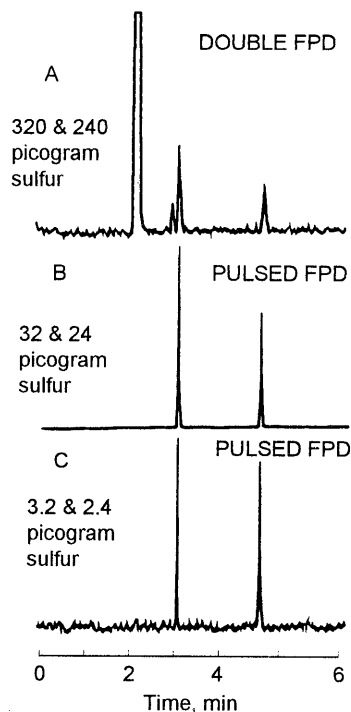


Figure 1.12: Comparison between the commercial double flame photometer (DFPD) (Varian) and the pulsed-FPD (PFPD). Standard Varian FPD test sample was used containing 20 ng/ μ L each 1-dodecane-thiol, tributyl phosphate, methylparathion and 4000 ng/ μ L *n*-pentadecane in isooctane. A 30-m capillary (0.25 mm i.d. DB-1) column was used at 220°C. (A) 2 μ L were injected with a 20:1 split ratio with the DFPD being used in the sulfur mode. (B) 1 μ L was injected with a split ratio of 100:1. The PFPD was used in the sulfur mode. (C) 0.10 μ L was injected with a split ratio of 100:1. Again the PFPD was used in the sulfur mode. The detector response times are 1 sec for the DFPD and 0.3 sec for the PFPD. Reprinted with permission from *Anal. Chem.*, 65 (1993) 539 by S. Cheskis, E. Altar and A. Amirav. Copyright 1993 American Chemical Society.

1.4.2. Improvements in Sulfur Chemiluminescence Detection

In contrast to the flame photometric detector, which is already commercially available for almost 30 years, the sulfur chemiluminescence detector (SCD) only became available some 9 years ago. In the SCD sulfur containing components are converted to SO by means of a reducing flame or a furnace-based converter. Currently, two designs that differ in the way the SO converter is set-up are available. In the flame-based system a ceramic sampling probe and a vacuum system is used to collect the gases from the flame of an FID. SO is then sensitively detected based on an ozone-induced chemiluminescence reaction to form electronically excited SO_2^* which relaxes by emission of light in the wavelength range of 280-420 nm. The SCD can be coupled to the flame housing of a flame ionization detector (FID) and hence is compatible with most existing GC instruments. Apart from the SCD signal of the sulfur components also an FID signal is obtained, although the settings of both hydrogen and air are well outside the optimum. In the second design of the instrument conversion of the sulfur components to SO no longer takes place in the FID flame. The instrument contains an enclosed flame converter. In the absence of the FID the need for manual adjustment of the position of the ceramic tip in the FID flame is eliminated which greatly simplifies operation. The sensitivity of the flameless burner version of the SCD is claimed to be 5 to 10 times higher [49].

1.4.3. Mass Spectrometric Detection of Sulfur Compounds

The combination of gas chromatography with mass spectrometric detection is an extremely powerful tool in the analysis of unknown samples. Mass spectrometric detection offers a selectivity unsurpassed by any of the other selective detection devices. Whereas selective detectors such as those described above only reveal the presence of a certain hetero-atom, the mass spectrometer gives detailed information on the various structural groups present in a molecule. Among the various ionization modes available, especially electron ionization and chemical ionization have gained widespread acceptance. The combination of these two ionization modes with detection of either positive or negative ions results in four basic operational modes showing substantially different sensitivities towards different types of components.

Headley [63] used a bench-top GC/MS system in the electron ionization mode to detect organosulfur compounds in environmental samples, *e.g.* industrial efflu-

ents, surface waters, sediment and fish samples. The electron-impact ion source was used with the electron energy set up at 70 eV. The mass range was 45-450 amu and the scan rate was 1 Hz. Positive ion detection was employed. The compounds were detected in the approximate concentration range from 0.1 to 2000 ppb. Bandy *et al.* [15] developed an accurate technique for the determination of ppt levels of atmospheric CS₂. High accuracy and immunity to analyte losses were achieved by using ¹²C³⁴S₂ as an internal standard and by performing the analysis by GC/quadrupole MS. High sensitivity was achieved by careful tuning of the GC/MS and preconcentration of the CS₂ on a Carbosieve B adsorbent. Data acquisition was carried out in the multiple ion detection mode of the INCOS data system (Finnigan Instruments, Sunnyvale, CA). Mass windows of 75.75 amu to 76.25 amu and 79.75 amu to 80.25 amu were monitored for 0.2 sec each. Parent ions of ¹²C³²S₂ and ¹²C³⁴S₂, respectively, could be monitored in these windows. Optimization studies showed that an electron energy of 30 eV produced the best compromise between signal and background.

Giuze *et al.* [64] used GC/quadrupole MS to analyze sulfur compounds in gasoline. Specific detection of sulfur species could be achieved by using the quadrupole analyzer in the chemical ionization mode with ammonia as the reagent gas with detection of negative ions. The authors concluded that the selectivity gained by using the negative ion chemical ionization mode (NICI) was high enough to selectively detect sulfur components on low resolution quadrupole mass spectrometers, even without preliminary separation of the samples.

In low resolution MS, chemical ionization using ammonia as the reactant gas increases the selectivity. In this ionization mode, the mass spectra obtained are fairly simple. The pseudomolecular ion as the base peak is characteristic. Unfortunately, mercaptans have very low molecular weights. It is hence necessary to start mass acquisition below 34 amu, the molecular weight of H₂S. With positive ion detection the reactant gas produces a considerable background noise in the low mass range. On the other hand with negative ion detection, no background noise occurs in the low mass range resulting in an improved sensitivity for sulfur compounds [64]. Mass spectra obtained with positive CI is very similar to EI ionization, unlike negative CI which is totally different from it [64]. The high electron affinity and the low background noise level in the low mass range render negative ion-CI the most suitable ionization technique for GC/MS analyses of volatile sulfur compounds.

In high resolution mass spectrometry the principle is to measure only the CHS^+ fragment which is one of the fragments from R-CHS compounds. At mass 45, there are at least 7 other species that could interfere with CHS^+ at low mass resolution. Only CHS^+ , and $^{13}\text{CC}_2\text{H}_8$ fragments are issued from the sample. All the other ions are background impurities. $M/\Delta M$ is the resolution required to completely resolve other ionic species which have the same nominal mass. At a resolution of 3400, CHS^+ is totally isolated. The resolution of a quadrupole mass analyzer is only $2 \times M = 90$ at mass 45.

Recently, selective detection of sulfur-containing compounds by a new GC/MS combination technique, GC/Chemical Reaction Interface MS, was reported [65]. The principle of this new method is based on the creation of a reaction interface by addition of a reactant gas to a low-pressure microwave-induced plasma. In this interface complex molecules are converted into small polyatomic neutral species. For a given reactant gas the array of these small molecules reflects the elemental composition of the original analyte. Moini *et al.* found that HCl is highly effective as a reactant gas for selective detection of sulfur containing compounds. In a low pressure microwave-induced plasma (temperature of about 4000-6000 K [65]), the components eluting from the GC column are completely decomposed. When the decomposition products leave the hot region of the plasma they react rapidly with the reactant gas to produce thermodynamically stable neutral molecules. The mass spectra of selected neutral molecules identify and quantify the elements of interest. In the case of sulfur

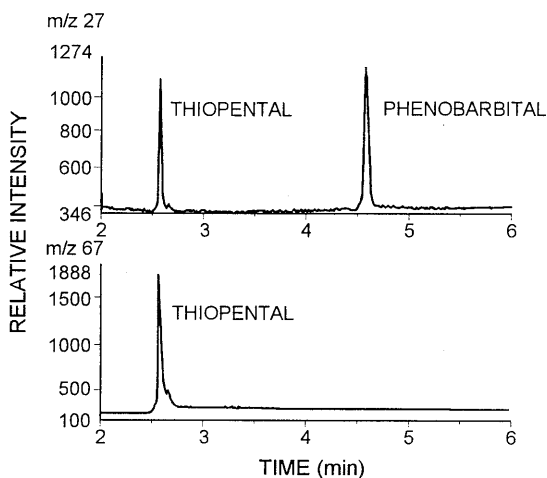


Figure 1.13: Selective detection of sulfur compounds by GC/Chemical Reaction Interface MS. Chromatogram at m/z 67 using a mixture of thio-pental (6.6 ng on-column) and phenobarbital (26.4 ng on-column) is the selective sulfur channel. The chromatogram at m/z 27 (HCN) is a non-selective carbon channel. Reprinted with permission granted by Elsevier Science, Inc. from *J. Am. Soc. Mass Spectr.*, 2 (1991) 250 by M. Moini, D. Chace, and F.P. Abramson. Copyright 1991 by the American Society for Mass Spectrometry.

compounds with HCl as reactant gas, sulfur predominantly (>95%) produced SCl at m/z 67 and 69 and detection at m/z 67 was completely selective for sulfur (Figure 1.13). Detection limits as low as 30 pg of a sulfur containing compound and a dynamic range of two orders of magnitude were achieved.

The high specificity of the GC/MS technique in sulfur analysis was also proved in a large series of other experiments, particularly in the determination of sulfur containing compounds in gas and oil fractions of local petroleum industry, *e.g.* the analysis of thiophenes in gas condensates of the Urtaubulak field of Uzbekistan [66,67], the study of the composition of sulfur compounds of Lyalmikar and Kokaity petroleums [68], and the analysis of organosulfur compounds of petroleums of the Ural - Volga region [69,70]. Mass spectrometers have also been used in comparative studies of different detection methods [71,72].

1.4.4. Other Detection Systems for Sulfur Analysis

Apart from the FPD, SCD and MS also other sulfur selective detectors have been employed in the determination of sulfur compounds in various matrices [73-77]. The basic principles and applications of these detection systems have recently been reviewed by Wardencki and Zygmund [45]. A comparison of the main characteristics of the different sulfur selective detection systems is presented in Table 1.2.

Table 1.2: Basic characteristics of various sulfur selective detectors.

Detector	Detection limit (g S/s)	Selectivity S/C	Linear dynamic range
FPD			
Single flame	10^{-11}	$10^4 - 10^6$	3*
Dual flame	10^{-10}	$10^3 - 10^4$	3*
Linear response	10^{-11}	10^3	4
Pulsed FPD	10^{-13}	$> 10^7$	2 - 3*
ECD	Variable, down to 10^{-15}	Variable	4
SCD			
Flame-based	10^{-13}	$10^6 - 10^7$	3 - 4
Flame-less	10^{-14}	$10^6 - 10^7$	4 - 5
AED	10^{-12}	10^4	3 - 4
HEICD	10^{-11}	$10^4 - 10^6$	3 - 5
PID	10^{-12}	poor	6
MS	10^{-11}	specific	2 - 5

* Linearized output from the quadratic response

1.5. CALIBRATION

GC based analytical methods are relative methods of determination which means that they require calibration, *i.e.* the relationship between detector signal and mass or concentration injected has to be established experimentally. The simplest way to calibrate an analytical instrument is to pass a sample containing the species of interest at a known concentration through the instrument and relate the instrument response to concentration. This simple description of the calibration process ignores the real problems that are generally encountered in the calibration process. These problems can be divided roughly into two areas [78]:

1. Preparation of the standards.
2. Assignment of concentration and uncertainty to the composition of the standard.

In this section various methods for the preparation of calibration standards are described. Special attention will be paid to methods for the preparation of calibration mixtures for sulfur analysis. Due to the adsorptive nature of sulfur components extreme care should be taken in both preparation of the standards as well in storage.

The most common procedure for calibration in quantitative instrumental analysis is the use of so-called calibration graphs [79]. In the *one point calibration graph*, one sample of known concentration is analysed in the analytical instrument under the same conditions as those subsequently used for the real samples. Next, a calibration line is constructed by drawing a straight line through the origin and the experimental point. For the *two point calibration graph* or for *multiple linear calibration*, the analyst takes a series of samples in which the concentration of the analyte is known. It is essential that the calibration standards cover the entire range of concentrations required in the subsequent analyses. The concentrations of the test samples are normally determined by interpolation and not by extrapolation. Furthermore, it is important to include the value of a "blank" sample in the calibration curve. The blank contains no deliberately added analyte, but does contain the same solvents, reagents, *etc.* as the other test samples and is subjected to exactly the same sequence of analytical procedures.

Non-linear calibration graphs can be used in situations where the relationship between the detector signal and the concentration or mass of compounds of

interest is clearly non-linear. Particularly common is the situation where the calibration plot is linear (or approximately so) at low analyte concentrations, but becomes curved at higher analyte levels. In other cases, *e.g.* classical FPD signal *vs.* concentration plots, it is obviously curved at all concentrations. For a more detailed discussion of the mathematics involved in linear and non-linear calibration the reader is referred to the excellent text-book written by J. C. Miller and J. N. Miller [79].

1.5.1. Methods for Preparing Standard Mixtures in Natural Gas Analysis

For the construction of the calibration graph, standards of accurately known concentrations are needed. A number of methods for the preparation of calibration gases for gas analysis is described by the ISO organisation. These methods can be roughly classified as static or dynamic. *Static methods* involve preparing and storing the mixture in a closed vessel, for example a cylinder, flask or plastic bag. The sample volume is thus limited to that of the container. Cylinders must be used to store mixtures at high pressures. Static systems are preferred when comparatively small volumes of mixtures are required at moderately high concentration levels, but losses of components by adsorption on the vessel walls may occur. *Dynamic systems* generate a continuous flow of mixture and can produce large volumes, with lower surface losses, owing to equilibrium between the walls and the flowing gas stream.

Figure 1.14 shows a schematic diagram of the preparation methods of calibration gas mixtures used in natural gas analysis. If the concentration in the component of a calibration gas mixture is directly related to the measurement of basic standard units (mass, time, length, etc.) then this mixture is a so-called *primary calibration gas mixture*.

If a primary calibration gas mixture is used for establishing the composition of another calibration gas mixture this last mixture is a so-called *secondary calibration gas mixture*.

The best claimed accuracies of these standardized methods [80] are summarized in Table 1.3.

One of the requirements of the analytical procedures in which the calibration gas mixtures are applied, is that the composition of the natural gas to be analyzed and that of the calibration gas mixture should have a close resemblance. In practice

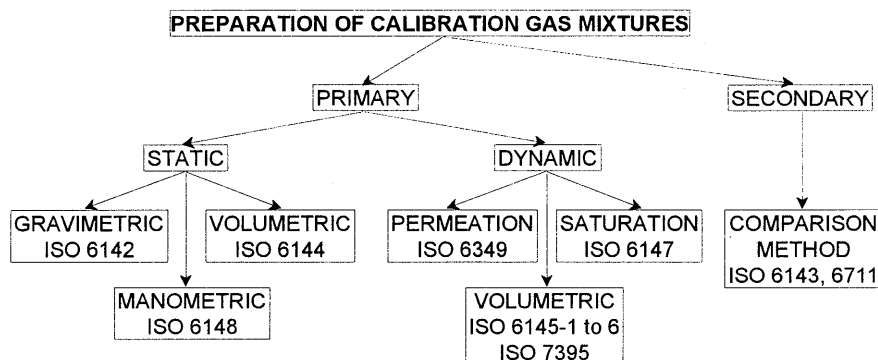


Figure 1.14: Schematic representation of the preparation methods for calibration gas mixtures used in the natural gas industry. For a more detailed discussion of the principles of the various preparation methods the reader is referred to the ISO standards summarized in Table 1.3.

Table 1.3: Best claimed accuracies of standardized methods for the preparation of calibration gas mixtures [80].

Method	Number of ISO	accuracy (%)
Gravimetric	ISO 6142	< 1
Manometric	ISO 6146	1
Permeation	ISO 6349	2
Saturation	ISO 6147	3
Dynamic volumetric	ISO 6145 - 1 to 6	2 - 5
	ISO 7395	
Static volumetric	ISO 6144	3 - 7
Comparison	ISO 6143, 6711	-

this means that a gravimetric preparation method should be used to prepare calibration gas mixtures. With the gravimetric method it is possible to prepare compositions very close to the desired composition. The precision of this gravimetric preparation method has been evaluated [81]. The following errors have to be taken into account when calculating the final composition of a calibration gas mixture prepared using this method:

1) Systematic errors, which are inherent to the procedures used. The use of different lots of reagent gases, different weight of gases, different operators and even different balances helps to reduce systematic errors arising in the process. A systematic error in the procedure however, can only be recognized by compari-

son of the standards to standards prepared by a totally different method or by analysis using an absolute method. The difference between the two methods of preparation, or the method of preparation and the method of analysis should be less than the statistically predictable difference based on all of the observed random errors.

2) Impurities in the pure gases: This error can be accounted for by carefully analyzing the pure gases and taking into account these impurities when calculating the final composition of the calibration gas mixtures.

3) Weighing errors: Koning and van Rossum found that the uncertainty in the concentration of methane of a gravimetrically prepared seven component calibration gas mixture caused by weighing errors can be as low as 1.6×10^{-4} mol% [81]. For this particular calibration gas mixture the total weighing error was 2.0×10^{-4} mol%.

4) Inaccuracy in the relative molecular masses. Large variation can occur in nature in the $^{13}\text{C}/^{12}\text{C}$ ratio of methane. This causes the molecular weight of methane to vary by 7.5×10^{-3} mol% depending on the origin of the methane. For the seven-component calibration gas mixture referred to above the total error caused by the uncertainty in the relative molecular masses is 8.2×10^{-3} mol%. Surprisingly, the inaccuracy in the relative molecular masses seems to be the largest error in the gravimetric preparation method of multi-component calibration gas mixtures.

Finally the conclusion can be drawn that in a 2-L high pressure gas cylinder, multi-component calibration gas mixtures can be prepared by a gravimetric method with a total error smaller than 0.01 mol% (total uncertainty of less than 0.5% relative [78]). In this conclusion the systematic errors of the gravimetric preparation method have not been taken into account. In practice this certainly means that the total error will be larger, depending on how correctly the preparation procedures will be followed.

1.5.2. Calibration Mixtures for Sulfur Components

In general, volatile sulfur compounds are very active, highly toxic and odorous. Furthermore, the analysis of sulfur components is only of importance for a limited number of companies. For these reasons calibration mixtures of sulfur compounds have never been "commercialized", this in contrast to the hydrocarbon

calibration gas mixtures described above. There are several methods for the preparation of sulfur calibration gas mixtures for use in laboratory experiments.

The choice of the materials coming into contact with the sulfur species is very important due to the reactivity of sulfur gases. Stability tests were conducted by Bishop *et al.* [82] on natural gas with high concentrations of sulfur components stored in Teflon, rubber, polyethylene, polypropylene and stainless steel containers. The following results were achieved. Mercaptans stored in all systems except Teflon and stainless steel suffered severe dissipation within two hours. Mercaptans stored in Teflon containers experienced less than 20% dissipation in 14 to 18 hours. In steel cylinders the mercaptans were found to dissipate substantially within the first day, with a very strong dissipation probably within the first few hours. Based on these results, the long-term storage of sulfur containing gases is apparently not feasible [82].

The *single rigid chamber* is a simple, easy to use mixing device. A known amount of the compound of interest is introduced into a single rigid chamber of known dimensions. A magnetic stirrer or a similar device is used for homogeneous mixing. The concentration of the standard mixture produced is given by equation 1.1.

$$C = C_0 \exp\left(-\frac{V_W}{V}\right) \quad (1.1)$$

C instantaneous concentration,
 C_0 initial concentration,
 V container volume,
 V_W volume of sample withdrawn.

Tangerman *et al.* [12] prepared gaseous standards for daily calibration in 15-mL glass sample vials. Ethylmercaptan (EtSH), DMS, and DMDS were injected into these vials as liquids (10 μL of each), while H_2S and MeSH were added in the gaseous state (2.5 μL at 20°C). In further experiments [13] Tangerman used this procedure for the preparation of sulfur gas standard samples. Unfortunately, no concrete statistical evaluations, *e.g.* accuracy of the method were reported.

The *exponential dilution flask*, shown in Figure 1.15A [83], is a hybrid static/dynamic system. A known amount of a pure component or a standard mixture is introduced into the vessel, which is stirred for efficient mixing. The vessel is continuously flushed with a steady stream of pure gas causing the

concentration of the vapour to decrease with time. This simple, reliable device is commercially available and has been widely used. It produces an outlet concentration described by equation 1.2.

$$C = C_0 \exp\left(-\frac{Qt}{V}\right) \quad (1.2)$$

Q volumetric gas flow rate,
 t time after sample introduction.

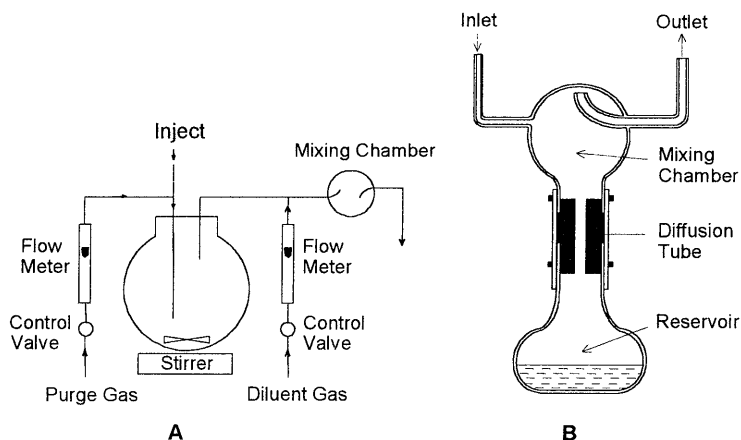


Figure 1.15: Apparatus for preparing standard mixtures of organic vapours. A - Exponential dilution flask; B - Diffusion tube system. Reprinted with permission granted by Elsevier Science Publishers BV from "Contemporary Practice of Chromatography" by C. F. Poole and S. A. Schuette, Elsevier Pub., Amsterdam, The Netherlands, 1984, p. 485.

The exponential dilution flask suffers from a number of principal problems such as losses by surface adsorption, mechanical wear of the mixing device, and the difficulty of accurately measuring the initial sample concentration. However, it is capable of providing adequate accuracy and precision for most of the analytical applications involving readily volatilized substances. Very low gas phase concentrations can be prepared by mixing the output from the flask with diluent gas.

De Souza [23] diluted standard high purity gases in both glass bottles or exponential flasks coated with Siliclad in order to passivate the flask towards the reactive sulfur gases. Nitrogen was used as the dilution gas. Standard mixtures of

sulfur compounds in CO₂ at ppb levels were prepared by Pick [25] using the exponential dilution apparatus. This apparatus consists of a 1.2 L glass flask with a large Teflon-coated magnetic stirrer bar which was rotated at maximum speed. Initial dilutions of the sulfur compounds were made up in glass vessels fitted with an injection septum and a magnetic stirrer in order to give concentrations in the range of 250 to 1000 ppm. Diluted samples were then injected into the CO₂ stream flowing into the exponential dilution flask to give concentrations between 50 and 1000 ppm. By using various initial concentrations the efficiency of the mixing process was checked and found to be satisfactory. However, the CO₂ flow rate could not be measured to an accuracy greater than ± 1 mL/min; therefore, in order to keep the error arising from flow measurements below *ca.* $\pm 3\%$ the contents of the exponential dilution flask were never diluted by more than a factor of 20.

Diffusion systems such as those described in Figure 1.15B [83], are useful and simple devices for preparing mixtures of volatiles and moderately volatile vapours in a gas stream. The method is based on the constant diffusion of a vapour from a tube of accurately known dimensions, producing a gas phase concentration described by equation 1.3 [83].

$$S = \frac{DMPA}{RTL} \ln \left(\frac{P}{P-p} \right) \quad (1.3)$$

- S* diffusion rate of vapour out of tube,
D diffusion coefficient,
M molecular weight,
P pressure in the diffusion cell,
A cross-sectional area of the diffusion tube,
R gas constant,
T temperature,
L length of the diffusion tube,
p partial pressure of the diffusing vapour at the outlet of the diffusion tube.

Within limits, broad concentration ranges can be prepared by varying the tube dimensions and/or the flow rate of the diluent gas.

Permeation tube devices are now very popular for generating standard vapor concentrations. The permeation tube contains a volatile liquid sealed in an inert permeable membrane, usually Teflon or a fluorinated copolymer of ethylene and propylene, through which the test compound diffuses at a fixed rate. The driving

force behind the process is the difference in partial pressures between the inner and outer walls of the tubes. This depends on the dissolution of the vapour in the membrane, the rate of diffusion through the membrane wall, and the rate at which the vapour is removed from the outer surface of the membrane. The mass permeation rate per unit tube length can be expressed by equation 1.4 [83], assuming that the membrane is in contact with the gaseous phase only.

$$G = \frac{730 PM}{\log\left(\frac{d_2}{d_1}\right)} \times P_1 \quad (1.4)$$

- G mass permeation rate in $\mu\text{g}/\text{min}$ per cm of tube length,
 P permeation constant for the vapour through the membrane in cm^3 ,
 M molecular weight of the vapour,
 P_1 gas pressure inside the tube in mmHg,
 d_2 outside diameter of the tube,
 d_1 inside diameter of the tube.

For samples with a low vapor pressure at room temperature, elevated temperatures are used to raise the permeation rates and to yield desirable concentration values. Gases or vapors with high membrane permeabilities require devices other than the standard single-walled tubes, *e.g.* multiple-walled tubes, microbottles, or permeation wafer devices to yield reasonable lifetimes. Commercially available permeation tubes have lifetimes of several months and provide a simple and inexpensive method of calibration for laboratories interested in determining only a few substances, or for those who need to perform measurements infrequently.

For the analysis of sulfur gases by gas chromatography, permeation devices offer an economical alternative to compressed gas standards. Moreover, the use of these devices offers a safety advantage in the handling of toxic sulfur gases while minimizing the chemical reactivity inherent to sulfide and mercaptan compounds [84]. Permeation devices are commercially available through a number of manufacturers and cover the concentration range of ppb to percent levels.

An international standardized method for the preparation of calibration gas mixtures by the permeation method is available: ISO 6349 - Gas Analysis - Preparation of Calibration Gas Mixtures - Permeation Method. The concentration C of the calibration gas mixture so prepared is a function of the diffusion rate of the tube and the flow rate of the complementary gas. It is given by the formula:

$$C = \frac{Q_m}{Q_V} \tag{1.5}$$

Q_m permeation rate in $\mu\text{g}/\text{min}$,
 Q_V sweeping flow rate in m^3/min .

Some examples of permeation tubes and permeation apparatus made in different laboratories are given in Figures 1.16 and 1.17. The use of a thermostatic device is essential to control the temperature of the bath to within 0.1°C because the tube diffusion rate may double at an increase in temperature of approximately 7°C . The accuracy of the concentration obtained depends on the knowledge of two parameters: the diffusion rate of the permeation tube and the flow rate of the complementary gas. In general it is within 5%.

The permeation rates are usually calibrated gravimetrically [85,86]. Primary calibration of a liquid-filled tube can be obtained by collecting weight data (losses) over a period of days, weeks, or months. Between weighing, the tube should be stored in a chamber maintained at a constant temperature ($\pm 0.1^\circ\text{C}$) and at low humidity (silica gel desiccant).

Common dilution gases are air [4,10,35], argon [7], helium [16] and nitrogen [24,26], which of course should be free of sulfur.

De Souza *et al.* [87] developed a calibration system for measuring the total reduced sulfur and SO_2 concentrations in ambient air. The system is based on the use of permeation tubes coupled with an exponential dilution flask. Reproducible calibration curves (log-log scale) were obtained for the concentration range of 1 to 100, 0.3 to 5, and 0.1 to 1 ppb SO_2 with $\pm 5\%$ relative error for eight determinations. However, only the calibration curve for the 0.3 to 5 ppb range

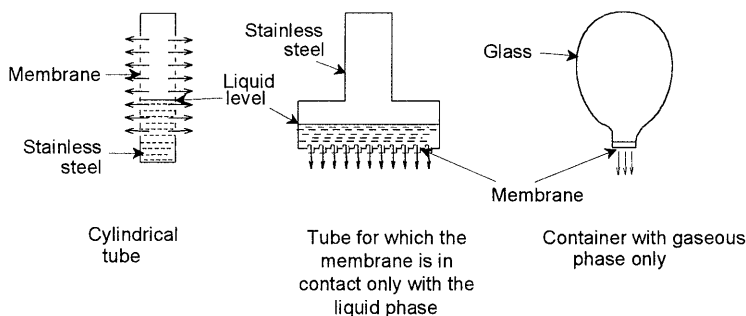


Figure 1.16: Examples of permeation devices.

was straight, while that of the 1 to 100 ppb range showed a slight deviation at the lower end and that for the 0.1 to 1.0 ppb range showed slight curvature throughout. For the calibration of six individual sulfur compounds, straight-line log-log calibration curves from 5 to 100 ng were obtained with slopes of

2.15, 1.87, 1.06, 2.26, 1.71, and 1.14 for H_2S , COS , SO_2 , CH_3SH , DMS , and DMDS , respectively. The low slope values for SO_2 and DMDS could be due to the very active nature of SO_2 and the heavy nature of the DMDS ; hence partial losses in the packing material of the sample preconcentrator might occur.

The G-Cal tube [84] is a commercially available permeation device which possesses sufficient thermal stability to permit usage without thermostatic control. The G-Cal device exhibits a 1-3%/°C change in permeation rate near ambient temperatures. To generate multi-component gas standards the permeation tubes can be hooked in series. The analyses of calibration mixtures containing 0.87 ppm of DMS and 1.30 ppm of MeSH represent a relative deviation of 2%, which is typically within the error limits expected from conventional permeation devices [86].

From the literature study described in this chapter it can be concluded that for the accurate calibration during the analysis of volatile sulfur compounds permeation tubes or diffusion devices are the best choice. However, for the "gross" determination of these components, when the demand posed on the accuracy is not so critical, a simple single rigid chamber is satisfactorily as well. In general, the use of gravimetrically prepared calibration gas mixtures yields a better repeatability and accuracy than these devices. For the particular case of sulfur components, however, it appears that this conclusion is no longer valid. The strong adsorptivity of sulfur components give rise to adsorption losses and hence, calibration errors unless special precautions, *e.g.* Teflon passivation of the inner wall, are taken. With higher boiling sulfur compounds such as EtSH and its higher

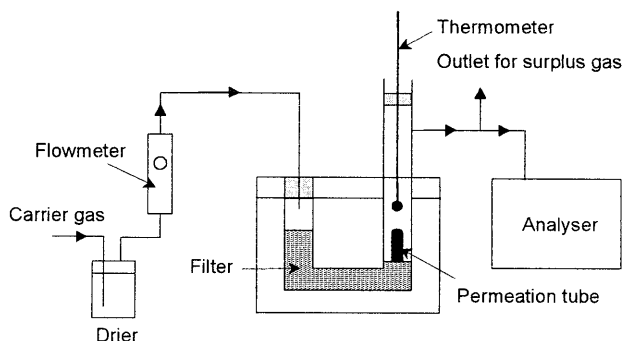


Figure 1.17: Example of a permeation system for the preparation of calibration standards.

homologes calibration solutions can be made in for example hexane. These mixtures should be stored in a refrigerator.

1.6. CONCLUSIONS

The determination of sulfur containing components in natural gas is a typical example of trace analysis in a complex and interfering matrix. Gas chromatography has proven to be an extremely useful technique for this difficult analytical problem. In order to obtain the maximum possible performance, each of the three steps of the analytical procedure, *i.e.* sample preparation, separation, and detection has to be carefully optimized and fine-tuned to meet the requirements of the other two steps of the procedure. In this respect the choice of the detector plays a key role. Despite tremendous progress in the field of especially flame photometric and sulfur chemiluminescence detection, at present no detector is available that provides the selectivity and sensitivity required to keep pace with the ever more stringent demands currently being imposed on sulfur detection limits and analytical accuracy. Optimized chromatographic separations have to be incorporated in the analytical procedure. Due to their high resolving power capillary columns are to be preferred over the classical packed columns. The sensitivity of the analytical system can be improved by preconcentration of the sulfur components on a suitable solid adsorbent prior to transfer of the sample on to the chromatographic column. Polar adsorbents appear highly promising as these materials could provide selective enrichment of the components of interest. For calibration of GC-based analytical techniques for sulfur determination in natural gas, dynamically generated calibration standards appear to be more reliable than statically prepared standards. Adsorption losses which are unavoidable in static calibration, are significantly lower or often even fully absent in dynamic system such as permeation or diffusion devices.

REFERENCES

1. A. L. C. Smit and E. Meijer, Proceedings of the Congress of "*Gas Quality - Specification and Measurement of Physical and Chemical Properties of Natural Gas*", Groningen, The Netherlands, 22 - 25 April 1986, Elsevier, Amsterdam, The Netherlands, 1986, p. 589.
2. ISO 6326 - 1 (E): International Standard: "*Natural Gas - Determination of Sulfur Compounds*" Part 1: "*General Introduction*", Geneva, Switzerland, 1989.

3. D. F. S. Natusch, H. B. Klonis, H. D. Axelrod, R. J. Teck, and J. P. Lodge, Jr., *Anal. Chem.*, 44 (1972) 2067.
4. H. D. Axelrod and S. G. Hansen, *Anal. Chem.*, 47 (1975) 2460.
5. P. W. West and G. C. Gaeke, Jr., *Anal. Chem.*, 28 (1956) 1816.
6. R. S. Braman, J. M. Ammons, and J. L. Bricker, *Anal. Chem.*, 50 (1978) 992.
7. R. A. Kagel and S. O. Farwell, *Anal. Chem.*, 58 (1986) 1197.
8. S. O. Farwell, D. P. Liebowitz, R. A. Kagel, and D. F. Adams, *Anal. Chem.*, 52 (1980) 2370.
9. M. S. Black, R. B. Herbst, and D. R. Hitchcock, *Anal. Chem.*, 50 (1978) 848.
10. P. A. Steudler and W. Kijovski, *Anal. Chem.*, 56 (1984) 1432.
11. A. Przyjazny, *J. Chromatogr.*, 333 (1985) 327.
12. A. Tangerman, M. T. Meuwese-Arends, and J. H. M. van Tongeren, *Clinica Chimica Acta*, 130 (1983) 103.
13. A. Tangerman, *J. Chromatogr.*, 366 (1986) 205.
14. J. J. Henatsch and F. Jüttner, *J. Chromatogr.*, 445 (1988) 97.
15. A. R. Bandy, B. J. Tucker, and P. J. Maroulis, *Anal. Chem.*, 57 (1985) 1310.
16. F. Caron and J. R. Kramer, *Anal. Chem.*, 61 (1989) 114.
17. S. O. Farwell, S. J. Gluck, W. L. Bamesberger, T. M. Schutte, and D. F. Adams, *Anal. Chem.*, 51 (1979) 609.
18. R. K. Stevens, J. D. Mulik, A. E. O'Keeffe, and K. J. Krost, *Anal. Chem.*, 43 (1971) 827.
19. F. Bruner, B. Cicciooli, and F. Di Natra, *Anal. Chem.*, 47 (1975) 141.
20. D. Suier and A. Hill, *J. Chromatogr. Sci.*, 20 (1982) 429.
21. T. L. C. de Souza, D. C. Lane, and S. P. Bhatia, *Anal. Chem.*, 47 (1975) 543.
22. C. A. Burgett, "The Rapid Determination of H_2S , CO_2 and SO_2 by Gas Chromatography", Hewlett-Packard Application Note ANGC5-75, Hewlett-Packard Company, Avondale, Pennsylvania, 1975.
23. T. L. C. de Souza, *J. Chromatogr. Sci.*, 22 (1984) 470.
24. C. D. Pearson, *J. Chromatogr. Sci.*, 14 (1974) 154.
25. M. E. Pick, *J. Chromatogr.*, 171 (1979) 305.
26. B. J. Ehrlich, R. C. Hall, R. J. Anderson, and H. G. Cox, *J. Chromatogr. Sci.*, 19 (1981) 245.
27. V. B. Stein and R. S. Narang, *Anal. Chem.*, 54 (1982) 991.
28. J. L. Genna, W. D. McAninch, and R. A. Reich, *J. Chromatogr.*, 238 (1982) 103.
29. P. Ronkainen, J. Densiow, and O. Leppänen, *J. Chromatogr. Sci.*, 11 (1973) 384.
30. K. J. Rygie, G. P. Feulmer, and R. F. Scheideman, *J. Chromatogr. Sci.*, 22 (1984) 514.
31. A. H. H. Tameesh, A. O. Bender, and T. M. Sarkissian, *J. Chromatogr.*, 321 (1985) 59.
32. P. A. Gibbons, *Chromatographia*, 19 (1984) 254.
33. L. Blomberg, *J. Chromatogr.*, 125 (1976) 389.
34. C. J. Barinaga and S. O. Farwell, *J. High Resolut. Chromatogr. & Chromatogr. Commun.*, 9 (1986) 388.
35. C. J. Barinaga and S. O. Farwell, *J. High Resolut. Chromatogr. & Chromatogr. Commun.*, 10 (1987) 538.
36. S. Jacobsson and O. Falk, *J. Chromatogr.*, 479 (1989) 194.
37. K. K. Gaines, W. H. Chatham, and S. O. Farwell, *J. High Resolut. Chromatogr.*, 11 (1990) 585.
38. F. Russo and F. Maghini, Proceedings of the Congress of "Gas Quality -Specification and Measurement of Physical and Chemical Properties of Natural Gas", Groningen, The Netherlands, 22 - 25 April 1986, Elsevier, Amsterdam, The Netherlands, 1986, p. 633.

39. S. E. A. Monks, Proceedings of the Congress of "Gas Quality - Specification and Measurement of Physical and Chemical Properties of Natural Gas", Groningen, The Netherlands, 22 - 25 April 1986, Elsevier, Amsterdam, The Netherlands, 1986, p. 641.
40. H. Obbens and L. Huber, Proceedings of the Congress of "Gas Quality - Specification and Measurement of Physical and Chemical Properties of Natural Gas", Groningen, The Netherlands, 22 - 25 April 1986, Elsevier, Amsterdam, The Netherlands, 1986, p. 649.
41. D. Jentzsch and E. Otte, "Methoden der Analyse in der Chemie" band 14: "Detektoren in der Gas-chromatographie", Akademische Verlagsgesellschaft, Frankfurt am Main, Germany, 1970.
42. J. Sevcik, *J. Chromatogr. Lib.*, Vol. 4 - *Detectors in Gas Chromatography*, Elsevier Pub., Amsterdam, The Netherlands, 1976.
43. M. Dressler, *J. Chromatogr. Lib.*, Vol. 36 - *Selective Gas Chromatographic Detectors*, Elsevier Pub., Amsterdam, The Netherlands, 1986.
44. H. V. Drushel, *J. Chromatogr. Sci.*, 21 (1983) 375.
45. W. Wardencki and B. Zygmund, *Anal. Chim. Acta.*, 255 (1991) 1.
46. S. S. Brody and J. E. Chaney, *J. Gas Chromatogr.*, 4 (1966) 42.
47. S. O. Farwell and C. J. Barinaga, *J. Chromatogr. Sci.*, 24 (1986) 483.
48. P. L. Patterson, R. L. Howe, and A. Abu-Shumays, *Anal. Chem.*, 50 (1978) 339.
49. M. Dyson, *Anal. Proceed.*, 30 (1993) 79.
50. A. R. Baig, C. J. Cowper, and P. A. Gibbons, *Chromatographia*, 16 (1982) 297.
51. J. Efer, T. Maurer, and W. Engewald, *Chromatographia*, 29 (1990) 115.
52. G. H. Liu and P. R. Fu, *Chromatographia*, 27 (1989) 159.
53. J. Zehner and R. Simonaitis, *J. Chromatogr. Sci.*, 12 (1976) 348.
54. W. A. Aue and C. G. Flinn, *J. Chromatogr.*, 158 (1978) 161.
55. T. Cardwell and P. Marriot, *J. Chromatogr. Sci.*, 20 (1982) 3017.
56. J. Sevcik and N. Phuong Thao, *Chromatographia*, 8 (1975) 559.
57. W. A. Aue, X.-Y. Sun, and B. Millier, *J. Chromatogr.*, 606 (1992) 73.
58. W. A. Aue and X.-Y. Sun, *J. Chromatogr.*, 633 (1993) 151.
59. W. A. Aue and X.-Y. Sun, *J. Chromatogr.*, 641 (1993) 291.
60. U. Schurath, M. Weber and K. H. Becker, *J. Chem. Phys.*, 67 (1977) 110; p. 112. Fig. 2B.
61. J. N. Driscoll and A. W. Berger, *J. Chromatogr.*, 468 (1989) 303.
62. S. Cheskis, E. Atar, and A. Amirav, *Anal. Chem.*, 65 (1993) 539.
63. J. V. Headley, *Biomed. Environ. Mass Spectrom.*, 14 (1987) 275.
64. J. Guieze, G. Devant, and D. Loyaux, *Int. J. Mass Spectrom. Ion Phys.*, 46 (1983) 313.
65. M. Moini, D. Chace, and F. P. Abramson, *J. Am. Soc. Mass Spectrom.*, 2 (1991) 250.
66. N. V. Agadzhanova, N. K. Lyapina, R. B. Alieva, V. S. Shmakov, and M. A. Parfenova, *Neftechimiya*, 26 (1986) 132.
67. N. V. Agadzhanova, N. K. Lyapina, R. B. Alieva, V. S. Shmakov, and M. A. Parfenova, *Neftechimiya*, 23 (1983) 424.
68. Kh. Khaitbaev, E. S. Brodskii, and S. L. Gusinskaya, *Dokl. Akad. Nauk Uzb. SSR*, 31 (1974) 26.
69. R. D. Obolentsev, T. I. Allilueva, G. V. Galeeva, R. P. Kruglyakova, S. S. Krivolapov, and I. M. Salimareeva, *Khim. Serrorg. Soedin., Soderzh. Neftiyakh Nefteprod.*, 9 (1972) 364.
70. R. D. Obolentsev, S. S. Krivolapov, T. I. Allilueva, G. V. Galeeva, V. S. Kaneva, R. P. Kaneva, and N. N. Lyushina, *Khim. Serrorg. Soedin. Soderzh. Neftiyakh Nefteprod.*, 8 (1968) 341.

71. Z. Schultheisz, S. Iglewski, M. Kantor, and E. Kerényi, *Magy. Asvanyolaj Foldgaz Kiserl. Intez. Kozlem.*, 10 (1969) 31.
72. I. Schultheisz, M. Kantor, K. Belafi, P. Szepesvary, and E. Kerényi, *Chromatographic and Spectrometric Study of Sulfur Compounds Of Cracked Gasolines*, paper pres. at Con. Chem. Chem. Process. Petrol. Natur. Gas, Budapest, 1965, p. 605.
73. J. E. Johnson and J. E. Lovelock, *Anal. Chem.*, 60 (1988) 812.
74. S. E. Eckert-Tilotta, S. B. Hawthorne, and D. J. Miller, *J. Chromatogr.*, 591 (1992) 313.
75. R. C. Mitchner, S. Nacson, and J. Wallace, *A portable GC analyzer for on-site analysis of natural gas odorant levels*, Paper pres. at IGT Gas Quality Symp. (June 12-13.1989), Chicago, Ill., USA.
76. R. G. Schiller and R. B. Bronsky, *J. Chromatogr. Sci.*, 15 (1977) 541.
77. F. Lindqvist, *J. High Resolut. Chromatogr.*, 12 (1989) 628.
78. E. E. Hughes, Proceedings of the Congress of "Gas Quality - Specification and Measurement of Physical and Chemical Properties of Natural Gas", Groningen, The Netherlands, 22 - 25 April 1986, Elsevier, Amsterdam, The Netherlands, 1986, p. 675.
79. J. C. Miller and J. N. Miller, *Statistics for the Anal. Chem.*, Ellis Horwood Ltd., 3rd Ed., West Sussex, England, 1993.
80. Internal publication: *Lab. Info. Bulletin No. 37*. NV Nederlandse Gasunie, Groningen, The Netherlands.
81. M. Koning and G. J. van Rossum, Proceedings of the Congress of "Gas Quality - Specification and Measurement of Physical and Chemical Properties of Natural Gas", Groningen, The Netherlands, 22 - 25 April 1986, Elsevier, Amsterdam, The Netherlands, 1986, p. 683.
82. H. K. Bishop, J. R. Bricarello, *Odorant Identification and Measurement in Natural Gas by Gas Chromatography*, AGA paper pres. at Distrib/Trans Conference, Boston, (1985) 601-605.
83. C. F. Poole and S. A. Schuette, *Contemporary Practice of Chromatography*, Elsevier Pub., Amsterdam, The Netherlands, p. 485, 1984.
84. D. G. Flowers, *Ind. Eng. Chem. Res.*, 29 (1990) 1565.
85. A. E. O'Keeffe and G. C. Ortman, *Anal. Chem.*, 38 (1966) 760.
86. F. P. Scaringelli, A. E. O'Keeffe, E. Rosenberg, and J. P. Bell, *Anal. Chem.*, 42 (1970) 871.
87. T. L. C. de Souza and S. P. Bhatia, *Anal. Chem.*, 48 (1976) 2234.

Chapter 2

DETECTORS FOR SULFUR ANALYSIS¹

ABSTRACT

In this chapter, the performance of a number of commercially available, selective as well as universal, detectors that can be used in the analysis of sulfur components in natural gas is evaluated in terms of sensitivity, selectivity, reproducibility, quenching effect, stability, and compound dependence of the sulfur response. Investigated detectors include the sulfur chemiluminescence, the flame photometric, the pulsed flame photometric, the atomic emission, the electron capture, the mass spectrometric, the thermal conductivity, and the flame ionization detector. The sulfur chemiluminescence detector was found to have the best overall performance, e.g., low picogram amounts of sulfur can be detected accurately and the linear dynamic range is more than five orders of magnitude. After careful optimization, the sulfur response of this detector was found to be almost compound independent. All other detectors, including the flame photometric and the electron capture detector, have more or less compound dependent responses.

¹ Partially published as "Evaluation of the Performance of Various Universal and Selective Detectors for Sulfur Determination in Natural Gas" by H. Pham Tuan, H.-G Janssen, C.A. Cramers, E. M. Kuiper-van Loo and H. Vlap in *J. High Resol. Chromatogr.*, 18 (1995) 333-342.

2.1. INTRODUCTION

In the development of gas chromatographic systems for sulfur determination the choice of the detector plays a key role as this determines the demands that have to be posed on sample pretreatment and chromatographic separation. Selective detection enables target compounds to be measured while other coeluting compounds are not sensed. If a truly selective detector is employed, it is sufficient if the sulfur components are separated from each other. A complete separation of the sulfur species from the hydrocarbons is not required. In this respect universal detectors such as the thermal conductivity detector (TCD) or the flame ionization detector (FID) behave clearly different. If these detectors are being used, high demands have to be posed on the chromatographic separation. All non-sulfur containing components such as alkanes have to be separated from the sulfur species as otherwise incorrect peak areas would be obtained. These non-selective detectors would yield peaks not only for the sulfur containing components but also for the alkanes present in the gas sample. Alternatively, it is possible to remove the interfering hydrocarbons in a selective pretreatment step. Ideally, only the sulfur components from a large volume of gas are introduced into the GC column, while the hydrocarbons are eliminated prior to transfer of the sample to the GC column.

The ideal detector for sulfur determination in natural gas would be a detector that has a sensitivity sufficiently high to yield the required detection limits at a sample size of some 0.1 to 1 mL. This volume of sample can be introduced easily into a capillary GC column without the need to employ refocusing techniques. Apart from being sufficiently sensitive, the ideal detector should also have an infinite sulfur-*over*-hydrocarbon selectivity. In this way one can be sure that a high concentration of a hydrocarbon is not accidentally identified as a sulfur-containing component. In addition to this, the ideal detector is free of quenching which means that the peak area of a sulfur compound is not affected by coelution with other non-sulfur containing species. Finally, the ideal detector is easy to use, stable, reliable, and preferably inexpensive. To investigate to what extent the various (sulfur selective) detectors meet the requirements for being an ideal detector, the performance of six detectors was studied in detail. From the reasoning outlined above it is clear that especially the sensitivity, the selectivity and the amenability to quenching are important parameters when investigating

the possibilities and limitations of the various potential detectors for sulfur analysis.

In this chapter the performance of a number of sulfur selective as well as universal detectors is evaluated experimentally. The detectors included in the experimental evaluation are the Sulfur Chemiluminescence Detector (SCD), the Flame Photometric Detector (FPD), the Thermal Conductivity Detector (TCD), the Pulsed-Flame Photometric Detector (PFPD), the Atomic Emission Detector (AED), and the Mass Spectrometric Detector (MSD). The detectors were evaluated with regard to the following points: sensitivity, sulfur-*over*-carbon selectivity, linearity, long- and short-term repeatability, quenching behavior and the compound dependence of the sulfur response.

2.2. DETAIL PROCEDURES FOR THE EVALUATORY STUDIES

2.2.1. Sensitivity

To evaluate the sensitivities of the various detectors, known volumes of the (liquid) test mixture that contained accurately known concentrations of the different sulfur species were injected. The sensitivity was then expressed in terms of the minimum detectable amount (*MDA*) here defined as the amount of sulfur that gives a peak with a signal-to-noise ratio of three. The *MDA* was calculated from the following equation:

$$MDA = \frac{3h_{bl}}{h_s} \cdot m_s \quad (2.1)$$

MDA minimum detectable amount in pg S,
h_{bl} noise level in mV (peak-to-peak),
h_s peak height of a sulfur compound in mV,
m_s amount of sulfur injected that gives a peak with height *h_s*, expressed in pg S.

The detection limit (*DL*) was calculated using the following equation:

$$DL = \frac{MDA \cdot 2.354}{\sqrt{2\pi} \cdot w_{1/2}} \quad (2.2)$$

DL detection limit expressed in pg S/sec,
w_{1/2} average peak width at half height in sec.

2.2.2. Sulfur-over-Carbon Selectivity

The sulfur-over-carbon selectivity is here defined as the ratio of the amounts of carbon over sulfur required to yield equal peak areas for a sulfur containing component and a hydrocarbon. The sulfur component considered in these studies was tetrahydrothiophene (THT). Nonane was used as the hydrocarbon. For the calculation of the sulfur-over-carbon selectivity the following equation was used:

$$S_{S/C} = \frac{m_C}{m_S} \cdot \frac{A_S}{A_C} \quad (2.3)$$

$S_{S/C}$	sulfur-over-carbon selectivity,
m_S	injected amount of THT expressed in ng S,
m_C	injected amount of <i>n</i> -nonane expressed in ng C,
A_S	peak area of THT,
A_C	peak area of <i>n</i> -nonane.

2.2.3. Linearity

In order to evaluate the linearity of the various detectors, calibration lines were constructed in which the peak areas observed were plotted *versus* the amount injected or the concentration of the sulfur components in the standard solutions. Here the concentration was expressed as weight of sulfur per volume unit. The linear dynamic range (*LDR*) was then calculated from:

$$LDR = \log \left(\frac{c_{\max}}{c_{\min}} \right) \quad (2.4)$$

Where c_{\min} is the minimum detectable concentration in the sample and c_{\max} represents the concentration at the end of the linear range. Equation 2.4 yields the *LDR* in decades.

2.2.4. Long- and Short-term Repeatability

The short-term repeatability was calculated from the peak area observed in a minimum of five replicate measurements and expressed in the relative standard deviation (RSD) of the peak areas. The long-term repeatability was calculated from the slopes of the calibration lines measured on three consecutive days. Due to the stability problems of the sample used (evaporation and adsorption) new standards had to be prepared freshly everyday. Again the data were expressed as RSDs.

2.2.5. Quenching Behavior

Even though a truly selective detector does not respond to non-sulfur containing components, its response can be affected by coelution of the sulfur-containing component with a sulfur-free species. This effect is called quenching. In order to study whether quenching occurs for the various detectors a situation of coelution of a sulfur component with a hydrocarbon was created deliberately. In the present study this situation was created in two different ways. Adding an alkane to the fuel gas supply of the detector created a continuous hydrocarbon background. The second method was based on deliberately selecting chromatographic conditions under which a sulfur component and an alkane (both present in the sample) coeluted. The quenching effect was then calculated as the carbon-*over*-sulfur ratio which resulted in an 50% reduction of the sulfur signal in comparison with the situation in which there was no coelution.

2.2.6. Compound Dependence of the Sulfur Response

Whether or not the response of the detector for sulfur depended on the structure of the molecule in which the sulfur atom was present was investigated from the slopes of the calibration lines of the various sulfur components present in the sample (see section 2.2.3).

2.3. EXPERIMENTAL

2.3.1. Chemicals

All pure liquid sulfur compounds except tetrahydrothiophene (THT), dimethylsulfide (DMS) and carbon disulfide (CS₂) were purchased from Polyscience (Niles, Illinois, USA). THT was bought from Aldrich (Milwaukee, Wisconsin, USA), DMS from Janssen Chimica (Beerse, Belgium) and CS₂ from Merck (Darmstadt, Germany). The main characteristics of these compounds such as their purities, boiling points, *etc.* are listed in Table 2.1. Because of the limited range of sulfur components that possibly occur in natural gas, higher boiling sulfur compounds were not taken into consideration.

Stock solutions of sulfur compounds in hexane (Merck, p.a.), cyclohexane (Merck, p.a.), and *n*-nonane (Janssen, p.a.), respectively, were prepared gra-

vimetrically in narrow-neck glass flasks to minimize vaporization of volatile sulfur components and were stored in a refrigerator. Working standard solutions in *n*-nonane were gravimetrically prepared freshly every day in small glass flasks.

Table 1.1: Main characteristics of liquid sulfur compounds.

compound	abbrev.	mol. wt.	boil. point (°C)	purity (%)
ethylmercaptan	EtSH	62.13	35.0	97.11
dimethyl sulfide	DMS	62.13	37.3	97.77
carbon disulfide	CS ₂	76.14	46.3	99.95
<i>iso</i> -propylmercaptan	<i>i</i> -PrSH	76.16	52.6	96.24
<i>tert</i> -butylmercaptan	<i>t</i> -BuSH	90.19	64.2	98.41
<i>n</i> -propylmercaptan	<i>n</i> -PrSH	76.16	67.5	98.24
<i>sec</i> -butylmercaptan	<i>s</i> -BuSH	90.19	85.0	98.28
<i>iso</i> -butylmercaptan	<i>i</i> -BuSH	90.19	88.7	98.83
diethyl sulfide	DES	90.19	92.1	97.91
<i>n</i> -butylmercaptan	<i>n</i> -BuSH	90.19	98.5	98.30
tetrahydrothiophene	THT	88.17	119.0	99.82

2.3.2. Instrumental set-up

GC: HP 5890A Hewlett-Packard (Avondale, PA, USA); oven temperature program: 30°C (5 min) to 150°C at a rate of 15°C/min in the case of MS detection and of 20°C/min in the case of the other detection techniques;

PTV: KAS II (Gerstel, Mülheim a/d Ruhr, Germany); empty deactivated glass liner; injection technique: cold splitless, injection volume: 1 µL of liquid solutions, splitless time: 1 min; temperature program: 30°C to 250°C at 12°C/sec;

Column: 35 m × 0.32 mm × 1.1 µm CP Sil-5 CB (Chrompack, Middelburg, The Netherlands);

Carrier gas: Helium, column head pressure 10 psi, column flow 1.6 mL/min, total flow rate 100 mL/min;

Cryotrap: DKK Cryofocuser (Atas, Veldhoven, The Netherlands) using gaseous CO₂ at 50 bars, restrictor 8 cm × 250 µm i.d. stainless steel inserted into a 60 cm × 3 mm i.d. PTFE tube; focusing time 1.75 min;

Detectors: Six detectors were included in the experimental work. A Sievers SCD 350B was purchased from Gerstel Benelux B.V. (Brielle, the Netherlands). The SCD was installed on the FID of the HP 5890 GC. Two modifications were

made to this FID: firstly, the capillary flame tip of the FID was replaced by a packed-column flame jet, and secondly, to allow higher hydrogen flow rates, the make-up gas line was used to supply additional hydrogen. The FPD was a Unicam 4600/04 FPD installed on a Unicam 4600 GC (Cambridge, UK). For mass spectrometric detection an HP 5970B MSD. The helium purge gas flow rate was set at 0.5 mL/min. The temperature of the interface was 200°C. TCD experiments were performed on a Gow Mac TCD (Clare, Ireland) installed in a Varian 3400 GC. Helium was used as the make-up gas for both the analytical and reference channel with a flow rate of 30 mL/min. The detector temperature was set at 200°C, the filament temperature at 300°C. The operating range was 0.05 mV with attenuation 1. Because the FPD and the TCD were installed in separate gas chromatographs, a transfer line was used to lead the compounds eluted from the analytical column to the detector. In case of the FPD the transfer line was a 10 m × 0.32 mm × 0.2 μm OV-1 column coupled to the analytical column with a 0.32-0.32 glass pressfit connector purchased from Hewlett-Packard. For the TCD the last part (approximately 1 m long) of the analytical column was drawn out from the oven and led to the Varian GC where the TCD was installed. Details of the detector settings are presented in the Results and Discussion section. More details on the experimental set-ups used for the PFPD and the AED are given in section 2.5.5 and 2.5.6, respectively.

2.4. OPTIMIZATION OF THE EXPERIMENTAL CONDITIONS

For the accurate determination of detector sensitivities, accurately known amounts of the test components must be introduced onto the chromatographic column. Moreover, the solvent should not interfere with the peaks of the components of interest.

2.4.1. Choice of the Injection Technique

Because of the high volatility and wide boiling point range of the investigated sulfur compounds, introduction of known volumes is only possible using the cold splitless injection technique. Only this way it is possible to eliminate losses of components due to volatility. Therefore all experiments were performed using cold splitless injection, except those on the AED and PFPD. In the experiments on the PFPD hot splitless injection was used. For the AED experiments, hot split

injection using an autosampler was employed. This might give rise to somewhat larger variation in the amounts introduced onto the column and therefore to a somewhat poorer repeatability.

2.4.2. Choice of the Solvent

Signals of sulfur compounds can be reduced, totally lost or become undetectable in the case of co-elution with the solvent peak. To avoid this problem, *n*-nonane was chosen for subsequent experiments because it elutes after all sulfur components of interest.

2.5. RESULTS AND DISCUSSION

2.5.1. Sulfur Chemiluminescence Detector

Sulfur chemiluminescence detection is based on the reaction of SO formed during the combustion of sulfur containing species in a hydrogen rich FID flame with ozone to form electronically excited SO₂*. The SO₂* species relax afterwards by emission of light in the wavelength range of 280-420 nm. The SO is drawn into the SCD by means of a ceramic sampling probe attached to the FID flame housing and a vacuum system. In this flame-based system apart from the SCD signal also an FID signal is obtained. To facilitate the positioning of the ceramic sampling probe in the FID flame a Gerstel adjustable connector was used, which allowed placing the tip of the ceramic sampling probe exactly 4 mm above the FID jet tip. The SCD vacuum system had a pumping speed of approximately 500 mL/min. If the total flow of FID gases is under this value, air from outside will be drawn into the system thereby reducing the signal of the sulfur compounds. Therefore it is recommendable to use a total FID air- plus hydrogen flow of at least some 550 mL/min. In this way at least 90% of the FID flame gases are drawn into the SCD. Because the FID is not operated at optimum gas flow settings, the sensitivity of the FID is only about 10% of its normal value. Still this signal can be of great benefit during, for example, method development.

The SCD performance was found to be strongly dependent on the ratio of the FID air and hydrogen flow rates. Figure 2.1 shows the effects of the air/hydrogen flow-rate ratio on the experimental response factors (A) and the signal-to-noise ratios (B) of 11 investigated sulfur compounds. In general the SCD signal was

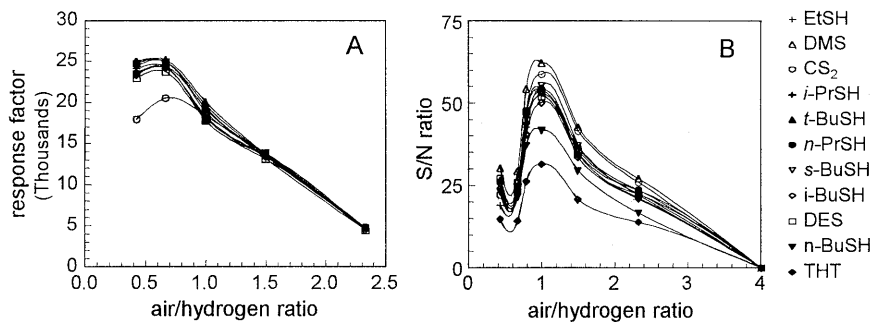


Figure 2.1: Influence of air/hydrogen flow-rate ratio on SCD performance: A) response factor = area/injected amount in pg S; B) S/N = (peak height in mV/injected amount in pg S)/noise in mV.

found to be less compound dependent at higher air/hydrogen ratios. Unfortunately, however, at these flow ratios the sensitivity is lower. The maximum sensitivity, in terms of the highest signal-to-noise ratio (S/N), was achieved with an air/hydrogen ratio of one. Under these conditions an adequate compound independent sulfur response was observed. The sulfur-over-carbon selectivity under these conditions was better than 10^6 .

Another aspect that should be taken into consideration is the lifetime of the ceramic sampling probe. The flame temperature increases significantly at higher air/hydrogen ratios and, hence, considerably shortens the lifetime of the probe. At gas flow settings of 150 mL/min for hydrogen, 250 mL/min for air and 100 mL/min for nitrogen (make-up gas) the tip of the probe was totally destroyed after approximately four weeks of continuous operation. With flow rates of 350 mL/min for hydrogen and 150 mL/min for air the ceramic probe was still fully functional after 12 weeks of continuous operation. To achieve these high hydrogen flow rates the make-up gas line was connected to the hydrogen line.

From the experimental results discussed above it is evident that the optimum SCD performance is a compromise between the sensitivity (in terms of signal and signal to noise ratio), the compound independence of the sulfur response, and the lifetime of the ceramic probe tip. All further experiments were performed at an air to hydrogen flow rate ratio of one (air flow = hydrogen flow = 250 mL/min). Under these conditions a good sensitivity was obtained and the SCD signal was virtually independent of the molecular structure of the sulfur compounds.

Figure 2.2 shows SCD calibration graphs for 11 sulfur compounds on a log-log scale. From Figure 2.2 a number of interesting conclusions can be drawn. First of all it can be seen that the SCD response is compound independent. The slopes of the calibration graphs for the various sulfur compounds range from 0.95 to 1.02. The linear dynamic range is over five orders of magnitude. The reproducibility,

based on areas of three subsequent injections, is generally in the range of 5% relative standard deviation (RSD). The detection limit, based on $S/N = 3$, is approximately 2 pg S/sec. An SCD chromatogram of 11 sulfur compounds at concentrations near the detection limits is given in Figure 2.3. As can be seen from this figure reasonable chromatograms can be obtained for picogram quantities. The long-term stability of the SCD was established by measuring the slopes of the calibration graphs of the 11 sulfur components on three consecutive days. The RSD of the absolute sensitivities was below 6%. Under the SCD settings used in the present study, large amounts of hydrocarbons give negative signals. For example the baseline drop at the end of the chromatogram in Figure 2.3 is caused by the elution of *n*-nonane, which was used as the solvent.

A first series of experiments to investigate the quenching behavior of the SCD upon coelution of sulfur compounds with large quantities of sulfur-free species was carried out by measuring the sulfur signal on a hydrocarbon background and comparing this with the signal in a system free of hydrocarbons. These experiments were performed at the optimum flow settings identified above, *i.e.* air = hydrogen = 250 mL/min. The ozone generator was operated using air as the oxygen source. A simple dynamic headspace-sampling device was used to introduce pentane, hexane or heptane vapors, respectively, into the air supply of the FID in this way mimicking the elution of sulfur compounds on a hydrocarbon

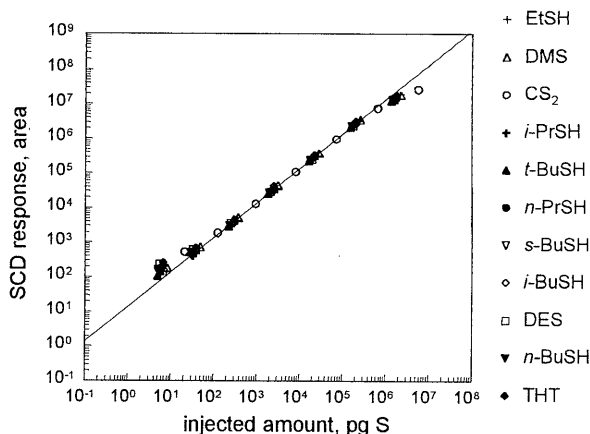


Figure 2.2: Calibration graph of sulfur compounds on the SCD. Chromatographic conditions: see Experimental.

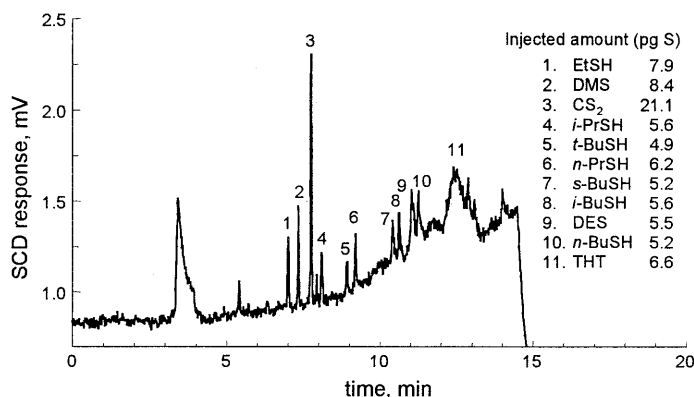


Figure 2.3: Chromatogram of sulfur compounds (picogram range) obtained using the sulfur chemiluminescence detector. Chromatographic conditions: see Experimental.

background. No significant quenching was observed with C/S ratio up to 10^5 . This result is in accordance with statements of the manufacturer claiming that the SCD is completely free of quenching. The loss of the sulfur signal when sulfur species coeluted with a hydrocarbon solvent such as cyclohexane in Figure 2.4B, however, indicates that the quenching effect on the SCD should be studied in more detail.

Quenching effects in the SCD signal are generally thought to be caused by incomplete combustion of coeluted hydrocarbons in the FID flame as well as by competitive reactions of combustion products of hydrocarbons and sulfur compounds for ozone in the reaction chamber [14]. At low air-to-hydrogen flow-rate ratios coeluting hydrocarbons will not be completely burnt in the FID flame. If now insufficient oxygen is fed into the ozone generator, the reaction of SO (combustion product of sulfur species) with ozone to form the electronically excited SO₂* will be incomplete as hydrocarbon combustion products compete with the SO for the ozone. Furthermore, if the total flow is not high enough, ambient air is likely to be drawn into the SCD reaction chamber, which in turn could also result in signal quenching. Summarizing, the parameters that could cause the SCD to show quenching, if not carefully optimized, are: *i/* air-to-hydrogen flow rate ratio; *ii/* amount of oxygen fed into the SCD ozone generator; and *iii/* total FID combustion flow rate.

In further experiments on SCD quenching, first the minimum required FID

combustion flow (air + hydrogen) was established by observing the SCD signal while injecting a gas mixture containing sulfur components directly into the FID flame housing. If a sulfur signal was observed immediately after the injection, the total flow of air and hydrogen is still too low and ambient air is drawn into the SCD. A total flow of 550 mL/min was found to be the minimum flow rate needed to prevent ambient air from entering the SCD.

To investigate the magnitude of the SCD quenching effect under non-optimized settings, chromatographic conditions were selected to create a situation in which a sulfur compound (*i*-BuSH) coeluted with a non-sulfur containing species (cyclohexane). A small amount of cyclohexane was added to a solution containing the 11 investigated sulfur compounds in *n*-nonane. To obtain true coelution of cyclohexane and *i*-BuSH the oven temperature program was changed to 30°C (3 min) to 150°C at 30°C/min. The calculated carbon-to-sulfur ratio (concentration of cyclohexane in g C/L over that of BuSH in g S/L), in case of complete coelution, was approximately 100.

Using the sample described above, the influence of the air-to-hydrogen flow rate ratio was studied. In these experiments the hydrogen flow rate was held constant at 250 mL/min while the air flow rate was gradually increased from 300 mL/min to 500 mL/min. Air was used for ozone generation in the ozone generator. The difference in response factors (peak areas divided by concentration) of *i*-BuSH and that of three other sulfur compounds eluting close to the *i*-BuSH peak (*s*-BuSH, DES, and *n*-BuSH) was found to decrease with increasing air/hydrogen ratio. Unfortunately, however, even at the highest air/hydrogen ratio quenching of the *i*-BuSH signal was not fully absent. Further increasing the air/hydrogen ratio is not recommendable because of the deleterious effects of flame temperature on the lifetime of the ceramic probe.

To investigate the influence of the amount of ozone generated in the ozone generator on the quenching behavior of the SCD, the amount of oxygen fed to the ozone generator was increased by applying a higher inlet pressure in the air supply line. No significant improvement was achieved. In a second series of experiments the air cylinder was replaced by an oxygen cylinder and the experiments described in the previous paragraph were repeated. When pure oxygen was used quenching was found to be less at all investigated FID air/hydrogen ratios. Quenching free chromatograms were obtained at an air/hydrogen ratio of two or higher. Representative chromatograms are shown in Figure 2.4.

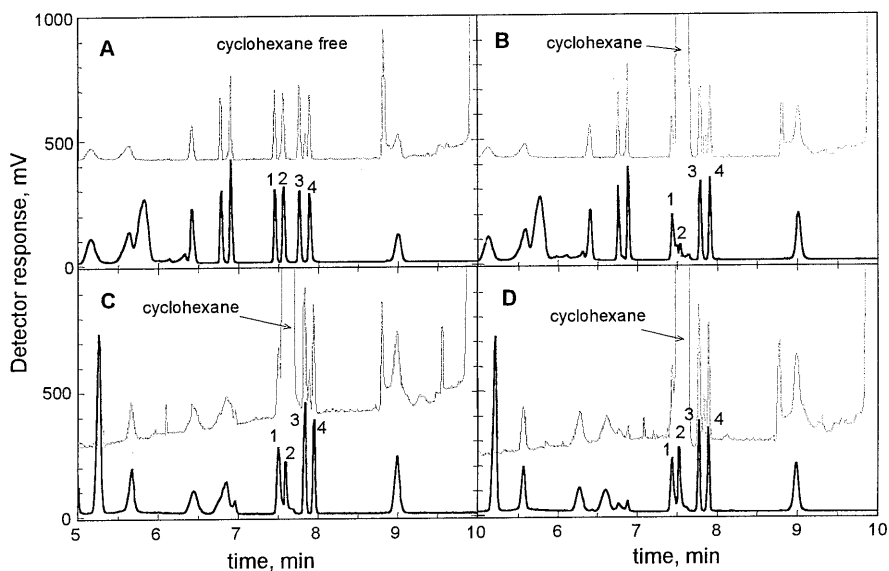


Figure 2.4: Quenching effect on the SCD signal. Full line: SCD signal; dotted line: FID signal. Fixed hydrogen flow rate 250 mL/min. Oven temperature program: 30°C (3 min) to 150°C at 30°C/min. Injection volume 1 μ L. Peak identification and concentration of sulfur compounds in the coeluting region (mg S/L): 1/ *s*-BuSH 58.2; 2/ *i*-BuSH 62.9; 3/ DES 62.5; and 4/ *n*-BuSH 58.4. Chromatograms: A/ free of cyclohexane, air 360 mL/min, ozone generator gas: air; B/ with cyclohexane C/S = 100, air 360 mL/min, ozone generator gas: air; C/ with cyclohexane C/S = 100, air 505 mL/min, ozone generator gas: air; and D/ with cyclohexane C/S = 100, air 505 mL/min, ozone generator gas: pure oxygen.

From Figure 2.4 it can be seen that although equal response factors are obtained for the four sulfur components mentioned above at an air/hydrogen of two with oxygen as the ozone generator feed gas, the heights of *s*-BuSH and *i*-BuSH peaks are significantly lower than that of the DES and *n*-BuSH peaks. This is most likely caused by the band broadening that occurs in the column as the sulfur compounds elute together with a much larger amount of cyclohexane. Increasing amounts of cyclohexane injected into the chromatographic column will cause the column to become overloaded which will result in broadening of the coeluting sulfur compound. The resolution will decrease which will result in incorrect peak integration. This conclusion is evident from Figure 2.5, where the response factors of the four sulfur compounds investigated are plotted vs. the carbon-to-sulfur ratios. Up to carbon-to-sulfur ratios of approximately 2×10^4 , no errors in peak area integration are observed, although the peaks clearly show severe band

broadening and peak distortion. Carbon-to-sulfur ratios exceeding 2×10^4 lead to errors in integration of the individual peak areas, but the average of the peak response factors from these four sulfur compounds remains identical. This means that no quenching occurs. In further experiments no quenching was observed up to carbon-to-sulfur ratios of 9×10^4 . Ratios above this value could not be evaluated because at higher carbon-to-sulfur ratios the peak areas of the sulfur components might be affected by some response of the SCD for hydrocarbons.

Figure 2.4 clearly illustrates the importance of having available the FID signal during development of a method using an SCD. If only the SCD signal would have been recorded, it would be impossible to see that peak No. 2 might be affected by coelution of a large amount of a hydrocarbon. This statement is not only true for situations in which an SCD is used but even more so when other, less selective or more quenching-sensitive detectors are employed.

From the study described above it can be concluded that for optimum sensitivity of the SCD an air-to-hydrogen flow rate ratio of one should be used. However, for quenching free operation, which is of utmost importance in natural gas analysis, a higher air-to-hydrogen flow rate ratio is beneficial. A value of two is an optimum compromise between quenching free operation and lifetime of the ceramic probe. Under these conditions the SCD sensitivity is approx. 30-50% of the maximum achievable sensitivity. It is finally recommendable to use pure oxygen instead of air for the SCD ozone generator. The sulfur-over-carbon selectivity is then better than 10^5 .

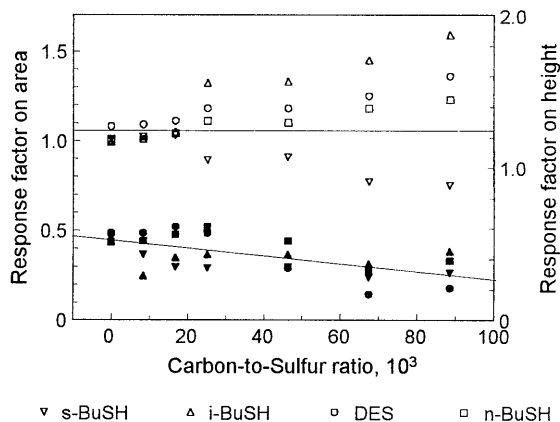


Figure 2.5: Extent of the quenching effect on the SCD. SCD conditions: air 400 mL/min, hydrogen 200 mL/min, ozone generator gas: pure oxygen 60 mL/min. Oven temperature program: 30°C (3 min) to 150°C at 30°C/min. Empty markers: response factors on a area basis (area/concentration); filled markers: response factors on a height basis (height/concentration). Injected amounts of sulfur compounds (ng): *s*-BuSH 1.46; *i*-BuSH 1.58; DES 1.57; and *n*-BuSH 1.47.

2.5.2. Flame Photometric Detector

Flame photometric detection is based on measuring emission light from S_2^* species which are formed when sulfur compounds are burnt in a hydrogen rich flame. The optimization of the FPD performance was carried out in the same manner as with the SCD, *i.e.* the influence of the air/hydrogen flow rate ratio and the nitrogen make-up flow rate on the response factor and the signal-to-noise ratio of all 11 sulfur compounds was studied. Figure 2.6 shows that the optimum FPD performance is obtained at an air/hydrogen ratio of approximately 0.6 (air 25 mL/min, hydrogen 40 mL/min). From this figure it is also evident that the FPD signal exhibits a much stronger compound dependency than the SCD signal. The make-up gas flow rate was found to have only a marginal effect on the FPD performance. In all further experiments a make-up flow of 30 mL/min was used. The detector temperature was set at 250°C.

Calibration graphs of the 11 sulfur compounds present in the sample are shown in Figure 2.7. From this figure it is clear that the FPD signal shows a square dependence on the concentration of the sulfur species. The slopes of the calibration graphs for the various sulfur compounds range from 1.8 to 2.2 on a log-log scale. The "linear dynamic" range of the square FPD response after linearization (log-log scale) is limited to two orders of magnitude. The reproducibility of absolute peak areas, based on three subsequent measurements, is generally in the range of 6% RSD. The detection limit ($S/N = 3$) was 0.15 ng S/sec and was, hence, about 100 times higher than that achieved with the SCD. The carbon-to-sulfur selectivity is in the range of $5 \times 10^4 - 1 \times 10^5$. The long-term stability of the

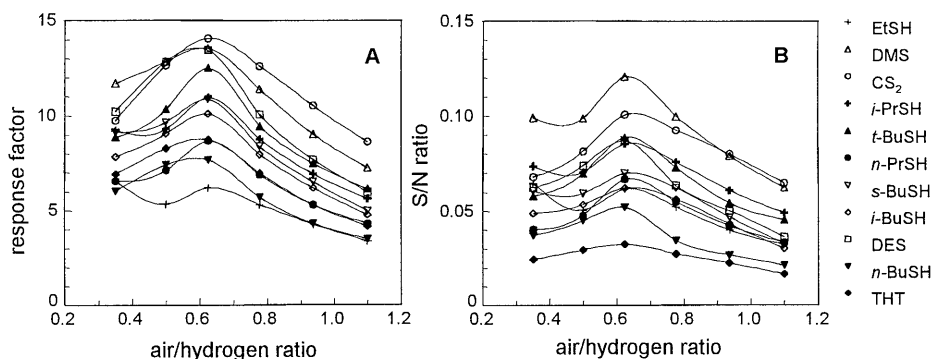


Figure 2.6: Influence of air/hydrogen flow rate ratio on FPD performance: A) response factor = area/concentration; B) S/N ratio = (peak height/concentration) divided by the noise level.

FPD was somewhat better than that of the SCD. The FPD can be left on overnight, whereas the FID flame of the SCD must be shut off because of the high consumption of flame gases. Moreover, the ceramic sampling probe of the SCD had to be taken out overnight to vent the water accumulated in the vacuum pump during operation. These two factors result in a slightly poorer long-term stability for the SCD. The slopes of the FPD calibration graphs, measured on three different days, have RSDs of less than 3%.

The quantitative study of the quenching effect of the FPD was performed in the same manner as with the SCD in the first series of quenching effect experiments. Now, however, the hydrocarbons were fed into the make-up gas supply line. Figure 2.8 shows a plot of the response factors of the sulfur compounds for various carbon-

to-sulfur ratios. It was found that the sulfur signal was reduced by 50% when sulfur species coelute with a 20-fold excess of hydrocarbons. Natural gas contains numerous higher hydrocarbons that elute in the elution range of the sulfur species of interest. Although the concentrations of these hydrocarbons are low, they still vastly exceed the concentration levels of the sulfur species. Hence, there is a serious risk of quantitation errors when using an FPD in natural gas analysis. Only detectors that are sufficiently selective and (sufficiently) free of

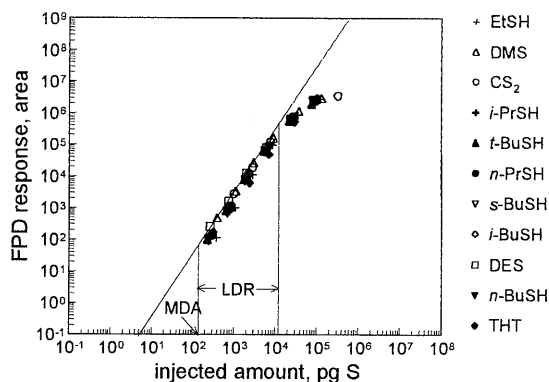


Figure 2.7: Calibration graphs of sulfur compounds obtained for the FPD. Chromatographic conditions: see Experimental, section 2.3.2.

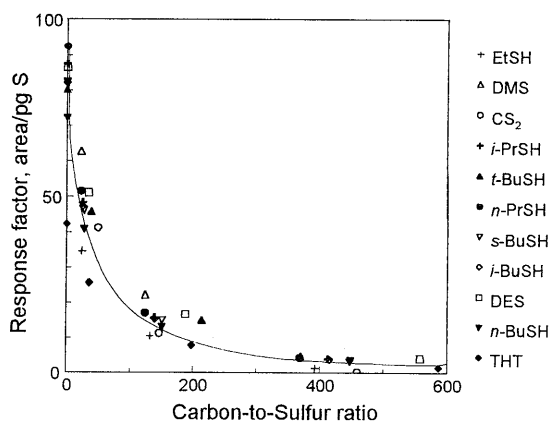


Figure 2.8: Results of quenching effect study on the FPD.

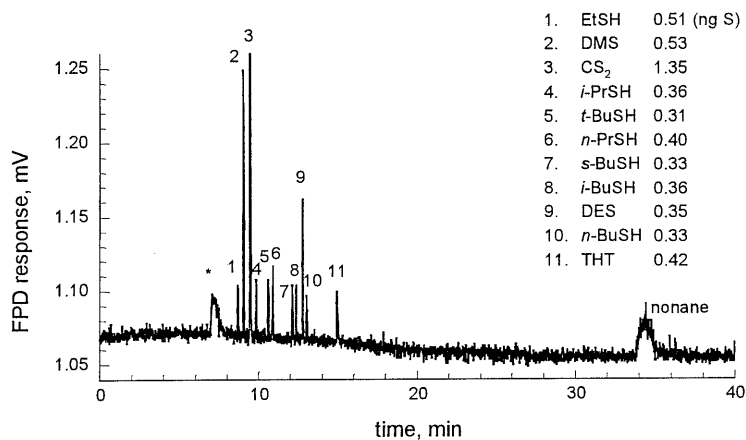


Figure 2.9: FPD chromatogram of a standard containing 11 sulfur compounds in *n*-nonane. Chromatographic conditions: see section 2.3.2. Experimental.

quenching give unbiased results in this particular field of application.

Figure 2.9 shows a representative chromatogram of 11 sulfur compounds at concentrations close to the detection limits.

2.5.3. Mass spectrometric detector

Mass spectrometric detection is based on detecting the ion fragments of the components eluting from a GC column. In the ion source of an (electron-impact) mass spectrometer, low energy electrons of approx. 70 eV, emitted from the filament, cause the neutral molecules to fragment and form ions. Owing to their different mass, these ions then can be differently accelerated, detected and identified. This type of detection appears to be highly attractive for sulfur determination in natural gas owing to its ability to identify unknown components. Because the mass spectrometer was very sensitive to column bleeding from the thick-film column the heating rate of the oven was decreased from 20°C/min to 15°C/min.

To obtain maximum sensitivity, the mass spectrometer was operated in the selected ion monitoring (SIM) mode. First, a series of full scan experiments was performed to identify the ions with the highest abundances. For most of the sulfur compounds the molecular ions were found to have the highest abundances and, hence, these ions have been chosen for further quantitative determination using

selected ion monitoring (SIM). The experimental conditions are summarized in Table 2.2. Calibration graphs for the sulfur compounds measured in the SIM mode are illustrated in Figure 2.10.

From Figure 2.10 it can be seen that the linear dynamic range of the MSD in the SIM mode is over five orders of magnitude. The detection limit ($S/N = 3$) varies from 1.5 pg S/sec for THT to 9.5 pg S/sec for EtSH. In the full scan mode the detection limit is approximately 100 times higher. The reproducibility, based on three measurements, was very good with RSDs in the range of 1-3%. The "long-term" stability, based on slopes of three calibration graphs measured on three different days, was also very good. Here values of 1.5 to 3.5% were obtained.

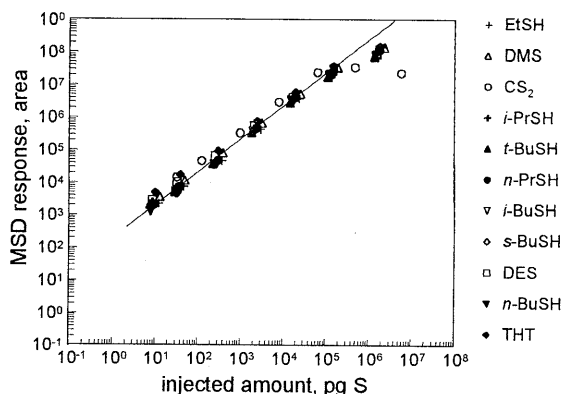


Figure 2.10: Calibration graphs of sulfur compounds obtained on the MSD in the SIM mode. Chromatographic conditions: see section 2.3.2 and Table 2.2.

Table 2.2: Conditions set on the mass spectrometric detector:

SCAN mode:	amplifier voltage 1600 V			
	scan range 10-100 amu			
	scan speed 2 scan/sec			
SIM mode:	amplifier voltage 1800 V			
group No.:	1	2	3	4
start time (min):	5.50	8.25	10.00	12.00
selected ions (amu):	62; 76	76; 90	90	88
dwel time (msec/ion):	100	100	150	150

2.5.4. Thermal conductivity detector

This detection technique is based on the change of the thermal conductivity of the gas stream through the detector cell when a compound elutes from the chromatographic column. As an universal detector the TCD responds to all compounds

that elute from the chromatographic column. In general, its response depends on the molecular weight of the eluting compounds, *i.e.* the detector is generally more sensitive for the heavier species. A proof of this principle is shown in Figure 2.11, which shows calibration graphs for the 11 sulfur compounds used in this study. The minimum detectable amounts for this detector are around 30 ng S.

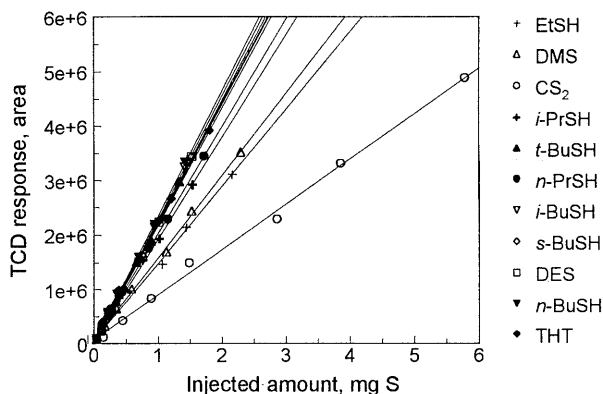


Figure 2.11: Calibration graphs of sulfur compounds obtained on a TCD. Chromatographic conditions: see section 2.3.2.

Figure 2.12 shows a representative chromatogram of the sulfur compounds near the detection limits. The linear dynamic range of this TCD is over 3 orders of magnitude. Here it is important to emphasize that the upper limit of this range is not dictated by the detector but by overloading of the chromatographic column. The reproducibility was in the range of 10% RSD, which is poor in comparison with other detectors. This is caused by fluctuations in the make-up flow rate. The long-term stability was in the range of 1-6% RSD.

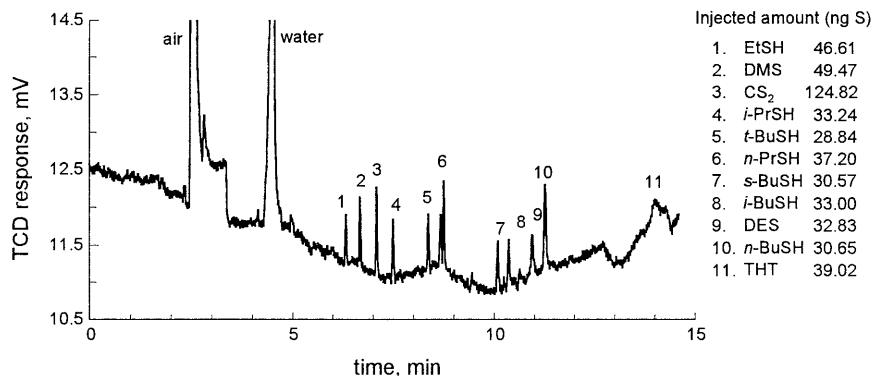


Figure 2.12: Typical chromatogram of sulfur compounds on a TCD at concentrations close to the detection limits. Chromatographic conditions: see section 2.3.2.

2.5.5. Pulsed-Flame Photometric Detector

2.5.5.1. Principle of the Pulsed-Flame Photometric Detection

The Pulsed-Flame Photometric detector (PFPD) was first described by Cheskis, Atar and Amirav in 1993. This detector recently became commercially available from Varian (Palo Alto, CA, USA). The PFPD is based on a flame source and a combustible gas flow rate that cannot sustain continuous-flame operation. Thus, the ignited flame propagates back to the combustible gas mixture source and is self-terminated after the combustible gas mixture is burnt. The continuous gas flow creates ignition in a periodic fashion.

The main feature that characterizes the PFPD is the pulsed nature of the emitted light. Time domain information is added to the heteroatom-specific emission with time dependent emission being observed. A more detailed discussion of the principles of the PFPD is given in Chapter 1. The PFPD is claimed to have an improved sensitivity for S and P, much higher selectivity against carbon, lower gas consumption, reduced emission quenching and the ability to detect selectively other heteroatoms such as nitrogen or to simultaneously detect sulfur and carbon (multi-atom detection). The sulfur concentration dependence of the PFPD is quadratic and its response is said to be independent of the structure of the sulfur-containing molecules. Owing to the incorporation of a special hardware data processing feature on the electronic board in the Varian gas chromatograph, the PFPD can be operated in either the normal (NORM) or the square root (SQRT) mode. In the NORM mode the PFPD output signal exhibits a square dependence on the injected amount of sulfur. The SQRT mode gives a linearized output signal by performing an electronic square root operation on the total detector signal. Therefore, any baseline offset is treated in the same manner as the sample peak signal. Because of this characteristic, it is always necessary to operate with as low as possible a baseline offset in order to obtain a linear peak-height response in this mode. The SQRT mode is best suited for sulfur analysis at moderate to high concentration levels. It is generally not very useful for trace analysis because of the high baseline noise level caused by the hardware electronic treatment of the signal.

2.5.5.2. Experimental Conditions

Injector: 1077 split/splitless Capillary Injector (Varian); splitless time 0.75 min; injector temperature 200°C.

Oven: programmed from 35°C (3 min) to 150°C at 20°C/min.

Detector: PFPD Varian; sulfur mode: deep violet optical filter, narrow-bore (2 mm i.d) quartz combustor, photomultiplier voltage 580 V.

2.5.5.3. Optimization of the PFPD

The pulse frequency of the PFPD is limited to the range of 2 to 4 Hz, and can be changed in this region by adjusting the air2 flow rate (see Figure 1.10 in Chapter 1). With the air2 supply line an extra portion of air is led to the upper (ignition) chamber of the detector and mixed with the combined hydrogen-air flow that comes from the lower (combustion) chamber. The higher the air2 flow rate, the easier the ignition process and, hence, the faster the detector pulses. The influence of the air2 flow on response factors and calculated minimum detectable amounts (MDA) of 10 investigated sulfur compounds is shown in Figure 2.13.

Similar to other flame-based sulfur selective detectors, the PFPD signal is strongly influenced by the ratio of the flow rates of the fuel gases. In case of the PFPD these are the hydrogen and air1 flow rate. The combined flow hydrogen-air1 is split into two flows before entering the detector. One of these is led along the outside of the wall of the quartz combustor to the upper chamber and has the role of the igniting mixture. The other flow fills the combustor, where components eluting from the column are burnt by the flame propagated down from the upper (ignition) chamber. For complete flame propagation the combustor must be filled slightly before the upper chamber. On the other hand, the second flow should not be too high to avoid losses of the components before the flame propagates. For these reasons a careful

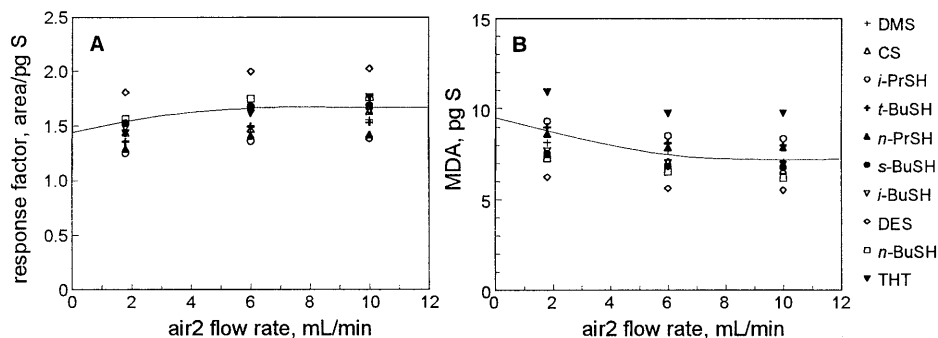


Figure 2.13: Influence of air2 (ignition) flow rate on PFPD performance. The detector was operated in the NORM mode: A) response factor = peak area/injected amount; B) MDA = minimum detectable amount. (Errors in concentrations can be up to 10%).

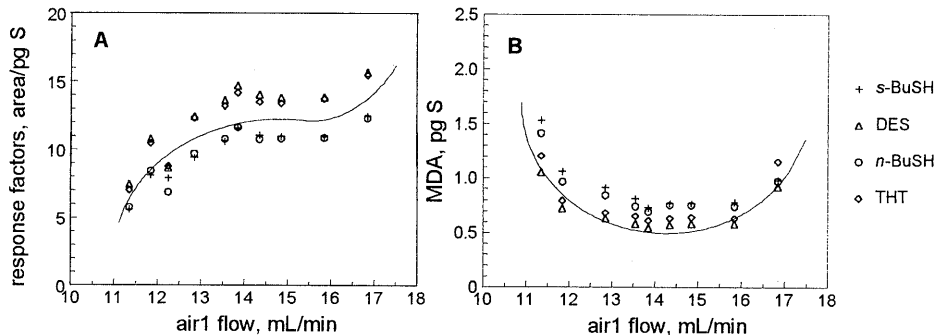


Figure 2.14: Influence of air1 (combustion) flow rate on PFPD performance. The detector was operated in the NORM mode: A) response factor = peak area/injected amount; B) MDA = minimum detectable amount.

optimization of the two fuel flows is important. Careful adjustment of the needle valve is necessary anytime the hydrogen and/or air1 flow is changed. Figure 2.14 shows the plot of the response factors (A) and the MDAs (B) of the investigated sulfur compounds *versus* the flow rate of air1. The hydrogen flow rate was fixed at 12.75 mL/min.

From Figure 2.14 it can be seen that the optimum flow setting for the PFPD sensitivity is: hydrogen - 12.75 mL/min, air1 - 13.75 mL/min, and air2 - 10 mL/min. At these flow settings the resulting pulse frequency was 3.2 Hz. Low air1 flows cause the burning process to be incomplete. Under these conditions the response factors as well as the signal-to-noise ratios decrease. Too high an air1 flow, on the other hand, causes the flame propagation to become unstable. This results in too high baseline noise levels, which in turn increase the detector minimum detectable amounts.

2.5.5.4. Quenching Behavior of the PFPD

The quenching effect of the PFPD was investigated by studying the influence of a coeluted hydrocarbon on the signal of a sulfur component. For this purpose cyclohexane was added to the *n*-nonane solution of sulfur compounds. With the column used in this study cyclohexane will coelute with *i*-BuSH. For a complete overlapping of these two peaks the oven temperature program was changed to 50°C (1.5 min) to 150°C at 20°C/min. Figure 2.15 shows the recoveries (on both area and height basis) of the cluster of three peaks *s*-BuSH, *i*-BuSH, and DES. *s*-BuSH elutes just before and DES after the quenched *i*-BuSH. The relative peak area (*RPA*) of for example *i*-BuSH were calculated by the following equation:

$$RPA^{i-BuSH} = \frac{A_x^{i-BuSH}}{A_0^{i-BuSH}} \times \left[\frac{1}{2} \times \left(\frac{A_x^{n-PrSH}}{A_0^{n-PrSH}} + \frac{A_x^{n-BuSH}}{A_0^{n-BuSH}} \right) \right]^{-1} \times 100 \quad (2.5)$$

- RPA Relative peak area expressed in %,
- A_x peak area (or height, respectively) measured with C/S = x,
- A_0 peak area (or height, respectively) measured with C/S = 0,

This equation gives the average degree of quenching for *i*-BuSH expressed relative to a component eluting slightly before and a component eluting slightly after the *i*-BuSH. *n*-PrSH elutes just before *s*-BuSH and *n*-BuSH just after DES. The RPA or RPH (relative peak height), respectively, calculated this way is free from possible fluctuations due to variations in peak width caused by for example inadequate cryofocusing. From Figure 2.15 we can conclude that the sulfur signal reduces to 50% if the sulfur component coelutes with a 10⁴-fold excess of a coeluting hydrocarbon.

To investigate the influence of the air-to-hydrogen ratio on the quenching behavior of the PFPD a sulfur-cyclohexane solution in *n*-nonane (C/S = 45,000) was used. From the RPA or RPH of the *i*-BuSH peak shown in Figure 2.16, it is evident that higher

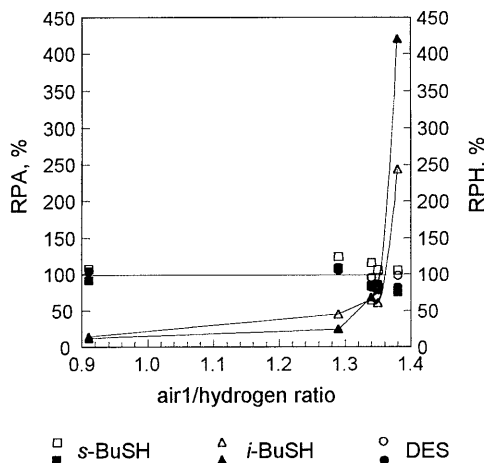
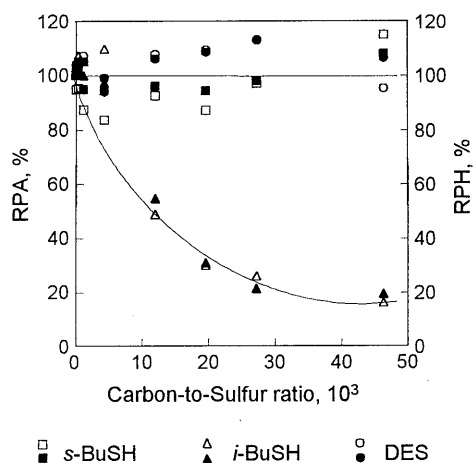


Figure 2.15: Extent of quenching effect on the PFPD. Flow settings: hydrogen 12.7 mL/min, air1 13.7 mL/min, air2 10 mL/min. The PFPD is operated in the NORM mode. Empty markers: relative peak area. Filled markers: relative peak height.

Figure 2.16: Influence of air1 flow rate on the PFPD quenching behavior. Flow settings: hydrogen 12.7 mL/min; air2 10 mL/min. The PFPD is operated in the NORM mode. Empty markers: relative peak area. Filled markers: relative peak height.

air/hydrogen ratios will suppress quenching due to more complete burning of the coeluting hydrocarbon species. On the other hand the selectivity of the PFPD seems to decrease with increasing air/hydrogen ratio. This explains the over 100% recovery of the *i*-BuSH peak at an air/hydrogen ratio of 1.38. A solution of only cyclohexane in *n*-nonane also gave a positive signal on the PFPD when the air/hydrogen ratio was set higher than 1.32. This observation is in contrast to what is stated in the instrument manual. According to the manufacturer better selectivity can be obtained at higher air/hydrogen ratios. In principle it is possible to optimize the selectivity of the detector (unfortunately at the expense of sensitivity) by changing the electronic gate settings. This has not been evaluated experimentally. Similar to the situation in the flow setting optimization experiments, in this quenching behavior study the PFPD was also operated in the NORM mode.

2.5.5.5. Calibration Graphs

Preliminary experiments indicate that the repeatability of replicate measurements on the PFPD using the square root mode (SQRT) is much better than that of the normal mode (NORM). This is obviously due to the non-linear dependence of the sulfur signal on the injected amounts in the NORM mode.

Calibration graphs were measured at fuel gas flows set for optimum detector sensitivity, *i.e.* 12.7 mL/min of hydrogen, 13.7 mL/min of air1, and 10 mL/min of air2.

Chromatograms of standard sulfur solutions in *n*-nonane were recorded in both the NORM and the SQRT mode in order to allow a comparative study. Due to some fluctuations in the background level of the electronic circuits in the square root mode care had to be taken for the zero level of the baseline to be

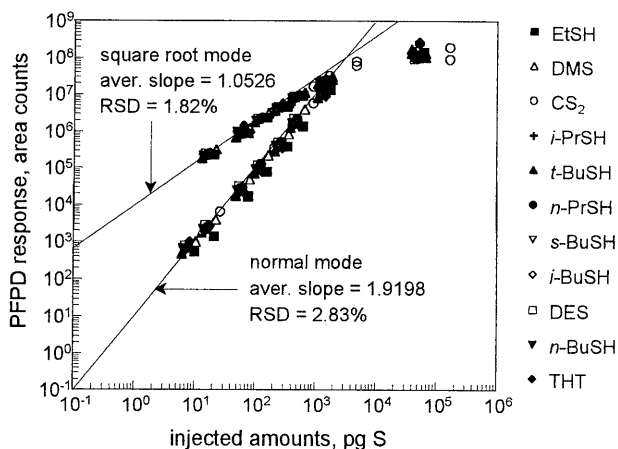


Figure 2.17: Calibration graphs of 10 investigated sulfur compounds on a log-log scale measured using the PFPD. Flow settings: hydrogen 12.7 mL/min, air1 13.7 mL/min, air2: 10 mL/min.

kept as low as possible without going below zero. Figure 2.17 shows calibration graphs of the 10 investigated sulfur compounds on the log-log scale in both the NORM and the SQRT mode. Previous (rough) experiments indicated that the PFPD had a compound independent response. Here a series of experiments with carefully prepared standards was carried out in order to study whether the response was truly compound independent. All calibration points for the 11 compounds are on one single straight line. More or less similar results were also obtained when plotting these calibration graphs on the normal scale, which indicate that the PFPD gives a virtually compound independent signal. A summary of the main characteristics of the PFPD is presented in Table 2.3.

From Table 2.3 we can conclude that for quantification purposes it is better to work in the square root mode because of the better repeatability achieved in this mode. Figure 2.18 shows representative chromatograms of sulfur components in both the normal and the square root mode at concentrations near the detection limit.

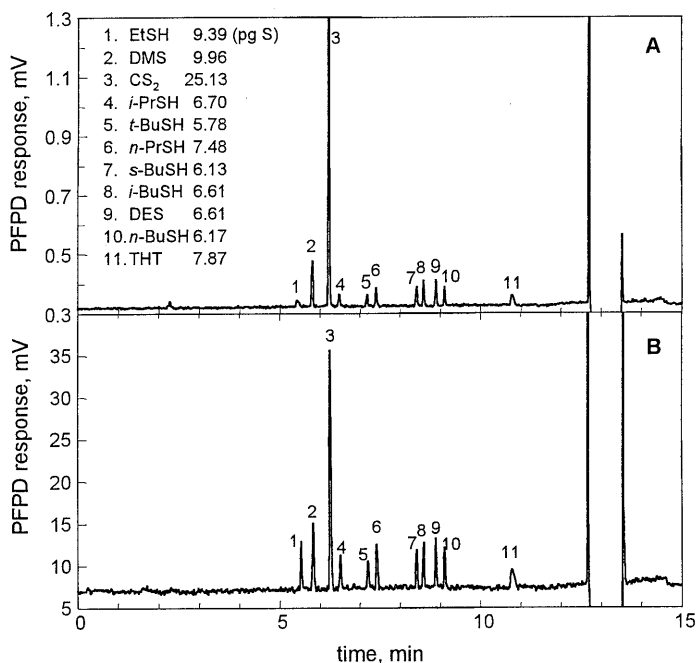


Figure 2.18: Chromatograms of 11 investigated sulfur components on a PFPD. Flow settings: hydrogen 12.7 mL/min, air1 13.7 mL/min, air2 10 mL/min. The PFPD is operated in the NORM mode (A) or the SQRT mode (B).

Table 2.3: Features of the PFPD. Comparison of the normal and the square root mode.

Parameter	Normal mode		Square root mode	
	value	RSD (%)	value	RSD (%)
<u>Calibration lines:</u>				
slope	1.9198	2.83	1.0526	1.82
correlation coefficient	0.9991	0.07	0.9987	0.09
<u>MDA (pg S)</u>	1.25	9.54	3.72	29.28
<u>DL (pg S/s)</u>	0.54	9.54	1.52	19.84
<u>LDR (decades)</u>	~3.0		~3.0	
<u>Quenching behavior (C/S)</u>	~10,000		nm ^a	
<u>Reproducibility (% RSD) (from 5 replicate absolute peak areas):</u>				
high conc. 10 ³ µg S/L	~2.0		~1.5	
mid. conc. 10 ² µg S/L	~12.5		~6.5	
low conc. 10 ¹ µg S/L	~22.5		~17.5	
<u>Selectivity (S_{SIC})^b</u>	0.5-2×10 ⁵		0.5-2×10 ⁵	

^a nm...not measured.

^b The PFPD selectivity was calculated on the basis of peak heights. On the area basis the selectivity would be considerably lower

2.5.6. Atomic Emission Detector

2.5.6.1. Principle of the Atomic Emission Detection

In contrast to the “normal” selective detectors that only reveal the presence or absence of a certain heteroatom in the effluent of the GC column, the Atomic Emission Detector (AED) provides information on the presence (or again absence) of all atoms in the gas eluting from the chromatographic column. In GC with AED detection the carrier gas is transported into a helium discharge chamber, powered (or heated) with a microwave generator. Here, the molecules are cleaved into atoms that are raised to an excited state and emit light. The light is focused, then dispersed by a diffraction grating into its component wavelengths and measured by a light sensor. The sensor converts the energy to an electrical signal measured by a recording device coupled to a computer or a dedicated signal analyzer. The plot of the detector output at a certain wavelength *versus* time produces a chromatogram. Each wavelength is specific for a given element. In this way chromatograms can be obtained for sulfur, carbon, hydrogen, nitrogen *etc.* The record of the spectral detector’s output across a range of wavelengths at a moment in time produces a spectrum that can be used for identification.

2.5.6.2. Instrumental conditions:

GC: HP 5890 Series II, Hewlett-Packard.
 Column: 30 m x 0.25 mm x 1 μ m DB 5 MS (J&W, Folsom, CA, USA).
 Carrier gas: Helium; head pressure 125 kPa; split flow 38.6 mL/min, column flow 2.26 mL/min.
 Oven: 40°C (3 min) to 225°C at 20°C/min.
 Injector: Autosampler HP 7673B Hewlett-Packard, hot split injection at 250°C, split ratio 17:1.
 Detector: AED HP 5921A, Hewlett-Packard,
 Sulfur signal measured at 181 nm, Carbon at 193 nm.

2.5.6.3. Experimental results:

A summary of the main characteristic of the AED is given in Table 2.4.

When comparing the chromatograms recorded on both channels (sulfur and carbon), the sulfur signal showed significantly more peak tailing than the carbon signal (obtained for the same peak). This indicates improper operation of the plasma chamber. Most likely, the sulfur atoms are adsorbed onto the wall of the fused-silica

Table 2.4: Performance characteristics of the AED

Parameter	Sulfur signal		Carbon signal	
	meas. value	RSD. (%)	meas. value	RSD. (%)
<u>Calibration line on log-log scale</u>				
slope	0.9058	3.35		
intercept	1.9397	1.11		
correlation coefficient	0.9980	0.16		
<u>Calibration line on normal scale</u>				
slope	71.9592	7.65		
intercept	12.1134	107.12		
correlation coefficient	0.9992	0.07		
<u>MDA (pg element)</u>	140.8	7.64	22.61	19.24
<u>DL (pg element/sec)</u>	48.4	11.04	9.53	26.69
<u>LDR (decades)</u>		~3		~3
<u>Reproducibility (% RSD)</u>				
high conc. 10^7 μ g/L		~4		~3
mid. conc. 10^5 μ g/L		~7		~5
low conc. 10^4 μ g/L		~15		~10
<u>Selectivity ($S_{S/C}$)</u>	very selective ($>10^5$)			

plasma cavity. This causes tailing of the signal and a significant loss of sulfur atoms and, hence, a poor sensitivity.

From the data shown in Table 2.4 and the poor peak shapes obtained for sulfur it can be concluded that the AED is clearly not at its optimum performance. The experimentally observed detection limits are 10 to 30 times higher than those specified by the manufacturer, *i.e.* the DL is 2 pg S/sec for sulfur and 1 pg C/sec for carbon. Also the LDR value found is 10 times worse than that given by Hewlett-Packard. Due to a heavy working load of the AED in the Shell Research Laboratory the experiments on the AED could not be repeated.

2.5.7. Comparison of the Various Detectors Investigated

For the sake of comparison the main characteristics of the six above-mentioned detectors are summarized in Table 2.5. These parameters include the minimum detectable amount (MDA), the "in-cell" detection limit (DL), the linear dynamic range (LDR), the repeatability expressed by RSD calculated from five subsequent measurements, and the "long-term" stability expressed by RSD calculated from slopes of calibration graphs measured on three different days.

Table 2.5: Summarized parameters of six investigated universal and sulfur selective detectors.

Detector	MDA (g S)	DL (g S/sec) ^b	LDR ^a	Repeat. (RSD %)	Stability (RSD %)	Select. (S _{S/C})	Quenching (C/S) ^c
SCD	5×10^{-12}	2×10^{-12}	$>10^6$	5	3-6	$>10^6$ ^d	90,000
FPD	$3-6 \times 10^{-10}$	1.5×10^{-10}	$<10^2$	6	<3	$<10^5$	20
MSD ^e	$4-14 \times 10^{-12}$	$2-11 \times 10^{-12}$	$>10^5$	1-3	2-4	na ^f	na
TCD	$1-4 \times 10^{-8}$	$1-4 \times 10^{-2}$ ^b	$>10^3$ ^g	10	1-6	na	na
PFPD	$1.5-4 \times 10^{-12}$	$0.5-2 \times 10^{-12}$	10^3	2-13	<10	$<2 \times 10^5$	10,000
AED ^h (exp.)	1.5×10^{-10}	5×10^{-11}	10^3	4-7	nm ⁱ	$>10^5$	nm
AED (manfac.)		2×10^{-12}	10^5			$>10^5$	

^a linear section on the calibration graph (log-log scale),

^b only for mass flow sensitive detectors. For the TCD the unit was mg S/m³,

^c carbon concentration, relative to the sulfur concentration, that gives a 50% reduction of the sulfur peak height.

^d hydrocarbons give negative response under the experimental conditions used in this study (under the conditions for quenching free operation, hydrocarbons give positive peaks. The selectivity in that situation was found to be better than 10^5)

^e in the selected ion monitoring mode

^f na...not applicable

^g the range is limited by column overloading.

^h during the experiments the AED was not in optimum condition. This explains the substantial difference between the experimental results obtained on this detector and the specifications of the manufacturer. Previous experience with the AED indicates that the manufacturer specifications are realistic.

ⁱ nm ... not measured.

2.5.8. Other Possible Detection Techniques Not Included in the Evaluatory Studies

Apart from the six detection techniques mentioned above, there are several other universal as well as “sulfur-selective” detectors available. These include, for example, the electron capture detector (ECD) and the flame ionization detector

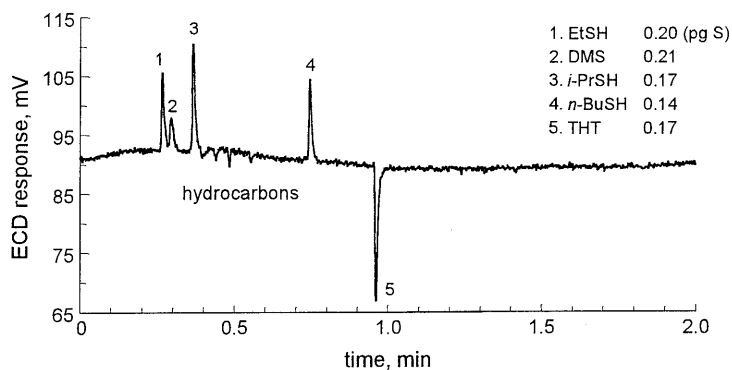


Figure 2.19: Chromatogram of sulfur compounds obtained on an ECD in a high-speed GC instrument with hot split injection.

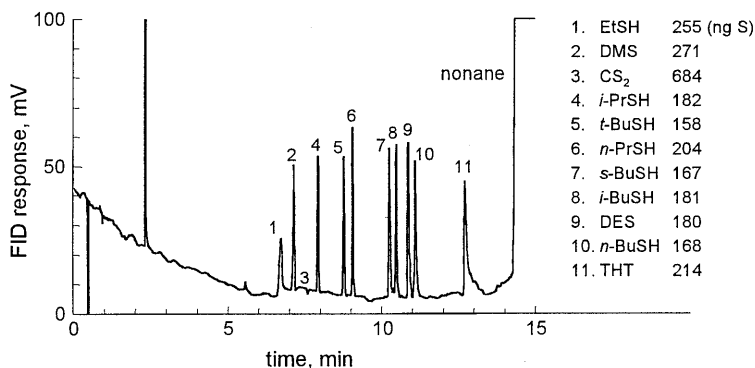


Figure 2.20: Chromatogram of sulfur compounds on an FID. Chromatographic conditions: see section 2.3.2.

(FID). The ECD, sensitive to electron-capturing elements, has been quoted as very sensitive for sulfur species. One of the disadvantages of this detector, however, is the strong compound dependence of its response. Figure 2.19 shows a representative chromatogram of sulfur compounds recorded on an ECD. An example of flame ionization detection of sulfur compounds is shown in Figure 2.20.

2.6. CONCLUSIONS

The performance characteristics of the detection device to a great extent determine the requirements that have to be met by sample pretreatment and chromatographic analysis if complex samples are considered. For the analysis of sulfur components in natural gas in principle various detectors can be used. Considering all technical as well as non-technical aspects, however, it is obvious that for the selective, sensitive, and reliable determination of sulfur components in a complex matrix such as natural gas, the SCD is the best choice. This detector offers the highest selectivity and sensitivity and has a large linear dynamic range. Moreover its response is largely compound independent. This implies that the detector can be calibrated using just one standard component. Last but not least, the detector is free of quenching over a wide concentration range. Universal detectors such as the TCD or FID can, at least in principle, also be used as the system detector. In practice, however, the resulting requirements for sample pretreatment and chromatographic separation quality will be almost impossible to meet. Disadvantages of the SCD detector are its rather high operational cost and high level of experience required for the operator. This, however, is partly compensated by advantage of the SCD of having an FID signal available simultaneously with the sulfur signal. This particular property of the flame-based SCD was found to be very helpful in the stage of method development and evaluation. Once the SCD is chosen for use in routine analysis, an upgraded version or a flame-less SCD can be used. These detectors have much lower operational and maintenance costs. Moreover, they are easier to operate.

The PFPD, a detector that was introduced only recently, appears to be highly suitable for trace analysis of sulfur in natural gas. This detector is easier to operate and cheaper than the SCD. Quenching is significantly less than in the normal FPD. For these reasons this detector is a good replacement for the normal FPD. Its technical performance characteristics (mainly linearity and linear dynamic range), however, are not as good as those of the SCD.

Chapter 3

DESIGN CONSIDERATIONS OF A GC METHOD FOR SULFUR DETERMINATION¹

ABSTRACT

In this chapter other fundamental steps, apart from detection, of a GC-based analytical procedure designed for sulfur analysis such as sample preconcentration/enrichment, chromatographic separation and calibration are evaluated and optimized. A number of adsorption materials for selective sulfur enrichment from natural gas are evaluated in terms of sulfur-over-carbon selectivity. Experimental conditions such as for example the adsorption temperature, the purge time and the desorption/transfer time, also are optimized. Among the adsorption materials tested, Chromosorb 104 is shown to have the best sulfur-over-carbon selectivity. The sampling process is carried out at -75°C. Depending on the amount of hydrocarbons present in the sample, the optimum purging time varies from 2 to 10 minutes.

The ideal column to be used in gas chromatographic sulfur analysis should provide adequate separation for all sulfur components present in natural gas samples under mild chromatographic conditions, i.e. no cryocooling of the oven should be required. The cluster hydrogen sulfide/carbonyl sulfide (H_2S/COS) is a critical peak pair due to their similar volatility and polarity. A very thick-film apolar methylsilicone column and a PLOT Q column were shown to provide adequate resolution for this peak pair. The PLOT Q column can be operated at higher than ambient oven temperatures, but shows some activity towards some of the sulfur components of interest.

Several methods, static as well as dynamic, for generating sulfur gas standards are evaluated in this chapter. The study focuses on the stability, stabilization time, accuracy and precision of the standards generated. Moreover, operational costs and user friendliness of the individual methods are also considered and compared.

¹ Published as a part of the article: "Improved Method for the Determination of Sulfur Components in Natural Gas" by H. Pham Tuan, H.-G. Janssen, E. M. Kuiper-van Loo, and H. Vlap in *J. High Resol. Chromatogr.*, 18 (1995) 525-534.

3.1. INTRODUCTION

When the detection system that is to be used for detection of the sulfur components in the gas sample has been selected, the requirements that have to be met by the sample pretreatment step and the required quality of the chromatographic separation are known. From the detection limits of the detector and the required minimum detectable concentration in the gas sample the amount of natural gas that has to be introduced on to the column can be calculated. Next, the selectivity and the quenching behavior of the detector determine the required quality of the pre-separation and the actual chromatographic separation. Below, the design criteria of a system for sulfur analysis in natural gas based on the use of an SCD detector for detection will be discussed in more detail. The work described here is mainly of an experimental nature. For more background information the reader is referred to Chapter 1.

3.1.1. Injection Volume

The required quantification limits for sulfur analysis in natural gas are 0.1 mg S/m^3 for H_2S and COS and 0.01 mg S/m^3 for the mercaptans, sulfides and odorants such as tetrahydrothiophene (THT) which are added to the natural gas to impart a characteristic smell to the gas. The detection limit of the SCD ranges from 5 pg S if optimized for maximum sensitivity to $10\text{-}15 \text{ pg}$ if optimized for being quenching free (see Chapter 2). This means that the required injection volume ranges from 0.5 mL (maximum sensitivity conditions) to 1 or 1.5 mL if the detector is optimized for minimum quenching. For a reliable quantitative analysis in a real sample, however, a safety margin of a factor of 5 to 10 is generally included. If we assume that the detector is optimized for maximum sensitivity, this means that the desired injection volume is 5 mL . This volume clearly exceeds the maximum allowable injection volume on capillary columns. Hence, for these columns selective enrichment is necessary. For packed columns on the contrary, an injection volume of 5 mL would be allowable. Here, however, the detection limits are clearly unfavorable in comparison with those on a capillary column due to the much larger chromatographic band broadening. For packed columns the estimated detection limits are approximately 25 picogram of sulfur. It is hence clear that also with these columns pre-

concentration of the natural gas sample is required if detection limits of 0.01 mg S/m^3 are to be met.

To meet the desired quantification limits at least some 5 mL of natural gas have to be introduced onto the GC column. More precisely, the sulfur compounds from some 5 mL of natural gas have to be retained in some type of an adsorption device while at the same time the hydrocarbons from this sample are eliminated as completely as possible. This is necessary because of selectivity constraints (see below). In the above discussion it is assumed that the SCD is operated under conditions where maximum sensitivity is obtained. If, however, the detector is operated under conditions which are optimized with regard to being quenching-free, the sensitivity is only approximately 30% of the maximum attainable sensitivity. Therefore, the desired injection volume in case a capillary column is used is approx. 15 mL.

3.1.2. Required Quality of Pre-Separation

It is evident that for a reliable specification and quantification of the various sulfur components in natural gas an adequate separation of the individual sulfur peaks is required. As the number of sulfur compounds that is present in natural gas (at a concentration level that can give rise to environmental or catalyst problems) is limited, this separation is not too complex. In general, the cluster $\text{H}_2\text{S}/\text{COS}$ is the most difficult peak pair. Various columns or column combinations (both packed and capillary) for sulfur separation have been discussed in literature (see Chapter 1). Some problems sometimes arise due to the reactive and adsorptive nature of the sulfur species.

Whether or not it is necessary to separate the individual sulfur species from the hydrocarbons in the gas sample depends on the quenching behavior and the selectivity of the detector employed. Because (after a careful optimization!) the SCD is free of quenching, it is possible to accurately detect and quantify a sulfur compound even if this compound coelutes with a hydrocarbon. Hence, there is no need to chromatographically separate the sulfur compounds from the hydrocarbons. This, by the way, would be extremely difficult due to the extremely large number of different hydrocarbons present in the gas sample. Apart from the quenching behavior of the detector, also the selectivity of the detector has to be considered. If the detector has a poor selectivity, non-sulfur-containing com-

pounds could incorrectly be identified as being sulfur species or incorrect peak areas could be obtained in case of coelution.

The detector employed in the present study has a Sulfur-over-Carbon selectivity ($S_{S/C}$) better than 10^6 (10^5 if optimized for quenching free operation). This means that the detection limits of the detector for hydrocarbons are at least 10^6 times higher than for sulfur species. In the present study we aimed at sulfur detection limits of 0.01 mg S/m^3 . At an $S_{S/C}$ of 10^6 this means that the detection limits for the hydrocarbons are higher than approximately 10^4 mg C/m^3 or 10 g C/m^3 . Hydrocarbons that are present in the gas sample at concentrations in excess of this value will show up as peaks on the SCD chromatogram. To avoid such peaks being inadvertently identified as sulfur components, it is preferable to eliminate these components in the sample preparation step. Hydrocarbons that occur at lower concentration levels do not hamper correct operation as these components are not sensed by the selective detector. For the particular case of the average "Groningen" natural gas (for composition see Table 3.1) this means that methane, ethane and preferably also propane have to be eliminated in the sample preparation procedure. Higher hydrocarbons do not have to be eliminated as these components are not sensed by the SCD detector. If another, less selective detector is used or if a detector that exhibits quenching is applied (e.g. FPD), the criteria specified above will be much more stringent.

3.1.3. Selective Enrichment

Adsorption followed by thermal desorption is nowadays widely used to introduce large volumes of gaseous samples onto capillary GC columns. This technique is, strictly spoken, not a large volume sampling technique because not the entire sample is injected onto the column. Merely the components of interest from a large volume of gas are transferred onto the column. Adsorption/thermal desorption is hence a selective technique. Only the components of interest are enriched and transferred to the column. The other components are eliminated by purging the adsorption device with an inert gas or by selecting an adsorbent that has no interaction with the dilution gas. Dedicated instrumentation for adsorption-thermal desorption (ATD) is commercially available. In our case the adsorption-thermal desorption procedure is carried out inside the liner of a programmed temperature vaporizing injector (PTV). The liner of the injector is packed with a selective adsorption material and kept at a controlled temperature.

Table 3.1: Composition of a typical Dutch natural gas (Groningen gas). Data taken from "Physical Properties of Natural Gases - N.V. Nederlandse Gasunie".

Component	Concn. (mol%)	Concn. (g/m ³)
Methane	81.3	580
Ethane	2.85	38.3
Propane	0.37	7.3
Butanes	0.14	3.64
Pentanes	0.04	1.29
Hexanes*	0.05	1.93
Nitrogen	14.35	180
CO ₂	0.89	17.52

* The concentration assigned under the term "hexanes" includes also higher hydrocarbons.

During adsorption and purging the split exit of the injector is open. After purging the split exit is closed and the components are desorbed and transferred to the column by heating the injector. An advantage of the use of a PTV injector for adsorption-purge-desorption is the fact that in this set-up there is no transfer line. The components that are desorbed from the adsorption material are transferred directly into the column. This minimizes the possibility for adsorption losses of the sulfur species.

The choice of the adsorbent plays an important role in the ATD technique. The adsorption material should quantitatively trap all sulfur components from a gas volume of at least 5 mL. Methane and ethane (and preferably also propane) should not be retained by the material. Due to their high concentrations these components would give an appreciable signal on the SCD despite the excellent selectivity of this detector. Moreover, the sulfur components should be desorbed quantitatively and rapidly from the adsorbent at mild temperatures. Finally, the material should exhibit a good thermal stability.

In the present study some eight different adsorption materials were investigated on the basis of the properties specified above. In particular the ability of the materials to retain sulfur species while at the same time allowing elimination of hydrocarbons was evaluated.

3.1.4. Requirements for the Chromatographic Separation

The keyword in trace analysis in complex matrices is selectivity. Accurate determination of low concentrations of sulfur species in natural gas, for example,

is only possible if the sulfur components in the sample are separated from each other as well as from interfering components. As the exceptionally selective SCD is chosen and an enrichment step is employed, the demands imposed on the column are to some extent less stringent. Because the detector is free of quenching, the sulfur compounds of interest do not have to be separated from the interfering hydrocarbons. Moreover, the hydrocarbons that are present in natural gas at high concentration levels are removed by using a selective sample enrichment procedure. Hence, there cannot be false peaks in the chromatogram because of a limited detector selectivity. The column in this case has to be efficient only for the separation of the individual sulfur components. Due to the wide boiling point range of the components of interest and, additionally, the high volatility of some of these, this is, however, not an easy task. The column chosen should give sufficient resolution for, for example, COS from H₂S, which is the most critical cluster, while at the same time show no band broadening for high boiling components such as butyl mercaptan (BuSH) and tetrahydrothiophene (THT). Moreover, the column should not give rise to adsorption losses, a problem which is very characteristic for sulfur components.

Capillary columns have a number of advantages over packed column systems. Among these the most important ones are a high speed of analysis, a high separation efficiency and low residual surface (re)activity. Owing to the higher efficiency it is easier to obtain sufficient resolution between the individual sulfur components as well as between sulfur peaks and residual hydrocarbons. The lower surface activity is due to the much lower specific surface area and to the better degree of deactivation. For these reasons we concentrated in the evaluatory study only on capillary columns. Four columns were included in this study, *i.e.* two wall coated open tubular (WCOT) thick- and ultra-thick film non-polar columns, a Carbon porous layer open tubular (CarboPLOT) column, and a PorraPLOT Q column.

3.1.5. Problem Definition for the Calibration

GC based analytical methods are relative methods of determination, which means that they require calibration, *i.e.* the relationship between detector signal and mass or concentration injected has to be established experimentally. The simplest way to calibrate an analytical instrument is to pass a sample containing the species of interest at known concentrations through the instrument and relate

the instrument's response to concentrations. This simple description of the calibration process ignores the real problems that are generally encountered in the calibration process. These problems can be divided roughly into two areas:

1. Preparation of the standard,
2. Assignment of concentration and uncertainty to the composition of the standard.

In this chapter different methods for the preparation of calibration standards are evaluated. Special attention was paid to dynamic methods for the preparation of standard mixtures (*vide infra*).

3.2. EXPERIMENTAL

3.2.1. Chemicals

For the evaluation of adsorption materials, mixtures of sulfur compounds were made-up in glass vials. The first (gaseous) mixture contained H₂S and COS in hydrogen (dilution gas) at concentrations of about 5% (v/v) of the former and 1% (v/v) of the latter. Ethyl mercaptan (EtSH), dimethyl sulfide (DMS) and *iso*-propyl mercaptan (*i*-PrSH) were injected as pure liquids (10 μL each) and 1-butyl mercaptan (*n*-BuSH) and tetrahydrothiophene (THT) (20 μL pure liquid each) into a 2-L glass vial washed with methanol and acetone before use. Methane, ethane, propane and butane were used as pure gases. Pentane up to decane were introduced as liquid mixture, which was prepared by mixing 10 μL of the pure liquids. For the analysis, 10 μL of each gas or gas mixture and 1 μL of the liquid solution was injected. The FID was employed for the analysis of the alkane mixtures, while sulfur compounds were analyzed using the SCD.

A gaseous standard mixture (Scott Specialty Gases, Breda, the Netherlands) containing eight sulfur components in methane was used in the column study: H₂S, COS, MeSH (methyl mercaptan), EtSH, *i*-PrSH, *n*-PrSH (1-propyl mercaptan), *n*-BuSH and THT are present at ppm concentration levels.

3.2.2. Instrumental Set-up

GC: HP 5890A Hewlett-Packard (Avondale, PA, USA); oven temperature program: 30°C (5 min) to 150°C at 20°C/min for a 35 m × 320 μm × 1.1 μm CP

Sil-5 CB column (Chrompack, Middelburg, the Netherlands). Helium was used as carrier gas with a column head pressure of 10 psi, a column flow rate of 1.8 mL/min and a total flow rate of 100 mL/min. Conditions set for the other columns during the evaluatory studies are summarized separately in section 3.4.

PTV: KAS II (Gerstel, Mülheim a/d Ruhr, Germany); temperature program: initial -75°C, -60°C, -30°C, and 30°C, respectively; liquid CO₂ cooling; heating rate 12°C/sec; desorption temperature 170°C and 180°C (3 minutes); splitless time 2 min;

Cryo trap: DKK Cryo focusser (ATAS, Veldhoven, the Netherlands); gaseous CO₂ 50 bar; restrictor 8 cm × 250 μm i.d. stainless steel inserted into a 60 cm × 3 mm i.d. Teflon tube; focussing time 4 min;

FID-SCD: Sievers SCD 350B (purchased from Gerstel Benelux B.V., Brielle, the Netherlands); FID housing temperature 250°C; fuel gas flow rates: air 350 mL/min, hydrogen 150 mL/min².

3.3. RESULTS AND DISCUSSIONS

3.3.1. Selective Enrichment of Sulfur Components from Natural Gas

3.3.1.1. Adsorption Materials and Procedure

The ideal adsorbent would quantitatively retain sulfur components from a large volume of gas while at the same time it should not exhibit interaction with the sulfur-free species (hydrocarbons). Eight adsorbents were studied experimentally. An overview of the properties of these adsorption materials is presented in Table 3.2. All materials were purchased from Chrompack.

The properties of the materials with respect to the selective enrichment of sulfur from natural gas were evaluated in a series of model experiments. The equipment used in these experiments is shown schematically in Figure 3.1. It consisted of a Gerstel KAS II PTV injector, an HP 5890A GC, a DKK cryofocusser cold trap and a Sievers SCD 350B with a Gerstel adjustable probe assembly.

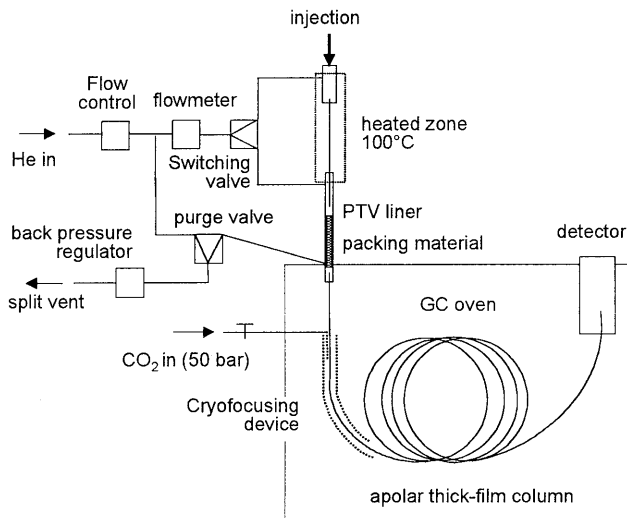
² Gas flow settings as recommended by the manufacturer. These settings later turned out to be non-optimum with regard to sensitivity (see Chapter 2).

Table 3.2: Properties of investigated adsorption materials.

Material	Abbrev.	Type*	Polarity	Surface area (m ² /g)	Mesh	T _{desorption} (°C)
CP Wax 51 (10%) on Chromosorb AW	CPWax51		very polar		60-80	150
Porapak Q	PorQ	EVB-DVB	slightly polar	500-700	50-80	180
Porapak T	PorT	EGDMA	very polar	250-300	80-100	170
Chromosorb 102	Chr102	STY-DVB	slightly polar	300-500	80-100	180
Chromosorb 103	Chr103	Polystyrene	non-polar	15-25	80-100	180
Chromosorb 104	Chr104	ACN-DVB	very polar	100-200	80-100	180
Chromosorb 105	Chr105	Polyaromatic	moder. polar	600-700	80-100	180
Chromosorb 107	Chr107	Acrylic ester	polar	400-600	60-80	180

* STY = styrene; DVB = divinyl benzene; ACN = acrylonitrile; EVB = ethylvinylbenzene; EGDMA = ethylene glycol dimethylacrylate.

The adsorption material to be investigated was packed into the liner of the PTV injector, held in place at both ends by two small plugs of deactivated glass wool. This packed liner was then conditioned under helium at a temperature about 20°C above the desorption temperature used in subsequent experiments. Care was taken not to exceed the maximum allowable temperature of the material.

**Figure 3.1:** Instrumentation used for the evaluation of the different adsorbents

The sulfur mixtures and the normal alkanes were introduced into the PTV liner at sub-ambient initial temperature (-75°C, -60°C and -30°C, respectively). The liner, still held at sub-ambient initial temperature, was then purged with Helium at a flow rate of 100 mL/min. In this step the actual elimination of the hydrocarbons occurs. After purging the liner with helium for some time the split valve

was closed and the liner was heated to the desorption temperature. Simultaneously the oven temperature program was started and the chromatogram was recorded. Finally, recoveries of the sulfur species and the alkanes were calculated using peak areas relative to a cold splitless injection. To obtain sharp peaks a (gaseous) CO₂ cooled cryotrap was employed. Later the CO₂ cooling was found to be insufficient for the most volatile components such as H₂S, COS, MeSH, and EtSH. Care was taken to avoid contact between the sulfur species and metal surfaces. This precludes losses due to (ir)reversible adsorption.

3.3.1.2. Results and Discussion

During the experimental part of the work, the influence of various operational parameters on the recoveries of the sulfur species and the alkanes were studied. Table 3.3 shows the results obtained for the adsorbent Porapak Q at an adsorption temperature of -75°C, a purge time of 4 min and a purge flow of 100 mL/min. The desorption temperature was 180°C. The desorption time was 2 min.

It is clear from the data presented in this table that Porapak Q (under these conditions) is not a suitable adsorbent for the present application. The material shows a lack of selectivity. The sulfur compounds are retained quantitatively, but also the alkanes are strongly retained. The material does not meet the requirement that states that methane and ethane (and preferably also propane) should be eliminated completely.

Tables similar to Table 3.3 were prepared for each of the adsorption materials investigated under the different experimental conditions studied. Below a summary of these tables is given. The purge time used in each experiment was 7 minutes at a purge flow rate of 100 mL/min. From Table 3.4 it is also clear that the polar materials have a better selectivity than the non-polar counterparts. If a polar material is used this provides the required selectivity, *i.e.* the non-polar hydrocarbons do not adsorb while at the same time the more polar sulfur species

Table 3.3: Selection of a suitable adsorbent. An example of a poorly selective material. Recoveries of some alkanes and sulfur compounds on Porapak Q.

Component	Recovery (%)
Methane	0
Ethane	49
Propane	99
Butane	102
H ₂ S	100
COS	91
EtSH	88
THT	111

Table 3.4: Recoveries of the investigated components using the APD technique with 7 min helium purging (100 mL/min) at -75°C.

Component	CPWax51	PorQ	PorT	Chr102	Chr103	Chr104	Chr105*	Chr107
Methane	0	0	0	0	0	0	0	0
Ethane	0	15	3	0	0	2	0	0
Propane	0	96	70	71	19	2	94	90
Butane	0	99	98	70	56	15	80	88
Pentane	1	100	91	86	83	75	96	98
Hexane	1	99	97	89	115	82	100	96
Heptane	4	97	97	94	103	83	107	98
Octane	5	93	92	103	107	83	100	97
Nonane	61	100	84	112	92	84	99	97
H ₂ S	0	95	65	91	0	97	105	133
COS	0	74	109	75	80	105	92	85
EtSH	0	87	100	90	97	97	104	91
DMS	0	89	100	102	93	98	98	90
<i>i</i> -PrSH	0	98	101	96	98	98	99	90
<i>n</i> -BuSH	2	102	86	83	90	93	91	113
THT	95	118	75	95	88	106	81	107

* Experiment on Chromosorb 105 was carried out at initial temperature of -60°C

are retained by selective interaction with the adsorbent.

With Chromosorb 104 the best results were obtained in terms of sulfur over hydrocarbon selectivity as well as break-through volume. Under optimized conditions this material allows almost complete elimination of methane, ethane and propane. Butane was retained for only a few percent. The recoveries of all sulfur components were 100%. It is therefore evident that this material clearly meets the requirements summarized earlier. A recovery of 100% was also found if the liner was purged with Helium for 10 minutes at a flow rate of 100 mL/min. This shows that the break-through volume of the sulfur components of interest on the adsorbent Chromosorb 104 is more than 1 L, which is well above the desired injection volume of 15 mL. The selectivity of this new material is illustrated in Figures 3.2 and 3.3. Figure 3.2A shows a reference chromatogram of an alkane test sample that was used for measuring the recoveries of alkanes. The test mixture contained the alkanes C₂ to C₉ and was injected in the cold splitless mode. Figure 3.2B shows the chromatogram that is obtained when the test mixture is injected into a cooled liner packed with the adsorbent. After flushing the injector with a helium flow of 100 mL/min for 7 minutes the hydrocarbons

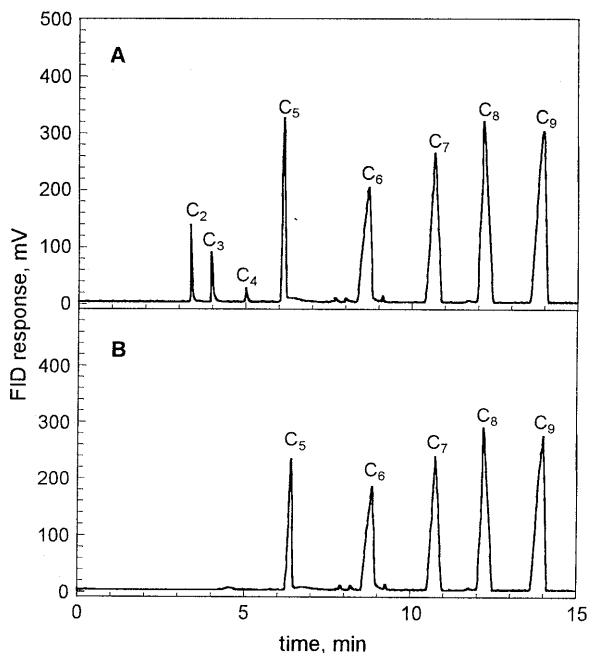


Figure 3.2: Elimination of lower alkanes by the ATD technique. Material: Chromosorb 104. Conditions: see experimental. A - FID chromatogram of a mixture of alkanes before elimination using cold splitless injection: PTV temperature program 30°C to 180°C at 12°C/sec. B - FID chromatogram of the same mixture of alkanes after elimination with APD technique; PTV initial temperature -75°C, purge time 7 min, then programmed to 180°C at 12°C/sec.

up to C₄ were completely eliminated.

In Figure 3.3 the results of a similar experiment but now with sulfur species are given. Figure 3.3A shows a cold splitless injection of the test mixture. Figure 3.3B shows the chromatogram that is obtained after adsorbing the sulfur species on the adsorbent and flushing it again for 7 minutes with a high flow of Helium. From the Figures 3.2 and 3.3 it is clear that the sulfur components are quantitatively retained at conditions under which the lower alkanes are eliminated completely. This adsorption material clearly

provides the selectivity required for the enrichment of sulfur components from a natural gas matrix.

It is interesting to compare the elution times of H₂S and COS in the two chromatograms shown in Figure 3.3. Whereas these components are separated when they are injected in the cold splitless mode, coelution occurs when sampling is performed using adsorption with subsequent thermal desorption. This is due to the pre-separation that occurs in the packed liner. In the case of the cold splitless injection an empty liner was used. Hence, the observed separation is caused by the capillary column solely. If, on the contrary, a packed liner is used for pre-concentration, a partial separation occurs already in the liner. The system basically behaves as a multidimensional set-up. A pre-separation is performed on

the packed liner, which in principle closely resembles a short packed column. Unfortunately, elution from the liner occurs in reverse order as compared to that on the capillary column. The result is coelution of the H₂S and the COS peak at the end of the chromatographic column. This problem can easily be solved by incorporating a more efficient, *e.g.* liquid nitrogen cooled, cold trap in the set-up or by using a separation column with a more retentive stationary phase.

3.3.1.3. Conclusions on Selective Enrichment

Selective enrichment of sulfur species from a hydrocarbon matrix such as natural gas can be performed inside the liner of a cooled PTV-type injector. If the liner of the injector is packed with a polar adsorbent, sulfur species from large sample volumes can be enriched on the packing material, while at the same time the lower hydrocarbons that could interfere with SCD detection are eliminated. From the study described above the adsorbent Chromosorb 104 was found to have the best sulfur-over-carbon selectivity and loadability among the eight adsorption materials investigated. The breakthrough volume of the Chromosorb 104 material is well above the 15 mL required to meet the specified detection limits. The PTV-based instrumentation for selective enrichment is easy to use and cheap in comparison with dedicated adsorption/thermal desorption instruments. As there is no transfer line between the ad-

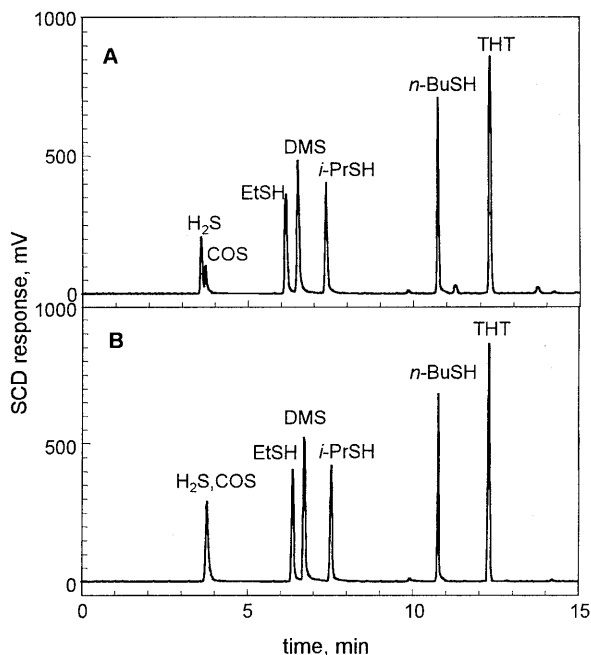


Figure 3.3: Selective adsorption of sulfur components on Chromosorb 104. Conditions: see Experimental. A - SCD chromatogram of a gaseous mixture of sulfur components using cold splitless injection, PTV temperature program: 30°C to 180°C at 12°C/sec. B - SCD chromatogram of the same mixture of sulfur components using the ATD technique, PTV initial temperature -75°C, purge time 7 min then programmed to 180°C at 12°C/sec.

sorption unit and the GC, the risk of loosing sulfur components by adsorption is minimized. The detection limits that can be achieved for sulfur analysis in natural gas are around $0.3 \mu\text{g}/\text{m}^3$ if preconcentration is used (with a sample volume of approx. 100 mL). Without preconcentration, the achievable limits are approx. 100 times higher.

3.3.2. Columns for Sulfur Analysis

3.3.2.1. Experimental Conditions

A number of capillary columns were evaluated in this study: a $35 \text{ m} \times 0.32 \text{ mm} \times 1.1 \mu\text{m}$ CP Sil-5 CB (Chrompack, Middelburg, The Netherlands), a $30 \text{ m} \times 0.32 \text{ mm} \times 4 \mu\text{m}$ SPBTM-1 SULFUR (Supelco, Bellefonte, PA, USA), a $23 \text{ m} \times 0.53 \text{ mm} \times 25 \mu\text{m}$ Carbo PLOT P7 (Chrompack), and a $30 \text{ m} \times 0.53 \text{ mm} \times 10 \mu\text{m}$ AT Q (Alltech Nederlands BV, Breda, the Netherlands).

For the evaluation of the performance of the various columns the chromatographic conditions were as specified below. The PTV was equipped with an empty deactivated glass liner or a liner packed with Chromosorb 104. Cold splitless injection was carried out with a splitless time of 2 min. A six-port VICI AG Valco Europe (Schenkon, Switzerland) with 1-mL sample loop made of 0.030 inch i.d. Teflon tubing was used to inject the gaseous sample into the PTV injector. The temperature program set on the PTV ran from 30°C to 250°C at $12^\circ\text{C}/\text{sec}$ for the empty glass liner and from -75°C to 180°C at $12^\circ\text{C}/\text{sec}$ when the packed liner was used.

3.3.2.2. Non-Polar Thick-Film Column

The polarity, adsorptivity, and reactivity of the investigated sulfur components logically lead to the choice of a non-polar thick film column for their separation. The apolar nature of the stationary phase prevents possible reactions of the sulfur components on the column surface, which could lead to peak tailing and band broadening. At the same time, the thick film provides an effective shield for the sulfur species against residual reactive/adsorptive sites on the wall of the fused silica column. Moreover, a column with a low phase ratio will give sufficient retention to the volatile compounds investigated in our study.

Figure 3.4A shows an SCD chromatogram of the sulfur gas mixture on a $1.1\text{-}\mu\text{m}$ CP Sil-5 CB thick-film column (phase ratio 75) using cold splitless injection

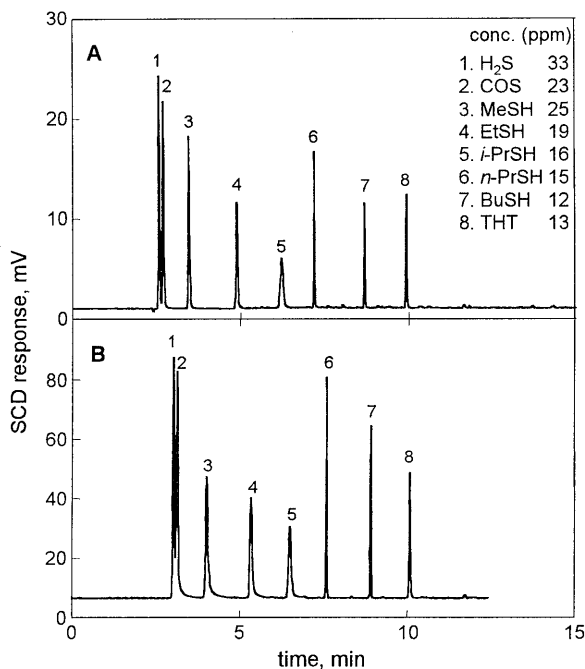


Figure 3.4: Chromatogram of sulfur components on a 1.1- μm thick-film non-polar capillary column. Oven temperature program: 30°C (5 min) to 150°C at 20°C/min. Injection: A - cold splitless with syringe, inj. volume 20 μL , PTV temperature program: 30°C to 250°C at 12°C/sec, splitless time 2 min; B - ATD technique, inj. volume 1 mL with loop, adsorption at -75°C on Chromosorb 104 liner, PTV temperature program: -75°C to 250°C at 12°C/sec, splitless time 2 min.

shown in Figure 3.4B. In this experiment the PTV was equipped with a Chromosorb 104 packed liner and the temperature of the liner was programmed from -75°C to 180°C at 12°C/sec. The high polarity of the Chromosorb 104 packing material caused the H₂S and COS to be pre-separated in a reverse order relative to that of the following chromatographic separation on the non-polar column. Hence, the final separation between those two critical components was largely reduced, which can lead to errors in quantification.

The effect of preconcentration using a liner packed with a polar adsorption material is reflected in the significantly higher degree of tailing for the MeSH,

(syringe injection). For this purpose the PTV was equipped with an empty glass liner and programmed from 30°C initially, followed by heating to 250°C at 12°C/sec. The oven temperature was programmed as follows: 30°C (5 min) to 150°C at 30°C/min. It is clear from the figure that at the lowest achievable initial oven temperature, this column gives adequate baseline separation between H₂S and COS if syringe injection is used. This, however, is no longer true, when a sample pretreatment procedure based on the adsorption-thermal desorption (ATD) technique (see Section 3.3.1) is incorporated in the method. A chromatogram recorded in this case is

EtSH and *i*-PrSH peaks. The use of this procedure gives rise to a somewhat broadened injection band, because desorption of the components from the adsorbent is not infinitely fast. This band broadening is only partially eliminated by cold trapping in the beginning of the GC column. The later eluting peaks, *i.e.* *n*-PrSH, BuSH, and THT, did not show tailing due to more efficient cold trapping on the column. It is for this reason that commercial adsorption/desorption devices or purge and trap systems very often contain a cryotrap.

3.3.2.3. Ultra-Thick-Film Non-Polar Column

For improving the separation between H₂S and COS an ultra thick-film column ($d_f = 4 \mu\text{m}$ of SPBTM-1 SULFUR, phase ratio 20) was used. With this column it was expected that a better cold trapping of the components would be obtained. Figure 3.5 shows a chromatogram of the gaseous sulfur mixture on this column obtained using the ATD injection technique. From the figure it can be seen that with this thicker stationary phase the cold trapping effect indeed works more efficiently for the lower boiling compounds, *i.e.* *i*-PrSH. Despite this, the more volatile components still show some peak broadening and tailing. This problem can be solved by using a more efficient cryotrapping device, cooled with liquid nitrogen, or by using another column with an even higher retention power.

3.3.2.4. CarboPLOT P7 Column

It was tested whether a good separation between highly volatile compounds without the need of using a low initial oven temperature and a cryo cooled trapping device could be obtained by using the newly developed CarboPLOT column. In this column a

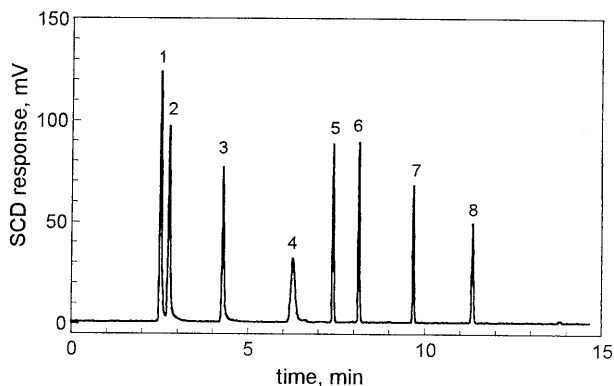


Figure 3.5: Chromatogram of sulfur components on a 4- μm thick-film non-polar capillary column. Injection: ATD technique, inj. volume 1 mL with loop, adsorption at -75°C on Chromosorb 104 liner, PTV temperature program: -75°C to 250°C at $12^\circ\text{C}/\text{sec}$. splitless time 2 min. Oven temperature program: 30°C (5 min) to 150°C at $20^\circ\text{C}/\text{min}$. Elution order and concentration: see Figure 3.4.

layer of deactivated carbon black deposited on the wall of the open tubular capillary column provides a very strong retention power for the separation of highly volatile compounds and even permanent gases. In our application the CarboPLOT column was found to be too strong. No single sulfur component had eluted, even after 60 min at 115°C, which is the highest allowable temperature for this column. Therefore, this column could not be used for the analytical problem at hand.

3.3.2.5. PoraPLOT Column

After the experiments with the CarboPLOT column, a PoraPLOT column was studied. This column combines the advantages from both capillary- and packed columns, *i.e.* strong retention (but less than CarboPLOT) and good resolving power. Figure 3.6 shows a chromatogram of the sulfur mixture on the PoraPLOT Q column. A good separation was obtained on the $30\text{ m} \times 0.53\text{ mm} \times 10\text{ }\mu\text{m AT Q}$ column. Despite the fact that this column did not contain a particle trap no problems with detector stability were seen.

3.3.2.6. Conclusions on Columns for Sulfur Separation

From the study described above, it can be concluded that the $4\text{ }\mu\text{m}$ thick-film SPBTM-1 SULFUR column and the AT Q column are the best choices for the separation of sulfur components from natural gas. While the former gives good peak shapes for all components of interest and adequate separation of the most critical peak pair H₂S/COS, the latter provides an excellent separation for this cluster even at higher initial oven temperatures. The only disadvantage of this column is the slight peak tailing and band broadening for some compo-

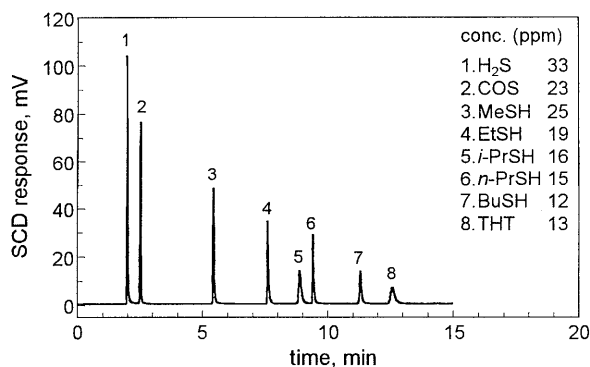


Figure 3.6: Chromatogram of sulfur components on a PLOT Q column. Injection: ATD technique, inj. volume 1 mL with loop, adsorption at -75°C on Chromosorb 104 liner, PTV temperature program: -75°C to 250°C at 12°C/sec. splitless time 2 min. Column $30\text{ m} \times 530\text{ }\mu\text{m} \times 10\text{ }\mu\text{m AT Q}$; oven temperature program: 70°C (3 min) to 200°C at 20°C/min.

nents such as *i*-PrSH and THT (Figure 3.7). This results in somewhat higher detection limits for these components. The main features of the two columns are listed in Table 3.5. It should be emphasized here that the SPBTM-1 column gives good results only if it is used in combination with a (CO₂ cooled) cryotrap. The use of a cryotrap is not necessary if an AT Q column is used.

Table 3.5: Main features of the capillary columns suitable for sulfur determination in natural gas.

Column	Length (m)	i.d. (mm)	d _f (μm)	Plate number	repeatability of t _R RSD (%)	adsorption
SPB TM -1	30	0.320	4	49×10 ³	0.1-0.5	no
AT Q	30	0.543	10	24×10 ³	0.2-0.5	no

3.3.3. Calibration Techniques

The final step in qualification of sulfur components in natural gas is the conversion of peak areas to concentrations. For this purpose calibration mixtures are required. Methods for the preparation of gaseous standard mixtures can be roughly classified as static or dynamic. Static methods involve preparation and storing the mixture in a closed vessel such as a gas cylinder. These methods are preferred when comparatively small volumes of mixtures are required at moderately high concentration levels. Unfortunately, however,

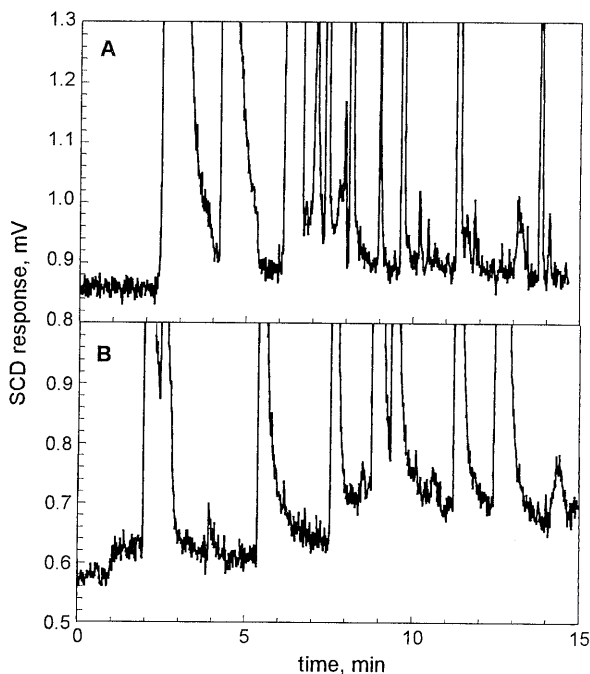


Figure 3.7: Enlarge chromatograms of sulfur components separated on the SPBTM-1 SULFUR column (A) and the AT Q column (B). Injection: ATD technique, inj. volume 1 ml with loop, adsorption at -75°C on Chromosorb 104 liner, PTV temperature chromatogram: -75°C to 250°C at 12°C/sec, splitless time 2 min.

losses of components by adsorption on the vessel walls may occur. Dynamic systems generate a continuous flow of mixture and can produce large volumes, with lower surface losses, owing to the equilibration of the walls by the flowing gas stream.

3.3.3.1. Static Methods for the Preparation of Standards

Principles

Static standards for sulfur analysis are generally prepared by the gravimetric method. A known amount of the components of interest is weighed into a gas cylinder which is then pressurized with a so-called 'balance gas' and weighed again. From the weight of the test component and the weight of the balance gas the concentration of the standard can be calculated. The standard prepared in this way is called a primary standard (but not necessarily a certified reference material!) because the concentration of the component in the calibration mixture is directly related to the measurement of basic standard units (mass, time, length *etc.*). With the gravimetric method it is possible to prepare compositions very close to the desired composition. For a more detailed overview of the backgrounds of this method as well as for a discussion of the possible errors in this method the reader is referred to Chapter 1, section 1.5.

Practical evaluation

Several single- as well as multiple component (sulfur) calibration gas cylinders were analyzed to evaluate the applicability of cylinders containing gaseous standards. All gas cylinders were purchased from Scott Specialty Gases and BOC Special Gases (London, UK). In all cylinders methane was used as the balance gas.

Figure 3.8 shows a schematic diagram of the dilution system used in the present study to investigate the features of the static calibration technique. Pure methane supplied from a separate cylinder (AGA Gas BV, Amsterdam, the Netherlands) was used as the dilution gas to produce lower concentrations of sulfur compounds in the gas stream. For proper operation it is extremely important that the system is free of pressure drops. Otherwise the flow rate of the pure calibration gas might depend on the total gas flow rate applied. This might lead to errors in the calculation of the actual concentration. The main characteristics that were investigated included: *i/* overall stabilization time of the gas sampling system

and *ii*/ accuracy and precision (repeatability) of concentrations of sulfur components in gas standards as well as in diluted gas streams (prepared using the system shown in Figure 3.8).

In Figure 3.9 peak areas of H₂S from a single-component gas standard cylinder recorded on an SCD are plotted against the

volume of gas passed through the system. The gas flow rate of the calibration gas was set at 1 L/min. No dilution gas was added. The first chromatogram was recorded immediately after opening the cylinders. From Figure 3.9 it is clear that the system requires a fairly long stabilization time (two hours). This is most likely due to the slow saturation of surfaces exposed to the gas stream (metal coupling pieces in particular). It is therefore advisable to reduce the number of coupling pieces to an absolute minimum, or preferably use PTEF (Teflon) couplings solely.

To calculate the concentrations (ppm vol) in the diluted gas streams the following equation was applied:

$$C = \frac{C_0 \cdot t_{tot}}{t_0} \quad (3.1)$$

C_0 original concentrations in the calibration cylinder (ppm vol),

t_0 time needed for 1 L of the gas standard to pass through the system (measured from volumeter) (minutes),

t_{tot} time needed for 1 L of the diluted gas stream (combined gas stream) to pass through the system (measured from volumeter) (minutes).

In order for equation 3.1 to be valid, the pressure drop in the gas sampling system and in particular downstream of the mixing chamber should be negligible. To achieve this a Teflon tube with a very large inner diameter (4 mm) was used for mixing the combined gas streams. Also the venting line was constructed of

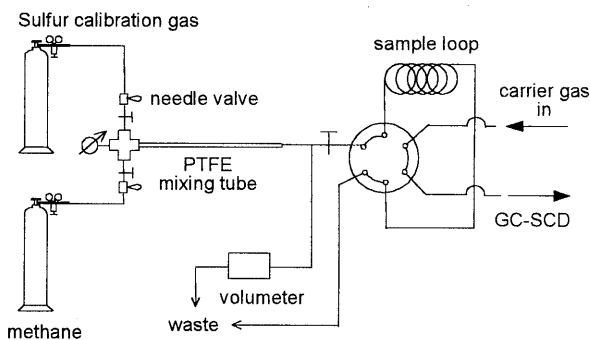


Figure 3.8: Instrumentation used for diluting gaseous calibration standards. Valve and coupling devices are made from stainless steel 316.

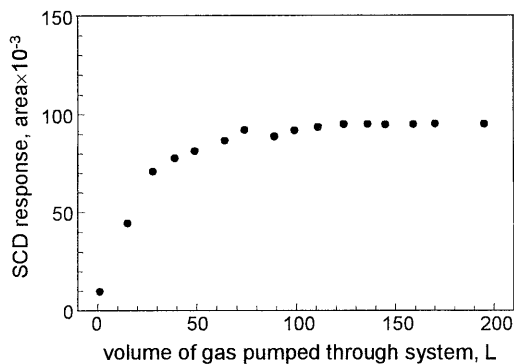


Figure 3.9: Intensity of the H₂S peak measured on the SCD versus the volume of gas purged through the gas sampling system shown in Figure 3.8. The total gas flow rate was 1 L/min. The internal volume of the system was approximately 50 mL.

tubing with a large inner diameter, again to prevent high pressure drops, also downstream of the sample loop. A less critical system can be obtained if the needle valves are replaced by (electronic) mass flow controllers. In this case the system automatically corrects for differences in the pressure drop.

Apart from calculation according to equation 3.1, the concentrations of the sulfur components in the combined

gas stream were also calculated from the peak areas measured on the SCD by comparison with peak areas found for gaseous mixtures prepared using the permeation and the diffusion device, respectively (*viz.* section 3.5.2). A comparison of calculated sulfur concentrations with repeatability data expressed by the relative standard deviation (RSD) value found in replicate peak area measurements obtained using the two methods described above are shown in Table 3.6. From this table a number of interesting conclusions can be drawn. On the first place it is obvious that it is not recommendable to dilute the original gas sample with more than a factor of 10. At higher dilution factors high RSD values are observed. Moreover, low concentration gas cylinders are not recommended because of the high uncertainty. The uncertainties specified by the manufacturer can be up to 40 or 50%. In our case, for the single-component gas cylinders evaluated the difference between the measured and specified concentration was as large as a factor of 2-3! It is also interesting to see the strong decrease in the concentration of EtSH in cylinder No 5700336 that occurred over a period of 7 months. Thus, for reasons of reliability, this static method should be used only in case of relatively high concentrations (*i.e.* 10 ppm or higher levels).

3.3.3.2. Dynamic Methods for the Preparation of Standards

Basically two different methods for the dynamic preparation of sulfur standards can be distinguished. The first method makes use of diffusion devices such as

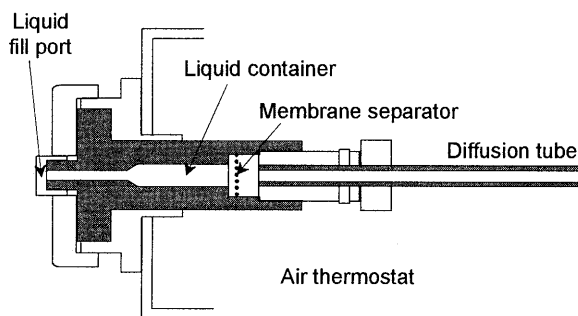


Figure 3.10: Schematic representation of a diffusion device for the preparation of gas standard.

the one schematically depicted in figure 3.10. The diffusion technique is based on constant diffusion of a vapor through a narrow tube or a capillary.

Diffusion devices such as the one described in Figure 3.10 are useful and simple devices for preparing mixtures of (moderately) volatile liquids. Within limits, broad concentration ranges can be prepared by varying the tube

dimensions and/or the flow of dilution gas. The actual concentration can be calculated from the measured weight loss of the tube and the total volume of dilution gas passed through the diffusion cell using the following equation:

$$C_{gas} = \frac{\Delta m \cdot V_{mol} \cdot 10^6}{Q_{gas} \cdot M_{comp}} \quad (3.2)$$

- C_{gas} Concentration of the test component in the calibration gas (ppm vol),
 Δm Weight loss rate of the test device (g/min),
 Q_{gas} Volumetric flow rate of the dilution gas passed through the diffusion cell (L/min, measured at temperature T),
 V_{mol} Molar volume of the test component at temperature T and ambient pressure (L/mole).
 M_{comp} Molecular weight of the test component (g/mol).

Because the concentrations are calculated from weights and volumes the standards prepared in this way are primary standards. Practical experiences with the DKK diffusion devices evaluated in the present study will be described in the next sections.

Table 3.6: Evaluation of gas standard cylinders

Multi-component gas cylinder		Dilution factor																			
Cyl. No.	Compound	1.0				2.2				3.0				6.7				36.7			
		C _A (ppm)	C _B (ppm)	RSD (%)	Note	C _A (ppm)	C _B (ppm)	RSD (%)	Note	C _A (ppm)	C _B (ppm)	RSD (%)	Note	C _A (ppm)	C _B (ppm)	RSD (%)	Note	C _A (ppm)	C _B (ppm)	RSD (%)	Note
5700568	H ₂ S	33	30.7	2.65	14.8	14.8	2.35	11.0	11.2	1.96	3.8	3.22	2.76	0.9	0.76	4.85		0.9	0.76	4.85	
	COS	23	26.8	2.87	10.3	15.5	2.41	7.7	11.8	1.94	2.7	3.74	4.26	0.7	1.02	5.83		0.7	1.02	5.83	
	MeSH	25	22.7	3.46	11.2	12.2	1.98	8.3	9.2	1.33	2.9	2.74	2.67	0.7	0.65	4.95		0.7	0.65	4.95	
	EtSH	19	18.5	3.78	8.5	9.7	2.57	6.3	7.3	3.23	2.2	2.14	2.26	0.5	0.50	1.53		0.5	0.50	1.53	
	<i>i</i> -PrSH	16	15.5	2.37	7.2	8.1	2.31	5.3	6.1	2.37	1.8	1.82	2.10	0.4	0.43	4.20		0.4	0.43	4.20	
	<i>n</i> -PrSH	15	15.4	2.45	6.7	7.9	2.09	5.0	6.0	1.40	1.7	1.81	2.76	0.4	0.41	4.72		0.4	0.41	4.72	
	BuSH	12	12.7	2.54	5.4	6.3	2.77	4.0	4.8	1.50	1.4	1.45	1.80	0.3	0.32	2.04		0.3	0.32	2.04	
	THT	13	11.8	2.96	5.8	6.3	2.50	4.3	4.7	1.15	1.5	1.51	2.76	0.4	0.35	3.47		0.4	0.35	3.47	
Single-component gas cylinders																					
Cyl. No. (Scott)	Compound	C _A (ppm)	C _B (ppm)	RSD (%)	Note	Cyl. No. (BOC)	Compound	C _A (ppm)	C _B (ppm)	RSD (%)											
5700247	H ₂ S	2	0.89	6.28		105668	H ₂ S	1.8	1.57	2.24											
5700464	EtSH	8	6.86	4.83		105663	H ₂ S	3.7	3.50	5.01											
5700476	MeSH	8	9.35	8.09		95543	COS	3.5	4.64	6.62											
5700140	MeSH	2	0.31	9.40		106664	COS	2.3	3.29	4.70											
	DMDS	0	2.92	1.12																	
2700336		2	4.65	2.61	Measured in June 1994																
		2	2.79	1.01	Measured in January 1995																

C_A Original manufacturer's quoted concentration in ppm mol,
 C_B Concentration (ppm mol) calculated from measured peak areas using the MeSH permeation device for generating a calibration gas mixture
 RSD All the relative standard deviations relate to C_B, calculated from the replicate peak area measurements.

A second method for the dynamic generation of gaseous calibration mixtures relies on the use of permeation devices. Permeation tube devices are nowadays very popular. The permeation tube contains a volatile liquid sealed in an inert permeable membrane, usually polytetrafluorethylene or a fluorinated copolymer of ethylene and propylene, through which the test compound diffuses at a fixed rate. The driving force behind the process is the difference in partial pressure between the inner and outer walls of the tube. This depends on the dissolution of the vapor in the membrane, the rate of diffusion through the membrane wall and the rate at which the vapor is removed from the outer surface of the membrane. The actual concentration of the test component in the dilution gas is again calculated from the weight loss of the tube and the total volume of gas used (equation 3.2).

For samples with a low vapor pressure at room temperature, elevated temperatures are used to raise the permeation rates and to yield the desired concentration values. Gases or vapors with a high membrane permeability require devices other than the standard single-walled tubes. For both diffusion devices as well as permeation tubes the use of an accurately thermostated oven (temperature fluctuations $< 0.1^{\circ}\text{C}$) is essential because the diffusion rate may vary strongly with temperature. As a rule of thumb, the permeation rate doubles at an increase in temperature of approximately 7°C . Because the concentrations in the test gas are calculated from weight and volume data, the standards prepared in this way are again primary standards.

Practical experiences with the DKK diffusion and permeation system

Instrumentation: An instrument for the dynamic generation of gas standards according to the diffusion or permeation method is fairly simple from its basic principles. The instrument should contain an accurately thermostated oven and an accurate flow controller. In the present study a commercially available gas generator (DKK, model GST-1, Tokyo, Japan) was used. A schematic overview of the instrumentation is given in Figure 3.11. Model experiments were performed with permeation tubes filled with MeSH and COS which were purchased from Bester B.V. (Amstelveen, the Netherlands). For the diffusion experiments, the diffusion device and diffusion tubes supplied by DKK were used. Air filtered over an activated carbon and a Molsieve filter was used as the dilution gas. The dilution air flow rate that can be used ranges from 200 mL/min to 2 L/min. Higher flow rates are possible if the PTFE restrictor inside the instru-

ment is changed. For maximum stability an air flow rate of around 1 L/min should be used.

Concentration range: In the present project calibration gases with extremely low concentrations of the components of interest had to be prepared. This can be achieved by using extremely high dilution gas flows or by working under conditions where the delivery of the test component by the permeation device is low.

In the experiments air flows in the range of 0.2-2 L/min were used. It was found that the minimum concentration that could be prepared was about 0.5 mg/m^3 for the diffusion device and 0.2 mg/m^3 for the permeation tubes. Lower concentrations can be prepared by using conditions under which the delivery of the permeation/diffusion tube is lower. Under these conditions, however, it is extremely difficult to determine the weight loss of the devices. This is especially true for the diffusion device which has a higher overall mass than the permeation tube (70 g vs. 5 g). For each permeation tube the manufacturer supplies a certificate in which the weight loss of the tube (under standardized conditions) is specified. The experimentally determined weight losses were found to be in good agreement with the values specified by the manufacturer. This could mean that it is not necessary to measure weight losses experimentally. As only two permeation tubes were tested it is uncertain whether this is always the case. In principle it is possible to apply both the diffusion and permeation system also for the preparation of calibration gases with lower concentrations by incorporating an additional gas dilution step in the procedure. This has not been evaluated in detail. The maximum concentration that can be prepared is approximately 100 mg/m^3 for both systems. More detailed information will be presented below.

Practical experiences with the DKK diffusion device

The liquid sulfur component that was used for evaluation of the DKK diffusion

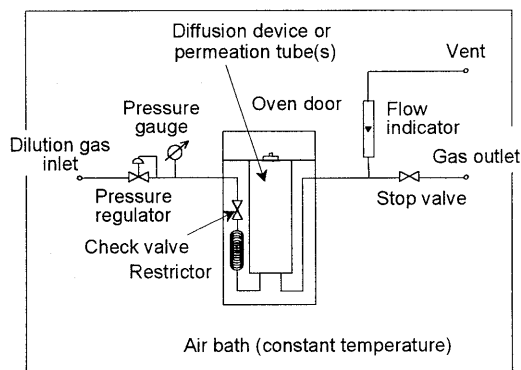


Figure 3.11: Schematic representation of the DKK GST-1 instrument for dynamic generation of calibration gases.

device was THT. The stabilization experiment was carried out in the same manner as in the case of the static calibration method. The peak area of THT measured on the SCD is plotted *versus* time in Figure 3.12. Here the time axis represents the time passed from the moment the diffusion cell was installed in the thermostated oven of the gas generator. From this figure one can conclude that the stabilization time of the diffusion device is approximately two hours.

The dependence of the THT "loss rate" on the bath temperature is also depicted in Figure 3.12. Here the loss rate is determined by the peak areas of the sulfur peak at a constant injection volume.

The dependence of the THT loss rate (expressed as its concentration in the gas stream) as a function of the diffusion tube diameter is studied as well. From the data collected we can conclude that a linear relationship exists between the concentration of the THT in the gas stream and the square of the diffusion tube inner diameter. This is in accordance with theory. Some deviation was observed for the 5 mm i.d. tube. The most likely reason is that the liquid standard had flown into the test tube once this tube is put on its side, thereby shortening the effective length of the tube. This problem did not occur when smaller diameter tubes were applied. The bath temperature used in the experiments was 30°C. The dilution gas (air) flow rate was set at 1 L/min. These values of bath temperature and gas flow rate are recommended by the manufacturer because they yield maximum stability for the gas generator operation. Shortening the tube's length by a factor of two, *i.e.* using a diffusion tube of 5 cm instead of 10 cm, increased the concentrations of THT by a factor of two. This is also expected from theory.

The relative standard deviation values (RSD) of peak areas obtained for a 1 mL injection of the calibration gas stream generated using the diffusion device was approximately 6% (provided that the system was giving sufficient time for stabilization). This number includes also deviations in the injection loop volume and errors in detection. Hence, it can be concluded that the deviations caused by the generation of the calibration gas mixture itself are significantly less than 6%. The accuracy of the method strongly depends on the concentration level of the sulfur species in the gas mixture prepared. The procedure for the calculation of the actual concentration is based on measuring the weight loss of the diffusion device. For low concentrations ($< 1 \text{ mg/m}^3$) the weighing error (about 1 mg absolute) will result in errors in the actual concentration easily exceeding 20%.

Here it should be realized that the total mass of the diffusion device is approximately 70 g. Weighing a weight loss of only some milligrams at this absolute level is very inaccurate unless special, dedicated weighing devices are used. When higher concentrations are considered, the error in the determination of the concentration of the sulfur species in the natural gas is significantly lower. The error in the concentration level at a concentration of 100 mg/m^3 is less than 0.1% to 0.4%

Practical experiences with the DKK permeation device

An important advantage of permeation devices over the diffusion methods occurs in the weighing procedure of the tube. Because the overall weight of a permeation tube is low in comparison to that of the diffusion device, weighing errors are much lower. Here another interesting feature of permeation devices should be mentioned. For every tube-type the manufacturer gives the approximate value of the emission rate of the tube under standard conditions as well as the standard deviation of this parameter. This standard deviation for most of the tubes is lower than 10%. If this error is acceptable in the calibration, it is possible to use the permeation tube without the need to perform weight-difference measurements. Experiments in our laboratory indicate that the weight loss found experimentally for the two tubes that were used were in good agreement with the value specified by the manufacturer. An additional advantage of permeation tubes is that it is possible to prepare multi-component calibration mixtures simply by putting more than one tube in the oven compartment.

The long stabilization times required are a well-known disadvantage of permeation tubes. In our case a stabilization time of 1 week was found. This is in agreement with values quoted in literature. The influence of the flow rate of the

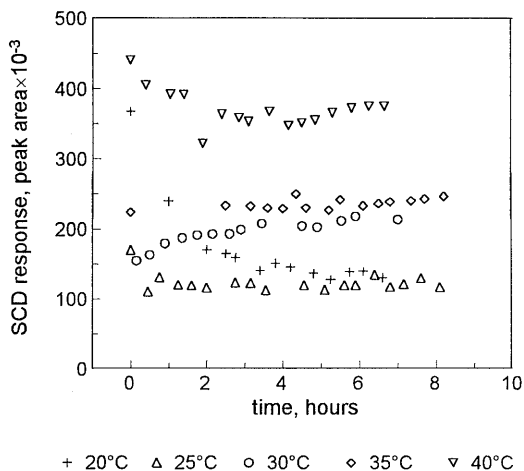


Figure 3.12: Equilibration of the calibration gas standard prepared using the DKK diffusion device. THT was used as the test compound. Diffusion tube i.d. 1 mm, length 10 cm.

dilution gas on the concentration of the test component in the calibration gas mixture is illustrated in Table 3.7. For the calculation of the concentrations (and hence the loss rate) of MeSH at various dilution gas flow rates the loss rate at 1 L/min dilution gas (air) was set at 39 ng/(min.cm). This is the loss rate value specified by the manufacturer. The other values were then calculated from the peak areas measured on the SCD.

From Table 3.7 it can be concluded that the flow rate has no effect on the weight loss of the diffusion tube. It is therefore possible to prepare different concentrations by changing the flow rate of the dilution gas. Care should be taken not to leave the region between the minimum flow rate and the maximum flow of the dilution gas for the present instrument (200 mL/min to 2 L/min). The repeatability of absolute peak areas for a 1 mL injection of the calibration gas was in the range of 4% to 9%. This again includes errors in sampling and detection as well. The high precision and the flexibility with regard to the preparation of different concentrations by using different dilution gas flow rates render the permeation method very attractive and highly promising. Apart from the long time required for stabilization the only disadvantages of the method are the high cost (approximately 250 to 700 NLG) and limited lifetime of the permeation tubes. Depending on the volatility of the component a permeation tube has

Table 3.7: Evaluation of the MeSH and COS permeation tubes purchased from Bester (Amstelveen, the Netherlands).

	MeSH		COS	
	loss rate (ng/min/cm)	Precision RSD (%)	loss rate (ng/min)	Precision RSD (%)
<i>Manufacturer's quoted value</i>	39	+/-10	450	+/-25
<i>Measured by weighing</i>	37.8	11.73	472.2	10.20
<i>Calculated from peak areas*</i>				
dilution gas flow (L/min)				
0.2	38.2	3.87	465.6	6.76
0.6	39.0	3.94		
1.0	39.0	5.22		
1.4	36.9	4.27		
1.8	38.8	8.52		
2.0	37.9	8.79		

* The loss rate at dilution gas flow rates other than 1 L/min were calculated using the relative peak areas measured on the SCD. The peak area of MeSH at a dilution gas flow rate of 1 L/min was used as a point of reference. At this point the manufacturer quoted loss rate of 39 ng/min/cm for MeSH was used.

a lifetime of 2 to 12 months. If the permeation tubes are compared with gas standard cylinders (with purchase prices of NLG 1,000-2,000 per cylinder and a lifetime of 1 to 2 years) the operational costs are approximately the same. The use of diffusion and permeation devices, however, requires a gas generator, which costs some NLG 20,000.

3.3.3.3. Conclusions on the Preparation of Gaseous Calibration Standards

From the study described above it can be concluded that for the preparation of concentrated calibration gas mixtures (higher ppm level) the use of cylinders with calibration gases is the best choice. When lower concentrations are required or if standards covering a fairly wide concentration range are needed, dynamic preparation techniques should be the techniques of choice. In case of sulfur determination in natural gas where typical total sulfur concentrations are in the low ppm range, the use of calibration gas cylinders can result in large errors in quantitation. Of the two techniques for dynamic generation of standards, diffusion and permeation methods, the use of permeation devices is more attractive owing to its higher accuracy and precision as well as due to its ruggedness, simplicity and ease of use. A disadvantage of this method is the very long stabilization time required. Stabilization can take weeks, but once equilibrium has been achieved the tubes can be used for 2 to 12 months, depending on the volatility of the component in the permeation tube. If the laboratory is equipped with highly accurate weighing facilities, diffusion devices may be preferable due to their much lower operating costs. The operational costs of the permeation device and of gas standard cylinders are of the same magnitude. However, the use of diffusion or permeation devices requires an initial investment in a gas generator oven (approximately NLG 20,000).

3.4. CONCLUSIONS

The selection of the detector to be used for a given application defines the requirements being imposed on the sample preconcentration step and the subsequent GC separation. Based on the choice of the SCD, the calculated desired injection volume is approx. 15 mL. As this value exceeds the maximum injection volume in capillary GC, an enrichment step must be employed. To this end the ATD technique was evaluated. A number of solid adsorption materials was

investigated using a PTV injector as the ATD device. The best material in terms of sulfur-*over*-carbon selectivity and loadability was found to be Chromosorb 104. Adsorption is carried out at -75°C . Purge times of 2 to 10 minutes are needed to eliminate hydrocarbons from C_1 to C_4 .

The column in use does not have to separate sulfur components from hydrocarbons due to the quenching-free feature of the SCD. It should, however, separate the individual sulfur species, especially the critical peak pair $\text{H}_2\text{S}/\text{COS}$. An ultra-thick film apolar $30\text{ m} \times 320\ \mu\text{m} \times 4\ \mu\text{m}$ SPBTM-1 SULFUR column fulfills this requirement. The AT-Q column is an attractive alternative, although some reactivity towards sulfur components has been observed.

For the preparation of concentrated calibration gas mixtures (higher ppm level) the use of cylinders with calibration gasses is the best choice. When lower concentrations are required or if standards covering a fairly wide concentration range are needed, dynamic preparation techniques, especially those based on permeation devices, should be the technique of choice.

Chapter 4

NEWLY DESIGNED PROCEDURE FOR DETERMINATION OF SULFUR COMPONENTS IN NATURAL GAS¹

ABSTRACT

The evaluatory studies described in previous chapters resulted in a new procedure for sulfur determination in natural gas. The system proposed consists of a preconcentration platform based on a programmed-temperature vaporizer injector equipped with a liner packed with Chromosorb 104, a very thick-film apolar capillary column for separation, and detection using a sulfur chemiluminescence detector. In this chapter, the newly proposed procedure is evaluated in terms of precision and accuracy, as well as with regard to detection limits in relation to the sample volume injected. It is shown that with the current set-up sulfur components present in natural gas at extremely low concentration level, i.e. sub-microgram sulfur per cubic meter, can be detected.

¹ Published as a part of the article: "Improved Method for the Determination of Sulfur Components in Natural Gas" by H. Pham Tuan, H.-G. Janssen, E. M. Kuiper-van Loo, and H. Vlap in *J. High Resol. Chromatogr.*, 18 (1995) 525-534.

4.1. INTRODUCTION

From the previous chapters it can be concluded that the optimum instrumental set-up for the determination of low concentrations of sulfur containing species in natural gas consists of a selective sample enrichment procedure based on the selective adsorption of the components of interest on Chromosorb 104, followed by a separation step performed on a non-polar ultra-thick film column in combination with a sulfur selective detection device such as the sulfur chemiluminescence detector. In this chapter such an instrument is constructed and evaluated. The results of the new method are compared with those obtained using the technique currently in use (packed column GC - FPD). The quantitative aspects of the new method (repeatability, precision and accuracy) will be studied by the analysis of natural gas samples with accurately known concentrations of sulfur components.

4.2. EXPERIMENTAL

4.2.1. Instrumental Set-up

The complete instrumental set-up used for sulfur determination in natural gas is shown in Figure 4.1.

Injector: Programmed temperature vaporizer (PTV) KAS II (Gerstel, Mülheim a/d Ruhr, Germany); liquid CO₂ cooling; liner packed with Chromosorb 104; splitless time: 2 min; temperature program: -75°C to 180°C (5 min) at 12°C/sec;

Sampling valve: six-port VICI AG Valco Europe (Schenkon, Switzerland) with 1-mL, 13-mL or 100-mL loop, respectively, made from PTFE tubing;

GC: HP 5890A Hewlett-Packard (Avondale, PA, USA);

Column: 30 m × 0.32 mm × 4 μm SPBTM-1 SULFUR (Supelco, Bellefonte, PA, USA);

Carrier gas: Helium, column head pressure 10 psi, split flow rate 100 mL/min;

Oven temperature program: 30°C (5 min) to 150°C at 20°C/min;

Detector: A Sievers SCD 350B was purchased from Gerstel Benelux B.V. (Bri-

elle, the Netherlands). The SCD is mounted on top of the FID (Hewlett-Packard) using an adjustable adapter (Gerstel). The temperature of the FID housing was set at 250°C. The hydrogen flow rate was 190 mL/min and air 400 mL/min. Pure oxygen with a flow rate of 50 mL/min was used for the SCD ozone generator.

Calibration: A COS permeation device with a loss rate of 450 ng/min ($\pm 25\%$ at 30°C)² and a

MeSH permeation tube with a loss rate of 39 ng/min/cm ($\pm 10\%$ at 30°C) (VICI Metronics, Santa Clara, CA, USA) were purchased from Bester (Amstelveen, the Netherlands). These permeation devices were inserted into the oven of a DKK Model GST-1 calibration gas generator (DKK Corporation, Tokyo, Japan). The temperature was set to 30°C. Air was used as the dilution gas at a flow rate of 200 mL/min.

Data system: A two-channel Nelson Omega 5.2 data system (Perkin-Elmer) was used for collecting data from both the FID and SCD simultaneously.

Natural gas samples: Stainless steel bottles containing natural gas samples with sulfur components at various concentration levels obtained from various locations within the Netherlands (samples A, B, C, etc.) were supplied by Gasunie Research (Groningen, the Netherlands).

4.2.2. Sampling Procedure

The gas sample is filled into the sample loop. During flushing of the loop the

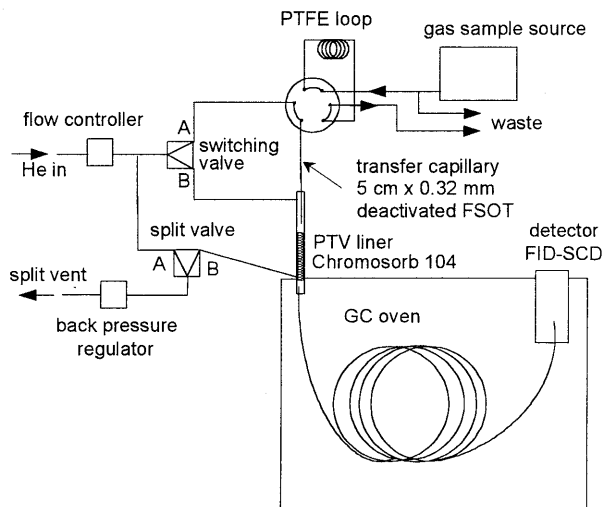


Figure 4.1: Schematic diagram of the final instrument for sulfur determination in natural gas as constructed for use in the laboratory. Sampling valve is in the "load" position.

² The manufacture quotes the uncertainty as $\pm 25\%$. The exact meaning of this is unknown.

PTV liner is cooled to the adsorption temperature (-75°C). During this stage of the procedure the switching valve is in position A and the split valve in position B - open (see Figure 4.1) to lead the carrier gas through the sampling valve. Next the content of the sample loop is transferred to the PTV liner by switching the sampling valve from the "load" position to the "inject" position. Depending on the volume of the sample loop, *i.e.* 1 mL, 13 mL, or 100 mL, respectively, the transfer times used were increased from 30 sec to 5 min to ensure that the entire volume of sample was flushed to the PTV liner. During this period of time the sulfur components are trapped inside the liner. The helium flow rate during flushing was 100 mL/min. After completing transfer, the switching valve remains in position A for approximately 15 sec for flushing the transfer capillary and the valve. After that the switching valve was turned to position B in order to purge the liner (4 min). During this time the volatile hydrocarbons (up to C₄) are eliminated. Here a transfer capillary is used to direct the sample to the bed of adsorption material, in this way preventing possible adsorption losses in coupling devices and tubing, which are mostly made from stainless steel. Then the split valve is closed (changed to position A), the temperature programs of both the PTV and the GC oven are started, and the chromatogram is recorded.

The calibration process involved analysis of the external standards prepared using permeation tubes. The gas sample source in Figure 4.1 was replaced by the gas standard prepared using the calibration permeation device and the procedure described above was repeated.

4.3. RESULTS AND DISCUSSION

Using the procedure described above with a 1-mL sample loop, chromatograms such as that shown in Figure 4.2 were obtained. To compare the results obtained here with those obtained with the standardized method currently in use, *i.e.* packed column GC - FPD, a chromatogram of the same sample but now obtained using the old procedure is shown in Figure 4.3. From these two figures it is clear that the new procedure is superior in several aspects. Firstly the new procedure is more selective. No hydrocarbon peaks show up in the chromatogram. This in contrast to the situation with the standardized procedure where high peaks of methane, ethane, and propane are seen in the FPD chromatogram. Further, the signal-to-noise ratio is better in the new chromatogram leading to

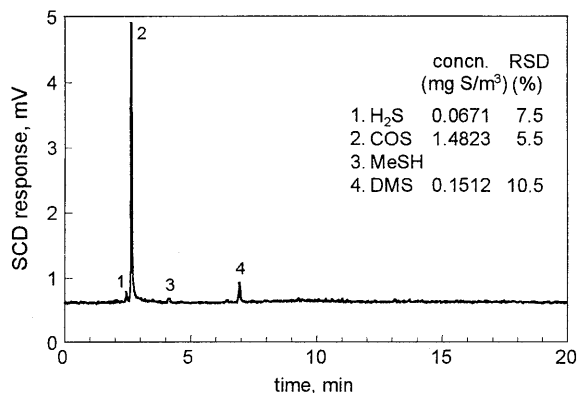


Figure 4.2: Chromatogram of sulfur components in natural gas sample A analyzed by the new method with a 1-mL sample loop. Chromatographic conditions: see section 4.2.1.

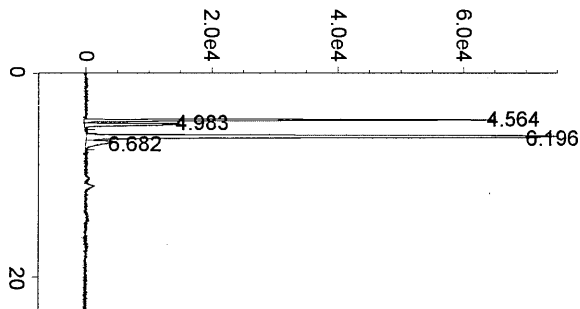


Figure 4.3: Chromatogram of sulfur components in natural gas sample A analyzed by the standardized method based on packed column GC - FPD. With increasing retention times the peaks are identified as methane, ethane, COS, and propane.

improved detection limits. In the new method four sulfur peaks, *i.e.* H₂S, COS, methyl mercaptan (MeSH) and dimethyl sulfide (DMS), can be seen, of which three can be quantified. In the standardized method only one sulfur peak (COS) can be seen and quantified. Last but not the least, the separation efficiency of the new method is higher ensuring the H₂S peak to be fully separated from the COS peak which is the main component. This allows completion of the analysis in a shorter time and results in more accurate peak area measurements for these two peaks.

If a larger sample loop is used the signal-to-noise ratio is further improved and also other sulfur components can now be quantified accurately (Figure 4.4). If a 13-mL loop is

used the quantitation limits now are 0.01 mg S/m³ (S/N = 10) and the detection limits are as low as 0.003 mg S/m³ (S/N = 3). With this set-up which incorporates a 13-mL sample loop, it is possible to detect a large number of sulfur components, which are undetectable if the old standardized method is used.

A summary of the results obtained from the analysis of the same sample (natural gas sample A) by the two methods, new- and standardized is shown in Table

4.1. With the old method quantitation was performed using gas standard mixtures taken from calibration gas cylinders. In the new method dynamic generation of calibration standards using permeation devices was employed. This table clearly illustrates the superiority of the new method in terms of detectability. Because of the higher overall selectivity of the method, also the risk of false positive sulfur analysis is greatly reduced. The precision of peak quantitation, expressed by the relative standard deviation (RSD) from three replicate peak area measurements, is generally in the range of 4-9%.

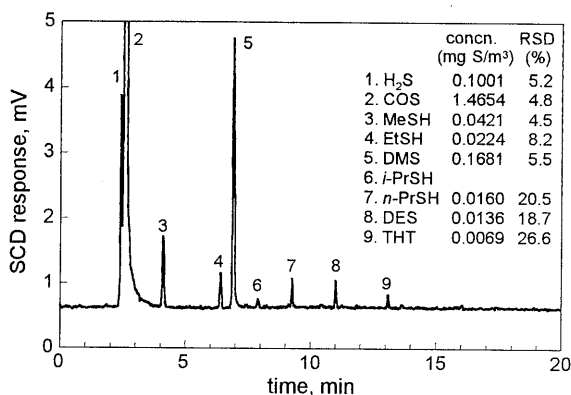


Figure 4.4: Chromatogram of sulfur components in natural gas sample A analyzed by the new method with a 13-mL sample loop. Chromatographic conditions: see section 4.2.1.

To estimate the accuracy of the new method, two more samples (natural gas samples B and C) were analyzed and the results were compared with those obtained by the old standardized method using statistical techniques. In each sample the COS content (the only sulfur compound that the old standardized method can detect and quantify) was measured three times using the 13-mL sample loop. From these data the statistical values such as mean, standard deviation, and confidence intervals are calculated. The accuracy is then calculated as the difference in COS concentrations (between average measured COS contents and those reported by old method) relative to the results obtained by standardized method. This calculation is summarized in Table 4.2. Using the Student's *t*-test for paired samples, the *t* value calculated is -1.22. From a comparison of this value with the tabulated critical value at a 0.05 significance level and 2 degrees of freedom (4.30) it can be concluded that the old and new method do not give significantly different values for the COS content. The large difference (decrease) in the COS content of the natural gas samples B and C is probably due to instability of this component during storage and transportation. The time between the two measurements was approximately 1 week.

Table 4.1: Comparison of the features of the new analytical procedure and the standardized method.

Compound detected	Standardized method		New method 1-mL loop		New method 13-mL loop	
	conc. (mg S/m ³)	RSD (%)	conc. (mg S/m ³)	RSD (%)	conc. (mg S/m ³)	RSD (%)
H ₂ S	nd ^a		0.0671	7.5	0.1001	5.2
COS	1.366	na ^b	1.4823	5.5	1.4654	4.8
MeSH	nd		nd		0.0421	4.5
EtSH	nd		nd		0.0224	8.2
DMS	nd		0.1512	10.5	0.1681	5.5
<i>i</i> -PrSH	nd		nd		DL ^c	
<i>n</i> -PrSH	nd		nd		0.0160	20.5
DES	nd		nd		0.0136	18.7
THT ^d	nd		nd		0.0069	26.6

^a nd = not detected;

^b na = not available,

^c DL = at the detection limit;

^d THT does not occur in untreated natural gas. The peak that elutes at the same retention time as THT may be thiophene, which is often found to be present in petroleum fractions.

Table 4.2: Evaluation of the accuracy of the new method using the 13-mL sample loop. Concentration of the target component COS is expressed in mg COS/m³

Sample	Old method	New method			Difference (mg/m ³)	Accuracy (%)
	conc. (mg/m ³)	conc. (mg/m ³)	std. dev. (mg/m ³)	conf. interval* (mg/m ³)		
A	1.59	2.74	0.13	±0.25	+1.15	+72.3
B	1.20	1.11	0.05	±0.09	-0.09	-7.5
C	0.61	0.65	0.03	±0.07	+0.04	+6.2
				average:	+0.37	
				std. dev.:	±0.68	

* Confidence intervals are calculated on a confidence level of 0.05. The degree of freedom was 2.

After analysis at the University of Eindhoven the natural gas samples were returned to the Gasunie and analyzed again using the standardized procedure. It was found that the COS content in both samples decreased over 200% relative to the first measurement performed by the Gasunie. From the results obtained on natural gas sample A we can conclude that the accuracy of the new method is within 10% relative to the standardized method.

In general, the number of sulfur components that are present in natural gas at relatively high concentration levels, *i.e.* 0.5 mg S/m³ or higher, is limited. In most cases the old standardized method can detect only COS, as in the previous example, and/or H₂S, which most natural gas samples contain before the sweetening process. Figure 4.5 shows a chromatogram of natural gas sample D. This

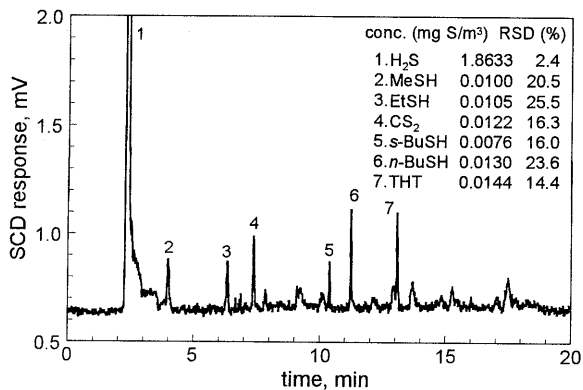


Figure 4.5: Chromatogram of sulfur components in natural gas sample D analyzed by the new method with a 13-mL sample loop. Chromatographic conditions: see Experimental.

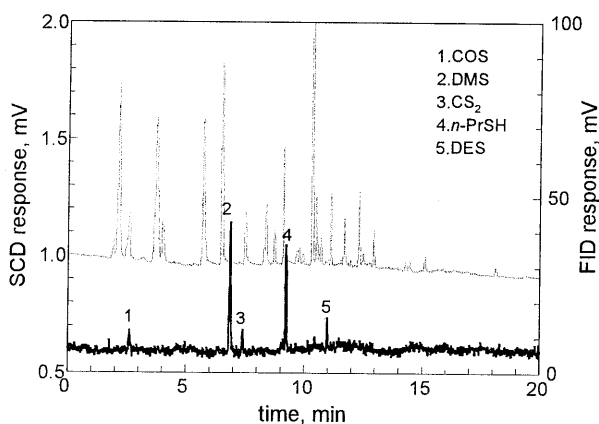


Figure 4.6: Chromatogram of sulfur components in natural gas sample E analyzed by the new method with a 13-mL sample loop. Chromatographic conditions: see Experimental. The dotted line is the FID signal. The full line is the SCD signal.

gas has a high content of H₂S. Figure 4.6 gives the result of the analysis of gas sample E, a gas that contains only few sulfur components at very low concentration levels.

Higher boiling sulfur components such as the higher mercaptans and sulfides are present in natural gas at extremely low concentrations. For these components the newly developed method with a 13-mL sampling loop gives peaks at detection limit level (see Figure 4.5 and 4.6). A logical approach for the accurate determination of these components is to increase the sample volume. For this purpose a direct sampling technique was employed. The natural gas bottle was connected directly to the transfer capillary that was lead into the injector via an open/close valve. When the PTV liner was ready at sub-ambient

adsorption temperature, *i.e.* -75°C , the carrier gas line was closed and the gas sample line opened. A volume-meter was connected to the split vent to control the volume of gas sample passing through the PTV liner. After the desired vol-

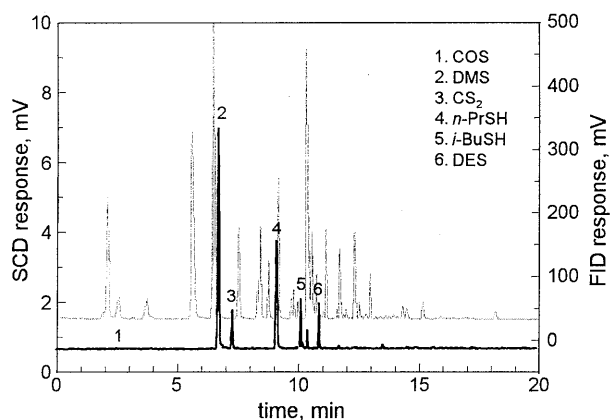


Figure 4.7: Chromatogram of sulfur components in natural gas sample E analyzed by the new method with 100 mL direct sampling. Chromatographic conditions: see Experimental. The dotted line is the FID signal. The full line is the SCD signal.

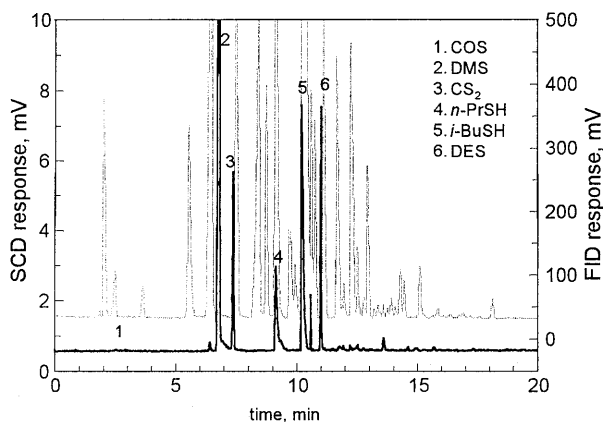


Figure 4.8: Chromatogram of sulfur components in natural gas sample E analyzed by the new method with 500 mL direct sampling. Chromatographic conditions: see Experimental. The dotted line is the FID signal. The full line is the SCD signal.

ume of natural gas was pumped through the liner, the sampling valve was closed and the carrier gas line opened to purge the liner. The desorption process and the chromatographic run were started simultaneously 4 min afterwards. Chromatograms of sample E are shown in Figure 4.7 and 4.8, where the sample volume was 100 mL, and 500 mL, respectively.

When comparing Figure 4.6 and Figure 4.7 it is clear that with larger sample volumes, the detection limits are greatly improved. This allows accurate quantitation of trace sulfur components. The sample volume, however, can not be increased unlimitedly. Together with the sulfur components, also the higher hydrocarbons, which are present in natural gas in large numbers and at relatively high concentrations, are ad-

sorbed. These components cannot be eliminated by using longer helium purging times due to their strong interaction with the adsorbent. The larger the sample volume, the higher the amounts of these hydrocarbons trapped in the liner. This is evident from the FID signals shown in figure 4.7 and 4.8. Large amounts of coeluting hydrocarbons can cause peak broadening of the sulfur species, such as seen from peak No. 4 in figure 4.8. The broadening complicates peak integration and can, hence, lead to quantitation errors. Large hydrocarbon peaks can also show up in the SCD chromatogram despite the extremely high detector selectivity. For example, the peak between peaks No. 5 and 6 in Figure 4.8 can incorrectly be identified as a sulfur peak. Depending on the concentrations of the higher hydrocarbons in the natural gas, the maximum allowable sample volume varies. If flame-based SCD is used for sulfur selective detection it can easily be verified whether a peak in the SCD signal originates from a sulfur containing component or from a high concentration of an alkane. If the peak is an alkane, a very high peak should also appear on the FID trace. If there is no peak or just a small peak on the FID chromatogram, the SCD peak originates from a sulfur component.

Having simultaneous FID and SCD signals is a very large advantage of the flame-based SCD. If other selective detectors are used one can never be sure that a peak is a sulfur peak and not a very high concentration of an alkane. Whether an alkane peak will show up in the chromatogram of a sulfur selective detector can be calculated from the concentration of the alkane in combination with the selectivity and sensitivity of the detector. An example of such a calculation is given below. At a detector sulfur-*over*-carbon selectivity of 10^6 and a detector detection limit of 15 pg S, an alkane will show up in the chromatogram if at least 15 μg C of this alkane is introduced into the chromatographic column. Assuming that the alkanes above C_6 are quantitatively trapped in the sample enrichment step and transferred onto the column, the maximum of gas that can be enriched can be calculated. Assuming that the concentration of C_6 in the gas is 0.01% vol (a typical value for hexane in natural gas) and further assuming that the column provides an optimum chromatographic performance, then the corresponding allowable sample volume will be approximately 40 mL. In practice the concentration of individual alkane isomers are lower by factor of 2-3. Moreover, large amounts of hydrocarbons often show severe peak broadening. Therefore, the sample volume can be larger by factor of 2-3 without the risk of

alkane peaks showing up in the chromatogram of the selective detector. In our study a sample volume of 100 mL is used as a safe upper limit.

When a large sample volume, *e.g.* 100 mL, is used, another important factor, the sampling flow rate, must be taken into consideration. During transfer of the loop contents into the liner, the adsorbent is purged with natural gas for a prolonged period. Due to the non-ideal behavior of natural gas the breakthrough volumes of the adsorbed sulfur species, especially of the most volatile ones H_2S and COS , were found to strongly depend on the gas flow rate. Figure 4.9 shows the effect of the sampling flow rate on the COS content of the gas sample B, relative to the value obtained with the 13-mL loop. From this figure it can be seen that with sampling flow rates up to approx. 50 mL/min, no component losses are observed. At higher sampling flow rates part of the adsorbed COS starts to break through, most likely due to displacement effects or a low plate number of the trap. At a small sample volume, *e.g.* 13 mL, no effect of the sampling flow rate on the recovery was observed.

Up till now, the adsorption-purge-thermal desorption (ATD) has been used for sample introduction. One question remains: can we achieve the required detection limits, *i.e.* 0.01 mg S/m^3 without using the sample enrichment technique?

To answer this question, two other injection methods were evaluated: hot split and direct on-column injection. The former was employed in order to avoid the cryofocusing step. To obtain sharp peaks for sulfur components, the time needed for the sample to be transferred onto the column must be in the range of seconds. This can easily be achieved by splitting the sample prior to introduction on to the column. In order to meet the detection limit, however, the split ratio must be as low as possible. Figure 4.10 shows a chromatogram of the gas sample

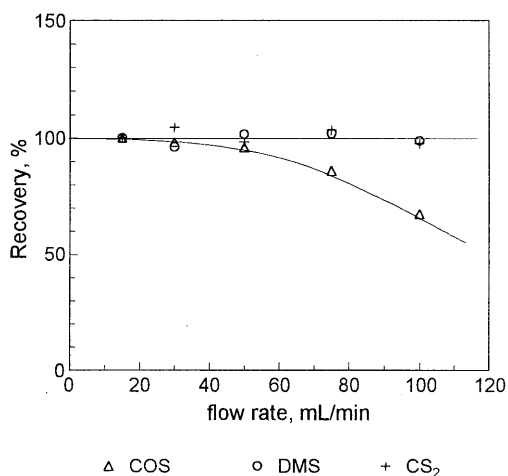


Figure 4.9: Effect of sampling flow rate on the recoveries of COS , DMS , and CS_2 . Gas sample B, sample volume 100 mL. The COS content measured using the 13-mL sample loop is used as reference value. Sampling and chromatographic conditions: see Experimental.

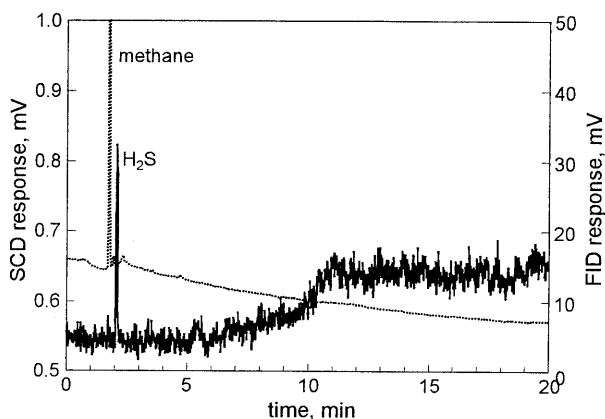


Figure 4.10: Chromatogram of sulfur components in natural gas sample D analyzed by the hot split injection technique. Sample volume 1 mL via loop, PTV: 150°C isothermal, empty narrow quartz liner. Split ratio 1:10. Other chromatographic conditions: see Experimental. The dotted line is the FID signal. The full line is the SCD signal.

D recorded in this manner. In this experiment the packed PTV liner was replaced by an empty narrow quartz liner. The injector temperature was set at 150°C. The injection volume was 1 mL. The split ratio was 1:10. As can be seen from the figure, the only sulfur peak that is above the detection limit, is H₂S. The other components cannot be detected. A possible solution is the use of a large sample loop. A large sample volume, however,

will need a longer time for sample transfer and, hence, will lead to broadened peaks. This can be avoided only by using a cryofocusing step (see below).

The PTV injector can also be used as a cryofocusing device in combination with the on-column injection technique. In this case the capillary column is led through the empty PTV liner and connected directly to the injection port of the sampling valve. In this way the entire content of the sample loop is injected onto the column. In order to obtain sharp peaks, the PTV is cooled to sub-ambient temperature and now acts as a cryofocuser. Figure 4.11 shows that even at -75°C, which is the lowest temperature achievable with liquid CO₂ cooling of the PTV, the cryofocuser is still not able to focus H₂S. This problem can be resolved by using a more powerful coolant such as liquid nitrogen. For practical reasons this method was not used. Another option is to use a column with a higher retention power such as the PoraPLOT Q column (see Chapter 3, section 3.4.4). Even with this column, H₂S and COS cannot be quantitatively retained at temperatures above -50°C. This means that a cryogenic coolant is still needed for proper chromatographic performance. It is therefore clear that this method is not more convenient than the use of selective sample enrichment techniques. Moreover, if a very strong column, capable of efficiently trapping

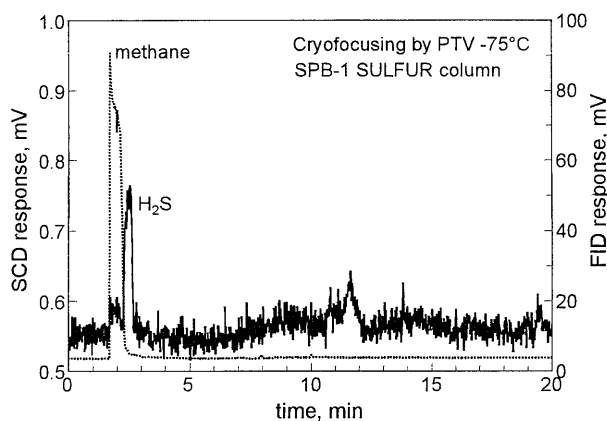


Figure 4.11: Chromatogram of sulfur components in natural gas sample D analyzed by the on-column injection technique. Sample volume 1 mL via loop, PTV: -75°C (2 min) to 200°C at $12^{\circ}\text{C}/\text{sec}$, empty narrow quartz liner. The column is led through the liner and connected directly to the sampling valve. Other chromatographic conditions: see Experimental. The dotted line is the FID signal. The full line is the SCD signal.

COS and H_2S is used, this column would most likely also trap the lower alkanes. As these components are present at extremely high levels in comparison with the sulfur species, they might show up as peaks even on the extremely selective SCD. It is therefore highly recommendable to selectively eliminate the alkanes before introducing the sample into the column.

From these experiments it can be seen that without

the selective sample enrichment step, the requirements imposed on detection limits cannot be fulfilled. Moreover, alkanes could be incorrectly identified as sulfur components. It is therefore clear that the above-described techniques for introduction without selective sample enrichment cannot replace the proposed procedure in case accurate and sensitive sulfur determination in natural gas is required.

Since 1995 the above-proposed procedure has been successfully used in routine analysis of sulfur components in natural gas in a number of industrial laboratories of companies involved in natural gas production or processing. For samples with relatively high contents of sulfur, a 13-mL loop is used (Figure 4.12). For sample with extremely low concentrations of sulfur species, a direct sampling of 500 mL of gas sample is employed (Figure 4.13). In these analyses the SCD was equipped with a flameless combustor. Higher sulfur-over-carbon selectivity of this SCD compared to that of the flame-based SCD allows a larger maximum volume of gas to be sampled without the risk of alkanes showing up as sulfur peaks.

4.4. CONCLUSIONS

The ideal GC-based analytical instrument for trace analysis in complex matrices consists of three components: a selective (preferably on-line) sample pre-treatment/enrichment device, a high resolution chromatographic column, and a sensitive, selective, and quenching-free detector. Each of these three steps has to be optimized in close conjunction with the other two. The instrumental set-up that we proposed in this chapter is an example of this idea. A programmed temperature vaporizing injector with a liner packed with the selective adsorbent Chromosorb 104 acts as an on-line sample enrichment device. The sulfur components from a large volume of natural gas are selectively collected while the more volatile hydrocarbons such as methane, ethane, propane, and partially also butane, are either not retained or further eliminated by purging the liner with helium. In this way, the effects of the interfering matrix, the natural gas background, are minimized. The enriched sulfur components are then directly transferred to a 4- μm ultra-thick non-polar capillary column, and separated. The column provides adequate resolution for all sulfur components of interest, pre-

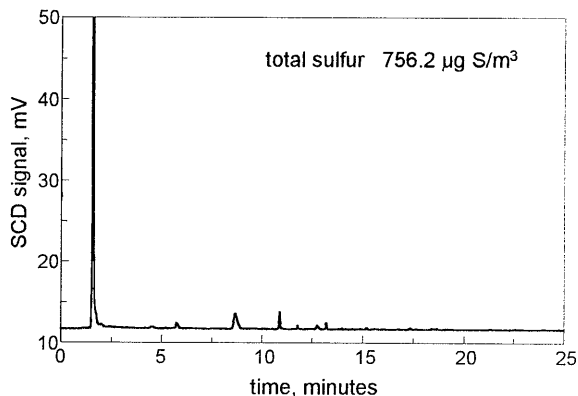


Figure 4.12: Example of analysis of a natural gas sample with a high sulfur content using the proposed method. The 13-mL sample loop was used.

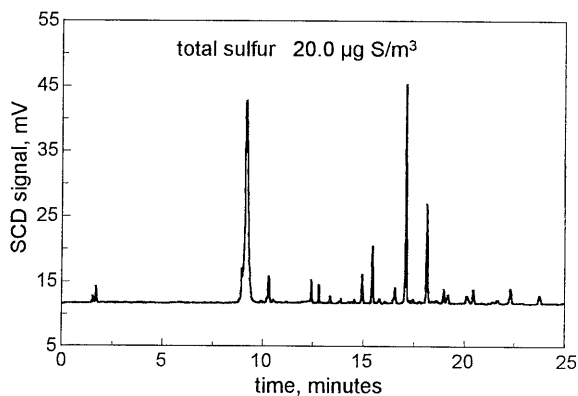


Figure 4.13: Example of the analysis of a natural gas sample with a low sulfur content using the proposed method. Sampling volume was 500 mL.

venting possible errors in quantitation. The accuracy and precision of peak quantitation is further secured by employing a selective and sensitive sulfur detector, the SCD. This detector is tuned to operate under quenching-free conditions ensuring the most reliable performance of the entire system. With the proposed instrumental set-up equipped with a 13-mL sample loop, the detection limit achievable is approx. $3 \mu\text{g S/m}^3$ (for individual peak). The accuracy and precision of the new method are, in general, under 10% RSD. A good agreement between the new procedure and the standardized method was obtained for the limited set of samples tested. Differences that were sometimes observed are most likely because of losses of sulfur components from the gas samples due to adsorption/reaction during storage. The analysis time, including sampling time, does not exceed 30 min. These parameters are clearly superior to the standardized method based on packed column GC-FPD without sample enrichment. With the latter technique, the risk of false positive identification is much larger. Moreover, quantitation is prone to errors by quenching or inaccurate calibration due to the non-linear calibration graphs. If proper care is taken to ensure maximum selectivity and quenching-free operation, extremely low level of sulfur in natural gas samples can be detected using a direct sampling technique with larger sample volumes, *e.g.* 100 to 500 mL.

Part 2

EMISSION MONITORING USING A PORTABLE GAS CHROMATOGRAPH

Chapter 5

GAS CHROMATOGRAPHY IN PROCESS AND EMISSION MONITORING

ABSTRACT

An overview of gas chromatographic instrumentation for field applications is given. This special branch of gas chromatographs can be divided into three classes: on-line process gas chromatographs, transportable gas chromatographs, and portable GC instruments. Although evidently based on the same separation principles, the designs of those classes of equipment differ dramatically. The selection of the various components to be integrated into the overall analytical system depends strongly on the target components as well as on the environment where the system will be installed and operated. Field gas chromatographic systems, especially the portable ones, have benefited strongly from recent progress in microprocessor technology and electromechanical micromachining.

5.1. INTRODUCTION

Gas chromatographs as problem solving analytical instruments have many applications in a wide range of disciplines. Much recent interest has focused on “field analytical chemistry”. The definition of this important concept can be revised as “the practice of producing appropriate qualitative and/or quantitative information with analytical instruments that are operated at or near the sample collection location and which convert data to chemical information in a time frame that is consistent with near real-time applications” [1]. Among the field applications listed in Table 5.1, environmental and process monitoring are the most frequently mentioned areas.

Table 5.1: Possible application areas for field GC analyzers

Environmental	boundary monitoring site investigation continuous emission monitoring work safety / industrial hygiene indoor air monitoring
Process monitoring	product / raw material monitoring BTU calculation safeguard of chemical accidents
Energy exploration, geologic evaluations	
Medical diagnostics	
Detection of explosives and/or chemical warfare agents	
Doping, drugs detection	
Foodstuff analysis	

The highest priority in process control and emission monitoring is to get the analytical results in the shortest possible time and on a continuous basis. The real-time response requirements come from the need of prompt actions that should be taken when a dangerous or an economically non-optimal situation as a consequence of a change in composition of target components occurs. In those cases either the production process or public health are at stake. For example in chemical industry an early detection of deviations from normal compositions in feed and/or intermediate streams can be used in the plant’s operational feed-back control system to eliminate the “up-sets” before a product goes out of specifica-

tion. More precise and accurate analysis of specific components along the production streamline will be needed in order to boost the efficiency. This will require analytical instruments to be installed as integral parts at the process stream rather than in a centralized laboratory [2]. An area where on-line and/or portable GC analyzers have been used extensively is in the analysis of natural gas, either for BTU (British Thermal Unit) calculation [3-6] or for control/regulation of the odorant level in the gas [7]. In environmental applications field-(trans)portable analyzers have been used for monitoring emission from vent stacks [8] or during site investigation and remediation [9,10]. They can be valuable tools in rapid analysis of soil gases as part of the cleanup excavation [11], and in detecting emissions that can migrate off site. Handy analyzer can give a quick warning when hazardous components are present above a certain level in the in-door atmosphere [12], the space station as a special example [13]. The data acquired are of tremendous importance for effective public safety decisions. In some still rather exotic instances, a portable GC instrument was used for criminal investigation such as forensic analysis in clandestine drug manufacturing laboratories [14].

Under the time-constraint situations mentioned above, analytical processes, which take hours to days as a norm in laboratory-based procedures, are clearly unsuitable. The analysis time must be reduced dramatically, down to the range of seconds and minutes. To achieve this goal, the time scales of every step involved in the analytical procedure - sampling, separation, detection, data collection and interpretation - must be shortened to a minimum. With the help of powerful computers and automation processes the time delay in the last two steps has become incomparably short. Even if the conversion from analytical data into chemical information and its consequent feeding into a decision making loop is included, this output process nowadays hardly takes longer than a few minutes to perform. This leaves the sampling and separation step to be the most time-consuming steps that have to be further optimized. The current development need therefore comprises two aspects: design of an on-line and/or field-(trans)portable analytical system including sampling and sample pretreatment and the application of high-speed separation techniques, fast GC in this particular case, in these systems.

Fast GC theory has been extensively developed in the last 20 years. In many publications on this subject Gaspar *et al.* [15-16] and the Eindhoven group [17-20] have concluded that an effective way to reduce the GC analysis time while maintaining the excellent level of resolution is to use narrow-bore capillary col-

umns. The theoretical plate numbers per unit length of a narrow-bore column are much higher compared to that of normal or mega-bore columns. This results in much shorter columns having the same plate numbers. The combination of short length and high optimum linear velocity of the carrier gas results in chromatograms recorded in a fraction of the time compared to that obtained on "conventional" columns. Moreover, columns with small dimensions can be much easier integrated into micromachined analytical instruments.

The technology of micromachining has been developed in the last 15 years to produce Micro Electromechanical Systems (MEMS). A special application of this technique in analytical chemistry is the production of Micro Total Analysis System (μ TAS) [21,22]. A μ TAS is an analytical system equipped with sample treatment units, reaction chambers, mixing devices, washing and cleaning systems, valves, pumps, sensors and waste outlets, all to be etched on a single small silicon chip [23]. For the particular case of miniaturized chromatographic instruments, the silicon micromachining process, which consists of a number of chemical and photochemical steps [24], is now capable of making injection and detection devices with extremely low dead volumes. Even the column, the heart of the separation system, can be also integrated on a chip. This is so far applied more often for liquid chromatography (LC) and capillary electrophoresis (CE) than for gas chromatography (GC) [25]. The main reason is the strict requirement of a circular cross-sectional profile of the capillary column used in GC. Moreover, deactivation and coating of the in-silicon-wafer etched capillary, either with a liquid phase or with a porous adsorption material, are still difficult at best. Conventional fused silica capillary columns, with an unsurpassed chromatographic performance, are readily available in extremely small dimensions and thus fully compatible with other micromachined parts. Conventional columns, therefore, are employed in most of the (trans)portable as well as process gas chromatographs.

The distinction between process, transportable and portable gas chromatographs is based on the operational mode of the instrument. As the name reveals, a process gas chromatograph is installed on-line at a fixed location somewhere along the production stream to provide a continuous flow of data. These instruments are dedicated to one or limited number of predetermined analytical tasks. The dimensions of the instrument are usually not a critical criterion in this case. The transportable and portable gas chromatographs, on the other hand, are under strict requirements of portability. Despite still being dedicated instruments, the range of target components to be analyzed by these systems is somewhat wider,

which make them more universal in use. Each class of the above-mentioned instruments is discussed in more detail in the following sections.

5.2. PROCESS GAS CHROMATOGRAPHS

Process Gas Chromatographs (PGCs) have been commercially available for over 30 years and are the most widely used process analyzer in the world today [26]. Primary characteristics of a PGC are as follow [27]:

- Located in the plant, near the sample point,
- Dedicated to monitor one or more components in one or more process streams,
- Designed for short analytical cycles,
- Designed for continuous, unattended operation,
- Designed for operation in hazardous environments,
- Designed for possible exposure to rough weather, humidity, dust and corrosive atmospheres,
- Provides integral communications with a process control system.

Except for utilizing the same separation concept, the process gas chromatograph is very much different from its laboratory analog. These differences result primarily from the need for continuous, reliable operation. To meet that need, the PGC must deliver its analytical results to the process measurement and control system with the speed and timeliness needed to achieve the possibility for proper control action. It must be compatible with the environment in which the unit is placed, easily accessible for maintenance and highly user-friendly. Finally, the PGC must be able to communicate with modern computer-based process control systems. Thus, the ideal PGC features a simple, reliable design to ensure a low mean failure rate; provides for simple, rapid re-

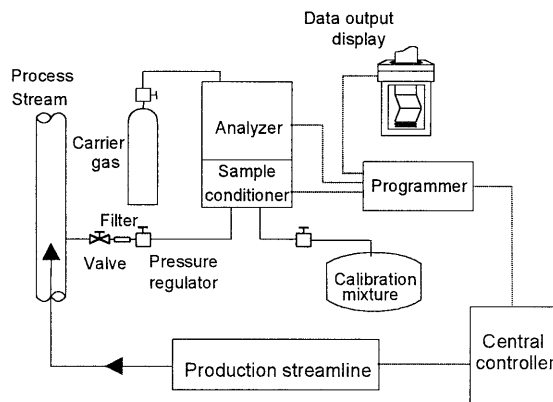


Figure 5.1: Schematic diagram of a PGC system.

pair when required; places appropriate sensors strategically in the system to aid in diagnosing problems; and provides adequate alarms in case of failure of the unit [2]. Basic elements of a PGC are shown in Figure 5.1.

5.2.1. Analyzer

The analyzer contains all components of a conventional GC system in a thermostated oven: columns, switching valves, and detectors. Due to the relatively simple nature of the mixture of components to be analyzed and for the desire of having as short as possible an analytical cycle, chromatographic operation is mostly isothermal. Although temperature-programming options have recently been also offered, isothermal operation still produces better reproducibility and reliability over longer periods of time. These two aspects are clearly the most important demands for a PGC system. Electronics and control units are generally located inside the oven, this to exclude environmental effects, *e.g.* temperature, humidity, *etc.*

5.2.2. Sampling System

The sampling system is usually designed for a particular process stream in operation. The objective of this system is to take a small sample representative for the process stream and condition it prior to transfer of the aliquot to the analyzer. Conditioning processes can include removing particles or water, and for example vaporization of the sample into a homogeneous stream for easy sampling by gas valves. For this purpose it must be mounted close to the analyzer and must have its own thermostated oven. Important components of the system are filters, pressure regulators, flow controllers, *etc.* Switching valves are also needed for alternate sampling from process streams and calibration mixtures.

In an attempt to improve the detection limits of an on-line gas chromatographic analyzer, several enrichment techniques have been integrated into the sampling system. Most of the methods in use are based on the adsorption/thermal desorption (ATD) principle. Mitra *et al.* [28-31] and Frank [32] have proposed the use of a trap packed with a solid adsorbent to preconcentrate the target components from the gas stream and inject them into the GC column by flash heating of the trap in a periodical manner. Enrichment methods using the membrane extraction principle are currently also under development [33, 34].

5.2.3. Columns

Packed columns have been standard for PGC systems for a long time due to their robustness. Compared to their capillary counterparts, packed columns can handle larger sample volumes and are less prone to contamination. Recently, however, capillary columns have gradually gripped stronger foothold in the PGC business owing to the advent of the tough polyimide coated fused-silica columns and stabilized stationary phases [35]. With their larger theoretical plate numbers, capillary columns will provide faster analyses or demand less selectivity of the stationary phases.

For complex samples and given the requirement of isothermal operation, separation on a single column is sometimes impossible. A larger number of columns and valve configurations have been developed to accomplish the task [36]. Some very helpful column switching techniques, based on valve systems [37] or, alternatively, on pressure balancing as invented by Deans [38,39], are used to improve the resolution power of the PGC system:

- Backflush: a reverse column flow removes late eluting components from the column to vent or directly to the detector as one single peak,
- Heart cut: A middle part eluted from the first column is introduced into the second column for a better resolution,
- Multiple columns: arranged in parallel to cover the entire range of the components of interest [40].

5.2.4. Detector

The thermal conductivity detector (TCD) and the flame ionization detector (FID) are still the most popular detectors due to their high robustness, reliability, ease of use and low costs. There are manufacturers who offer a silicon micromachined version of the TCD in a PGC unit designed specially for the BTU application [41]. Occasionally, selective detection such as the flame photometric detector (FPD) are used for monitoring, *e.g.* the sulfur content of gases.

5.2.5. Data Processing System / Communication

An extremely important part of a modern PGC system is the programmer/controller/communication section [2]. It contains all the electronics to power the system, the controller, the data reduction hardware and software, and the

communication package. The gigantic leaps in electronic design that followed the introduction of integrated circuit technology and fast microprocessors had a profound effect on the design of this module. This part has undergone the most radical changes in a short period of time. Discarding the split architecture of the mid 70s, when much of the programmer/controller functions were resident in a central computer [42], the modern PGC is designed as a stand alone microprocessor-based unit that is as powerful as any of the older computer-controlled chromatographs. It can execute all of the complicated calculations necessary to extract accurate and precise data from a complex analysis. Moreover, as an integral part of the process control architecture, contributing important information to the process management, data analysis and control system, the PGC must be able to communicate with the decision making loop. The advance in computer technology has made it easy to fulfill this requirement.

5.3. TRANSPORTABLE GAS CHROMATOGRAPH SYSTEMS

A simple alternative in bringing the analytical instrument to the field is putting the entire GC system on some means of moving platform and drive to the site. This in fact can be called a laboratory-on-the-road. Apart from several minor adjustments, any conventional GC system can be used. Carrier gas and detector gases are supplied from cylinders or generators instead of gas pipelines as common in the lab. Power supplies can be hooked up on the spot. The field-lab is then more likely to be stationed on a fixed spot on-site and the samples are collected either off-line by sample bags or on-line by sample tubing systems. Because there are almost no limitations in power and gas consumption, virtually all additional techniques can be employed such as for example mass spectrometric detection to identify the analytes, temperature programming and cryo-refocusing to have the best GC resolution or sample enrichment to improve the sensitivity [43-45].

To improve the mobility of the system, larger modifications must be applied which result in a narrowed range of functionality. Meuzelaar *et al.* [12,46] proposed a roving GC/MS system capable of analyzing up to 1000 VOC samples per hour while mounted on an electric "golf cart style" platform, moving at up to 20 miles/hour. At this speed, VOC samples could be taken every 100 ft or so and a 1 × 1 mile area could be covered in approx. 2.5 hour. The roving system is equipped with a differential global positioning system (GPS) and radio trans-

ceiver capability thereby permitting remote tracking of the vehicle location and local VOC concentration. Detection limits of less than 20 ppb for BTEX mixtures were reported.

Field-deployable GC/MS systems, such as Viking Spectra Trak (Viking Instruments, Reston, VA, USA) [14] weigh approx. 150 pounds, and utilize an existing commercial mass spectrometer vacuum system which requires dolly transport. The power consumption is between 1000 and 1500W depending upon the operational mode. The instrument can be operated remotely and transmit data to remote locations.

5.4. PORTABLE GAS CHROMATOGRAPHS

A gas chromatograph can be defined as portable if an operator can carry and operate it at remote sites without extra power or gas supplies and transportation means. At present the primary target for portable gas chromatographs are gaseous samples. Compared to liquid and solid samples, gaseous samples are prone to degradation or adsorption and far more difficult in handling and storage. As a result they need more immediate attention and in-the-field treatment. Relevant operational characteristics of portable GC devices are listed in Table 5.2. The most important feature of these instruments is their high portability. The portable gas chromatograph, thus, has to have a compact size (with a volume less than

Table 5.2: Relevant operational parameters of portable gas chromatographs [1].

Analytical capability

1. sensitivity, detection limits
2. selectivity, resolution power
3. precision and accuracy
4. range of applications

Operational parameters

1. size, portability
 2. analysis cycle time
 3. power and gas consumption
 4. ruggedness, reliability
 5. ease of use: hardware, software
 6. cost, capital and operational
 7. service quality: maintenance, part change, repair...
 8. software capability of data interpretation
-

50 L) and light weight (less than 30 kg), and should have a build-in battery and carrier gas cylinder, which can be easily recharged. As continuous on-line analysis is not the prime objective for the portable GCs, operational times of several hours can be considered appropriate. In this limited time span the GC analyzer ought to give as much as possible data. This means short analytical cycles must be applied. Regarding the ruggedness and reliability of the instrument, more or less the same requirements in design as in the case of PGC apply for the portable GC instruments. Recently an extensive list and detailed guide for the selection of portable and miniaturized GCs has been published [47].

In order to have a compact dimension while trying to maintain as much as possible the analytical characteristics inherent to GC systems, portable GCs have to extensively use state-of-the-art technology in electronics as well as electromechanical micromachining. In general a portable GC consists of four main parts: controlling electronics, pneumatic hardware, battery and gas reservoir, and, evidently, analytical GC modules.

5.4.1. Controlling Electronics

One or more printed circuitry boards represent this part. With the implementation of powerful microprocessors the portable GC is having a build-in microcomputer and can operate as a stand-alone instrument. Connections for remote control and data acquisition by an external computer have also become standard. A laptop computer can be used for short-term investigations. Connection to a central computer can be considered for longer-term studies with the perspective for on-line installation.

5.4.2. Pneumatic Hardware

This part of the instrument controls the pressure of the gas which is used as carrier gas and/or actuation gas for the micromachined valves. This part also includes a small vacuum pump used for pulling the gas samples into the analyzer.

5.4.3. Power and Gas Supplies

Carrier gas, usually helium for safety reasons, is pressurized in a small stainless steel cylinder with a volume of *ca.* 1 L. With a full pressure of *ca.* 120 bar this gas tank can provide gas for continuous operation from 8 to 48 hours, depending

on the columns in use. If narrow-bore columns are used, gas consumption rates are low and the portable GC can operate longer before refill and *vice versa*.

Much more problems occur with the power supply. At isothermal operation conditions, a 12V accumulator can provide a maximum of a few hours of power before recharging is required. The more components need to be temperature controlled, the higher the power consumption. Due to the limitation in accumulator lifetime, "power hungry" features such as temperature programming have been rarely implemented. For stationary on-line versions or for instruments on special locations where a network power supply is available, temperature-programming capabilities can be considered [48].

5.4.4. GC Analytical Module

This is the heart of the entire system and has the function of a normal GC system, albeit with certain limitations. Each module has its own injector, column and detector. The philosophy behind the module configuration is that with this design changing the column is easy as in conventional GCs. The entire module is simply replaced. Moreover, lower resolution power due to the lack of the temperature program feature can be partially compensated for by installing more than one column module with complementary selectivities in parallel.

5.4.4.1. Injector

Several injection techniques have been used in portable GCs such as for example silicon micromachined injection valves, loop-type injection valves and ambient vapor sampling systems. As stated before, these injectors are designed to handle mainly gaseous samples.

The silicon micromachined injector has been so far the most widely used injection device in portable GC busi-

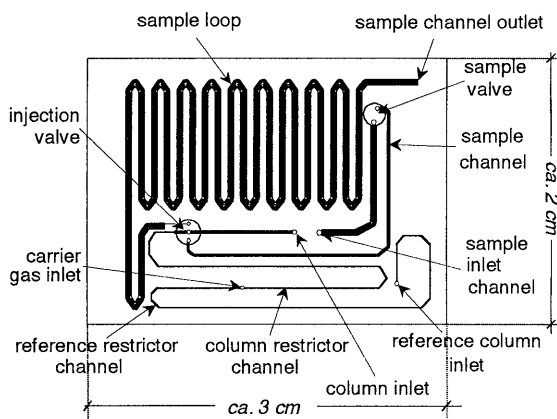


Figure 5.2: Schematic diagram of the silicon-etched sample injection system of the micro GC.

ness [49]. Its design, shown in Figure 5.2, combines two-sided silicon etching and bonding techniques in the generation of microvalves and gas flow channels. The microvalves serve as stream-switching devices such as a means of introducing a dense aliquot of analyte into the carrier gas stream for separation on the chromatographic column. The injection microvalve (Figure 5.3) has an internal volume of only approximately 200 nL. The pneumatically actuated polymeric membrane serves as the valve diaphragm, opening and closing the microvalve by deflecting several microns. The closed state provides a helium leak-tight seal against a valve set ring. The volume of sample to be injected onto the column depends on the time duration during which the valve seal is opened. This time period, for example in the Chrompack CP 2002 Micro GC software adjustable from 10 to 255 msec, will produce an injection volume of 0.5 to 10 μL . Little or no sample dilution occurs during injection. This minimizes the sample band broadening. The injected aliquot mixture is then introduced into a microchannel continuously swept by carrier gas and is subsequently carried to the analytical column for separation. In this pre-column microchannel, however, some band broadening might occur, especially for early eluting components (*viz.* Appendix), contributing to the total extra-column instrument band broadening.

Early versions of silicon micromachined injectors were not temperature controlled. In these injectors, higher boiling and active polar compounds tended to condense or react with residual active sites on the cold microchannels. This could result in serious band broadening and losses of components [8]. The implementation of heated injectors, easily applicable due to their small size, has greatly reduced this undesired side effect. The heating of the injector is software controllable from ambient to about 110°C. Higher injector temperatures, 350°C, have recently been reported as achievable in a new design of silicon micromachined injector [50].

The use of loop-type injection valves [11] is less popular. It is based on a principle similar to the

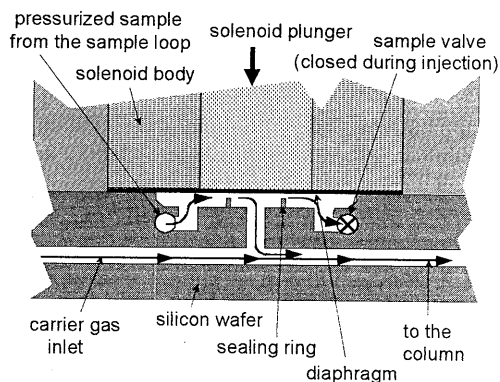


Figure 5.3: Cross-sectional diagram of the silicon micromachined injection valve. The valve is in the open (inject) position.

high-performance liquid chromatography (HPLC) injection technique. An advantage of this injector design is that it can handle also liquid samples.

The ambient vapor sampling (AVS) inlet system (US patent 4,970,905) is usually operated in combination with a short capillary GC column and sub-ambient pressure detector such as a mass spectrometer [12]. The principle of its operation [51] is schematically depicted in Figure 5.4. The AVS module is fully automated, capable of performing repetitive on-column injections of nanoliter quantities of gaseous samples within 20-30 msec. Furthermore the AVS is made from quartz and can be heated. No valves or mechanically moving parts are involved in the design.

5.4.4.2. Column

Column on the chip

The first wafer-scale GC was made over 20 years ago by S. C. Terry [52] (Figure 5.5). A 1.5-meter long capillary column was isotropically etched on a silicon wafer together with an injection valve and a micro thermal conductivity detector. The cross section of the column was not circular but rectangular with 200 μm in width and 30 μm in depth. The column was coated with an OV-101 liquid stationary phase. The number of theoretical plates varied between 380 and 2300 and the analysis of a gas mixture containing nitrogen, pentane and hexane was completed under 5 sec [53]. Unfortunately, this development did not evoke the enthusiasm of other researchers, since capillary GC technology was still in its infancy at that time and chromatographers lacked the technological experience required to use such devices. Effective technology of producing a homogeneous and stable

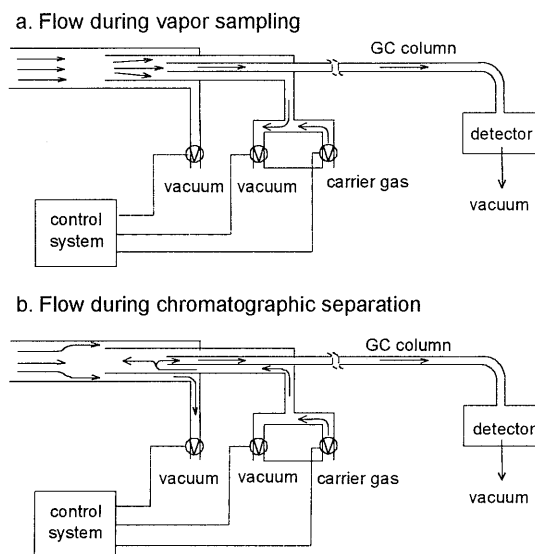


Figure 5.4: Schematic representation of an AVS system and modes of operation.

chemically bonded stationary phase on the capillary wall was not available since the beginning of the 80's [54].

Recently Kolesar and Reston [55,56] have reported the production of a $0.9 \text{ m} \times 300 \text{ }\mu\text{m} \times 10 \text{ }\mu\text{m}$ silicon-etched capillary coated with a $0.2 \text{ }\mu\text{m}$ thick copper phthalocyanine stationary phase. This rather "exotic" stationary phase was used to analyze ammonia and nitrogen dioxide. The chromatograms, however, showed very broadened peaks indicative of the low theoretical plate number achieved on this column. What is the major contributor to the poor peak shapes, column geometry or nature of the stationary phase, is unfortunately not yet clear.

One of the decisive factors contributing to the large band broadening in the above mentioned silicon micromachined capillary columns is their rectangular shape. The propagation front of the gas and how it diffuses into- and back out of the column itself are highly dependent on the inside cross-sectional geometry of the column. A circular cross-sectional column is ideal and produces the best results, because it presents a uniform path regardless of the direction of outward diffusion of component molecules to the column walls. The etching methods used so far have resulted in squared-bottom trenches in one wafer that are capped by another wafer, usually Pyrex glass that produces a problem with thermal expansion coefficients. In order to overcome this problem, Yu *et al.* [57] have patented a new method to produce circular etched columns. Two new procedures are encountered. First, two mirror-imaged semi-circular microchannels are etched on separate silicon wafers. Isotropic etching was used to erode the silicon equally in all directions from the slit entries. Second, the microchannels are placed face-to-face, are aligned and bonded together by a pin forced through exactly matched

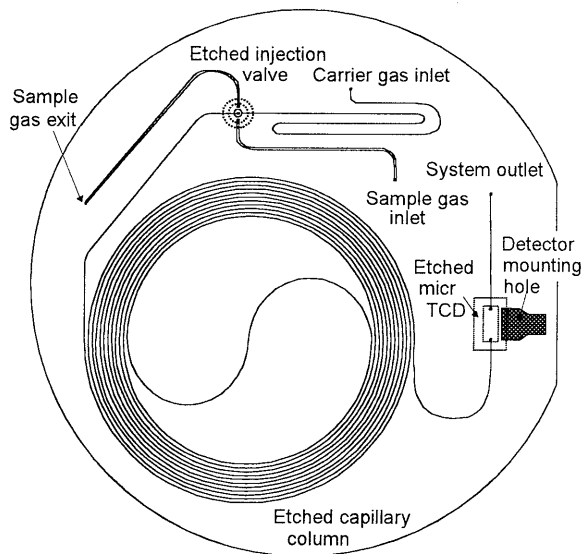


Figure 7.5: Schematic diagram of a gas chromatograph integrated on a silicon wafer.

vertical alignment holes etched on both wafers. No chromatographic results obtained on this device have been published so far.

Fused-silica columns

Due to difficulties in producing silicon-etched capillary columns, most of the portable GCs use fused-silica capillary columns. Well established technology enables the preparation of high-quality columns with exceptionally stable and homogeneous stationary phase layers with a wide range of polarities and film-thicknesses. Different column dimensions can be readily produced to satisfy the resolution power required. In addition to existing liquid stationary phases, a number of Porous Layer Open Tubular (PLOT) columns have recently been introduced boosting the applicability of the portable GC module, especially towards the more volatile components. A schematic diagram of a typical column module is shown in Figure 5.6.

Short columns, from 4 to 10 meters, are used in order to fit into the small module and to facilitate heating with a low-power heating device. To obtain the required plate numbers, narrow-bore columns, typically 100 and 150 μm i.d., are employed. For PLOT applications the column inner diameter can be as large as 250 μm . The small size of a module, typically 20 cm \times 10 cm \times 6 cm, enables the portable GC to accommodate two or even more modules at the same time. Each module, with its own injection system, column and detector acts as an independent GC. Different columns with complementary polarities in these modules give the system a combined resolution power which can not be achieved with a separate module due to the lack of temperature

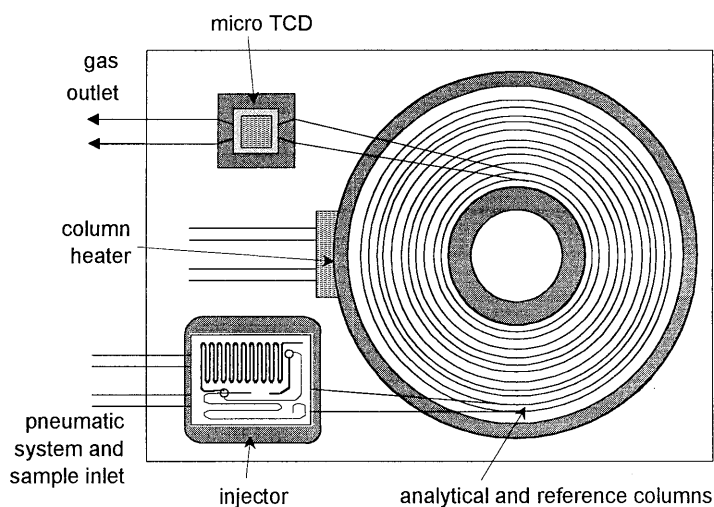


Figure 5.6: Schematic diagram of a portable GC module.

programming [7,8,58]. The compact module design also facilitates a quick and easy maintenance, or exchange of the module to adapt to the target components to be analyzed. Because of the elegance of this idea, the modular design is intensively explored for its possible implementation in conventional GCs in the future.

Another design of the column module is employed in portable GC/MS systems. Apart from the chromatographic function, the column in this case also plays the role of a transfer line [12,59]. The GC separation is then actually performed in the capillary flow restrictor of a mass spectrometry system, known as “transfer line”. GC conditions are, therefore, optimized (based on both separation and flow rate considerations) using variations in the column length and radius in the context of fixed pressure drops from ambient conditions to the detector [60]. Column length typically varies from 5 to 10 meters with column diameters ranging from narrow-bore (100 μm) to normal-bore (320 μm).

5.4.4.3. Detectors

The thermal conductivity detector (TCD), with its well-tested ruggedness and reliability, is still the most powerful candidate in portable GC systems. Moreover, the TCD requires no extra gases and has an extremely low power consumption. The simple response mechanism, based on the difference in thermal conductivity between eluting analyte molecules and a reference gas stream, enables the detector to respond to virtually every component. The TCD has been traditionally regarded to lack the sensitivity and speed of response necessary for use with high-speed narrow-bore capillary columns. The main reason is the large volume, in the order of 100 μL , of the conventional TCD. This drawback has definitely been overcome by the introduction of silicon micromachined TCDs.

The micro TCD measures $0.52 \text{ cm}^2 \times 0.17 \text{ cm}$ and has an internal volume of only 240 nL [49]. For most gases, it exhibits a linear response over its entire sensitivity range of 1 ppm to 100% (*i.e.* 6 orders of magnitude) with only 10% RSD (relative standard deviation). The time constant of a micro TCD is less than 10 msec, making it the fastest chromatographic detector available today. Because of its compact size and low heat capacity, this detector can warm-up and stabilize within one minute [61]. This detector is *ca.* 250 times more sensitive than conventional TCDs [62].

A serious disadvantage of the TCD is its lack of selectivity which, evidently, can not be overcome by down-sizing. For detecting specific target components in a

complex matrix, which is the norm rather than exception in field applications, more selective detectors must be employed. Portable GCs equipped with a photoionization detector (PID) or an electron capture detector (ECD) are commercially available [47]. The former is used for detecting aromatic hydrocarbon mixtures while the later has been proved to be very sensitive to halogenated volatile organic compounds (VOCs). These two detectors can be readily integrated into portable GC systems due to the fact that no auxiliary gas is required and power consumption is relatively low.

The power of mass spectrometric detection techniques in detecting specific components has attracted researchers to apply this technology in field applications. The classical bench-top mass spectrometer that requires high vacuum and is power demanding, clearly cannot be transferred to a portable device without radical modifications. For field monitoring of VOCs in air Meuzelaar *et al.* [12] used a 5971A HP MSD with an extensively modified "hybrid" (bulk/ion getter pump combination) vacuum system [63]. Power supply was changed from 110V AC to 24V DC. The "bulk" getter method cannot handle noble gases. Hydrogen, therefore, was used as carrier gas. Detection limits at the ppb levels were claimed to be achieved.

Andersen *et al.* [64] have patented a portable GC/MS system which is small (can be incorporated in a 9.5×18×27 inch suitcase), light weight (less than 70 pounds), with low power consumption (under 600W at peak power). The system is controlled by a laptop computer. Hydrogen was used as carrier gas, which is demanded by the light-weight vacuum-sorption pumping system. The pump uses pelletized stable-state zirconium getter metals to sequester the hydrogen carrier gas in combination with an ion getter pump to remove any extraneous gases.

Another technology, Ion Mobility Spectrometry (IMS), initially developed in the late 60's [65], has been developed and incorporated with the Ambient Vapor Sampling – Transfer Line Gas Chromatography (AVS-TLGC) technique into a hand-portable instrument used primarily to detect volatile compounds in air [13,59]. Scrubbed air is used as carrier gas in this system. Compounds elute from the TLGC to the ionization region of the IMS. A radioactive ^{63}Ni foil provides high energy beta particles ionizing water molecules $[\text{H}+(\text{H}_2\text{O})_n]$ to form a charge-reservoir that can be transferred to the analyte molecules. In the negative mode, electrons are transferred to sample molecules from the charge-reservoir residing in O^{2-} ions. Positive or negative charges applied to the repeller determine which

ions are accelerated towards an electronic gate that leads to the drift region. When the gate voltage drops to zero, a narrow band of ions enters the drift region. In a weak electric field, the ions traverse the drift region to a collector electrode in a characteristic time that depends on their size and shape. A counter-flowing drift gas (usually air) maintains the integrity of the narrow sample band. The reduced mobility, corrected for pressure and temperature, of an ion is the time it takes to travel from the gate to the collector. Reduced mobilities and mobility spectra are used to identify and quantify the molecules that elute from the GC.

Traditionally IMS has been classified as a specific detector sensitive to compound classes such as ketones or chlorinated species, but was not considered as a universal detector because of its minimal response to compounds without functional groups. Several improvements have been incorporated in the new design of the IMS to improve its capabilities to a new level. The new IMS cell with reduced dead volume, which is further swept by scavenger gas, can be heated to a temperature as high as 250°C. The heated IMS is still most sensitive for halogenated components with a detection limit of 0.2 pg, but the detection limits achieved for non-functional species such as toluene are only an order higher, *i.e.* 2 pg. Typical IMS peak widths are similar to the gating pulse duration of 20 μ sec thus making the IMS fully compatible with the high-speed GC.

Recently several novel detection techniques which have great potential for full integration into portable instruments, have been published. Time-gated emission detectors such as pulsed-flame photometric detectors (PFPD) [66] and windowless pulsed discharge detectors [67] look particularly promising. The use of micromachined emitters, similar to those in flat screen computer displays, have been suggested as a mechanism to produce ions by field ionization or to produce thermal electrons for electron capture [68]. These can be used to manufacture flameless ionization detectors or electron capture detectors with no radioactive materials.

5.5. CONCLUSIONS

Gas chromatographic instruments employed in field applications have to meet far more rigorous design requirements than their laboratory counterparts. The strictest demands include intrinsic safety, ruggedness, reliability and stability of op-

eration as well as low gas and power consumption. This sometimes results in severe sacrifices in GC performance: lower sensitivity and selectivity, and narrow range of applicability. In most cases field GC instruments are dedicated analytical instruments, specifically build for a particular analysis.

Silicon micromachining technology, together with the introduction of microprocessors and microcontrollers, has pushed the production of field analytical instruments a giant step forward. The integration of micromachined mechanical and electrical components will allow high performance analytical instruments to be packaged as chemical sensors. When equipped with proper software this new breed of field analytical instruments will be able to solve problems in many applications sectors currently not accessible with conventional analytical instruments.

REFERENCES

1. E. B. Overton, H. P. Dharmasena, U. Ehrmann, K. R. Carney, *Field Anal. Chem. Technol.*, 1996, 1(2), 87-92.
2. R. Annino, *Am. Lab.*, 21 (1989) 60-67.
3. P. E. Kiezer, *Proc. 71st Int. Symp Hydrocarbon Meas.*, 1996, p. 544-548.
4. L. N. Cox, *Proc. 70th Int. Symp Hydrocarbon Meas.*, 1995, p. 514-516.
5. E. Brown, *Proc. 71st Int. Symp. Hydrocarbon Meas.*, 1996, p. 522-524.
6. T. Hawkins, *Chem. Eng. World*, 31 (1996) 211.
7. R. C. M. de Nijs, J. van Dalen, A. L. C. Smit, and E. M. van Loo, *J. High Resolut. Chromatogr.*, 16 (1993) 379.
8. H. Pham Tuan, H.-G. Janssen, C. A. Cramers, P. Mussche, J. Lips and N. Wilson, *Proc. 18th Int. Symp. Capillary Chromatogr. Electrophoresis*, Riva del Garda, Italy, May 20-24, 1996, p. 2213.
9. G. Etiope, *J. Chromatogr. A*, 775 (1997) 243-249.
10. G. Matz, W. Schroeder, T. Ollesch, *J. Chromatogr. A*, 750 (1996) 151-153.
11. H. B. Jones III, *Report*, Rose-Hulman Institute of Technology, 5500 Wabash Avenue, Terre Haute, Indiana 47803, USA, May 1996.
12. H. L. C. Meuzelaar, W. H. McClennen, J. P. Dworzanski, N. S. Arnold, and W.-H. Du, *Air and Waste Management Assoc.*, Paper presented at the 88th Annual Meeting & Exhibition, San Antonio, Texas, USA, June 18-23, 1995.
13. T. Limero, J. Brokenshire, C. Cumming, E. Overton, K. Carney, J. Cross, G. Eiceman, and J. James, *SAE Technical Paper Series*, ISSN 0148-7191, Paper presented on the 22nd Int. Conf. of Environmental Systems, Seattle, Washington, USA, July 13-16, 1992.
14. R. J. Matejczyk, *Proc. SPIE- Int. Soc. Opt. Eng.*, SPIE, 1997 (2941) 140-146.
15. G. Gaspar, R. Annino, C. Vidal-Madjar, and G. Guiochon, *Anal. Chem.*, 50 (1978) 1512.
16. G. Gaspar, C. Vidal-Madjar, and G. Guiochon, *Chromatographia*, 15 (1982) 125.

17. C. P. M. Schutjes, *Ph.D. Thesis*, Eindhoven University of Technology, the Netherlands, 1983.
18. C. A. Cramers, P. A. Leclercq, *CRC Crit. Rev. Anal. Chem.*, 20 (1988) 117.
19. A. J. J. van Es, *Ph.D. Thesis*, Eindhoven University of Technology, the Netherlands, 1990.
20. P. G. van Ysacker, *Ph.D. Thesis*, Eindhoven University of Technology, the Netherlands, 1996.
21. P. Bergveld, *Proc. μ TAS Workshop*, MESA Research Institute, 21-22 November 1994, p. 1-4.
22. A. Manz, *Proc. μ TAS Workshop*, MESA Research Institute, 21-22 November 1994, p. 5-23.
23. J. A. Dziuban, L. Nieradsko, A. Grecka-Drzazga, and J. Mróz, *Microsystem Technology News Poland*, 1 (1997) 8-10.
24. G. T. A. Kovacs, K. Petersen, and M. Albin, *Anal. Chem. News & Features*, July 1, 1996, 407A.
25. A. Manz, D. J. Harrison, E. Verpoorte and H. M. Widmer, "Planar Chips Technology for Miniaturization of Separation Systems: A Developing Perspective in Chemical Monitoring" in "Advances in Chromatography" by P. R. Brown and E. Grushka, Eds., Vol. 33, 1993, Marcel Dekker, Inc., New York, USA.
26. H. M. McNair, *Am. Lab.*, 19 (1987) 17-20.
27. R. Villalobos and F. Glow, *Advances in Instrumentation*, 40 (1985) 1435-1461.
28. S. Mitra and C. Yun, *J. Chromatogr. A*, 648 (1993) 415.
29. Y. H. Xu and S. Mitra, *J. Chromatogr. A*, 688 (1994) 171.
30. S. Mitra and A. Lai, *J. Chromatogr. Sci.*, 33 (1995) 285.
31. S. Mitra, Y. H. Xu, W. Chen, and A. Lai, *J. Chromatogr. A*, 727 (1996) 111.
32. W. Frank and H. Frank, *Chromatographia*, 29 (1990) 571.
33. S. Mitra, X. Guo, N. Zhu, and X. Guo, *J. Microcolumn Separations*, 8(1) (1996) 21-27.
34. T. Górecki, J. Pawliszyn, M. Yang, Y. Luo, and M. Adams, *Proc. 19th Int. Symp. Capillary Chromatogr. Electrophoresis*, Wintergreen, Virginia, USA, May 18-22, 1997, p. 184.
35. R. Villalobos and R. Annino, *Analysis Instrum.*, 21 (1985) 73.
36. R. Villalobos and R. Annino, *ISA Calgary '89 Symp. Proc.*, April 3-5, 1989, p. 57-86.
37. R. Villalobos, R. O. Brace, and T. Johns, "The Role of Backflushing in Gas Chromatography", in "Gas Chromatography" by H. J. Noebels, R. F. Wall, and N. Brenner, Eds. (Academic Press, New York, NY, 1961), p. 39-54.
38. D. R. Deans, *J. Chromatogr.*, 18 (1965) 477.
39. D. R. Deans, *Chromatographia*, 1/2 (1968) 18.
40. R. Annino, *J. Chromatogr.*, 678 (1994) 279-288.
41. Applied Automation, Bartlesville, UK.
42. D. W. Stevens and R. Villalobos, *ISA Trans.*, 9(1) (1970) 61.
43. G. Matz, W. Schröder, and T. Ollesch, *J. Chromatogr. A*, 750 (1996) 151-153.
44. J. González, S. P. Levine, and R. E. Berkley, "The Development and Evaluation of a Transportable Fast Flow Chromatograph for the Monitoring of Organic Vapors in Air", Report EPA/600/A-93/213, reproduced by US Department of Commerce, National Technical Information Service, Springfield, VA 22161, USA.
45. A. C. Lewis and K. D. Bartle, *Proc. 19th Int. Symp. Capillary Chromatogr. Electrophoresis*, Wintergreen, Virginia, USA, May 18-22, 1997, p. 394-395.

46. W. H. McClennen and H. Meuzelaar, *Proc. 19th Int. Symp. on Capillary Chromatogr. Electrophoresis*, Wintergreen, Virginia, USA, May 18-22, 1997, p. 136-137.
47. D. Di Benedetto, *Spectra Analyse*, 193 (1996) 30.
48. R. E. Berkley, M. Colón, Jesús González, I. Droz, J. Adams, C. Fortune, K. Oliver, D. R. Coleman, and C. Wood, *At-Onsite*, 2(1) (1996) 161-170.
49. M. W. Bruns, *Proc. 1992 Int. Conf. Ind. Electr., Control, Instrum. Autom.*, Volume 3, New York: IEEE, 1992, p. 1640-1644.
50. C. M. Yu, "Microminiature Gas Chromatograph", *US Patent 5,583,281*; Dec. 10, 1996.
51. N. S. Arnold, W. H. McClennen, H. L. C. Meuzelaar, *Anal. Chem.*, 63 (1991) 299-304.
52. S. C. Terry, *Ph.D. Thesis*, Stanford University, USA, 1975.
53. S. C. Terry, J. H. Jerman, and J. B. Angell, *IEEE Trans. Electrom. Devices*, ED-26 (1979) 1880.
54. K. Grob, G. Grob, and K. Grob, Jr., *J. Chromatogr.*, 211 (1981) 243-246.
55. R. R. Reston and E. S. Kolesar, Jr., *J. Microelectromech. Syst.*, 3(4) (1994) 134-146.
56. E. S. Kolesar, Jr. and R. R. Reston, *J. Microelectromech. Syst.*, 3(4) (1994) 147-154.
57. C. M. Yu and W. C. Hui, "Method for Making Circular Tubular Channels with Two Silicon Wafers", *US Patent 5,575,929*; Nov. 19, 1996.
58. L. M. Dominguez, B. M. Gordon, W. M. Coleman, and J. C. Serne, "Commercial Gas Chromatographic Continuous Emissions Monitoring System for Determination of VOCs and HAPs", *Air & Waste Management Association*, For Presentation at the 88th Annual Meeting & Exhibition, San Antonio, Texas, June 18-23, 1995.
59. N. S. Arnold, D. L. Hall, R. Wilson, and A. P. Snyder, "A New Hand-Portable Gas Chromatography / Ion Mobility Spectrometry for Chemical Detection Applications", *Proc. 1995 US Army ERDEC Sci. Conf. Chem. Defense*, November 14-16, 1995, APG, MD.
60. A. P. Snyder, C. S. Harder, A. H. Brittain, M. G. Kim, N. S. Arnold, and H. L. C. Meuzelaar, *Anal. Chem.*, 65 (1993) 299-306.
61. S. J. Santy, "Portable Gas Chromatography", presented at *the Institute of Gas Technology's Gas Quality Measurement Symposium*, Chicago, Illinois, June 10-12, 1991.
62. M. W. Bruns, *Proc. 17th Int. Symp. Capillary Chromatogr. Electrophoresis*, Wintergreen, Virginia, USA, May 7-11, 1995.
63. N. S. Arnold, P. A. Cole, and W. Du, *Proc. 1993 Int. Symp. Field Screening Methods for Hazardous Wastes and Toxic Chemicals*, Vol. 2, Las Vegas, 1993, p. 915-931.
64. B. D. Andersen, J. D. Eckels, J. F. Kimmons, and D. W. Myers, "Portable Gas Chromatograph - Mass Spectrometer", *US Patent 5,525,799*; Jun. 11, 1996.
65. R. H. St. Luis and H. H. Hill, *Anal. Chem.*, 62 (1990) A1201.
66. A. Amirav and H. Jing, *Anal. Chem.*, 67 (1995) 3305-3318.
67. G. German, W. E. Wentworth, A. Zlatkis, R. Swatlovski, E. C. Chen, and S. D. Stearns, *J. Chromatogr. A*, 724 (1995) 235-250.
68. C. A. Spindt, *Surf. Science*, 266 (1992) 145-154.

Chapter 6

ANALYSIS OF VENT STACK GASES USING A PORTABLE MICRO GAS CHROMATOGRAPH¹

ABSTRACT

Stricter environmental regulations currently being imposed on the emission of toxic components from chemical plants into the atmosphere initiate the need of new, fast, reliable and accurate methods for environmental monitoring of vent stack effluents. An additional complication in this type of analyses is often the presence of high concentrations of water vapor in the gaseous samples. For the vent-stack emission-monitoring program described in this chapter, the components of interest include methanol, methyl bromide, methyl formate, methyl acetate, benzene, toluene, p-xylene and acetic acid. Moreover, the analytical device in use should be capable of operating in a harsh environment and should be (trans)portable. The micromachined gas chromatograph (micro GC) CP 2002 (Chrompack) is shown to meet these requirements. An evaluatory study in the laboratory resulted in the selection of two independent GC modules employing a CP Sil-8 CB column and a PoraPLOT U column, respectively. The detection limits for all components obtained on this dual column system are in the parts-per-million range. A heated injection system was proven to be useful for increasing the sensitivity owing to the lower adsorption losses of the components in the injection system.

A field trial at a vent stack showed that the analytical results of the on-line at-site GC measurements are in good agreement with those obtained using the laborious off-line method currently in use. The concentrations of benzene and toluene found in the effluent gas were relatively stable at 5 ppm and 3 ppm, respectively. Methyl acetate and p-xylene were found to strongly fluctuate in the range of 100-160 ppm for the former and from 10 to 30 ppm for the latter. Methanol, methyl bromide and methyl formate were found at detection limit level, i.e. from 2 to 10 ppm. The concentration of acetic acid was below the detection limit (c.a. 30 ppm).

¹ Partially published as "Analysis of a Strongly Acidic Component in Very Humid Samples Containing Various Non-polar Components Using a Micro GC", by H. Pham Tuan, H.-G. Janssen, C. A. Cramers, P. Mussche, J. Lips, and N. Wilson in *Proceedings of the 18th Symposium on Capillary Chromatography*, Riva del Garda, Italy, May 20-24, 1996, p. 2213-2224.

6.1. INTRODUCTION

The ever higher demands on accurate and precise analysis in every stage of a chemical industrial process encourages the growing involvement of gas chromatography. The analytical tasks range widely from the determination of the composition of the materials along the production line to trace analysis of toxic components in the surrounding environment. Emission monitoring is an important step in the process of minimizing the impact of a production process on its environment. Vent stack analysis is generally one of the most difficult emission measurements. The large diversity in characteristics of the components of interest, *e.g.* their boiling points, polarity and especially acidity/basicity, render method development for such analyses a difficult task. Moreover, the presence of high water vapor contents and rather harsh conditions such as for example high temperatures and pressures at the sampling points cause additional problems.

Most of the analytical procedures currently in use for emission monitoring, non-chromatographic as for example titration, as well as chromatography-based, employ off-line and very elaborate, cumbersome and time-consuming sampling steps. This leads in many cases to an unacceptable inaccuracy in the determination due to almost unavoidable losses of components and/or contamination during the sampling process and the following sample storage and transportation. Another disadvantage is that no "on the fly" data can be generated, which can be a serious drawback in case of radically changing process conditions or compositions during production. In order to overcome these drawbacks, a (trans)portable analytical device is required capable of operation at remote locations under rough conditions. Moreover, this device should be able to handle the analysis of the target components in a relatively complex and interfering matrix, containing large amounts of water vapor and other non-polar compounds without compromising the precision and accuracy. It was the aim of the present study to investigate to what extent a micromachined portable gas chromatograph could meet these requirements for the particular application of the analysis of humid vent stack components. The components of interest differ widely in polarity and volatility. One of the target components is extremely acidic: acetic acid.

The micro gas chromatograph used in this project falls into the third category defined in the previous chapter, portable gas chromatography systems. Each of the two analytical modules contains a silicon micromachined injection system, a FSOT capillary column, and a micro TCD. Due to the strict requirement of portability, the micro GC has some limitations in hardware and thus in analytical capability compared to those of a conventional GC. The injector, consisting of a fast switching valve system, for example, can handle only gaseous samples. Only isothermal operation can take place, either at ambient or elevated temperatures. The micromachined GCs have so far almost exclusively been used for applications where the composition of the target mixture is not too complex [1,2] or if only a few components from a complex matrix were of interest [3]. Recently the application of the micro GC in the analysis of a more complex mixture of VOCs has been described [4]. The range of components to be handled by the micro GC can be extended significantly by employing two or more different column modules with complementary chromatographic application ranges.

In the present vent stack emission monitoring project target components were methanol, methyl bromide, methyl formate, methyl acetate, benzene, toluene, *p*-xylene and acetic acid. Due to the wide range of volatility and polarity covered by this sample, the development of a suitable analytical method is complicated. An additional complicating factor is the very high concentration of water vapor in the vent gas. In the first phase of the project, a portable micro-GC CP 2002 (Chrompack, Middelburg, The Netherlands) was evaluated and optimized for this particular application. Owing to its compact size, low weight, as well as the low gas and electricity consumption, this instrument is suitable for field operation. In the second phase the micro GC was installed on the plant for a field trial.

6.2. MICRO GC EVALUATION AND OPTIMIZATION

6.2.1. Problem Definition

The goal of this stage of the work is to find the best chromatographic conditions to meet the requirements on resolution and detection limits as well as the working ranges for the entire set of components of interest. Parameters to be

evaluated include: the selection of suitable columns to be integrated in the analytical modules, column temperatures and pressures, the use of heated injectors and the effects of the water vapor content and sample pressure on the chromatographic performance of the micro GC. Detection limits and linear dynamic ranges of the micro GC for the individual components were also established.

6.2.2. Experimental

The bench-top micro GC CP 2002 (26 cm × 40 cm × 15 cm in size and 10 kg in weight) used in the evaluatory study was equipped with two separate standard column modules: a 4 m × 100 μm × 0.2 μm CP Sil-8 CB column and a 10 m × 250 μm × 10 μm PoraPLOT Q column. Column temperature can be set isothermally in the range from ambient to 180°C. Each module is equipped with a silicon micromachined TCD. The micro TCD consists of four precisely matched nickel filaments. Two of these filaments are placed in the column effluent stream and two are fed with pure carrier gas acting as reference channel. The detector cell volume is approx. 100 nL per channel. No make-up gas is used. Helium from the laboratory supply line was used as carrier gas. The injector accommodates a built-in 8-μL sample loop and two silicon micro valves. Just before the injection, carrier gas compresses the sample in the sample loop. By opening the micro valve between the sample loop and the analytical column, a small volume of sample can be injected as an extremely narrow injection band. The time the valve is in the open position can be set in the range of 0-255 msec with 5-msec increments. Gaseous samples are drawn through the sample loop by means of a vacuum pump at a sampling flow of *ca.* 10 mL/min. The micro GC is controlled by Maestro software ver. 2.3 (Chrompack) running on a Hill-top Inca 486 PC.

The synthetic gas mixture used in the laboratory evaluation of the instrument comprised of acetic acid, methanol, methyl formate, methyl acetate, benzene, toluene and *p*-xylene in air to provide an atmosphere that is representative for the type of samples which could be encountered when performing vent stack analyses. Synthetic mixtures were prepared using a laboratory-made head space device [5]. Air was used as dilution gas. Pure liquids (methanol, methyl acetate, acetic acid, benzene, toluene, *p*-xylene, all p.a. grade and purchased from Merck, Darmstadt, Germany) or a mixture of these pure liquids were used to fill the head space reservoir. A wide range of concentrations could be generated by

different air dilution flows. High water vapor contents in the sample were prepared by bubbling the air through water prior to sending it through the head-space device.

Low concentrations (at detection limit level) of the components of interest in air streams were generated using the DKK gas generator Model GST-1 (DKK Corporation, Tokyo, Japan) in combination with the DKK diffusion device.

Three cylinders containing gas standard mixtures in helium were purchased from BOC Special Gases (London, UK). The first cylinder contains benzene, toluene, *p*-xylene at a concentration of 25 ppm each, the second cylinder acetic acid (150 ppm), methyl acetate and methyl formate (25 ppm each) and the last cylinder methyl bromide (25 ppm). These gas standard cylinders were used to calibrate the micro GC as well as to study the effect of sample pressure on the peak heights and areas of the components.

6.2.3. Results and Discussion

6.2.3.1. Selection of Modules

The GC analysis of samples covering a wide range of boiling points and/or polarities very often requires the use of temperature programmed analysis. The temperature programming feature, which is standard in all modern laboratory GC instruments, is not available on portable GC's. This means that instead of analyzing a sample temperature programmed on one column, analysis on a micro GC has to be carried out on more than one column, each of which is operated isothermally. Careful selection of the chromatographic columns is therefore of utmost importance.

Among the target components, the most critical one is obviously acetic acid. Due to its high polarity and acidity acetic acid strongly reacts with active sites in the column as well as in the sampling/injection line. This easily results in peak tailing or loss of the component. Figure 6.1 shows chromatograms of a gaseous test mixture on a CP Sil-8 CB and a PoraPLOT Q column. In both chromatograms the acetic acid peak has significant tailing making its detection very difficult, not mentioning quantitative determination. To overcome this problem another module must be selected. As acetic acid has an extremely high polarity, the column of choice is a very polar column. An FFAP column and a PoraPLOT U column were investigated as alternatives.

Figure 6.2 shows the chromatogram of a test mixture on a thick-film CP FFAP column: $6\text{ m} \times 150\ \mu\text{m} \times 0.4\ \mu\text{m}$. A thick film of the FFAP stationary phase was chosen in order to reduce the contribution of the column to the overall acetic acid band tailing. Although the acetic acid peak shape was improved significantly compared to that obtained on the previously tested Sil-8 and/or PoraPLOT Q columns it still did not reach the desired level of symmetry.

Figure 6.3 shows the chromatogram of a test mixture on the PoraPLOT U column. On this column the band shape of the acetic acid peak is comparable to that of the nearest eluting peak, *i.e.* benzene. The long elution time of acetic acid is due to the relatively low column temperature that had to be used, *i.e.* only 150°C . In order to obtain adequate separation for the other components a higher column temperature could not be used. A critical peak pair is methanol

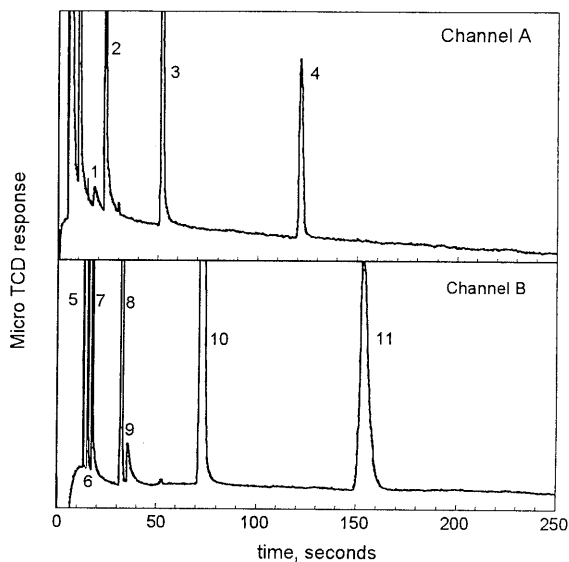


Figure 6.1: Chromatograms of the gaseous test mixture on the standard micro GC. Channel A: $4\text{ m} \times 150\ \mu\text{m} \times 0.2\ \mu\text{m}$ CP Sil-8 CB, 150 kPa, 40°C ; channel B: $10\text{ m} \times 250\ \mu\text{m} \times 10\ \mu\text{m}$ PoraPLOT Q, 250 kPa, 180°C . Peak number: 1/ acetic acid, 2/ benzene, 3/ toluene, 4/ *p*-xylene, 5/ air, 6/ water, 7/ methanol, 8/ methyl acetate, 9/ acetic acid, 10/ benzene, and 11/ toluene.

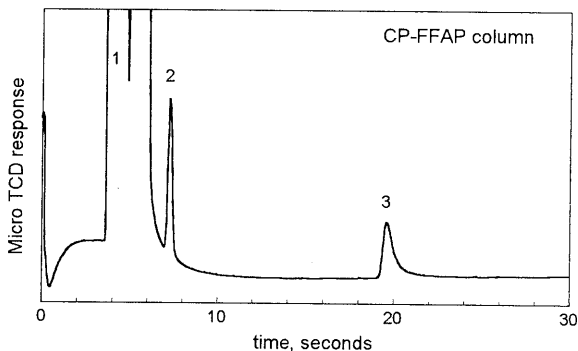


Figure 6.2: Chromatogram of a test mixture containing *p*-xylene and acetic acid on the thick-film $6\text{ m} \times 150\ \mu\text{m} \times 0.2\ \mu\text{m}$ CP-FFAP column. Column head pressure 200 kPa, column temperature 110°C . Elution order: 1/ air, 2/ *p*-xylene, and 3/ acetic acid.

and methyl bromide. These components can be separated on the PoraPLOT Q column but only at a lower column temperature of approximately 120°C.

For the particular emission monitoring problem under study, separation of the entire range of components on the micro GC could only be obtained if the GC was equipped with two column modules with

complementary selectivities. The optimal module combination consists of either a PoraPLOT Q column with a thick-film FFAP column or, alternatively, a Sil-8 column with a PoraPLOT U column. With the first column set-up the FFAP column is used for analysis of *p*-xylene and acetic acid exclusively, while the rest of the components is separated on the PoraPLOT Q column. Here two sets of chromatographic conditions (or two micro GCs) must be used in order to analyze the entire range of components. A lower column temperature (120°C) is needed to obtain adequate separation of methyl bromide from methanol and a higher column temperature (180°C) is necessary to elute benzene and toluene. The disadvantage of two different sets of chromatographic conditions needed to complete one analysis is eliminated if the second column combination is used, *i.e.* a CP Sil-8 CB column and a PoraPLOT U column. Benzene, toluene and *p*-xylene can be comfortably analyzed on the former column, while the rest is adequately separated on the later. The PoraPLOT U column at 150°C gives a good separation for the methanol/methyl bromide peak pair as well as a good peak shape for acetic acid. Benzene can also be analyzed on this column and thus can serve as a “bridge” component for improving the quantitative analysis. Although the detection limits achievable on this combination of modules are slightly worse than that on the FFAP/PoraPLOT Q combination (Table 6.1), they still meet the requirements specified in the project. The CP Sil-8 CB col-

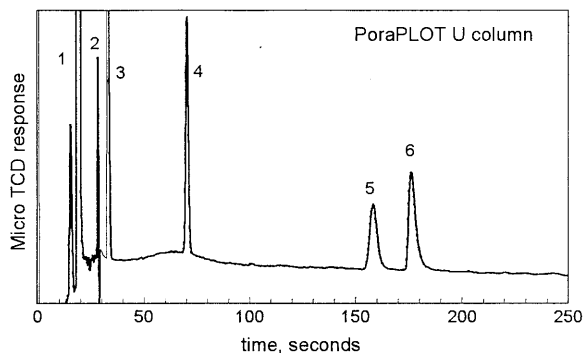


Figure 6.3: Chromatogram of a test mixture containing acetic acid on the 10 m × 320 μm × 10 μm PoraPLOT U column module. Column head pressure 300 kPa, column temperature 150°C. Elution order: 1/ air, 2/ water, 3/ methanol, 4/ methyl acetate, 5/ benzene, and 6/ acetic acid.

umn and the PoraPLOT U columns are therefore selected for the micro GC to be used in the field application.

Table 6.1: Summary of the detection limits and upper limits of the linear dynamic range for the individual test components.

Compound	Detection Limit ^a (ppm)	Upper Limit ^b (%)	Module used
Water	nd ^c	0.6	PoraPLOT Q
		1.0	PoraPLOT U
Methanol	1.0	10.0	PoraPLOT Q
	1.0	7.5	PoraPLOT U
Methyl bromide	2.0	nd	PoraPLOT U
Methyl formate	2.0	nd	PoraPLOT U
Methyl acetate	1.0	5.0	PoraPLOT Q
	5.0	5.0	PoraPLOT U
Benzene	2.0	3.0	PoraPLOT Q
	21.0	3.0	PoraPLOT U
	0.5	3.0	CP Sil-8 CB
Toluene	3.5	2.0	PoraPLOT Q
	0.5	1.0	CP Sil-8 CB
p-Xylene	0.5	0.6	FFAP
	1.0	0.5	CP Sil-8 CB
Acetic acid	2.0	1.5	FFAP
	30.0	0.2	PoraPLOT U

^a DL is calculated on peak height basis (S/N = 3).

^b UL is the concentration where the calibration graph (on peak area basis) starts to deviate from linearity.

^c At low concentrations the TCD gives a negative peak at the elution position of water. Accurate DL determination is, hence, impossible.

nd not determined.

6.2.3.2. Evaluation of the Heated Injector

The serious tailing of the acetic acid peak that was seen even when a thick-film FFAP column was used, indicates that most likely adsorption occurred in the injection system which caused the band tailing. To overcome this disadvantage, the standard micro GC was upgraded with heated injection systems. The sample line and injectors now could be heated to a temperature of 110°C. Figure 6.4 shows the acetic acid peak shape on the thick-film FFAP column module at different injector temperatures. Compared to the acetic acid peak obtained at the lowest injector temperature (*e.g.* 50°C), the peak observed at an injector tem-

perature of 110°C was four times higher while at the same time the peak width at half height is reduced by a factor of two (Table 6.2). A similar series of experiments was repeated with the PoraPLOT U column module. The acetic acid peak shape on this column at different injector temperatures is shown in Figure 6.5. From this figure and the data in table 6.2 it can be seen that the use of the heated injector is more important for the FFAP column than for the PoraPLOT U column. The latter column has a lower plate number and therefore the injection bandwidth is slightly less critical.

Table 6.2: Influence of injector temperature on the acetic acid peak parameters.

Injector Temp. (°C)	FFAP column				PoraPLOT U column			
	t _R (sec)	Height (μV)	Area	W½ (sec)	t _R (sec)	Height (μV)	Area	W½ (sec)
50	25.4	31338	24045	0.58	176.5	30423	174048	5.01
60	25.1	37390	25909	0.50	176.3	29988	175518	4.98
70	25.0	45708	27833	0.47	176.3	33194	170315	4.51
80	24.8	54785	30992	0.43	176.5	34290	159100	4.16
90	24.8	60358	33257	0.41	176.4	36011	155713	4.12
100	24.7	70724	35640	0.40	176.1	36336	145495	3.57
110	24.7	100873	48543	0.39	176.1	36931	147092	3.50

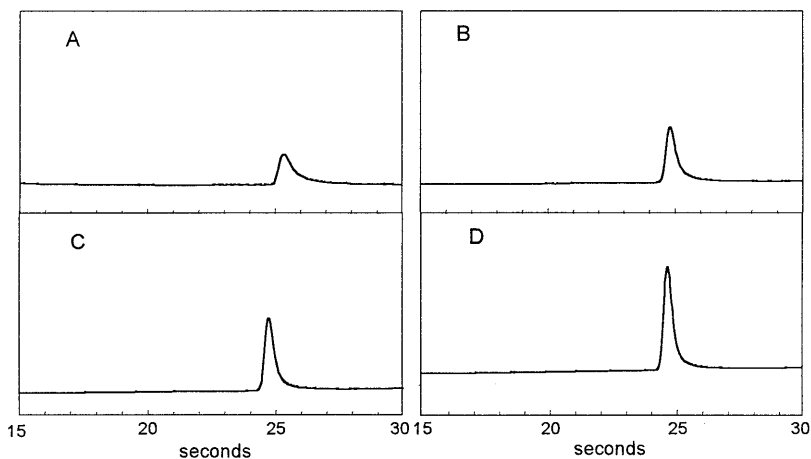


Figure 6.4: Acetic acid peak shape at different injector temperatures. Column: 6 m × 150 μm × 0.4 μm CP-FFAP, 200 kPa, 100°C. Injection time 50 msec. Injection temperature: A/ 50°C, B/ 80°C, C/ 100°C, and D/ 110°C.

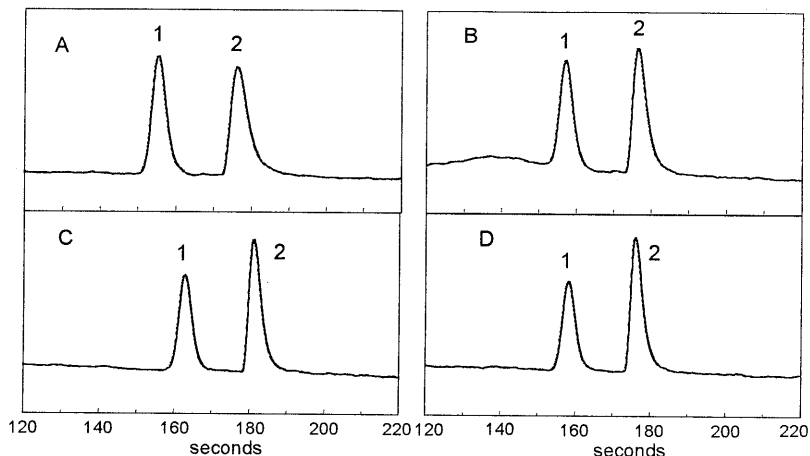


Figure 6.5: Acetic acid peak shape at different injector temperatures. Column: 10 m \times 320 μm \times 10 μm PoraPLOT U, 300 kPa, 150°C. Injection time 50 msec. Injector temperature: A/ 60°C, B/ 80°C, C/ 100°C, and D/ 110°C. Peak number: 1/ benzene and 2/ acetic acid.

The peak shapes of the other components were only marginally affected by the use of the heated injector. Peak areas of high boiling components such as for example toluene and *p*-xylene were found to be somewhat higher when working at elevated injector temperatures. This is most likely due to reduced condensation/adsorption of these components in the injection system. From these results it can be concluded that the use of a heated injector is certainly advisable if either highly polar solutes or low volatility components have to be analyzed. All further experiments were performed using a micro GC equipped with heated injectors.

6.2.3.3. Effect of Injection Times

The amount of sample injected onto the analytical column and therefore also the sensitivity of measurements is determined by the opening time of the valve. This parameter can be varied from 0 to 255 msec. Unfortunately, however, the injection time also affects the total band broadening of the peak. This effect can be quite significant, especially for the early eluting peaks that have an average peak width at half height of approximately 300-700 msec.

Figure 6.6 shows chromatograms of a mixture of benzene, toluene and *p*-xylene on the CP Sil-8 CB module with an injection time of 255 msec in the upper

trace and of 150 msec in the lower one. All other chromatographic conditions were identical. Good peak responses are observed for toluene and *p*-xylene in the upper trace while no peaks can be seen in the lower trace. Longer injection times thus improve the detection limits.

Chromatograms recorded at different injection times for a mixture containing methanol, methyl bromide and methyl formate using the PoraPLOT U column are shown in Figure 6.7. The injection times used here were 50 msec, 150 msec and 255 msec, respectively. As can be seen from this figure, baseline separation between the methanol and methyl bromide peaks can be obtained only at a short injection time. Longer injection times cause band broadening which in turn results in errors in quantitation due to the poor separation of the two components.

From this study we can conclude that the injection times of the two channels must be carefully optimized. A conflicting situation occurs where a selection has to be made based on sensitivity *versus* separation adequacy. For the CP Sil-8 CB column an injection time of 255 msec can be used whereas only a 50 msec injection time is allowed for the PoraPLOT U channel. In the first column sensitivity is preferred while separation is more critical in the latter.

6.2.3.4. Influence of Water Vapor on the Calibration Graphs

In order to investigate the influence of water vapor on the chromatographic performance of the target components calibration graphs of the components of interest were constructed using standard gas samples with or without water being

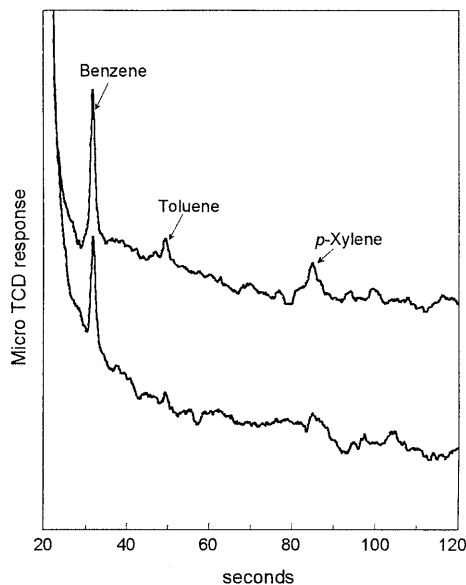


Figure 6.6: Effect of the injection time on the detection limit. Column: 4 m × 150 μm × 0.2 μm CP Sil-8 CB, 200 kPa, 70°C. Injection time: upper trace 255 msec, lower trace 150 msec.

added to the gas. Moreover, estimations of the detection limits as well as upper limits of the linear dynamic range were made based on these calibration graphs.

Calibration graphs were constructed based on both peak areas and peak heights of the components. Single-component gas mixtures in air were generated with the laboratory-made head-space sampling device. The reservoir was filled with a pure (liquid) component. The concentration of the component in the gas stream was calculated from the weight loss of the device and the air flow rate through the apparatus. By altering the air dilution flow rate, which could be set in the range of a few mL/min to some 2 L/min, a wide range of concentrations could be generated. To prepare concentrations near the detection limit levels the DKK gas generator, which operates on the diffusion principle, was used. Gas standard cylinders were used to cross-check the response factors found using the above mentioned methods for the generation of gas standards.

To investigate the effect of water vapor on the signal of the components of interest, similar calibration graphs were constructed also for high humidity samples. These samples were generated by leading the air dilution flow through a water reservoir before feeding it to the mixing chamber of the head-space sampling device. In this way the gas standard samples were saturated with water vapor.

Figure 6.8 shows the calibration graphs of acetic acid constructed with dry samples (A) and wet samples (B) measured on the FFAP column. Comparable parameters (Table 8.3) of these calibration graphs for dry samples vs. humid sam-

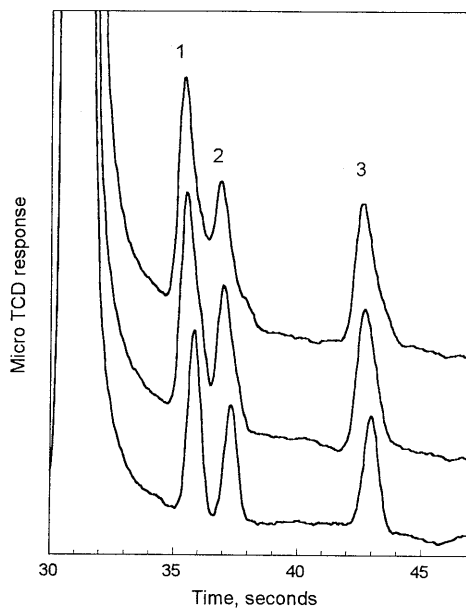


Figure 6.7: Effect of the injection time on the peak shape and chromatographic resolution. Column: 10 m \times 320 μ m \times 10 μ m PoraPLOT U, 300 kPa, 150°C. Injection time: upper trace 255 msec, middle trace 150 msec, and lower trace 50 msec. Peak number: 1/ methanol, 2/ methyl bromide, and 3/ methylformate.

ples, measured on the FFAP column as well as the PoraPLOT U column indicate that the water vapor has no significant adverse effect on the chromatographic performance of the system for acetic acid. The slightly lower values of the slopes of the calibration graphs in the latter case, *i.e.* with humid samples, are most likely due to higher adsorption/condensation losses in the sample generation system. Similar results were also obtained with other components. This indicates that the sampling line should also be heated to avoid losses of the components of interest due to adsorption into the condensed water layer.

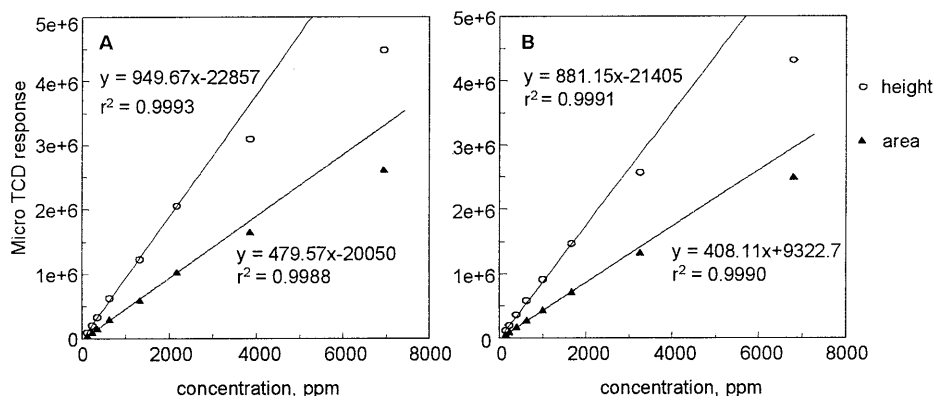


Figure 6.8: Calibration graphs of acetic acid measured on the FFAP (thick-film with heated injector) column module. A – dry samples, B – humid samples.

Table 6.3: Parameters of calibration graphs (on area basis) of several test components measured on different micro GC column modules.

Compound	Column	Dry samples			Humid samples		
		slope	intercept	r^2	slope	intercept	r^2
Acetic acid	FFAP	479	-20050	0.9988	408	9322	0.9990
	PoraPLOT U	297	-5210	0.9988	276	-2227	0.9995
Benzene	Sil-8	723	227754	0.9978	741	23748	0.9970
	PoraPLOT U	358	34253	0.9980	357	-3079	0.9991
	PoraPLOT Q	368	-30007	0.9979	332	-21411	0.9981
Methyl acetate	PoraPLOT U	326	106014	0.9941	305	115485	0.9993
	PoraPLOT Q	306	-4835	0.9989	299	31368	0.9985

As can be seen from Figures 6.8, A and B, in most cases the calibration graph based on peak areas has a larger linear dynamic range than that based on

heights. The effect of column overloading on the peak heights is obviously much stronger than that on peak areas. The presence of water had no significant effect on the quantitative performance of the components of interest, irrespective of the concentration level of the water. Estimations of the detection limits and upper limits of the linear dynamic ranges found for the various components on different micro GC column modules are summarized in Table 6.1.

A comparison of the response factors, defined as the ratios of the detector signal (area or height, respectively) over the concentration of the component, measured with gaseous standard mixtures generated via three different methods is shown in Table 6.4. Large differences in response factors of the acetic acid peak indicate that its calibration remains a difficult task. Compared to the response factors of the acetic acid gas mixtures generated using the head-space device, the lower response factors obtained when using the DKK diffusion device are obviously due to the fact that at lower concentration levels adsorption losses of acetic acid are relatively higher than at high concentrations. In case of the use of gas standard cylinders, adsorption of acetic acid onto the cylinder wall during storage is the most likely reason for the observed lower response factors.

Table 6.4: Comparison of response factors measured with three different methods for the generation of the (gaseous) standard mixture.

Compound (module)	Source	Concentration (ppm)	Response factor	
			height	area
Acetic acid (FFAP)	Dyn. head space *	100-1800	557	262
	DKK diffusion device	16	248	157
	DKK diffusion device	8	191	132
	BOC cylinder (0 bar)	150	296	149
	BOC cylinder (1 bar)	150	325	165
	BOC cylinder (2.5 bar)	150	377	191
<i>p</i> -Xylene (FFAP)	Dyn. head space *	40-3000	1627	432
	BOC cylinder (0.5 bar)	25	1598	408
Methyl acetate (PoraPLOT Q)	Dyn. head space *	150-12000	762	477
	DKK diffusion device	34	695	386
	BOC cylinder (0.5 bar)	25	751	368

* Response factors were taken as slopes of calibration graphs over a wide concentration range

6.2.3.5. Influence of the sample pressure

The influence of the sample pressure on the micro GC signal was investigated

in two ways, either by changing the input pressure at the sample inlet of the micro GC or by adjusting the “pulling” power of the built-in vacuum pump. In either way different pressures of the gas sample inside the micro GC’s sample line before injection onto the analytical column can be realized. Shortly before the actual injection the sample loop content is pressurized using carrier gas to a pressure slightly higher than the head column pressure. A part of the sample loop is then pushed into the carrier gas stream of the analytical column when the injection valve is open.

For the first series of experiments, *i.e.* changing the sample stream pressure applied at the sample inlet of the micro GC, a gas standard cylinder was used. The vacuum pump configuration was kept unchanged. The cylinder contains acetic acid, methyl formate and methyl acetate in helium. Figure 6.9 shows the effect of the sample inlet pressure on the signal of these components. The higher the pressure applied, which means the lower the difference in pressure of the sample loop and the pressurizing carrier gas, the higher the peak intensity.

A similar pattern was obtained in the second series of experiments where the sample inlet pressure was kept constant at ambient pressure while the pulling power of the vacuum pump was differently adjusted in the range of 350 to 900 mbar (Figure 6.10). To enable the adjustment of the vacuum power of the pump, a split line with a needle valve was added to the connection between the

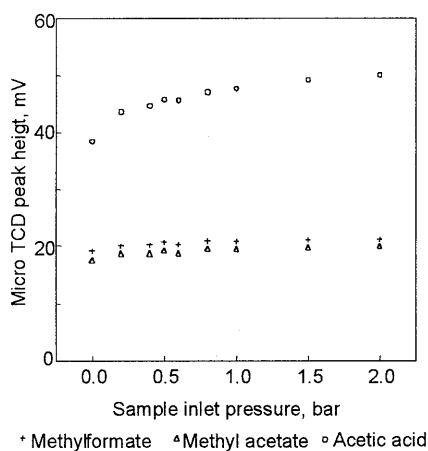


Figure 6.9: Effect of the sample inlet pressure (relative) on the component signals.

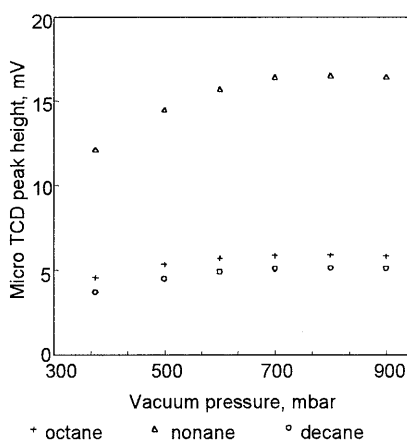


Figure 6.10: Effect of the pulling power (absolute pressure) of the built-in vacuum pump on the component signals.

pump and the outlet of the micro GC sample loop. The full vacuum power, *i.e.* 350 mbar, of the pump was obtained with the needle valve totally closed. As can be seen from the Figure 6.10 the peak signal is stable if the vacuum is above approximately 700 mbar. This phenomenon can be explained by the fact that the sample loop content is pressurized before being injected onto the analytical column. The short time period for pressurizing is fixed by the micro GC software. This time period is, however, not long enough to fully pressurize the sample loop to the preset level in case of too low vacuum (lower than 700 mbar). More precisely, in case the difference in pressure of the sample loop content and the preset carrier gas pressure is too large. The sample loop content is then less “dense” resulting in a lower amount to be injected onto the column. The component signals therefore become lower.

From this study it can be concluded that in order to obtain a stabilized maximum signal under various gas sample pressures while maintaining the highest possible sampling flow rate for the vacuum pump, the time period for pressurizing the sample loop before the actual injection should be prolonged for complete pressurization.

6.3. FIELD TRIAL

6.3.1. Selection of Column Modules and Instrumental Set-up

A boiler vent stack was chosen for the field trial. Based on the evaluatory study described above a system consisting of a CP Sil-8 CB column and a PoraPLOT U column was selected. This selection was made mainly because this module combination covers the entire range of the components of interest in one chromatographic run while maintaining a reasonable sensitivity.

A bench top micro GC was made suitable for field operation. The dimensions of the instrument are approximately 40 cm × 39 cm × 15 cm. The weight is 30 kg. An internal helium carrier gas tank and a battery were added. The gas tank is made from stainless steel, has a volume of 1 L and can be pressurized with helium up to 120 bar. This carrier gas tank allows continuous operation over approx. 48 hours. Due to the use of heated injectors, the build-in battery only allowed stand-alone operation for one hour. The micro GC was, therefore, run on an external power supply. The following chromatographic conditions were set

on the micro GC: channel A - 4 m \times 150 μm \times 0.2 μm CP Sil-8 CB column 70°C, 200 kPa; channel B - 10 m \times 250 μm \times 10 μm PoraPLOT U column 150°C, 300 kPa. The injector temperatures on both channels were set at 110°C unless stated otherwise.

Maestro 2.3 software (Chrompack) installed on a portable PC T1650CT (Toshiba, Tokyo, Japan) controlled operation of the micro GC. The laptop PC was also run on an external power supply.

Three gas standard cylinders were used for recalibration. The first cylinder contains methanol, benzene, toluene and *p*-xylene (50 ppm each) in nitrogen. The second cylinder contains methyl acetate in nitrogen at a concentration of 1000 ppm. Methyl bromide (50 ppm) in nitrogen was in the last cylinder. All cylinders were purchased from BOC.

At the boiler vent stack sampling point a tent was build with a power supply line. The sampling probe was a stainless steel tube of approximately 1.5 m allowing samples to be taken at different positions across the stack. A schematic diagram of the on-site sampling system is shown in Figure 6.11. Due to the limited sampling flow that the micro GC can manage, *i.e.* approx. 10 mL/min, and the large volume of the sampling probe, a split line was added in order to have a continuous flow of sample to the sample inlet of the micro GC.

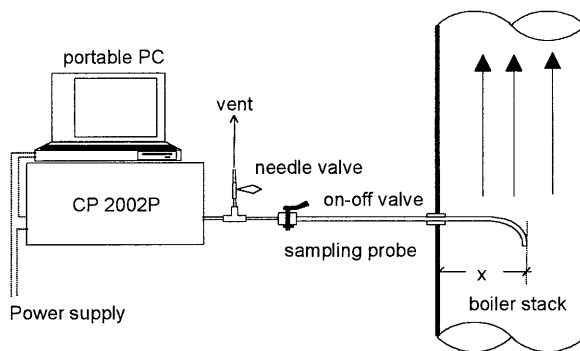


Figure 6.11: Schematic diagram of the instrumental set-up for the field trial at the boiler vent stack.

6.3.2. Laboratory Testing and Recalibration

The micro TCD was found to be the most vulnerable part of the micro GC. If the carrier gas is contaminated with oxygen, the filaments of the TCD are easily damaged. During upgrading of the bench-top version to a field instrument and

shipping the micro TCDs in both channels were damaged and had to be replaced. The micro GC, therefore, had to be re-calibrated using the gas standard cylinders. Detailed parameters of the micro GC in use is given in Table 6.5.

Table 6.5: Micro gas chromatograph CP 2002P configuration and characteristics

Channel	A		B	
<u>Column</u>				
Type	CP Sil-8 CB		PoraPLOT U	
Dimension	4 m × 150 μm × 0.2 μm		10 m × 250 μm × 10 μm	
Head pressure (kPa)	200		300	
Temperature (°C)	70		150	
<u>Injector</u>				
Temperature (°C)	110		110	
Time (msec)	255	150	150	50
<u>Detection Limits (ppm)</u>				
Benzene	1.0	1.5	8.0	15.0
Toluene	1.5	2.0		
p-Xylene	2.0	3.0		
Methanol			3.0	3.0
Methyl bromide			2.5	3.0
Methyl formate				
Methyl acetate			2.5	3.0
<u>Change in Response Factor (new/old)</u>				
Benzene	1.32	1.80	1.54	1.29
Toluene	1.25	1.72		
p-Xylene	1.19	1.59		
Methanol			1.72	1.47
Methyl bromide			1.69	1.45
Methyl formate				
Methyl acetate			1.59	1.56
<u>Reproducibility (area RSD %)</u>				
Gas standards			2-6	
Tedlar bag samples			4-15	

During testing in the laboratory the application of heated injectors in the micro GC was again confirmed to be very important. Apart from poorer detection limits, especially for higher boiling components, the standard CP Sil-8 CB module showed a rather long stabilization time. Without the heated injector this column module needed approximately one to two hours for the signal to stabi-

lize instead of only a few minutes as on the PoraPLOT U column module which was equipped with a heated injector. Adsorption in a cold injection system is the most likely cause for the lower signals found for the components in the system that did not contain a heated injector. A couple of hours is probably the time required for the temperature of the injector to stabilize and the surfaces to equilibrate.

6.3.3. On-site Analysis

The on-site analyses can be divided in two parts. The first part was an investigation of the fluctuation of the vent gas composition in time. The second part was dedicated to evaluate the effect of the sampling probe position on the concentrations of the components of interest.

The investigation of the time fluctuation of the vent gas composition was carried out when the plant started its normal operation again after a two-week shutdown due to technical problems. The sampling probe was placed in the middle of the stack. The micro GC was programmed to take a sample every 10 minutes. The sampling time was set at 30 sec per run. An analysis was completed within 5 min. The injector temperature on both channels was set at 70°C. At higher injector temperatures the baseline noise increased dramatically. This was most likely due to the disturbances of the carrier gas flow through the injection system at higher temperatures. Figure 6.12 shows the variations of the concentrations of the components over approx. 20 hours. Typical chroma-

Table 6.6: Composition of the boiler vent stack gas determined by micro GC and NMP adsorption analysis.

Component	micro GC analysis		NMP analysis	
	aver. concn. (ppm)	RSD (%)	Bottle 1	Bottle 2
Benzene	4.9	7.5	20.1	<2.0
Toluene	2.6	19.7	3.0	<2.0
<i>p</i> -Xylene	17.4	27.7	17.9	<2.0
Water	3595.3	2.4	na	na
Methanol	4.9	42.1	4.1	<2.0
Methyl Bromide	3.7	25.3	na	na
Methyl Formate	6.7	27.1	na	na
Methyl Acetate	127.1	11.8	127.7	19.1
Acetic Acid	nd		54.4	49.1

na ...not available,

nd ... not detected.

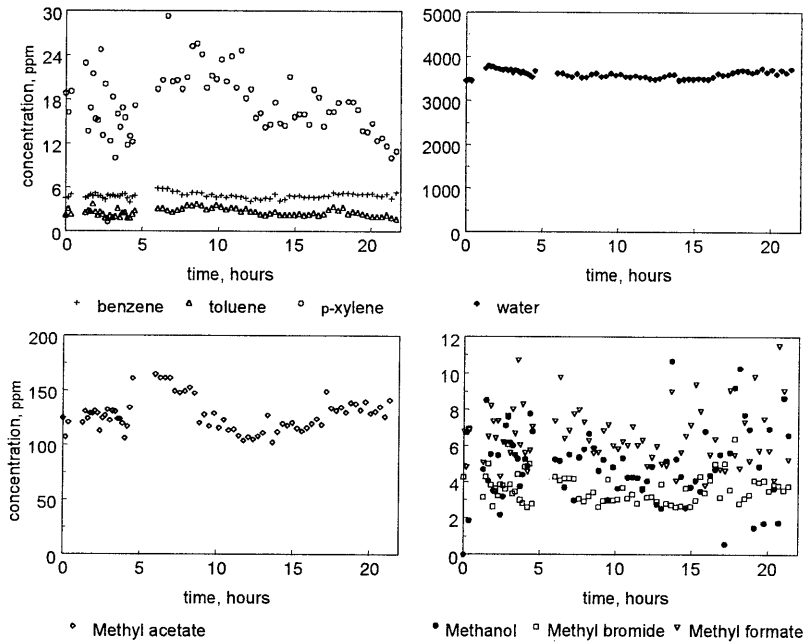


Figure 6.12: Time fluctuation of the vent-gas composition.

tograms of the vent stack gas are shown in Figure 6.13. Acetic acid, which should elute at a retention time of around 200 sec on Channel B, was not detected due to its low concentration (<20 ppm) in the gas sample. The mean concentration values and RSDs of the components detected are summarized in Table 6.6. For comparison a determination of the gas composition was carried out using the "old" method currently in use, *i.e.* bubbling the vent gas through a N-methyl-2-pyrrolidone (NMP) solution followed by GC analysis. Higher values obtained for benzene and acetic acid are believed to be due to the contamination of the NMP solution with these components.

To investigate the composition of the vent gas across the stack, the distance that the sampling probe was placed in the stack was varied. The stack has a diameter of approx. 1 meter. The probe was inserted to six different positions 5 cm, 25 cm, 40 cm, 60 cm, 75 cm and 95 cm, into the stack. Some 5 runs were carried out at each position. Figure 6.14 shows the average values and standard deviations of the concentrations of the components at each position. From this figure it can be concluded that the gas composition inside the stack is relatively

homogeneous. Only if the entrance of the sampling probe was very close to the inlet of the probe in the vent stack, lower concentrations of the components were found. This is most likely because now a large part of the probe is positioned outside the stack. In this cold part of the probe components could be lost due to condensation and/or adsorption. Heating the part of the probe that is outside the vent stack could be a solution to this problem.

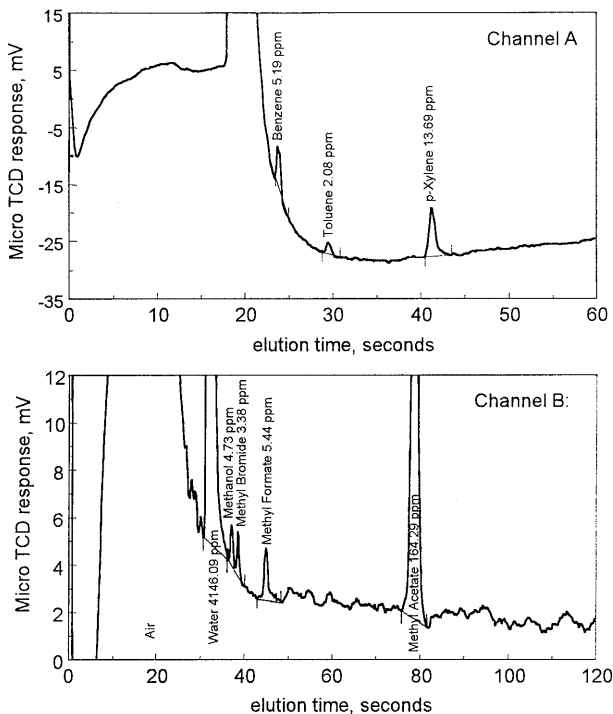


Figure 6.13: Typical chromatograms of a vent stack gas sample analyzed by the portable micro GC.

6.4. CONCLUSIONS

The study described in this chapter clearly illustrates the potentials of the micro GC as a (trans)portable device for precise and accurate analysis of gas streams containing a wide range of components largely differing in boiling points and polarities. The system is shown to be extremely powerful for on-the-spot analysis in the particular case of vent stack gas monitoring. The high content of water in the gas has no adverse effects on the chromatographic performance of the components of interest. A column system is proposed that enables accurate analysis of the components of interest in a humid gas stream. Detection limits were found to be in the low ppm range and the linear dynamic ranges were in general four orders of magnitude or better.

In the field trial the average values of the concentrations of the components of interest determined using the micro GC agree very well with those obtained us-

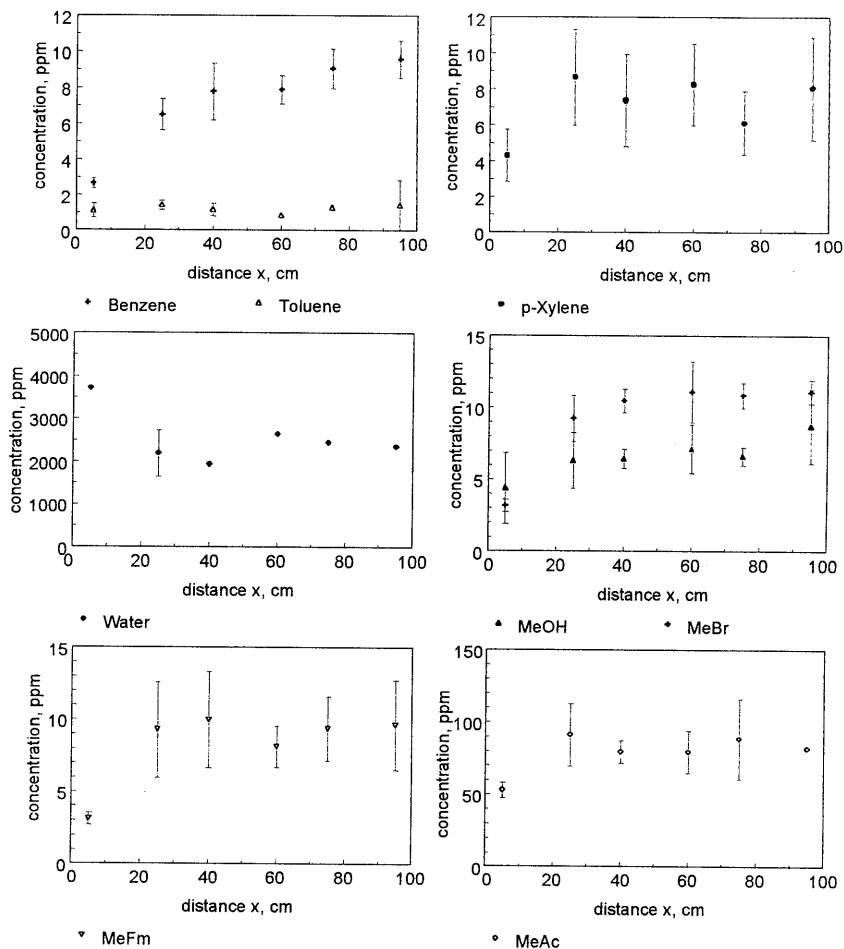


Figure 6.14: Composition of the vent gas at different locations inside the vent stack.

ing the analysis method currently in use. The micro GC has a number of advantages over the “old” method. A larger number of components can be analyzed. Moreover, the micro GC analysis can be automated and is much faster. The range of components amenable to analysis is extended, *i.e.* methyl bromide and methyl formate can be determined in the same analytical procedure applied for other components. A single analysis can be completed in only 5 minutes.

The most important improvement is the fact that the micro GC allows “on the spot” analysis. The risk of errors from either the loss of components or the in-

roduction of contaminants during sampling and transportation is, therefore, significantly reduced. The fluctuation of the vent gas composition in time can be closely and accurately monitored, allowing a detailed monitoring of the environmental impact of the plant and opening new possibilities for process control.

The field trial, however, has also shown that the concentration levels for some of the components of interest on the test point are close to the detection limits of the micro GC. In order to the concentration levels below the current detection limits further improvements in micro GC sensitivity are required.

Other recommendations are issued concerning the performance of the micro GC. First the heated injector should be improved to prevent distortion of the carrier gas flow when heating the injector and thereby improve baseline stability. Second the micro GC software should be adjusted to allow a longer pressurization time of the sample before injecting it into the analytical column. The effect of the pressure of the gas sample in the sampling line on the volumes injected thus could be eliminated. The micro GC should be evaluated over a longer time period to establish the reliability, especially of the electronics and detectors.

REFERENCES

1. R. Reston and E. S. Kolesar Jr., *J. Microelectromech. Systems*, 3 (1994) 134.
2. S. Kolesar Jr. and R. R. Reston, *J. Microelectromech. Systems*, 3 (1994) 147.
3. R. C. M. de Nijs, J. van Dalen, A. L. C. Smit and E. M. van Loo, *J. High Resolut. Chromatogr.*, 16 (1993) 379.
4. W. Bruns, *Am. Environm. Lab.*, 7 (1995) 29, 30, 32, 34.
5. H. Pham Tuan, H.-G. Janssen, C. A. Cramers, P. Mussche, J. Lips, and N. Wilson, *Proc. 18th Int. Symp. Capillary Chromatogr. Electrophoresis*, Riva del Garda, Italy, May 20th-24th, Volume III, p. 2213.

Chapter 7

SAMPLE ENRICHMENT BY EQUILIBRIUM (AB)SORPTION IN OPEN TUBULAR TRAPS. FUNDAMENTAL ASPECTS¹

ABSTRACT

In recent years there has been a substantial progress in the field of high-speed narrow-bore capillary gas chromatography in general, and in the development of (trans)portable gas chromatographs (GCs) for fast and accurate analysis in field applications in particular. Due to the limited (concentration) sensitivity of instrumentation for high-speed (portable) GC, environmental applications of this technique frequently require a preconcentration step. The equilibrium (ab)sorption technique developed here is found to be very promising for on-line coupling to high-speed narrow-bore capillary GC and field portable GC instruments. Enrichment factors up to at least 100 can be obtained rapidly without the use of complicated instrumentation. The new preconcentration technique is shown to have clear advantages over enrichment based on conventional adsorption - thermal desorption techniques. It can be carried out at ambient trapping temperatures, gives uniform desorption profiles, reduces water effects, uses inert adsorption materials and does not require a (cryogenic) refocussing step. Moreover, the new preconcentration method allows the enrichment factors to be predicted from tabulated chromatographic data, thereby facilitating calibration.

¹ Partially published as "Novel Preconcentration Technique for On-line Coupling to High-Speed Narrow-Bore Capillary Gas Chromatography: Sample Enrichment by Equilibrium (Ab)sorption. Part I: Principles and Theoretical Aspects" by H. Pham Tuan, H.-G. Janssen, and C. A. Cramers in *J. Chromatogr. A*, 791 (1997) 177-185.

7.1. INTRODUCTION

Despite the tremendous progress in detection techniques for gas chromatography (GC), the analysis of low concentrations of target solutes in gaseous samples still often requires enrichment of the sample prior to introduction into the gas chromatograph. Most of the sample enrichment techniques for gaseous samples currently in use in GC are based on the principle of adsorption-thermal desorption (ATD) using solid adsorption materials [1-4].

On-line coupling of an ATD-based enrichment device with high-speed narrow-bore capillary GC is complicated due to the very strict requirement for a narrow input bandwidth. One way to meet this demand is to incorporate a cryofocusing step to refocus the solutes on the analytical column. Van Es and Janssen [5] developed a microcryofocusing device that is capable of generating the very narrow input bandwidths required for high-speed narrow-bore capillary GC. The device was later improved by Borgerding *et al.* [6]. With such a system, ATD-based techniques are, at least in principle, also suited for combination with narrow-bore capillary GC. For reasons of portability, as in case of GC field applications, the use of cryogenic refocusing is, however, not possible. In this situation packed microtraps such as those reported by Frank *et al.* [7] and Mitra *et al.* [8-11] have to be used for on-line enrichment with narrow-bore fast GC analysis. Despite the extremely low volume of these traps, the bandwidth requirements of narrow-bore capillary GC are still not fully satisfied. A sufficiently fast transfer of the desorbed solutes onto the chromatographic system can only be obtained for a mega-bore, *e.g.* 530 μm i.d., analytical column, which allows a high gas flow rate during the desorption step.

An important and growing application area of high-speed narrow-bore capillary GC is the area of field (trans)portable analytical devices. Unfortunately these instruments have a limited applicability in environmental analysis as their detection limits are generally in the low ppm range [12]. For the analysis of components present at lower concentrations, the field-portable GC has to be equipped with a suitable preconcentration device. As explained above, the direct on-line coupling of ATD-based techniques to field portable GC instruments equipped with narrow-bore GC column is difficult at best [13]. This is not only because no cryogenics can be used in portable instruments, but also because these instruments

often use silicon-micromachined injection valves that operate according to the “time-slice” injection principle. Until now only an off-line enrichment technique compatible with portable high-speed GC was reported [14].

In order to overcome the above mentioned drawbacks we have developed a new sample preconcentration/enrichment technique - the technique of equilibrium (ab)sorption. With this new sample enrichment technique, the standard silicon-micromachined injection valves used as injectors in portable GC instruments can be used without modification. The new technique is capable of on-line generating a homogeneously enriched sample flow. Any part of this flow is representative for the entire sample and therefore enables reproducible injection into the GC system. The need to transfer the entire desorption volume onto the analytical column is thus eliminated. The volume to be injected now can be adjusted to the requirements of the chromatographic system and the use of a refocussing step is no longer necessary. This feature is clearly very advantageous for high-speed narrow-bore capillary GC, in which the injection volume is a critical parameter. In this chapter the principles and theoretical aspects of the new method are discussed. In Chapter 8, the analysis of selected hydrocarbons and volatile organic compounds (VOCs) in air using an on-line system consisting of a preconcentration device based on equilibrium (ab)sorption and a field-portable GC is described.

7.2. THEORY

In previous work silicon-micromachined injection valves have been found to be excellent systems for the introduction of (gaseous) samples in high-speed narrow-bore capillary GC [15]. The injection valves operate according to the principle of “time-slicing”. A schematic diagram of a silicon-micromachined injection valve as used in the field-portable GC can be found in Figure 5.4 (*viz.* Chapter 5). The gas sample is pressurized inside the sample loop. The silicon-micromachined injection valve is then opened for a fraction of a second to allow part of the content of the sample loop to enter the chromatographic column. Short injection times, typically in the range of 10 to 250 msec, result in a very narrow input bandwidth. This injection technique is not compatible with ATD enrichment techniques as with these methods unpredictable desorption profiles are obtained (Figure 7.1). If the “injection slice” is taken from the first part of the desorption volume, only the

volatile solutes are recovered and *vice versa*. Time-slicing injection techniques are only compatible with ATD if the trap is strictly miniaturized so that the entire volume of desorption gas can be transferred onto the GC column. When using narrow-bore columns (i.d. <math><100\ \mu\text{m}</math>) this is virtually impossible.

To overcome this disadvantage we developed a preconcentration method that produces a steady flow of homogeneous, preconcentrated sample gas - the method of equilibrium (ab)sorption. Any slice from this flow is virtually the same and representative for the entire enriched sample flow. An additional advantage of this technique is that the enrichment factors do not have to be established experimentally as they can be calculated from GC retention data. The theoretical backgrounds of this method are described below.

7.2.1. Equilibrium (Ab)sorption Procedure

In the equilibrium (ab)sorption technique a steady flow of enriched sample gas is generated. To do so a large volume of the gas sample that is to be enriched, is pumped through a tube containing an (ab)sorption material at a mild, *e.g.* (ambient) temperature. Sampling is continued until the (ab)sorption material in the trap is saturated with the components of interest. More precisely, sampling is continued until the sorbent phase is in equilibrium with the gas phase. Once this equilibrium has been achieved the trap is closed and the system is heated to shift the equilibrium from the sorbed state to the gas phase. Unlike the situation in the ATD method, sampling is continued beyond the breakthrough point. To avoid oxidation of the sorbent phase at high temperatures, the air is eliminated from the trap by shortly purging it with helium prior to starting the heating step. Heating is performed under stop-flow conditions to a predetermined (high) temperature.

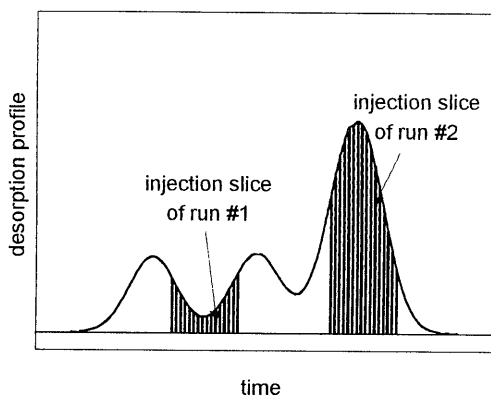


Figure 7.1: Desorption profile from an ATD-based trap and subsequent time-slice injections.

7.2.2. Prediction of Enrichment Factors

In order to allow rapid equilibration of the entire bed of (ab)sorption material in a reasonably short time while simultaneously allowing quantitative desorption of the trapped components at a mild temperature, the use of a weak (ab)sorption material is advisable. This in contrast to the conventional break-through sampling approach, where it is better to use a strong adsorbent or a combination of adsorbents with increasing strength. Moreover, to produce a stable desorption profile, the sorbent bed has to be homogeneous and the concentration of the solutes has to be fairly stable within the sampling time. In the current work we opted for the use of a mega-bore thick-film non-polar wall coated open tubular (WCOT) column as the preconcentration trap. Sorption of the components is now based on a pure partitioning mechanism which is relatively weak. This allows rapid equilibration of the sorption tube. In addition to this, the use of an open tubular preconcentration device gives the required homogeneity to the desorption plug. Moreover, because sorption is based on partitioning solely, displacement effects should be absent. Finally, the enrichment factor can be readily calculated from GC retention data. The enrichment factor that can be achieved by the procedure, $E_{T_1-T_2}$, can be defined as:

$$E_{T_1-T_2} = \frac{c_{m,T_2}}{c_{m,T_1}} \quad (7.1)$$

Where c_{m,T_1} is the concentration of the component of interest in the original flow of sample gas at temperature T_1 and c_{m,T_2} is its concentration in the enriched sample gas stream coming from the tube at temperature T_2 . Using standard chromatographic theory these parameters can be expressed as:

$$c_{m,T_2} = \frac{c_{s,T_2}}{K_{D,T_2}} = \frac{c_{s,T_2}}{k_{T_2} \beta} \quad (7.2)$$

$$c_{m,T_1} = \frac{c_{s,T_1}}{K_{D,T_1}} = \frac{c_{s,T_1}}{k_{T_1} \beta} \quad (7.3)$$

Where c_{s,T_1} and c_{s,T_2} are the concentrations of the component of interest in the stationary phase; k_{T_1} and k_{T_2} are the respective capacity factors and K_{D,T_1} and K_{D,T_2} are the partitioning coefficients at temperatures T_1 and T_2 , respectively. β is the phase ratio of the trapping column.

The total amount of a solute in the trap after sampling, m_{trap} , is given by:

$$m_{trap} = c_{m,T_1} \cdot V_m + c_{s,T_1} \cdot V_s \quad (7.4)$$

Where V_m and V_s are the mobile phase and the stationary phase volumes of the column. During the helium purging step that is applied to remove air, an amount roughly equal to the first term in the right hand side of equation 7.4 is lost. After heating the trap the total amount can again be expressed by an equation similar to equation 7.4, but now with the T_2 indexes. This results in:

$$c_{s,T_1} \cdot V_s = c_{s,T_2} \cdot V_s + c_{m,T_2} \cdot V_m \quad (7.5)$$

After substitution of equation 7.2 in this equation we have the following relationships:

$$\begin{aligned} c_{s,T_1} &= c_{m,T_2} \cdot k_{T_2} \cdot \beta \cdot V_s + c_{m,T_2} \cdot V_m \\ &= c_{m,T_2} \cdot k_{T_2} \cdot V_m + c_{m,T_2} \cdot V_m \\ &= (k_{T_2} + 1) \cdot c_{m,T_2} \cdot V_m \end{aligned} \quad (7.6)$$

or:

$$c_{m,T_2} = \frac{c_{s,T_1} \cdot V_s}{V_m \cdot (k_{T_2} + 1)} = \frac{c_{s,T_1}}{\beta \cdot (k_{T_2} + 1)} \quad (7.7)$$

Combining equations 7.1, 7.3 and 7.7 gives the final relationship for the enrichment factor:

$$E_{T_1-T_2} = \frac{k_{T_1}}{k_{T_2} + 1} \quad (7.8)$$

As can be seen from this equation the enrichment factor is roughly equal to the capacity factor of the solute at the sorption temperature used in the sampling process. This because at the high temperature used for desorption the solute's capacity factor is usually much smaller than one. Equation 7.8 also shows that the enrichment factor can be easily obtained experimentally by simply measuring the capacity factors of the solute at two temperatures on a column coated with the same stationary phase, not necessarily with the same film thickness.

Alternatively, the capacity factors of the solutes at the two temperatures employed in the preconcentration procedure can be extracted from the Kovat's retention indices or published enthalpy and entropy data using the procedures men-

tioned in ref. [16]:

$$\ln k = \ln \frac{\alpha}{\beta} + \frac{\Delta H}{RT} \quad (7.9)$$

Where (α/β) is the so-called entropy term and $(\Delta H/R)$ is the enthalpy term.

Using the same considerations we can calculate the minimum time required for sampling, *i.e.* the time required to reach the equilibrium state at a temperature T_1 . This time equals the elution time of the components using air as the carrier gas. If we neglect the pressure drop across the trapping column and if we further assume that the column has an infinitely large number of theoretical plates, the required minimum sampling time is given by:

$$t_{\text{sampl.}} = t_M \cdot (k_{T_1} + 1) = \frac{V_m}{v_{T_1}} \cdot (k_{T_1} + 1) \quad (7.10)$$

Where v_{T_1} is the sampling flow rate measured at the outlet of the trapping column.

Using helium as the desorption gas at a volumetric flow rate v_{He} and a desorption temperature T_2 and again neglecting pressure drop over the trap, the output plug width is now given by:

$$t_{\text{plug}} = \frac{V_m}{v_{He}} \cdot (k_{T_2} + 1) \quad (7.11)$$

In practical terms, after enrichment a continuous flow of homogeneous sample with duration of t_{plug} is obtained. Multiplication of t_{plug} with the flow rate gives the total volume of enriched gas available. This volume should be sufficient to flush the connecting lines between the enrichment unit and the micro GC.

7.2.3. Effect of Pressure Drop

In the previous section it was assumed that no pressure gradient exists over the trap, neither during sampling nor during desorption. Below it will be demonstrated that the compressibility of the gas streams can have a significant influence on the composition of the enriched sample.

The variation of the gas pressure $p(x)$ along a capillary column of length L is described by the following equation:

$$p(x) = p_o \cdot \sqrt{\left(\frac{p_i}{p_o}\right)^2 - \frac{x}{L} \left[\left(\frac{p_i}{p_o}\right)^2 - 1\right]} \quad (7.12)$$

Where x is the distance from the column inlet. p_i and p_o are the column inlet and outlet pressures, respectively. This relationship is graphically shown in Figure 7.2. The existence of a pressure gradient across the column has significant consequences for the local concentrations of the solute molecules. The concentration of the solute in the mobile phase, expressed as mass per volume

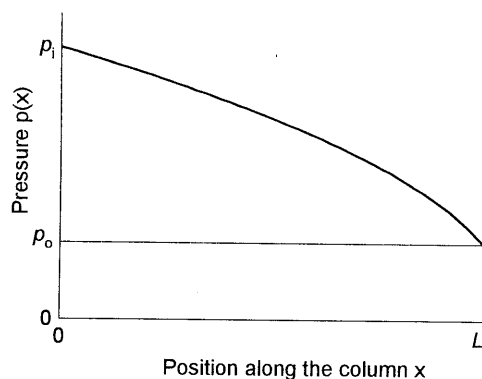


Figure 7.2: Pressure drop along the capillary column.

unit, follows the pressure pattern along the trapping column. This now means that also the solute concentration (expressed as mass per volume unit) in the stationary phase in equilibrium with the mobile phase decreases from a higher value at the inlet to a lower value at the outlet. A concentration gradient occurs in the stationary phase reflecting the pressure drop in the mobile phase.

To fulfill the requirement of a stable desorption profile, the concentration difference between the starting point and the end point of the concentration gradient should not be higher than (arbitrarily) 10%. This results in the requirement that the pressure drop over the trapping column during sampling is less than 10%, *i.e.* $(\Delta p/p_i) \leq 0.1$. In practice, in order to avoid possible contamination of the trap, the gas sample stream is pulled through the adsorption tube by means of a vacuum pump rather than pumped through the trap at elevated pressures. This means that the inlet pressure p_i will be maintained at ambient pressure (1 bar). The outlet pressure p_o then should not be lower than 0.9 bar.

7.2.4. "Vacuum Enrichment" Considerations

Section 7.2.2 demonstrated the calculation of enrichment factors based on their mass-per-volume concentrations. A more accurate definition of the enrichment, however, has to be based on the molar fraction of the components. This leads us

to an alternative possibility for improving the detector signal. In this section it will be demonstrated that the molar fraction of the component in the gas stream can be increased using the so-called “method of vacuum enrichment”.

In the method of vacuum enrichment proposed here, the trapping column is equilibrated and then purged with helium as described in section 7.2.1. Just before the column isolation step, the gas inside the column, *i.e.* the helium, is evacuated using the vacuum pump of the micro GC. The column that is now under vacuum is then closed and heated to release the trapped components and transfer them to the micro GC as described before. As the number of moles of helium mobile phase in the column is decreased due to the evacuation, the mole fraction of the released components in the enriched gas sample plug is now increased. This results in a higher sensitivity.

The concentration of the enriched component in the desorbed He gas stream is described by the equation:

$$c_{m,T_2} = \frac{f_{m,T_2} \cdot M \cdot n_{mp,des}}{V_m} \quad (7.13)$$

From equation 7.1 we have:

$$c_{m,T_2} = c_{m,T_1} \cdot E_{T_1-T_2} = \frac{f_{m,T_1} \cdot M \cdot n_{mp,sorp}}{V_m} \cdot E_{T_1-T_2} \quad (7.14)$$

Where $n_{mp,sorp}$ and $n_{mp,des}$ are the number of moles of matrix gas occupying the free volume V_m of the capillary column during the sorption or desorption process, respectively. In our case $n_{mp,sorp}$ is the number of moles of air in the trap during sampling and $n_{mp,des}$ is the number of moles of He purging gas occupying the trapping column after evacuation. M is the molecular weight of the component of interest. The terms f_{m,T_1} and f_{m,T_2} are the molar fractions of the component of interest during sorption and desorption, respectively. The “true” enrichment factor is then expressed as:

$$I_{T_1-T_2} = \frac{f_{m,T_2}}{f_{m,T_1}} = \frac{n_{mp,sorp}}{n_{mp,des}} \cdot E_{T_1-T_2} \quad (7.15)$$

This equation implies that in the final calculation of the enrichment factor we have to include the ratios of the pressures (or numbers of moles per trap volume) during the sampling and the desorption process. The number of air molecules in

the trap during the sorption process $n_{mp,sorp}$ is fixed due to the fact that ambient pressure sampling is used. The helium purge gas is evacuated by means of a vacuum pump prior to sealing the trap and starting the desorption, *i.e.* $n_{mp,des} < n_{mp,sorp}$. The enrichment factor, therefore, increases. We call this effect “vacuum enrichment”.

In practice, to reach a 10-fold enrichment with the vacuum effect, the vacuum system in use must be able to reduce the pressure in the trap to at least 100 mbar. This is not achievable with the micro GC’s build-in vacuum pump. The “vacuum enrichment” method has, hence, no practical importance as an individual preconcentration technique. It could, however, be a valuable addition to the equilibrium technique. An additional 2- to 5-fold enrichment, achieved by this vacuum effect, will reduce the preconcentration factor to be obtained for the equilibrium technique by the same factor. This means we might need only an enrichment factor of 200 to 500 instead of 1000 to be achieved in the equilibrium stage. Consequently, the demand for short a sampling time can be met more easily. Incorporating the vacuum effect into the overall enrichment process requires, however, more precise control of the vacuum system. It was therefore decided not to further pursue this option. Finally the vacuum effect enrichment described here proves that pressure effects have to be carefully taken into account when calculating/predicting the “true” enrichment factor using the technique of equilibrium (ab)sorption.

7.2.5. Sampling Flow Rate

For practical reasons the sampling time should be as short as possible. This means that the use of higher sampling flow rates for equilibration of the trap is desirable. However, this should not result in pressure drops exceeding 10% of the inlet pressure. In case of open tubular columns, the volumetric flow rate through the column at a given inlet and outlet pressure can be calculated according to the Hagen-Poiseuille equation [17].

$$F = \frac{\pi \cdot d_c^4}{128 \cdot \eta \cdot L} \cdot (p_i - p_o) \quad (7.16)$$

Where η is the viscosity of the sample gas stream. The results of the calculation for different column sizes at various pressure drops are shown in Table 7.1. For air samples the viscosity at 30°C is approximately $200 \mu\text{P} = 2 \cdot 10^{-4} \text{ g}/(\text{cm} \cdot \text{sec})$

[17]. For a number of columns also experimental values were measured. Lower measured values for the larger-bore columns compared to the calculated data are most likely due to extra restriction effects in the valves and tubing used in the experimental set-up.

Table 7.1: Inlet flow of gas through open-tubular trapping columns of different dimensions and at different pressure drops.

p_i (bar)	p_o (bar)	d_c (μm)	L (m)	V_c (mL)	F (mL/min)	
					calculated	measured
1.0	0.9	530	20.0	4.412	2.9	3.0
1.0	0.5	530	20.0	4.412	11.5	13.5
1.0	0.3	530	20.0	4.412	13.9	17.5
1.0	0.9	530	10.0	2.206	5.8	6.5
1.0	0.5	530	10.0	2.206	22.9	21.5
1.0	0.3	530	10.0	2.206	27.8	26.8
1.0	0.9	530	5.0	1.103	11.6	7.8
1.0	0.5	530	5.0	1.103	45.9	25.6
1.0	0.9	750	5.0	2.209	46.6	
1.0	0.9	1000	5.0	3.927	147.3	
1.0	0.9	1000	2.0	1.571	368.2	
1.0	0.9	1000	1.0	0.785	736.3	200.0
1.0	0.9	2000	5.0	15.708	2356.2	
1.0	0.9	2000	2.0	6.283	5890.5	
1.0	0.9	2000	1.0	3.142	11781.0	

7.2.6. Requirements for the Open Tubular Trapping Column

From the theoretical considerations described above, a number of requirements the trapping column has to meet can be identified. First of all the trapping column should generate a sufficiently large volume of enriched sample to flush the transfer lines to the GC injector. Furthermore, a certain minimum plate number is required to obtain a stable concentration profile. Moreover, there is a maximum allowable pressure drop. Below these parameters are examined in more detail.

The volume of enriched sample that is generated by the trapping column during desorption has to be large enough to thoroughly flush the connecting lines and sample loop of the GC instrument. The sampling and injection system of a portable GC instrument typically has an internal volume of 200 to 500 μL . The trapping column therefore should have a volume V_c of approx. 2 mL or more, suffi-

cient to flush the inlet system four to ten times. This criterium is met for all columns fulfilling the length/diameter requirements described by the following equation:

$$L \geq \frac{4 \cdot V_c}{\pi \cdot d_c^2} = \frac{2.548 \cdot 10^{-6}}{d_c^2} \quad (7.17)$$

Equation 7.10 indicates that the minimum sample volume that has to be passed through the trapping column to reach equilibrium is at least $(k_{T_1} + 1)$ times larger than the column volume itself. This relationship is valid only if the trapping column has an infinite plate number. In practice a correction factor must be incorporated into the equation to correct for the finite plate number of the trap. The sample volume needed for 95% breakthrough [18] is:

$$V_{\text{sampl}} = V_c \cdot (k_{T_1} + 1) \cdot \left(1 + \frac{2.326}{\sqrt{N}} \right) \quad (7.18)$$

Where N is the column plate number. If the trapping column has a volume of 2 mL, 100 theoretical plates and if the capacity factor of the component at the low sampling temperature is 100 (enrichment factor is approx. 100), the sample volume needed for 95% breakthrough is approximately 125 mL. To ensure full equilibration the sample volume should be even larger. In order to complete the sample pretreatment procedure in a reasonably short time, the sampling flow rate F should be sufficiently high. In our consideration a sampling flow rate of some 100 mL/min would be appropriate. This, however, should not result in an excessive pressure drop. The column dimensions that can give a flow rate of 100 mL/min at an inlet pressure of 1 bar and an outlet pressure of 0.9 bar are given by:

$$L = \frac{\pi \cdot d_c^4}{128 \cdot \eta \cdot F} \cdot (p_i - p_o) = 7.457 \cdot 10^{12} \cdot d_c^4 \quad (7.19)$$

A minimum column plate number is required in order to obtain a sharp desorption profile. Due to the low pressure drop over the trap the equation describing the theoretical plate height of the column for large k values can be simplified to:

$$H = \frac{2 \cdot D_m}{u} + \frac{11 \cdot d_c^2 \cdot u}{96 \cdot D_m} \quad (7.20)$$

Where D_m is the diffusion coefficients of the solute in the mobile phase and u is

the linear velocity of the mobile phase. In our case the mobile phase is air. The volatile organic compounds of interest have D_m values in air of around $0.1 \text{ cm}^2/\text{sec}$ [17]. By substituting $H = L/N$ and $u = 4F/\pi d_c^2$ and some simple mathematical operations we obtain the following equation describing the length required to obtain a plate number of 100 as a function of column diameter:

$$L = 2.433 + 942 \cdot d_c^2 \quad (7.21)$$

The three equations 7.17, 7.19 and 7.21 describing relationships between the column length L and diameter d_c that a useful trap should meet are graphically shown in Figure 7.3. The following numerical values are used: $F = 100 \text{ mL/min}$, $p_i = 1 \text{ bar}$, $p_o = 0.9 \text{ bar}$, $\eta = 2 \times 10^{-4} \text{ g/(cm}\cdot\text{sec)}$, $D_m = 0.1 \text{ cm}^2/\text{sec}$, and $N = 100$. Line 1 identifies columns with an internal volume of 2 mL. Line 2 shows columns with 100 theoretical plates at a flow rate of 100 mL/min. Line 3 finally represents columns that give a flow rate of 100 mL/min at an inlet pressure of 1 bar and an outlet pressure of 0.9 bar. From this figure it can be seen that the column of choice should be in the shaded area. Only columns with a diameter of 0.7 mm or larger can meet the requirements. These columns will have at least 100 theoretical plates, an internal volume larger than 2 mL and at the same time allow a sampling flow rate higher than 100 mL/min at a pressure drop of 0.1 bar (10%).

7.3. EXPERIMENTS

7.3.1. Experimental Set-up

A series of model experiments was performed to investigate the applicability of the equilibrium preconcentration approach developed here. A schematic diagram of the set-up is shown in Figure 7.4. The detector used in these experiments was an FID. The preconcentration system constructed consists of a high tempera-

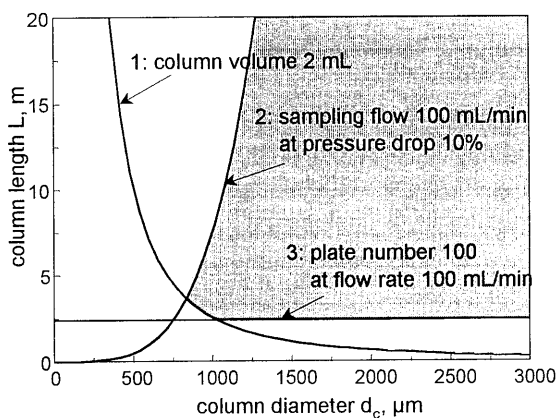


Figure 7.3: Requirements for the open tubular trapping column. Columns fulfilling the requirements of having more than 100 theoretical plates, having an internal volume larger than 2 mL and allowing higher flow rates than 100 mL/min at less than 0.1 bar pressure drop are in the shaded area.

ture six-port switching valve N6WT with 0.010-inch port diameter (VICI Valco, Schenkon, Switzerland) and a 20 m \times 530 μm \times 5 μm CP Sil-5 CB (Chrompack, Middelburg, the Netherlands) open-tubular trapping column in-

stalled inside the oven of a Varian 3400 GC (Sunnyvale, CA, USA). Trap columns with larger diameters meeting the requirements stated in section 7.2.6 were not available by the time these experiments were carried out. In order to have sufficient volume of the enriched gas sample available, a rather long column had to be employed which precluded the use of high sampling flow rates due to the fact that only a low pressure drop can be tolerated (*viz.* section 7.2.3).

Figure 7.4 shows the flow selection valve in the "sampling" position. The 0.010-inch bore of the valve and the 20-m long 530- μm i.d. column used here limited the sampling flow rate to *ca.* 15 mL/min without causing excessive pressure drop. After equilibrium had been established, the valve was switched to the "desorb-flush" position for about 2 minutes in order to purge the column with helium carrier gas to remove air. The helium flow rate during purging was about 3 mL/min. After this the valve was switched to the "isolation" position, an intermediate position between the "sampling" and the "desorb-flush" positions and the GC oven was heated to the desorption temperature. After the oven reached the desired temperature, the valve was switched to "desorb" and the enriched sample plug was pushed out of the column directly to an FID detector by the helium carrier gas. Gaseous standard samples of alkanes in air were generated using the laboratory-made dilution device described previously (*viz.* Chapter 2).

7.3.2. Results and Discussion

Figure 7.5 shows the desorption profiles of *n*-heptane (A), *n*-octane (B) and *n*-nonane (C). The sorption temperature was 30°C, the desorption temperature was 200°C. The low plateaus around 3, 7 and 18 minutes, respectively, show the

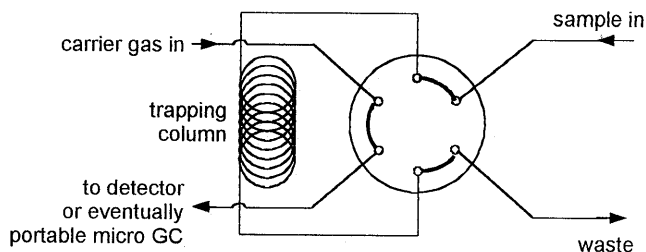


Figure 7.4: Schematic diagram of the experimental set-up for the equilibrium (ab)sorption procedure.

original gas samples. The high plateau signals the enriched samples. The narrow peaks at the beginning of a plateau are caused by flow disturbances. A flow distortion on the mass flow sensitive FID results in a peak, despite the fact that the concentration is stable. The figure clearly shows that stable, enriched gas flows can be generated using the approach developed here. Depending on the conditions used and the components studied, enrichment factors between 3 and 60 were found.

Table 7.2 shows a summary of calculated and experimentally observed capacity factors as well as enrichment factors. Calculated factors were obtained from published (α/β) and $(\Delta H/R)$ data [19]. The table shows that these values are in good agreement with the experimental data measured using conventional GC-FID. The differences sometimes observed are most likely due to small variations in the sampling and desorption flow rate and inaccuracies in the published enthalpy and entropy values. Enrichment factors now can be predicted either directly from the calculated capacity factors or from the experimentally obtained retention data. Direct experimental measurement of enrichment factors is possible by comparing the heights of the desorption plateaus with the heights of un-enriched gas sample signals. Values of

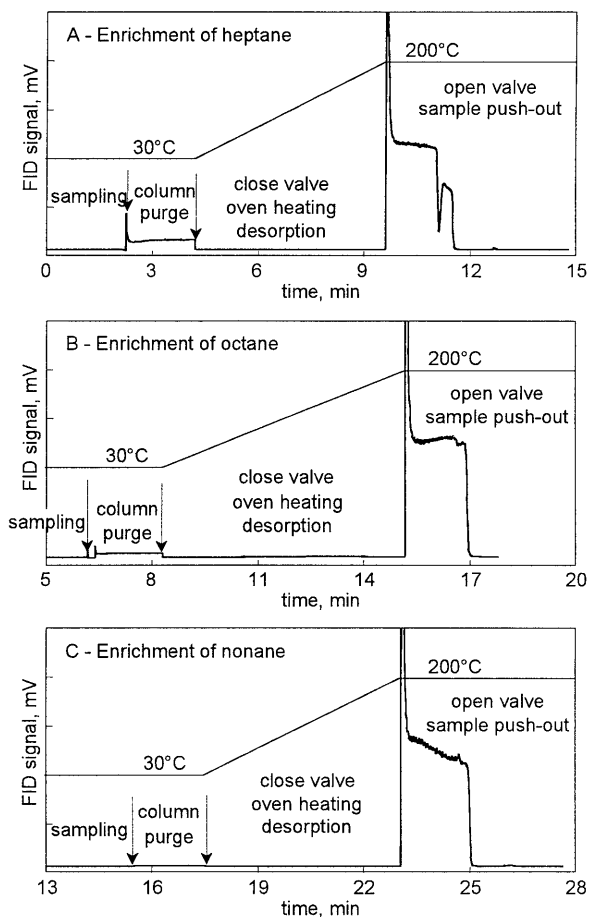


Figure 7.5: Examples of the desorption profiles of alkanes obtained using the equilibrium (ab)sorption technique.

experimentally measured enrichment factors are summarized in the lower part of Table 7.2. Again a good agreement with calculated values can be observed. Repeated retention time measurements, used for calculation of the capacity factors, have shown relative standard deviations (RSDs) lower than 1%. RSD's of the measured enrichment factors are generally in the range of 5-8%.

As can be seen from the equations in section 7.2.2, the enrichment factors strongly depend on the temperatures used for sorption and desorption and, to a lesser extent, on the phase ratio of the column. Lower sorption temperatures, higher desorption temperatures and lower phase ratios increase the enrichment factors substantially. The results in Figure 7.5 and Table 7.2 clearly illustrate the potentials of this new method of gas preconcentration. Further studies, described in the next chapter, are dedicated to exploring the full potentials of the new technique and evaluate the coupling of the preconcentration technique described here to portable instrumentation for high-speed GC for selected applications such as analysis of volatile organic compounds (VOCs) in air.

Table 7.2: Calculated and experimentally found enrichment factors of the tested *n*-alkanes.

Compound	thermodyn. term		capacity factor				enrichment factor		
	a/β	$\Delta H/R$	$k_{30^\circ\text{C}}$	$k_{140^\circ\text{C}}$	$k_{200^\circ\text{C}}$	$k_{250^\circ\text{C}}$	$E_{30^\circ\text{C}-140^\circ\text{C}}$	$E_{30^\circ\text{C}-200^\circ\text{C}}$	$E_{30^\circ\text{C}-250^\circ\text{C}}$
Calculated capacity factors and enrichment factors^a:									
<i>n</i> -hexane	136.0E-6	3163	4.62	0.29	0.11	0.06	3.59	4.17	4.37
<i>n</i> -heptane	67.0E-6	3680	12.54	0.50	0.16	0.08	8.39	10.81	11.65
<i>n</i> -octane	34.2E-6	4179	33.14	0.84	0.23	0.10	17.97	26.85	30.11
<i>n</i> -nonane	17.0E-6	4682	86.67	1.42	0.34	0.13	35.83	64.81	76.63
Measured capacity factors, calculated enrichment factors^b:									
<i>n</i> -hexane			3.75	0.23	0.15	0.06	3.05	3.26	3.53
<i>n</i> -heptane			10.00	0.39	0.23	0.09	7.19	8.13	9.17
<i>n</i> -octane			26.42	0.68	0.26	0.12	15.73	20.97	23.59
<i>n</i> -nonane			69.71	1.13	0.41	0.19	32.73	49.44	58.60
Measured enrichment factors^c:									
<i>n</i> -hexane							3.33	3.56	3.75
<i>n</i> -heptane							7.76	9.05	10.15
<i>n</i> -octane							16.67	21.67	22.25
<i>n</i> -nonane							36.25	52.50	61.25

^a Capacity factors were calculated using equation 7.9, enrichment factors from equation 7.8.

^b Capacity factors were calculated using measured retention data: $k=(t_R-t_M)/t_M$, enrichment factors were calculated using equation 7.8.

^c Enrichment factors were measured as ratio of plateau heights on the desorption profiles.

7.4. CONCLUSIONS

The study described in the present chapter clearly demonstrates the potentials of the new enrichment technique for preconcentrating gaseous samples for high-speed narrow-bore capillary GC in general or field-portable GC instruments in particular. Because the new method generates a homogeneously enriched sample flow, a preconcentration device based on the equilibrium (ab)sorption approach is compatible with silicon-micromachined injection valves as well as other "time-slice" injection devices used in high-speed narrow-bore capillary gas chromatography such as actuated sample valves. The large desorption gas volume that has to be transferred to the GC column in standard ATD techniques is no longer a limiting factor. The need for a refocusing step is eliminated and, last but not least, enrichment factors can be predicted in advance.

REFERENCES

1. G. Castello, M. Benzo, and T. C. Gerbino, *J. Chromatogr. A*, 710 (1995) 61.
2. H. Pham Tuan, H.-G. Janssen, E. M. Kuiper-van Loo, and H. Vlap, *J. High Resolut. Chromatogr.*, 18 (1995) 525.
3. M. R. Allen, A. Braithwaite, and C. C. Hills, *Int. J. Environ. Anal. Chem.*, 62 (1996) 43.
4. V. Camel and M. Caude, *J. Chromatogr. A*, 710 (1995) 3.
5. A. van Es, H.-G. Janssen, C. A. Cramers, and J. Rijks, *J. High Resolut. Chromatogr. Chromatogr. Commun.*, 11 (1988) 852.
6. A. J. Borgerding and C. W. Wilkerson, Jr., *Anal. Chem.*, 68 (1996) 701.
7. W. Frank and H. Frank, *Chromatographia*, 29 (1990) 571.
8. S. Mitra and C. Yun, *J. Chromatogr. A*, 648 (1993) 415.
9. Y. H. Xu and S. Mitra, *J. Chromatogr. A*, 688 (1994) 171.
10. S. Mitra and A. Lai, *J. Chromatogr. Sci.*, 33 (1995) 285.
11. S. Mitra, Y. H. Xu, W. Chen, and A. Lai, *J. Chromatogr. A*, 727 (1996) 111.
12. H. Pham Tuan, H.-G. Janssen, C. A. Cramers, P. Mussche, J. Lips, and N. Wilson, *Proc. 18th Int. Symp. Capillary Chromatogr. Electrophoresis*, Riva del Garda, Italy, May 20th-24th, Volume III, p. 2213.
13. T. Limero, J. Brokenshire, C. Cumming, E. Overton, K. Carney, J. Cross, G. Eiceman, and J. James, *SAE Technical Paper Series No. 921385*, ISSN 0148-7191, 1992, Society of Automotive Engineers, Inc.
14. M. W. Bruns, *Am. Environ. Lab.: On-Site Analysis*, Apr. 1995, p. 29.
15. A. van Es, H.-G. Janssen, R. Bally, C. A. Cramers, and J. A. Rijks, *J. High Resolut. Chromatogr. Chromatogr. Commun.*, 10 (1987) 273.
16. H. Snijders, H.-G. Janssen, C. A. Cramers, *J. Chromatogr. A*, 718 (1995) 339.
17. R. C. Weast and M. J. Astle, *CRC Handbook of Chemistry and Physics*, 1981-1982, 62nd Edition, CRC Press, Inc., Boca Raton, Florida, USA.

-
18. B. E. Werkhoven-Goewie, U. A. Th. Brinkman, and R. W. Frei, *Anal. Chem.*, 53 (1981) 2072.
 19. J. M. Curvers, *Ph.D. Thesis*, Eindhoven University of Technology, The Netherlands, 1985.

Chapter 8

VOC ANALYSIS BY COUPLING THE EQUILIBRIUM (AB)SORPTION ENRICHMENT DEVICE TO A PORTABLE MICRO GC¹

ABSTRACT

The technique of equilibrium (ab)sorption is proven to be a powerful method for pre-concentration of gaseous samples for high-speed narrow-bore capillary gas chromatography (GC) in general and field-portable GC instruments, often referred to as micro GCs, in particular. Using a simple experimental set-up equipped with an open-tubular enrichment column it is possible to produce a homogeneously enriched sample plug, allowing reproducible injections of an enriched sample into the portable micro GC. Using a non-polar trapping column, enrichment factors found for n-alkanes in the range of C₇ to C₁₀ ranged from 15 to 150 and were in good agreement with calculated values. No displacement effects were observed on this liquid phase. Using highly retentive Thermocap A columns at elevated sampling temperatures, the enrichment factors observed for volatile organic compounds (VOCs) were in the range of 500 to 1000. Sampling times were as short as 20 minutes. Displacement effects which can occur at high (total) concentrations, however, limit the applicability of this stationary phase to the enrichments of VOCs present at relatively low concentration levels. As the use of this new preconcentration method requires only minimum modification of the portable micro GC, the use of the preconcentration device does not compromise the chromatographic performance of the GC instrument. Examples of on-line enrichment with portable micro GC analysis of VOCs in air are shown. These examples clearly demonstrate the potentials of the new method in field analysis.

¹ Partially published as "Novel Preconcentration Technique for On-line Coupling to High-Speed Narrow-Bore Capillary Gas Chromatography: Sample Enrichment by Equilibrium (Ab)sorption. Part 2: Coupling to a Portable Micro Gas Chromatograph" by H. Pham Tuan, H-G. Janssen, C. A. Cramers, P. Mussche, J. Lips, A. Handley, and N. Wilson in *J. Chromatogr. A*, 791 (1997) 197-202.

8.1. INTRODUCTION

As stated in the previous chapter, the strict requirements imposed on the input bandwidth renders on-line coupling of a preconcentration device with instrumentation for high-speed narrow-bore capillary gas chromatography an extremely difficult task. Preconcentration devices based on conventional adsorption - thermal desorption (ATD) techniques cannot be directly coupled to narrow-bore GC without strict miniaturization and/or incorporation of a powerful cryofocusing step. These demands impose great difficulties in the construction of portable analytical instrumentation based on high-speed narrow-bore GC techniques.

Another approach, aiming to overcome the above mentioned drawbacks by the on-line generation of a flow of a homogeneously enriched gaseous sample, is the preconcentration method based on the principles of equilibrium (ab)sorption (see Chapter 7). The enriched sample flow generated allows highly reproducible injections onto narrow-bore columns using the "time-slice" injection technique of silicon-micromachined injection valves. The theoretical aspects and the principles of this technique have been described in detail in the previous chapter. Preliminary experiments with a mega-bore thick-film non-polar trapping column and an FID have given highly promising results. In this contribution the on-line coupling of this new preconcentration technique to a field-portable narrow-bore GC instrument has been realized. Different trapping columns, differing in dimension as well as in the nature and thickness of the stationary phase layer, have been evaluated. Gaseous standard samples containing the *n*-alkanes C₅ to C₁₀ were used. The new method has also been applied for VOC analysis in air. The results of this work will be described in detail.

8.2. ON-LINE COUPLING TO THE MICRO GC

8.2.1. Experimental Set-up

A schematic diagram of the instrumental set-up used for the experiments is shown in Figure 8.1. The field-portable narrow-bore GC instrument used in the present work was a CP 2002 Micro GC supplied by Chrompack (Middelburg,

The Netherlands). The micro GC was equipped with a $6 \text{ m} \times 150 \text{ }\mu\text{m} \times 0.4 \text{ }\mu\text{m}$ CP-FFAP column module and a $10 \text{ m} \times 250 \text{ }\mu\text{m} \times 10 \text{ }\mu\text{m}$ PoraPLOT Q column module. In order to minimize the dead volume of the sample inlet system as much as possible, the sampling line was disconnected from the original large connector where the sample flow is split for both channels and was reconnected directly to the sample outlet of the preconcentration system. The connection consisted of $320\text{-}\mu\text{m}$ i.d. empty fused-silica capillaries and Valco low dead-volume connectors (VICI Valco, Schenkon, Switzerland).

The gas enrichment system, which consists of a trapping column and high-temperature six-port switching valves, was placed inside the oven of a Varian 3400 GC (Varian, Palo Alto, CA, USA), thus providing constant temperature during sampling and desorption. Two high-temperature six-port switching valves (Valco) were used to switch the gas flows during the enrichment process. The lower valve, with 0.7-mm bore channels, directs either gaseous sample stream or helium purging gas through the trapping column. The upper valve, with smaller 0.4-mm bore channels, directs the desorbed effluent from the trapping column either to the micro GC for chromatography or to vent during post-run purging. The micro GC can also collect an original gas sample through this valve without the requirement to disconnect it from the system.

The micro GC contains a build-in vacuum pump for sampling gaseous samples into the sample loop. This vacuum pump was used to sample air through the enrichment device. To do so, a cross connector was installed in the line connecting the original sample inlet line of the micro GC and the build-in vacuum pump. A needle valve was installed in the vacuum line allowing the vacuum to be controlled. A flow

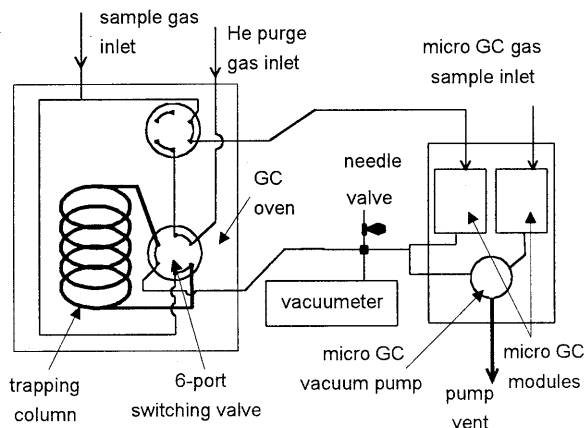


Figure 8.1: Schematic diagram of an equilibrium enrichment system coupled to a portable micro GC. The valve system is in the sampling position.

selection valve allows switching between enrichment and sample transfer to the GC. Using the needle valve the pressure drop over the trapping column can be adjusted to the desired value. As concluded from the theoretical deductions in Chapter 7, the use of outlet pressures below 900 mbar results in non-homogeneous desorption profiles.

The gaseous test samples were generated in a laboratory-made headspace device (*viz.* Chapter 2). The liquid reservoir was filled with either pure liquid components or with mixtures of liquids. The main characteristics of the compounds analyzed are summarized in Table 8.1. Air was used as the dilution gas. The pressure in the vessel was maintained at 1 bar (absolute).

Table 8.1: Physical characteristics of the test components.

Compound	MW (amu)	BP (°C)	Compound	MW (amu)	BP (°C)
<u>Pure hydrocarbons</u>			<u>VOC mixture</u>		
<i>n</i> -Pentane	72.15	36.1	Methylbromide*	94.94	3.6
<i>n</i> -Hexane	86.17	69.0	Dichloromethane	84.94	39.8
<u>Hydrocarbon mixture</u>			<i>trans</i> -1,2-Dichloroethene	96.95	47.2
<i>n</i> -Heptane	100.20	98.4	1,1,2-Trichlorotrifluoroethane	187.38	46.0
<i>n</i> -Octane	114.22	125.6	1,1-Dichloroethane	98.97	57.3
<i>n</i> -Nonane	128.26	150.8	Chloroform	119.39	61.5
<i>n</i> -Decane	142.29	174.1	1,1,1-Trichloroethane	133.42	74.1
<u>BTEX mixture</u>			<u>HVOC (Heavier VOC) mixture</u>		
Benzene	78.11	80.1	Chlorobenzene	112.56	131.5
Toluene	92.13	110.6	Bromobenzene	157.02	156.2
Ethylbenzene	106.16	136.3	Bromoform	252.77	149.5
<i>p</i> -Xylene	106.16	137.5	<i>i</i> -Propylbenzene	120.19	152.5
<i>m</i> -Xylene	106.16	139.3	<i>t</i> -Butylbenzene	134.21	168.5
<i>o</i> -Xylene	106.16	144.0	<i>s</i> -Butylbenzene	134.21	173.5
			1,2,4-Trichlorobenzene	181.46	213.0

* Methylbromide was available in a gas standard cylinder at a concentration of 25 ppm in Helium

Different trapping columns were used in the experiments:

- a 5 m × 530 μm × 5 μm CP Sil-5 CB column,
- a 10 m × 530 μm × 2 μm CP Sil-19 CB column,
- a 10 m × 530 μm × 2 μm CP-FFAP column,
- a 10 m × 530 μm × 10 μm Thermocap A column and
- a 5 m × 1 mm × 10 μm Thermocap A column.

All but the last column were made of fused silica. The last one was made from specially treated stainless steel. All columns were supplied by Chrompack.

8.2.2. Sampling and Desorption Procedure

Gaseous samples were pulled through the enrichment column by means of the micro GCs built-in vacuum pump. Due to software limitations, the maximum sampling time for the vacuum pump is 255 sec for each chromatographic run. The total sampling procedure, therefore, consisted of a series of subsequent 255-sec segments. During sample enrichment, the valve system is set in the position depicted in Figure 8.1. After the enrichment column reached equilibrium both valves were switched to the opposite positions, thereby allowing the helium carrier gas to purge the air out of the column. Depending on the volume of the trapping column, the total purging time was 1 to 2 minutes.

The trapping column is then sealed by switching the lower six-port valve to an intermediate position. The GC oven in which the entire preconcentration system is installed, is now heated from sampling temperature to the desorption temperature (*e.g.* 140°C, 200°C or 250°C). After temperature had stabilized, the six-port valve is switched back to the “inject” position and the micro GC is programmed for a series of consecutive chromatographic runs. During each run a “slice” of the enriched sample plug was injected into the micro GC’s column. To obtain the maximum sampling frequency, the transfer line between the enrichment system and the micro GC were only shortly flushed, *i.e.* 1 to 5 sec, prior to each injection. In the micro GC control software this is called the sampling time.

After the entire enriched sample was injected into the micro GC, the upper six-port valve was switched back to the sampling position to allow contaminants to be purged out of the trapping column. The GC oven could now be cooled down to the adsorption temperature thereby preparing it for the next run.

8.2.3. Results and Discussion

In the first series of experiments the enrichment process was monitored using the micro GC. By monitoring consecutive injections of the enriched sample, the desorption profile of the components of interest can be established simply by plotting the micro GC’s TCD signal for the individual components, *i.e.* peak ar-

eas, against the time during which enriched gas samples were taken and chromatograms were recorded. An example of this is shown in Figure 8.2. The gas eluting from the enrichment column was sampled every 40 seconds during desorption and the peak areas observed for a number of components were plotted *versus* time. These experiments were performed using the 5 m \times 530 μ m \times 5 μ m CP Sil-5 CB trapping column.

Two hours were needed to equilibrate the entire column using a gaseous sample containing *n*-alkanes from C₇ to C₁₀ at 30°C. As can be seen from Figure 8.2, the desorption profiles have sharp edges and long stable regions enabling repro-

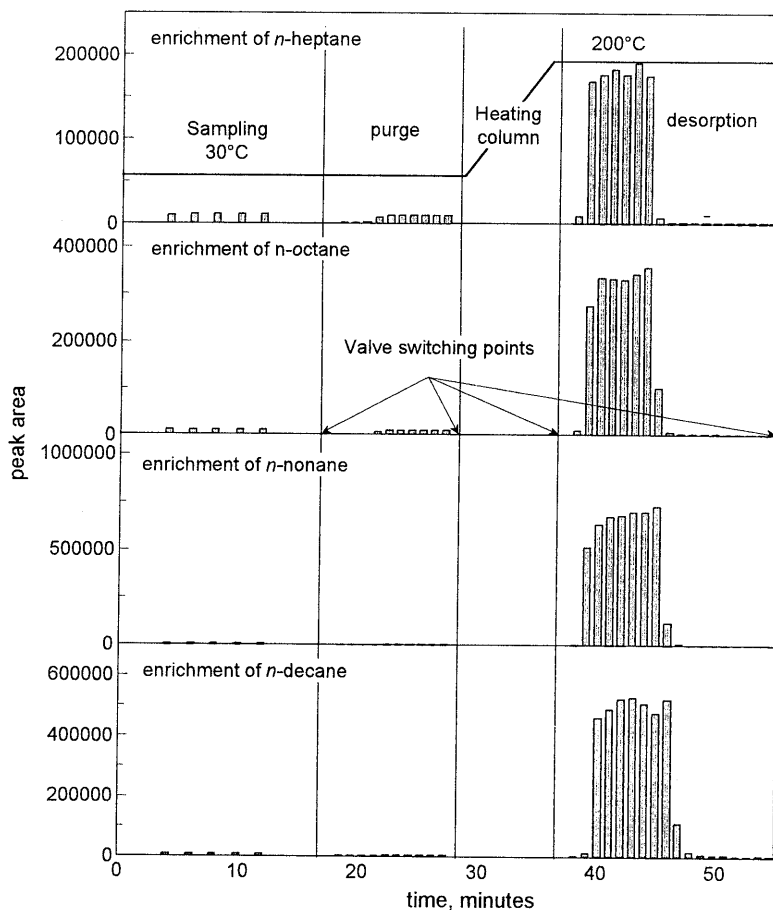


Figure 8.2: Desorption profile of *n*-alkanes after equilibrium (ab)sorption enrichment on a 5 m \times 530 μ m \times 5 μ m CP Sil-5 CB trapping column.

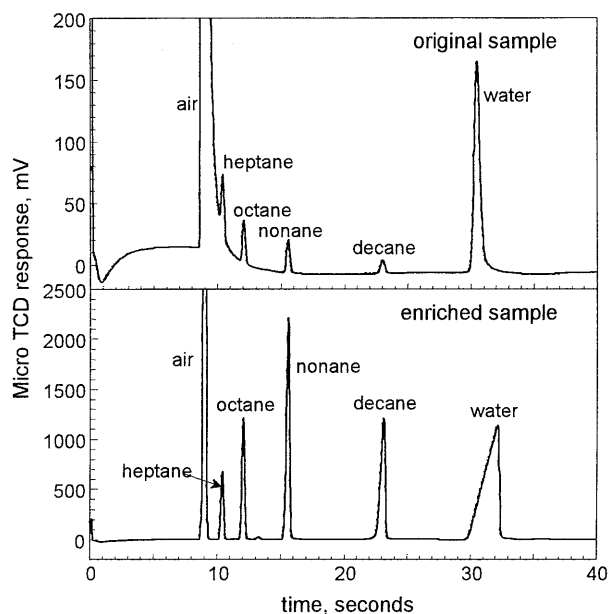


Figure 8.3: Chromatograms of the gaseous samples containing *n*-alkanes, measured on a micro GC. Chromatographic conditions: 6 m × 150 μm × 0.4 μm CP-FFAP column, 160 kPa, 40°C. Injection time 50 msec. Upper trace: original sample, lower trace: sample after equilibrium (ab)sorption enrichment from 30°C to 200°C on a 5 m × 530 μm × 5 μm CP Sil-5 CB trapping column. Note the difference in the y-scale.

Table 8.2: Calculated and experimental enrichment factors of the selected *n*-alkanes on the 5 m × 530 μm × 5 μm CP Sil-5 CB trapping column.

Compound	enrichment factor		
	$E_{30^{\circ}-140^{\circ}}$	$E_{30^{\circ}-200^{\circ}}$	$E_{30^{\circ}-250^{\circ}}$
<i>Calculated values</i>			
<i>n</i> -heptane	8.4	10.8	11.7
<i>n</i> -octane	17.9	26.9	30.1
<i>n</i> -nonane	35.8	64.8	76.6
<i>n</i> -decane	48.6	109.9	143.5
<i>Experimental values measured using the micro GC</i>			
<i>n</i> -heptane	10	15	15
<i>n</i> -octane	20	33	30
<i>n</i> -nonane	40	75	71
<i>n</i> -decane	65	110	150

ducible sampling onto the micro GC. The sampling time of two hours is, however, impracticably long for field operation. Chromatograms of the *n*-alkane mixture in air before and after enrichment are shown in Figure 8.3. From this figure it can be seen that the water present in the sample is significantly less enriched compared to the *n*-alkanes. This, hence, proves another advantage of this technique, *i.e.* water is largely eliminated. Enrichment factors at different desorption temperatures are shown in Table 8.2. The measured values are in reasonable to good agreement with the values calculated from published entropy and enthalpy data (*viz.* Chapter 7).

Entropy and enthalpy data of the components on a particular liquid stationary phase can also be deduced from

retention data measured on a capillary column coated with the same phase, regardless of the column dimension (*viz.* Appendix). Using this method enrichment factors of a number of components, especially VOCs, on various liquid stationary phases have been calculated. Their experimental values were obtained in a series of measurements conducted in the same way as with the *n*-alkanes. The data collected are summarized in Table 8.3.

Table 8.3: Calculated and experimental enrichment factors of selected VOCs using various trapping columns. Sampling temperature 30°C, desorption temperature 200°C.

Compound	CP Sil-5 CB column		CP Sil-19 CB column		CP-FFAP column	
	Cal.	Exp.	Cal.	Exp.	Cal.	Exp.
Chlorobenzene	47	48	31	29	38	36
Ethylbenzene	52	50	30	35	20	20
Bromoform	61	49	70	55	187	91
<i>p</i> -Xylene	39	37	34	39	21	22
<i>o</i> -xylene	135	120	42	50	30	28
Bromobenzene	155	151	73	72	86	75
<i>t</i> -Butylbenzene	75	68	96	105	44	38
<i>s</i> -Butylbenzene	47	45	99	110	48	44

Table 8.3 shows an excellent agreement between the enrichment factors calculated from retention data and the experimental values for most of the components tested except for bromoform. The large difference in case of this very polar component are apparently due to its strongly non-linear behavior on the liquid stationary phases in use. Chromatograms illustrating the enrichment of the test mixture on the FFAP column are shown in Figure 8.4.

Although the above mentioned experiments have clearly proven that the pre-concentration method works perfectly according to expectations, the technique still has many points that need to be improved. First of all higher enrichment factors are required. Furthermore the sampling time should be reduced. These two parameters are closely interrelated. In order to have a high enrichment factor, the trapping column must exhibit a strong retention for the component of interest at ambient sampling temperature. A column with a higher retention power, however, requires a longer equilibration time unless the column dimension, *i.e.* the column inner diameter and length, are changed facilitating higher sampling flow rates. At the same time all flow resistances, *e.g.* in the column as well as in tubing and valves, have to be reduced to an absolute minimum.

To increase the enrichment factors, a trapping column with a novel, much more retentive stationary phase, a $5\text{ m} \times 530\text{ }\mu\text{m} \times 10\text{ }\mu\text{m}$ Thermocap A column, was used. The enrichment of a gaseous sample consisting of *n*-heptane in air is shown in Figure 8.5.

This figure shows the breakthrough curve for *n*-heptane. From this figure it can be seen that *n*-heptane starts to break through and approach equilibrium only after 9 hours sampling. The sampling flow rate was *ca.* 10 mL/min which was

the maximum that could be used due to pressure drop limitations. Column equilibration with *n*-heptane required 11 hours! The flat plateau in the upper figure indicates the signal of the original sample. From the signal obtained during desorption (see lower trace in Figure 8.5) the enrichment factor of *n*-heptane can be estimated. Enrichment at 50°C followed by desorption at 140°C results in an enrichment factor of approx. 500.

The Thermocap A stationary phase, hence, appears very attractive for the pre-concentration of volatile components due to its extremely strong retention. The sampling time can be reduced to acceptable levels by applying a higher sampling flow rate. This can be achieved at an acceptable pressure drop by using a wider-bore trapping column. With a $2\text{ m} \times 1\text{ mm} \times 10\text{ }\mu\text{m}$ Thermocap A trapping column, the equilibration time for *n*-heptane could be reduced to approx. 2 hours. The desorption profile of *n*-heptane with the latter column is shown in

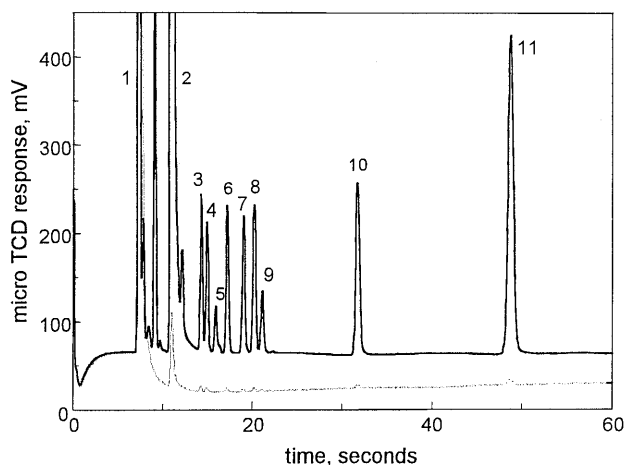


Figure 8.4: Chromatograms of an air sample containing several VOCs, recorded on the micro GC before (lower trace) and after (upper trace) equilibrium enrichment. Trapping column: $10\text{ m} \times 530\text{ }\mu\text{m} \times 2\text{ }\mu\text{m}$ CP-FFAP, sampling overnight at 30°C , desorption at 200°C . Micro GC chromatographic conditions: $6\text{ m} \times 150\text{ }\mu\text{m} \times 0.2\text{ }\mu\text{m}$ CP FFAP column at 80°C and 200 kPa, injection time 50 msec, injector temperature 110°C . Elution order: 1/ air, 2/ water, 3/ethylbenzene, 4/ *p*-xylene, 5/ isopropylbenzene, 6/ *o*-xylene, 7/ chlorobenzene, 8/ *t*-butylbenzene, 9/ *s*-butylbenzene, 10/ bromobenzene, and 11/ bromoform.

Figure 8.6. Compared to the desorption profile from Figure 8.5, it is obvious that the enriched sample plug is now less sharp rendering a more careful selection of the "slice" to be injected into the micro GC necessary. This is due to the lower plate number of the megabore trapping column.

The sampling time can be further shortened by increasing the flow rate through the column. Doing it without causing an excessive pressure drop over the column requires the careful reduction of every possible flow resistance in the sampling line. The six-port switching valve (lower valve

in Figure 8.1) with 0.4-mm bores used in the first series of experiments was replaced by a 0.7-mm bore valve. The length of the connecting tubing was reduced to a minimum. After all modifications, equilibration of the $2\text{ m} \times 1\text{ mm} \times 5\text{ }\mu\text{m}$ Thermocap A column could be completed within 50-60 min. A further reduction in sampling time could be achieved by using a shorter column, *i.e.* one meter instead of two meters. Even with the one-meter column the enriched gas volume obtained was sufficient for thorough flushing of the inlet line of the micro GC.

As stated above, however, the most effective way to reduce the time required for equilibration of the trap is to choose proper enrichment factors for the components of interest. In order to obtain detection limits in the ppb range, enrichment factors of, say, 500 must be achieved as the detection limits of a stand-alone micro GC are generally approximately 1-2 ppm. According to the equation for the enrichment factor we have derived in the previous chapter, and as-

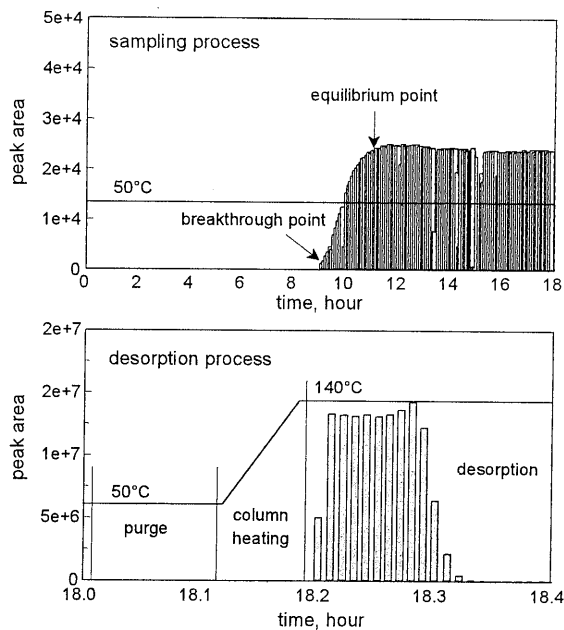


Figure 8.5: The time-dependent response of heptane measured on the micro GC during equilibrium (a) sorption enrichment process. Trapping column: $5\text{ m} \times 530\text{ }\mu\text{m} \times 10\text{ }\mu\text{m}$ Thermocap A, sampling at 50°C , desorption at 140°C .

suming the trapping column has a void volume of 1 mL and an infinite plate number, at least 500 mL of gas must be drawn through the column before equilibrium is established. Because of the fairly low plate number of the trapping column used in the experiments, equilibrium is only reached when sampling is continued far beyond the breakthrough

point. This means that in this case a sample volume of some 1000 mL is necessary. At a sampling flow rate of 100 mL/min, *ca.* 10 min is needed for the sampling process. The simple consideration presented above demonstrates how closely the two parameters, sampling time and enrichment factor, are interrelated. An unnecessarily high enrichment factor will result in excessively long sampling times, which are not acceptable for fast GC procedures. Sampling times of less than 20 minutes can be considered to be feasible. In order to achieve this goal all parameters, such as for example type of stationary phase and sampling temperature, must be carefully optimized.

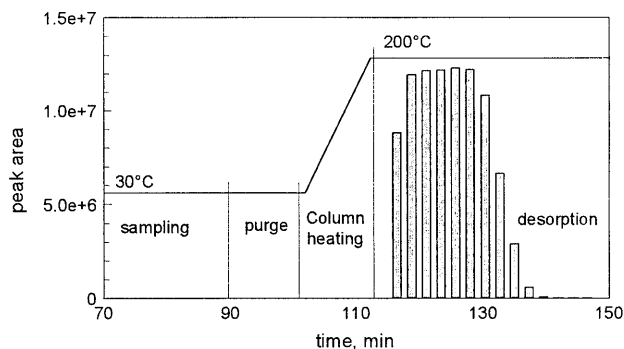


Figure 8.6: Desorption profile of heptane during equilibrium (ab)sorption enrichment using a 2 m × 1 mm × 10 μm Thermocap A stainless steel trapping column. Sampling 90 min at 30°C, desorption at 200°C.

8.3. APPLICATION IN VOC ANALYSIS

To demonstrate the potentials of the new preconcentration technique in field applications, it was applied for the analysis of VOCs in air. A 1 m × 1 mm × 10 μm Thermocap A column was used for these experiments.

8.3.1. Enrichment at Ambient Temperature

Several VOC mixtures in air were generated. The first mixture contained benzene, toluene and *p*-xylene (BTX) and was prepared by diluting a standard mixture of these components in helium (25 ppm each) with air in an exponential

dilution device. The concentration of the individual components in the final gas sample was approx. 1 ppm. The FFAP column module of the micro GC was used to analyze the gas samples. Chromatograms of this gas mixture before and after enrichment, recorded with the micro GC, are shown in Figure 8.7. The sampling process was continued for 3 hours at a sampling flow rate of 150 mL/min. The fronting peaks for toluene and *p*-xylene in the lower trace are obviously caused by overloading of the narrow-bore FFAP column.

Enrichment factors of the individual components are summarized in Table 8.3. Detection limits of 1-2 ppb can be achieved for benzene and toluene. *p*-Xylene, with its extremely high enrichment factor, can be detected at an even lower concentration level. The estimated detection limit for this component is approx. 0.5 ppb.

Other gas samples containing some 7 VOCs in air were generated in a laboratory-made head space device (see Table 8.1). The reservoir of the device was filled with a liquid mixture of VOCs consisting of methyl bromide, dichloromethane, *trans*-1,2-dichloroethene, 1,1,2-trichlorotrifluoroethane, 1,1-dichloroethane, chloroform and 1,1,1-trichloroethane. The diluting air flow was set at different values in order to generate gas samples at various concentration

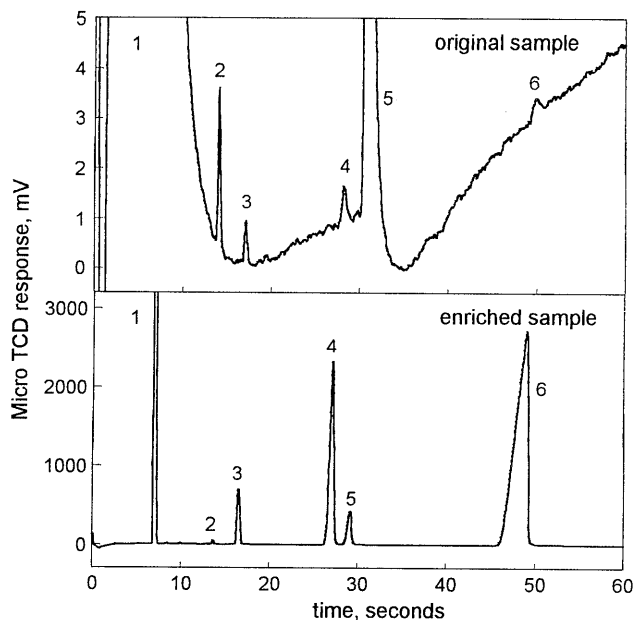


Figure 8.7: Enrichment of a gaseous sample containing benzene, toluene and *p*-xylene in air using the equilibrium (ab)sorption method. Chromatographic conditions: micro GC 6 m \times 150 μ m \times 0.2 μ m CP-FFAP column, 200 kPa, 40°C. Trapping column 1 m \times 1 mm \times 10 μ m stainless steel Thermocap A, sampling temperature 30°C, desorption temperature 200°C. Elution order: 1/ air, 2/ methanol, 3/ benzene, 4/ toluene, 5/ water, and 6/ *p*-xylene.

Table 8.3: Enrichment factors of selected VOC's using a 1 m × 1 mm × 10 μm Thermocap trapping column.

Compound	b.p. (°C)	Enrichment factor at		
		150°C	200°C	250°C
Benzene	80.1		570	
Toluene	110.6		2100	
<i>p</i> -Xylene	137.5		17000	
Methylbromide	3.6	11	17	21
Dichloromethane	39.8	71	96	101
<i>trans</i> -1,2-Dichloroethene	47.2	109	151	124
1,1,2-Trichlorotrifluoroethane	46.0	139	269	391
1,1-Dichloroethane	57.3	144	258	360
Chloroform	61.5	207	366	452
1,1,1-Trichloroethane	74.1	386	968	1570

levels ranging from approx. 0.05 to 5 ppm. The chromatogram of the gas sample with the lowest concentration level, *i.e.* 0.05 ppm, after enrichment is shown in Figure 8.8. For the analysis of highly volatile components the PoraPLOT column module of the micro GC was used. The enrichment factors of the VOCs at different desorption

temperatures are listed in Table 8.3. With the relatively low enrichment factors to be achieved the sampling time was only 30 min, much shorter than in case of the above mentioned BTX mixture. The estimated detection limits are in the range of 5-10 ppb.

The peak areas of the enriched components at different concen-

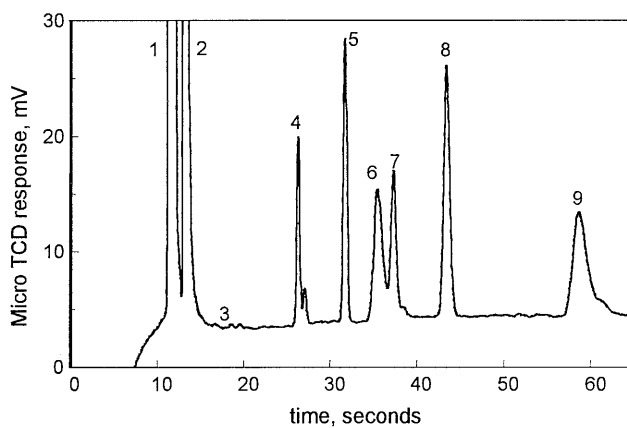


Figure 8.8: Chromatogram of an enriched gas sample containing some 7 VOCs in air at a concentration level of ca. 50 ppb. Elution order: 1/ air, 2/ water, 3/ methyl bromide, 4/ dichloromethane, 5/ *trans*-1,2-dichloroethene, 6/ 1,1,2-trichlorotrifluoroethane, 7/ 1,2-dichloroethane, 8/ chloroform, and 9/ 1,1,1-trichloroethane. Chromatographic conditions: 10 m × 250 μm × 10 μm PoraPLOT Q column at 180°C and 310 kPa. Trapping column: 1 m × 1 mm × 10 μm Thermocap A, sampling at 30°C, desorption at 250°C.

Table 8.4: Parameters of the regression equations: peak areas *versus* concentrations. The VOCs were enriched from air samples using the equilibrium (ab)sorption technique. Chromatographic conditions: micro GC 10 m × 250 μm × 10 μm PoraPLOT Q column at 310 kPa and 180°C. Trapping column 1 m × 1 mm × 10 μm stainless steel coated with Thermocap, sampling temperature 30°C, desorption temperature 250°C.

Compound	intercept (peak area unit)	slope (area unit/ppm)	corel. coef.
Bromomethane	50	1048	0.9953
Dichloromethane	952	94224	0.9989
<i>trans</i> -1,2-Dichloroethene	1895	166598	0.9986
1,1,2-Trichlorotrifluoroethane	-8074	210179	0.9997
1,1-Dichloroethane	-2086	145303	0.9994
Chloroform	4770	232413	0.9987
1,1,1-Trichloroethane	1965	251248	0.9993

tration levels were processed with the least square linear regression technique. Parameters of the regression equations are summarized in Table 8.4. These graphs show a good linearity which indicates that in the evaluated concentration range the (ab)sorption of an individual component is not affected by the presence of other components. All the components tested in this experiment were, however, at relatively low concentration level. In order to assess the displacement effect more accurately, larger concentration range of test components should be generated. These experiments are described in detail in section 8.3.3.

8.3.2. Enrichment at Elevated Temperatures

Sampling of the BTX mixture, as shown in the previous section at ambient temperature, *i.e.* 30°C, was too long to be considered practical in field applications. The enrichment factors for some components such as for example *p*-xylene, are excessively high which leads to long equilibration times. According to equation 7.8 deduced in chapter 7, the enrichment factor (or the required equilibration time) can be reduced to a more suitable level by decreasing the capacity factor of the component at the sampling temperature. Using the same stationary phase, there are two ways to realize this. The most obvious method is to reduce the film-thickness of the stationary phase. In practice this means that another trapping column has to be installed. A more practical alternative can be the use of a higher trapping temperature.

According to the technical data received from the manufacturer (Chrompack), in

the presence of air the Thermocap A stationary phase is stable up to 100°C. This exceptional characteristic enables sampling of air samples at elevated temperatures. The higher the sampling temperature, the lower the enrichment factor and, hence, the shorter the equilibration time.

Figure 8.9 shows chromatograms of a BTEX mixture at a concentration level of 5-10 ppb in air recorded on the micro GC after going through the preconcentration device. The sampling temperature ranged from 30°C to 70°C. The enrichment factors observed decrease roughly by a factor of 2 with every 10°C increasing in sampling temperature. The sampling time is reduced by the same factor. Three hours were required to equilibrate the trapping column with the BTEX sample at 30°C, only a little bit longer than one hour was needed at 40°C. At 70°C the sampling time was shortened to only 15 min. In these experiments the sampling time is determined by the component with the highest

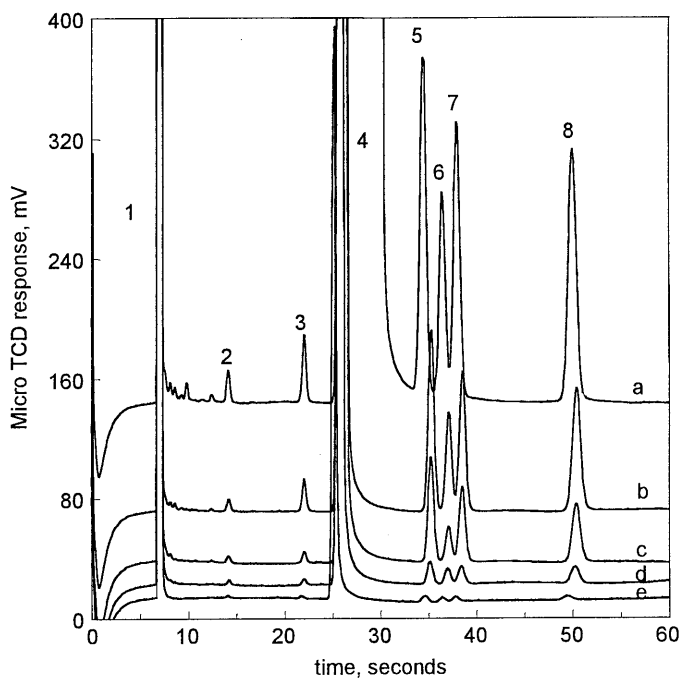


Figure 8.9: Chromatogram of an enriched gas sample containing a mixture of BTEX in air at a concentration level of ca. 5-10 ppb obtained using the equilibrium absorption technique. Micro GC chromatographic conditions: 6 m × 150 μm × 0.2 μm CP FFAP column, 40°C, 200 kPa. Elution order: 1/ air, 2/ benzene, 3/ toluene, 4/ water, 5/ ethylbenzene, 6/ *p*-xylene, 7/ *m*-xylene, 8/ *o*-xylene. Trapping column: 1 m × 1 mm × 10 μm stainless steel Thermocap A, desorption temperature 250°C, sampling temperature: a/ 30°C, b/ 40°C, c/ 50°C, d/ 60°C, and e/ 70°C.

capacity factor, which is *o*-xylene in this case. Components with lower capacity factors, *e.g.* benzene and toluene, have a lower enrichment factor and reach equilibration much earlier. For these solutes the sampling process can be completed in a much shorter time or lower temperatures can be used. At 50°C these components can be completely equilibrated within 20 min.

The feature of the Thermocap stationary phase that in air it is stable up to temperatures around 100°C makes a trapping column coated with this material very flexible. Based on the enrichment factor desired, the trapping temperature can be selected anywhere between 30°C and 100°C. If a very large enrichment factor is needed, 30°C can be used. In case that either a lower enrichment suffices or the solutes of interest have a very strong interaction with the Thermocap material, a higher temperature can be applied. Changing the trapping temperature from 30°C to 100°C results in approx. a 100-fold decrease in the enrichment factor (and, hence, the required equilibration time). With one trapping column,

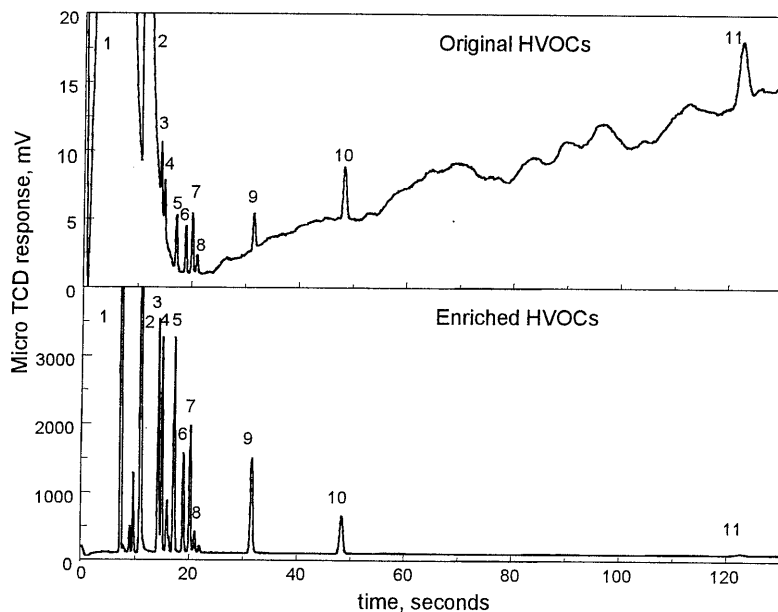


Figure 8.10: Chromatograms of a mixture of heavier VOCs in air before (upper trace) and after (lower trace) equilibrium enrichment. Concentration of the original sample: 5–10 ppm. Micro GC chromatographic conditions: 6 m × 150 μm × 0.2 μm CP-FFAP column at 80°C and 200 kPa. Trapping column: 1 m × 1 mm × 10 μm Thermocap A, sampling for 20 min at 70°C, desorption at 250°C. Elution order: 1/ air, 2/ water, 3/ ethylbenzene, 4/ *p*-xylene, 5/ *o*-xylene, 6/ chlorobenzene, 7/ *t*-butylbenzene, 8/ *s*-butylbenzene, 9/ bromobenzene, 10/ bromoform, and 11/ 1,2,4-trichlorobenzene.

hence, a very large range of solutes and enrichment factors can be covered.

The possibility to sample at elevated temperatures is thus found to be very useful for speeding up equilibration of the higher boiling point components on the Thermocap trapping columns. A gaseous mixture of heavier VOCs in air was sampled for 20 min at 70°C (Figure 8.10). In the chromatogram of the mixture after enrichment (lower trace), the peak of the heaviest component, *i.e.* 1,2,4-trichlorobenzene, is missing indicating that this component has not yet reached the breakthrough point. *t*-Butylbenzene and *s*-butylbenzene show peaks lower than expected. These two components broke through the trapping column but had not yet reached full equilibration. Figure 8.11 shows a chromatogram of a similar gas mixture, at a lower original concentration level, *i.e.* 50-100 ppb, after enrichment at a higher sampling temperature of 100°C. After 20 min sampling both butylbenzenes have reached full equilibrium and 1,2,4-trichlorobenzene has started to break through.

As indicated previously another way to reduce excessive enrichment factors and too long sampling times is to employ a trapping column with a lower phase ratio. Experiments similar to those described above were carried out on a 1 m × 1 mm × 5 μm Thermocap A column. Measured enrichment factors of several VOCs on this column and the previous one are listed in Table 8.5. At the same sampling temperature the 10-μm-film column roughly gives a two times higher enrichment factor compared to the 5-μm-film column. The sampling time, determined by the equilibrium time of the component with the highest capacity

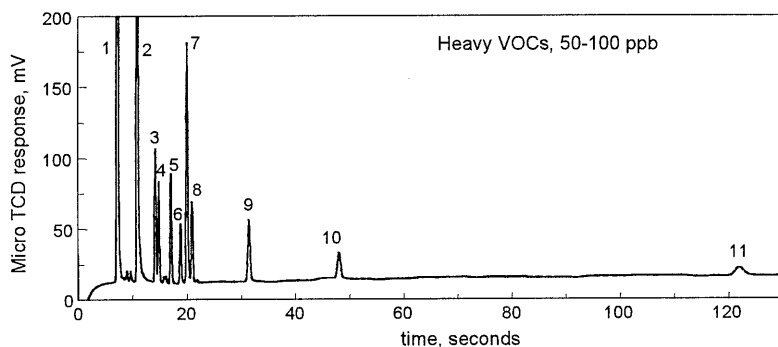


Figure 8.11: Chromatogram of an gas sample containing several VOCs in air at a concentration level of ca. 70-100 ppb enriched using the equilibrium enrichment technique. Elution order and micro GC chromatographic conditions: see Figure 8.10. Sampling temperature 100°C, sampling time 20 min.

factor, is also proportionally longer. In order to complete the sampling process within the same time period, *e.g.* equilibrate the column within 20 min, higher sampling temperatures must be applied for the thicker film column. To limit the sampling time to 20 min, a sampling temperature of 100°C was needed to equilibrate the thicker 10- μm -film column with the particular mixture of heavy VOCs tested in this series of experiments. On the other hand, 80°C was found to be sufficiently high for the 5- μm -film column.

Table 8.5 also shows the enrichment factor values calculated for the 5- μm -film column according to the theory derived in the previous chapter. Larger discrepancies between calculated and measured values in this case are due to more pronounced derivation of the behavior of the components on the Thermocap A stationary phase from ideal behavior. The calculated values, however, can still be used as a rough estimate in an optimization process.

Table 8.5: Enrichment factors of selected VOCs on different Thermocap A columns at various sampling temperatures. Components: 3/ ethylbenzene, 4/ *p*-xylene, 5/ *o*-xylene, 6/ chlorobenzene, 7/ *t*-butylbenzene, 8/ *s*-butylbenzene, 9/ bromobenzene, 10/ bromoform, 11/ 1,2,4-trichlorobenzene.

Sampling temp.(°C)	Component (Peak number)									
	3.	4.	5.	6.	7.	8.	9.	10.	11.	
<u>Column 1 m × 1 mm × 10 μm Thermocap A, measured values</u>										
60	1046	1171	974	575	2970	3279	655	227		
70	654	750	608	355	1493	1520	489			
80	475	546	462	254	1334	1613	401			
90	291	360	289	197	755	944	302			
100	196	205	179	97	541	713	156	41	870	
<u>Column 1 m × 1 mm × 5 μm Thermocap A, measured values</u>										
30	2189	2417	2222	1243	15615	17539	2318	145		
40	1425	1597	1501	750	5393	6416	1254	193		
50	972	991	958	435	2773	3339	871	176		
60	560	600	564	231	1393	1986	500	73		
70	312	369	367	158	1001	1481	327	94		
80	177	204	204	97	722	863	196	58		
<u>Column 1 m × 1 mm × 5 μm Thermocap A, calculated values</u>										
30	2762	2890	3468	1279	24331	28249	3145	1514	30505	
40	1337	1393	1663	656	10303	11856	1541	773	13134	
50	677	702	835	351	4601	5251	789	412	5958	
60	357	369	437	195	2156	2442	421	228	2834	
70	195	201	237	112	1056	1187	233	130	1408	
80	111	114	133	66	539	602	133	77	727	

Several rules of thumb can be derived from the results achieved in this series of experiments. First of all it has been proven that a large majority of the solutes on the EPA VOC list can be covered using a $1\text{ m} \times 1\text{ mm} \times 10\text{ }\mu\text{m}$ Thermocap A trapping column. For components with boiling points ranging from 50°C to 200°C enrichment factors in the 500-1000 range can be achieved within 20 minutes at properly selected sampling temperatures. Starting from ambient temperature, *i.e.* 30°C , every 10-degree increase in sampling temperature extends the accessible boiling point range by *ca.* 20°C . A few examples: allowing a sample time of 20 minutes, toluene (bp. 110°C) should be equilibrated at 50°C , ethylbenzene and the xylenes (bp. $130\text{-}140^{\circ}\text{C}$) at 70°C , and the butylbenzenes (bp. $170\text{-}180^{\circ}\text{C}$) at 90°C . The sampling temperature, therefore, must be set properly depending on the target components to be analyzed and the enrichment factor desired. Lower sampling temperatures can be used when a thinner film column is employed.

8.3.3. Displacement Effects

As stated in section 8.3.1, no displacement effects occur on the Thermocap A stationary phase when all the components tested are present at relatively low concentrations. In practice, however, a more common situation is that one or more interfering components are present at higher concentration levels. To investigate whether displacement occurs in this case a new series of experiments was carried out. The test mixture contained benzene, toluene and *p*-xylene (BTX) in air at a concentration level of approx. 2-3 ppm. To this mixture *o*-xylene was added as an interfering component at different concentration levels ranging from 2 to 100 ppm. Any decrease in enrichment factors of the test components due to the increasing concentration of *o*-xylene would indicate the occurrence of displacement.

First, enrichment factors were measured for the test components on a CP Sil-5 CB stationary phase. The data collected are summarized in Table 8.6. As can be seen from this table, the enrichment factors of all the components remained constant despite the increasingly higher content of *o*-xylene added to the sample flow. The signal of the BTX stayed unchanged even when the sample contains high amounts of *o*-xylene and is nearly saturated with water. Apparently, a pure partitioning mechanism governs the enrichment process on this CP Sil-5 stationary phase.

Similar experiments were then carried out on the Thermocap A column at different sampling temperatures. In this case an evident influence of the concentration level of the interfering component on the enrichment of the BTX mixture can be observed (Table 8.7). This leads to the conclusion that beside the partitioning mechanism other processes are taking place during the enrichment of BTX on the Thermocap A column. Hence, care should be taken when applying the Thermocap column for enrichment of components from a sample that containing high concentrations of interfering components. For such situations it is advisable to use liquid-phase coated enrichment columns.

Table 8.6: Influence of the content of an interfering component present in the sample on the enrichment of the test compounds. Trapping column: 1 m × 1 mm × 5 μm stainless steel coated with CP Sil-5 CB, sampling temperature 30°C, desorption temperature 200°C. Chromatographic conditions: 6 m × 150 μm × 0.2 μm CP-FFAP column, 35°C, 300 kPa.

Concentration of interfering <i>o</i> -xylene (ppm)	Enrichment factors of BTX mixture		
	Benzene	Toluene	<i>p</i> -Xylene
0	11	23	55
5	11	26	59
10	12	26	53
60*	11	25	53

* Sample is also saturated with water vapor.

Table 8.7: Influence of the content of an interfering component present in the sample on the enrichment of BTX mixture. Trapping column 1 m × 1 mm × 5 μm stainless steel coated with Thermocap A, desorption temperature 250°C. Chromatographic conditions: 6 m × 150 μm × 0.2 μm CP-FFAP column, 35°C, 300 kPa.

Concentration of interfering <i>o</i> -xylene (ppm)	Enrichment factors of toluene at				
	40°C	50°C	60°C	70°C	80°C
0	890	420	230	125	70
10	560	360	220		
20	340	310	210	120	70
50				125	73
100				100	72
400				50	40

8.4. CONCLUSIONS

The experimental results described above clearly show the compatibility of pre-concentration techniques based on the equilibrium (ab)sorption principle with

high-speed narrow-bore GCs. In case of field-portable micro GCs no major modification of the micro GC hardware is required. The chromatographic performance of the GC instrument, therefore, is not compromised. Experiments with gas samples containing *n*-alkane mixtures or selected VOCs showed very good results with excellent enrichment factors. The enrichment factors measured on trapping columns with different liquid stationary phases agree well with calculated values. Due to the weak retention of liquid stationary phases, however, rather low enrichment factors are obtained. For volatile components such as VOCs with boiling points in the range of 50°C-200°C, a more retentive Thermocap A stationary phase was used to obtain acceptable enrichment factors and correspondingly low detection limits, *i.e.* at the 1-2 ppb level. The exceptional stability of the Thermocap stationary phase under air at higher than ambient temperatures largely extends its applicability. Sampling at elevated temperatures helps to reduce the sampling times to practically acceptable levels, *i.e.* 15 to 25 minutes, while maintaining high enrichment factors, 500 to 1000, for most of the components tested.

Unfortunately, displacement effects that can occur restrict the application of Thermocap A enrichment columns to situations, when no interfering components are present in the sample at a high concentration levels. For such applications, thick-film liquid phases have to be used.

The lower end of the VOC rang, *i.e.* components with boiling points from -30°C to 50°C can be covered using trapping columns with even more retentive stationary phases, such as for example Thermocap C, PoraPLOT or ultra-thick film columns.

Appendix

PREDICTION AND OPTIMIZATION OF SEPARATION ON THE MICRO GC

A.1. INTRODUCTION

Extensive theoretical knowledge of gas chromatography has enabled chromatographers to predict the behavior of solutes during the separation process. Two basic parameters that characterize the interaction between a solute and a GC instrument are the solute's retention time and peak width. Knowing all the factors that influence the outcome of these parameters, chromatographers can predict and, hence, optimize the GC instrument for the analytical problem at hand prior to the actual experimental work. This can save a lot of work in the tedious task of optimization, which has till recently mostly relied on trial and error procedures.

To minimize laborious trial and error optimization efforts, numerous authors have tried to simulate the chromatographic process for optimization purposes [1-8]. A common procedure is to predict and optimize a temperature-programmed separation using the data of the solutes' isothermal behavior. The optimization process which we would like to apply for the micro GC, is in the reverse direction. A sample has been analyzed on a conventional GC using temperature programming. The questions which can be asked now: Can the same sample be analyzed on a portable micro GC? What conditions are then optimal for the micro GC separation?

Equation 7.9 in Chapter 7, section 7.2.2 describes the relationship between the capacity factor k of a solute and the enthalpy and entropy of its vaporization from the stationary phase to the mobile phase: $\ln k = \ln(a/\beta) + (\Delta H/RT)$. Here β is the column phase ratio and T is the column absolute temperature. Values of the enthalpy ($\Delta H/R$) and entropy (a/β) terms are usually assumed to be temperature independent. In a temperature-programmed GC separation the retention time of solute i is given by:

$$1 = \int_0^{t_R} \frac{dt}{t_0(1+k_i)} \quad (\text{A.1})$$

Where t is the time from injection of the sample and the start of the temperature program and t_0 is the column dead time. For linear or segmented temperature programs, this equation cannot be solved explicitly.

In an effort to avoid the above mentioned problem, the DryLab software (LC Resources Inc., Lafayette, CA, USA) uses the so-called linear-elution-strength (LES) approximation, a well-known technique used to describe retention in liquid chromatography with solvent gradients. The LES approximation is expressed as:

$$\log k \approx A - ST \quad (\text{A.2})$$

Where A and S are constant for a given solute and GC system. The DryLab GC optimization method, that clearly lacks a sound theoretical basis, uses two experimental temperature-programmed runs as input for further computer simulations. This analogous to the computer simulations that have been applied for method development in gradient elution High Performance Liquid Chromatography (HPLC). The prediction and optimization process using this software, however, has an inherent disadvantage of being non-transferable between different columns as the constant S is strongly dependent on the system used. This minimizes the applicability of the DryLab software for the problem described in this appendix. Transferring a method from a lab GC to a micro GC means that other GC instruments with different columns are used.

Prediction and optimization procedures based on enthalpy and entropy data have been proven to produce highly reliable results [7,8]. This approach is also applied here to solve our problem. The goal is to suggest a procedure to acquire input data and several rules of thumb assisting the selection of a micro GC module and operating conditions best suited for the sample to be analyzed.

A.2. EXPERIMENTAL

Enthalpy and entropy data for a number of volatile organic compounds (VOCs) were calculated from retention times measured at different temperatures on several capillary columns. Liquid samples of the test components were injected into

the column using split injection. A GC 8000 Series gas chromatograph (Fisons Instruments, Milano, Italy) equipped with an FID was used to perform isothermal runs. Oven temperature was set isothermally in the range of 30-140°C. The column head pressure was set variously depending on the column tested. The split flow was set to 100 mL/min. Injector temperature was 200°C and detector temperature was 250°C.

A number of different columns were used:

- 45 m × 320 μm × 0.52 μm HP-FFAP column (Hewlett-Packard, Avondale, PA, USA),
- 15 m × 530 μm × 1.91 μm CP-FFAP column (Chrompack, Middelburg, the Netherlands),
- 10 m × 530 μm × 1.84 μm CP Sil-19 CB column (Chrompack),
- 25 m × 530 μm × 3 μm DB 1701 column (J&W, Folsom, CA, USA),
- 25 m × 250 μm × 0.12 μm CP Sil-8 CB column (Chrompack),
- 25 m × 310 μm × 0.18 μm HP-1 column (Hewlett-Packard),
- 23 m × 150 μm × 0.13 μm HP-1 column (Hewlett-Packard),
- 60 m × 250 μm × 0.12 μm Thermocap A column (Chrompack),
- 60 m × 250 μm × 0.12 μm Thermocap B column (Chrompack).

All calculations were carried out using the Microsoft Excel 97 spreadsheet software.

A.3. THERMODYNAMIC DATA

The enthalpy ($\Delta H/R$) and entropy (a) data were calculated from values of the intercept and the slope of linear relationships between ($\ln k$) and ($1/T$). For every component at least 4 or 5 data points were obtained to guarantee optimal precision and accuracy. Thermodynamic data of a number of components on various stationary phases are summarized in Table A.1.

A.4. PREDICTION OF MICRO GC CHROMATOGRAPHIC RUNS

Calculation of the retention time t_R from the acquired thermodynamic data is a reverse process compared to that described in the previous section. The following equation is used:

Table A.1: Calculated entropy (a) and enthalpy ($\Delta H/R$) terms of the components tested on various stationary phases.

	CP Sil-5 CB		CP Sil-8 CB		CP Sil-19 CB		CP-FFAP		Thermocap A		Thermocap B	
	$a \times 10^7$	$\Delta H/R$	$a \times 10^7$	$\Delta H/R$	$a \times 10^7$	$\Delta H/R$	$a \times 10^7$	$\Delta H/R$	$a \times 10^7$	$\Delta H/R$	$a \times 10^7$	$\Delta H/R$
n-Hexane	29879.3	3300	37150.9	3248	51663.8	3082	100650.0	2246	575.4	5695	1118.3	5180
Ethylbenzene	12256.8	4225	14341.7	4250	14916.0	4343	15462.8	4166	658.8	6339	1435.3	5582
p-xylene	8819.5	4386	10779.5	4386	11948.1	4425	14947.7	4199	702.7	6379	964.4	5731
o-xylene	11132.5	4324	9758.5	4441	10860.1	4475	13393.8	4348	231.0	6890	459.8	6148
Chlorobenzene	7836.1	4450	12843.7	4387	10589.6	4557	11402.4	4466	211.3	6930	382.2	6228
t-Butylbenzene	7470.3	4523	9403.2	4515	28064.8	4481	8682.9	4598	224.0	6977	443.5	6213
s-Butylbenzene	7971.6	4584	32064.6	4226	8392.2	4816	8142.8	4647	424.4	6771	648.2	6091
Bromobenzene	3942.4	4993	4546.9	5017	4470.8	5086	9494.7	4802	35.5	8158	255.8	6811
Bromoform	3565.8	5074	4418.5	5073	4580.1	5090	3782.4	5323	31.7	8242	115.1	7172
1,2,4-Trichlorobenzene	1927.6	5656	2322.8	5699	3050.0	5702	3334.2	5760	98.3	8000	150.1	7243
MeAc			20036.2	3239			32179.5	3238				
MeOH			4844.0	3221			12197.0	3722				
Benzene			21660.3	3608			38587.2	3456				
Toluene			11160.6	4119			24328.8	3838				
Hac			6790.3	3773			2033.2	5579				

$$t_R = t_M(1+k) = \frac{L}{\bar{u}}(1+k) \quad (\text{A.3})$$

With:

$$k = \frac{\alpha}{\beta} + \exp \frac{\Delta H}{RT} \quad (\text{A.4})$$

Here t_M is the column dead time, L is the column length and \bar{u} is the average linear carrier gas velocity. Using the Poiseuille equation and the relationship between the average- and the outlet gas velocity (u_o) defined by James and Martin [9], the average gas velocity can be obtained as:

$$\bar{u} = u_o j = \frac{3d_c^2(p_i^2 - p_o^2)}{128\eta L(p_i^3 - p_o^3)} \quad (\text{A.5})$$

Where j is the gas compressibility correction factor, p_i is the inlet pressure, p_o is the outlet pressure and d_c is the column diameter. The helium carrier gas viscosity η ($\mu\text{Pa}\cdot\text{sec}$) is calculated according to Hawkes [10]:

$$a = -0.126516$$

$$b = -1.230553$$

$$c = +2.171442$$

$$T' = T/10.4$$

$$\alpha = 13.65299 - \ln T$$

$$\Omega = 0.00635209 \cdot \alpha^2 \cdot \left[1.04 + \frac{a}{(\ln T')^2} + \frac{b}{(\ln T')^3} + \frac{c}{(\ln T')^4} \right]$$

$$E = 1 - \frac{1}{4\Omega} \cdot \left[\frac{2\Omega}{\alpha} + 0.00635209 \cdot \alpha^2 \cdot \left(\frac{2a}{(\ln T')^3} + \frac{3b}{(\ln T')^4} + \frac{4c}{(\ln T')^5} \right) \right]$$

$$f = 1 + \frac{3}{196} (8E - 7)^2$$

$$\eta = 0.7840374 \cdot \frac{f}{\Omega} \cdot \sqrt{T} \cdot \left[0.995 + (T - 300) \cdot 2.5 \times 10^{-5} \right] \quad (\text{A.6})$$

The peak width at half height is calculated according to the following equation:

$$W_{1/2} = 2.354 \cdot \sigma \quad (\text{A.7})$$

Under isothermal conditions, the chromatographic band broadening σ^2 can be obtained from:

$$\sigma^2 = \frac{t_R^2}{N} = \frac{Ht_R^2}{L} = \frac{Ht_M^2(1+k)^2}{L} = \frac{HL(1+k)^2}{\bar{u}^2} \quad (\text{A.8})$$

The theoretical plate height can be calculated from the Golay equation [11], including the pressure drop correction factors derived by Giddings *et al.* [12]:

$$H = \left[\frac{2D_{m,o}}{u_o} + \frac{11k^2 + 6k + 1}{24(k+1)^2} \cdot \frac{d_c^2 u_o}{4D_{m,o}} \right] \cdot \left[\frac{9(p^4 - 1)(p^2 - 1)}{8(p^3 - 1)^2} \right] + \frac{2k}{3(k+1)^2} \cdot \frac{d_f^2 u_o}{D_s} \cdot \frac{3(p^2 - 1)}{2(p^3 - 1)} \quad (\text{A.9})$$

Where $p = p_i/p_o$. The binary diffusion coefficient of the solute in the mobile phase $D_{m,o}$ (cm²/sec) is estimated using the method developed by Fuller *et al.* [13]:

$$D_{m,o} = \frac{0.00143 \cdot T^{1.75}}{p \cdot \sqrt{M_{AB}} \cdot \left[\sqrt[3]{(\Sigma_v)_A} + \sqrt[3]{(\Sigma_v)_B} \right]^2} \quad (\text{A.10})$$

Where: M_A, M_B = molecular weights of A and B (g/mol)

$$M_{AB} = 2 / \left[(1/M_A) + (1/M_B) \right]$$

Σ_v = sum of atomic diffusion volumes listed in Table A.2 [14]

Table A.2: Atomic diffusion volumes.

Atomic and structural diffusion volume increments					
C	15.9	F	14.7	S	22.9
H	2.31	Cl	21.0	Aromatic ring	-18.3
O	6.11	Br	21.9	Heterocyclic ring	-18.3
N	4.54	I	29.8		
Diffusion volume of simple molecules					
He	2.67	H ₂	6.12	CO	18.0
Ne	5.98	D ₂	6.84	CO ₂	26.9
Ar	16.2	N ₂	18.5	N ₂ O	35.9
Kr	24.5	O ₂	16.3	NH ₃	20.7
Xe	32.7	Air	19.7	H ₂ O	13.1
		Cl ₂	38.4	SF ₆	71.3
		Br ₂	69.0	SO ₂	41.8

Using the equations and data listed above, retention times and peak widths were calculated for components analyzed in the vent stack gas analysis (chapter 6) and the VOC analysis (chapter 8). Calculated and measured values are summarized in Tables A.3 and A.4, respectively.

Table A.3: Calculated and measured values of retention times and peak widths for the components analyzed in the vent stack gas analysis. Chromatographic conditions: column 4 m x 150 μm x 0.2 μm CP-FFAP, 60°C, 200 kPa. Injector not heated, injection time 50 msec.

	t_R (sec.)			$W_{1/2}$ (sec)			$\sigma_{\text{instrm.}}^2$
	Cal.	Meas.	Error (%)	Cal.	Meas.	Error (%)	
MeAc	3.4	3.6	5.88	0.0376	0.19	405.51	0.0063
MeOH	3.9	4.0	2.56	0.0452	0.20	342.64	0.0069
Toluene*	6.2	6.3	1.61	0.1028	0.30	191.82	0.0143
p-Xylene	9.0	9.0	0.00	0.1742	0.27	55.01	0.0077
HAc**	56.3	55.7	-1.07	1.0524	1.14	8.33	0.0347
Aver. Value							0.0070

* Toluene elutes on the tail of a large water peak

** HAc peak shows severe peak asymmetry

Table A.4: Calculated and measured values of retention times and peak widths for the components analyzed in the VOC analysis. Chromatographic conditions: column 6 m x 150 μm x 0.2 μm CP-FFAP, 80°C, 200 kPa. Injector temperature 110°C, injection time 50 msec.

	t_R (sec.)			$W_{1/2}$ (sec)			$\sigma_{\text{instrm.}}^2$
	Cal.	Meas.	Error (%)	Cal.	Meas.	Error (%)	
Ethylbenzene	13.2	14.3	8.33	0.1325	0.30	126.50	0.0131
p-Xylene	13.6	15.0	10.29	0.1409	0.28	98.67	0.0106
o-Xylene	16.0	17.2	7.50	0.1762	0.30	70.24	0.0106
Chlorobenzene	17.8	19.0	6.74	0.1908	0.32	67.69	0.0119
t-Butylbenzene	18.9	20.2	6.88	0.2179	0.34	56.01	0.0123
s-Butylbenzene	19.9	21.2	6.53	0.2262	0.35	54.75	0.0129
Bromobenzene	30.5	31.8	4.26	0.4036	0.46	13.97	0.0088
Bromoform	48.0	48.8	1.67	0.6701	0.71	5.96	0.0099
1,2,4-Trichlorobenzene	132.0	124.0	-6.06	1.8893	1.91	1.10	0.0142
Aver. value							0.012

When comparing calculated and measured data in Table A.3 and A.4 a good agreement is observed for retention times. The errors are generally lower than 10%. For the peak width, however, the measured values are generally much larger than the calculated data, especially for the early eluting peaks. This clearly shows that there is a significant extra-column contribution of the instru-

ment to the overall band broadening. This is also indicated by the fairly constant values of $\sigma_{instrm.}^2$. The values for this parameter are calculated according to equation A.11:

$$\sigma_{instrm}^2 = \left(\frac{(W_{1/2})_{meas.}}{2.354} \right)^2 - \sigma_{calc.}^2 \quad (A.11)$$

The relatively large contribution of the instrument to the overall bandwidth originates from gas channels in the injector and the TCD of the micro GC. Once the value of extra-column band broadening is determined, it can be included in the calculation to improve the accuracy of the predictions. Unfortunately, these values are characteristic for the particular instrument in use and can only be measured experimentally. The small errors in the predicted retention times are most likely a result of pressure drop in the microchannels etched in the micro GC making column head pressure reading less accurate. This results in a shift of the measured retention times compared to the calculated values.

The extra-column band broadening is difficult to calculate as it is strongly influenced by a large number of parameters. To name a few, the injector temperature and the column head pressure. The effects of these parameters on $\sigma_{instrm.}^2$ are demonstrated in Tables A.5 and A.6. The results in these tables clearly show that extra-column band broadening decreases with increasing injector temperature and increasing column head pressure. Apparently, the solutes are slightly retained by the injector and some dead volumes exist in the instrument. Higher temperatures and higher volumetric gas flow rates reduce the effects of these sources of extra-column band broadening.

Table A.5: Effect of the injector temperature on the extra-column band broadening. Chromatographic conditions: 4 m x 150 μ m x 0.12 μ m CP Sil-8 CB column, 70°C, 200 kPa. Injection time 50 msec.

Injector temperature (°C)	Average σ_{instrm}^2
50	0.030
60	0.028
70	0.026
80	0.023
90	0.016
100	0.016

Table A.6: Effect of the column head pressure on the extra-column band broadening. Chromatographic conditions: 4 m x 100 μm x 0.5 μm CP Sil-8 CB column, 40°C. Injector not heated, injection time 50 msec.

Inlet pressure (kPa)	Average $\sigma_{instr.}^2$
153	0.025
200	0.015
250	0.011

A.4. OPTIMIZATION OF MICRO GC RUN CONDITIONS

For optimization purposes a chromatographic response function (CRF) has to be used. The CRF represents a proper conversion of the retention times and peak widths of all relevant chromatographic peaks into a single number which accurately reflects the optimization criterium, *i.e.* the quality of the chromatogram. In this work the CRF proposed by Dose [6] has been used with a small modification. Only resolution between adjacent peaks is taken into account instead of resolution of all possible peak pairs. This simplification has been adopted to shorten the calculation time of the spreadsheet software without significantly reducing the accuracy of the procedure. The simplified CRF then reads:

$$CRF = \frac{t_{R,n}}{t_{R,crit}} + \sum_j \exp\left(-\frac{R_{s,j,j+1}}{R_{s,crit}}\right) \quad (\text{A.12})$$

where the resolution $R_{s,j,j+1}$ is calculated as:

$$R_{s,j,j+1} = \frac{t_{R,j+1} - t_{R,j}}{2(\sigma_{j+1} + \sigma_j)} \quad (\text{A.13})$$

The required critical values were $t_{R,crit} = 4$ min and $R_{s,crit} = 1.5$. The CRF described by equation A.12 incorporates both retention time and resolution. With a fixed set of input parameters such as the column dimensions (length, diameter, film thickness) the CRF is calculated for every combination of column temperature and column pressure. The combination at which the CRF achieves its minimum, represents the optimum conditions for the separation of the test mixture on the column used. The column temperature was set in the range of 30°C to 180°C with 10°C increments. The column head pressure varied from 0.25 bar to 3 bar at 0.25 bar increments.

Table A.7 shows data calculated for a VOC mixture tested on a micro GC FFAP

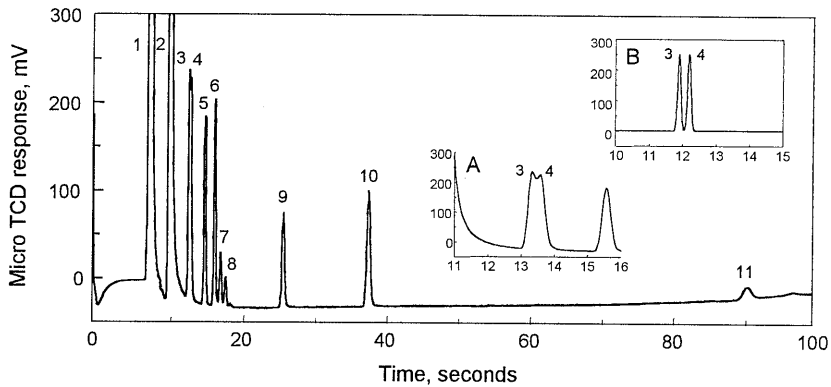


Figure A.1: Chromatogram of the VOC mixture tested under the calculated optimal condition. Chromatographic conditions: $6\text{ m} \times 150\ \mu\text{m} \times 0.2\ \mu\text{m}$ CP-FFAP column, 90°C , 1.75 bar. Injector temperature 110°C , injection time 50 msec. Elution order: 1/ air+hexane, 2/ water, 3/ ethylbenzene, 4/ *p*-xylene, 5/ *o*-xylene, 6/ chlorobenzene, 7/ *t*-butylbenzene, 8/ *s*-butylbenzene, 9/ bromobenzene, 10/ bromoform, and 11/ 1,2,4-trichlorobenzene. A – measured signal, B – signal constructed using calculated values.

column under theoretically optimal conditions. A chromatogram was recorded under the indicated conditions (Figure A.1) and the data collected were compared to the calculated values. The large extra-column band broadening has significantly worsened the resolution of the critical peak pair, which in this case is ethylbenzene/*p*-xylene (peak pair 3/4 in Figure A.1A). Under ideal conditions, *i.e.* without the extra-column band broadening, these two peaks should be baseline separated as depicted in the predicted chromatogram (Figure A.1B). The Chromatogram of the test mixture can be graphically constructed from calculated values of t_R and σ^2 using the Gaussian function:

$$c(t) = c_{\max} \cdot \exp\left[-\frac{(t-t_R)^2}{2\sigma^2}\right] \quad (\text{A.14})$$

Where $c(t)$ is the signal as a function of time and c_{\max} is the peak height.

Assuming the extra-column band broadening is known, for example by using the average value of 0.012 from Table A.4, it can be included in the calculations. A new (*CRF*) $\min = 1.786$ was reached under a new set of conditions, *i.e.*, column temperature of 80°C and column head pressure of 1.25 bar. A chromatogram was recorded (Figure A.2) and measured data are compared to the calculated values in Table A.8. A much better separation was now indeed achieved

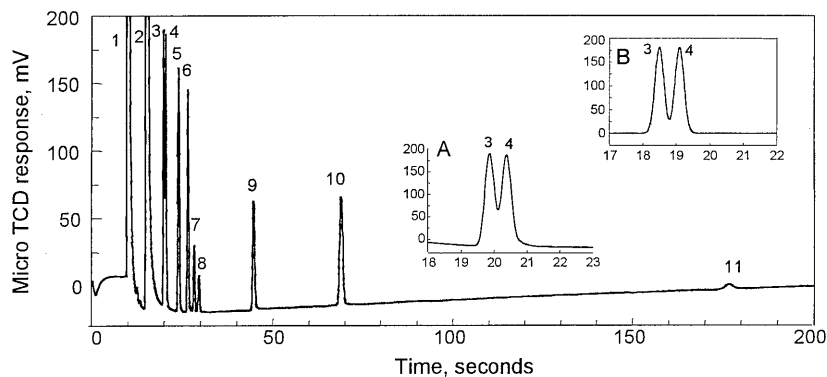


Figure A.2: Chromatogram of the VOC mixture tested under calculated optimal conditions (including extra-column band broadening contribution): 6 m × 150 μm × 0.2 μm CP-FFAP, 70°C, 1.25 bar. Injector temperature 110°C, injection time: 50 msec. Elution order: 1/ air+hexane, 2/ water, 3/ ethylbenzene, 4/ *p*-xylene, 5/ *o*-xylene, 6/ chlorobenzene, 7/ *t*-butylbenzene, 8/ *s*-butylbenzene, 9/ bromobenzene, 10/ bromoform, 11/ 1,2,4-trichlorobenzene. A – measured signal, B – signal constructed using the calculated peak data.

for the critical peak pair ethylbenzene/*p*-xylene. A much better agreement was now also obtained for the predicted and the experimental chromatograms (See Figure A.2 A and B).

Table A.7: Chromatographic data of the VOC mixture under theoretically optimal conditions: 6 m × 150 μm × 0.2 μm CP-FFAP, 90°C, 1.75 bar, *CRF* min = 1.168.

	t_R (sec.)			$W_{1/2}$ (sec)		
	Cal.	Meas.	Error (%)	Cal.	Meas.	Error (%)
<i>n</i> -Hexane*	7.3	7.7	5.40	0.0504	na	
Ethylbenzene	11.9	13.4	12.60	0.1115	na	
<i>p</i> -Xylene	12.2	13.6	11.47	0.1169	na	
<i>o</i> -Xylene	14.0	15.6	11.43	0.1413	0.30	112.31
Chlorobenzene	15.2	17.0	11.84	0.1525	0.31	103.31
<i>t</i> -Butylbenzene	16.0	17.8	11.25	0.1687	0.33	95.58
<i>s</i> -Butylbenzene	16.7	18.5	10.78	0.1746	0.33	88.97
Bromobenzene	24.2	26.5	9.50	0.2938	0.42	42.95
Bromoform	35.6	38.3	7.58	0.4603	0.57	23.85
1,2,4-Trichlorobenzene	90.7	91.1	0.44	1.2286	1.38	12.33

* Hexane coeluted with the the air peak.

na ... not available

Table A.8: Chromatographic data of the VOC mixture under theoretically optimal conditions, including extra-column band broadening: 6 m x 150 μ m x 0.2 μ m CP-FFAP, 80°C, 1.25 bar, CRF min = 1.786

	t_R (sec.)			$W_{1/2}$ (sec)		
	Cal.	Meas.	Error (%)	Cal.	Meas.	Error (%)
<i>n</i> -Hexane*	9.8	9.9	0.57	0.2685	0.67	149.53
Ethylbenzene	18.5	19.9	7.51	0.3134	0.35	11.67
<i>p</i> -Xylene	19.1	20.4	6.96	0.3172	0.36	13.51
<i>o</i> -Xylene	22.5	24.0	6.49	0.3434	0.37	7.75
Chlorobenzene	25.0	26.6	6.52	0.3632	0.39	7.38
<i>t</i> -Butylbenzene	26.6	28.3	6.27	0.3782	0.42	11.05
<i>s</i> -Butylbenzene	27.9	29.6	5.91	0.3890	0.43	10.54
Bromobenzene	42.8	44.7	4.38	0.5503	0.60	9.02
Bromoform	67.5	69.0	2.29	0.8388	0.89	6.10
1,2,4-Trichlorobenzene	185.5	176.7	-4.76	2.2686	2.33	2.71

* Hexane coeluted with air peak.

A.5. RECOMMENDATIONS

The study described above has shown the feasibility of prediction and optimization of chromatographic conditions for portable micro GC analysis. The method proposed, however, also has its limitations. There is no reliable method for direct translation of temperature-programmed chromatographic data, which are available from conventional GC runs, to that of the isothermally operated micro GC. The initial thermodynamic data of the components to be analyzed on a certain liquid stationary phase (not necessarily on the same column) have to be acquired by performing several isothermal input runs. Three to five temperature levels are recommended. If the mixture is analyzed by a conventional GC with a temperature program running from T_1 to T_2 , the temperature levels recommended for isothermal input runs are T_1 , T_2 , T_3 , T_4 , and T_5 , where T_3 , T_4 and T_5 are evenly spaced between T_1 and T_2 . A library of thermodynamic data can be established. Alternatively enthalpy and entropy data from literature can be used.

Prediction of retention times for a micro GC run was found to be fairly precise. The errors towards experimental values are under 10% and generally are the same for each of the peaks. Calculation of the peak widths is, however, much more difficult. The main obstacle is the large contribution of the instrument to the solute's final peak width. This extra-column band broadening is different for each individual instrument and can depend on a number of parameters. Once

an average value of this contribution is determined experimentally, it can be included into the calculation to improve the precision and accuracy. The optimization process then can be used as a useful tool to assist in the actual evaluation study.

To optimize the chromatographic performance of a micro GC for a specific sample, chromatographers still, however, have to rely very much on their own experience. A substantial part of the range of columns used in micro GCs are the Porous Layer Open Tubular (PLOT) columns. The theory developed in this appendix is virtually non-applicable to these columns. Generally PLOT columns are used to analyze the very volatile components. For higher boilers a few rules of the thumb can be pointed out from our study. Regarding the limitations in micro GC operation, a sample containing more than 25-30 components can hardly be separated on the micro GC. Moreover, it will be very difficult for any component which elutes after C_{15} or elutes at 250°C-300°C on a conventional GC column to be eluted from the micro GC column within the 4 minute time window. For the elution of such components micro GCs with higher column temperatures and/or maximum times exceeding the (current) limit of 4 minutes are required.

REFERENCES

1. G. Anders, M. Scheller, C. Schuhler, and H. G. Struppe, *Chromatographia*, 15 (1982) 43.
2. P. Y. Shrotri, A. Mokashi, and D. Mukesh, *J. Chromatogr.*, 387 (1987) 399.
3. S. Vezzani, P. Moretti, and G. Castello, *J. Chromatogr. A*, 677 (1994) 331.
4. N. H. Snow and H. M. McNair, *J. Chromatogr. Sci.*, 30 (1992) 271.
5. E. Dose, *Anal. Chem.*, 59 (1987) 2414.
6. E. Dose, *Anal. Chem.*, 59 (1987) 2420.
7. H. Snijders, H.-G. Janssen, and C. A. Cramers, *J. Chromatogr. A*, 718 (1995) 339.
8. H. Snijders, H.-G. Janssen, and C. A. Cramers, *J. Chromatogr. A*, 756 (1996) 175.
9. A. T. James and A. J. P. Martin, *J. Biochem.*, 50 (1952) 679.
10. S. J. Hawkes, *Chromatographia*, 37 (7/8) (1993) 399.
11. M. J. E. Golay, in *Gas Chromatography 1958* by D. H. Desty, Ed., Butterworths, London, 1958, p. 36.
12. J. C. Giddings, S. L. Seager, L. R. Stucki, and G. H. Stewart, *Anal. Chem.*, 32 (1960) 867.
13. E. N. Fuller, P. D. Schettler, and J. C. Giddings, *Ind. Eng. Chem.*, 58 (1966) 19.
14. E. N. Fuller, K. Ensley, and J. C. Giddings, *J. Phys. Chem.*, 75 (1969) 3679.

SUMMARY

Chromatography as a separation and analytical technique has been marked by a tremendous progress since its invention in 1903 by the Russian botanist, Mikhail S. Tswett (1872-1919). Its excellent separation power renders chromatography an extremely powerful tool when analyzing complex samples. Typical examples of the pressing issues chemical analysts have to face today are trace analysis of organic micropollutants in the atmosphere and process and emission monitoring in chemical industry. In the application area of atmospheric pollution control there is an urgent need for more sensitive, more accurate and faster analytical methods suited for environmental emission monitoring due to the ever more stringent regulations imposed by national and international environmental institutions. Similar demands apply for industrial process control due to the need of the chemical industries to improve the quality and efficiency of their production processes while simultaneously reducing the environmental impact of their activities. In order to meet these requirements, the selection of suitable analytical procedures have to involve the development and evaluation of instrumentation for indoor laboratory use as well as for field applications. While complex and dedicated analytical instruments used "in-door" in the laboratory excel in sensitivity, accuracy and adaptability, field-portable equipment has its advantages in terms of ruggedness and real-time on-the-spot response. As an illustration for this development process, two important and representative analytical problems have been addressed in this thesis. The first is the determination of sulfur components in natural gas. The analysis of volatile organic compounds in emission control and environmental monitoring is the second. Regarding the nature of the samples involved, gas chromatography clearly is the technique of choice.

Due to the differences in instrumentation involved, each of the problems mentioned above is addressed in a separate part of this thesis. **Part One**, consisting of chapters 1 to 4, is dedicated to the problem of the determination of sulfur components in natural gas. The main aim of the study is to develop a gas chromatography-based analytical procedure for sulfur measurement for use in the laboratory. The stringent requirements in terms of detection limits (micrograms of sulfur per cubic meter) for the individual sulfur components in the complex natural gas matrix resulted in the need for improvements in each of three essential

steps of the analytical procedure: sample pretreatment, chromatographic separation and target compound detection.

Chapter 1 of Part One concentrates on summarizing recent developments in the field of gas chromatography related to the analysis of sulfur components in a wide variety of matrices. This phase of the study resulted in a review article: "Determination of Sulfur Components in Natural Gas", which has been published in the Journal of High Resolution Chromatography, Vol. 17, June 1994 - a special issue on fossil fuel analysis. The literature study described in this chapter provides cornerstone information for the experimental part of the research work. Based on the knowledge gathered in the literature study, practical experiments were carried out in order to optimize sample pretreatment, separation and detection in a gas chromatography based procedure for sulfur determination in natural gas.

Chapter 2 is devoted to the evaluatory study of various potential selective as well as universal detectors for the analysis of sulfur components. When the detection system that is to be used for the detection of the sulfur components in the gas sample has been selected, the requirements that have to be met by the sample introduction step and the chromatographic separation are known. Evaluation of the performance of the detectors, hence, is the step to start with in the development of complex analytical methodologies. The detectors included in the experimental evaluation are the Sulfur Chemiluminescence Detector (SCD), the Flame Photometric Detector (FPD), the Thermal Conductivity Detector (TCD), the Pulsed-Flame Photometric Detector (PFPD), the Atomic Emission Detector (AED) and the Mass Spectrometric Detector (MSD). The detectors were evaluated with regard to the following points: sensitivity, sulfur-*over*-carbon selectivity, linearity, long- and short-time repeatability, quenching behavior and the compound dependency of the sulfur response. For the selective, sensitive and reliable determination of sulfur components in a complex matrix such as natural gas, the SCD is the best choice. This detector offers the highest selectivity ($>10^6$ for S/C) and sensitivity (2 pg S/sec). The linear dynamic range spans over 4 to 5 orders of magnitude. Moreover, its response is largely compound independent. Last but not least, the detector is free of quenching over a wide concentration range. Disadvantages of SCD detectors are their rather high operational costs and the high level of experience required for the operator. This, however, is partially compensated by the advantage of the SCD (flame-based version) of having an FID (flame ionization detector) signal available simultaneously with the sulfur signal.

This particular property of the SCD was found to be very helpful in the stage of method development and evaluation.

Based on the selection of the SCD as the system detector, it was calculated that the injection volume needed to meet the specified detection limits in case a capillary column is used is approx. 15 mL. This by far exceeds the maximum allowable injection volume for such columns which is only approx. 100 μ L for gaseous samples. It is, hence, evident that a sample enrichment step must be employed. The selective enrichment of sulfur components from natural gas is one of the subjects of **Chapter 3**. In this study a preconcentration device based on the adsorption/thermal desorption (ATD) technique using solid adsorption materials was used. This technique was carried out inside the liner of a programmed temperature vaporizer (PTV) injector. Eight different adsorption materials were investigated on the basis of their sulfur breakthrough volume, the sulfur-over-carbon selectivity, ease of thermal desorption and thermal stability. The adsorbent Chromosorb 104 was found to have the best sulfur-over-carbon selectivity and loadability. The breakthrough volume of the Chromosorb 104 material is well above the 15 mL required to meet the specified detection limits.

Chapter 3 also addresses the issue of optimizing the chromatographic separation in the sulfur analysis in natural gas problem. Due to the excellent sensitivity, the high selectivity and quenching-free nature of the SCD detector in combination with the outstanding performance of the enrichment step using Chromosorb 104, it is no longer necessary to separate each of the sulfur components from the complex hydrocarbon background. An adequate separation of the individual sulfur components is, however, still required. For the particular analytical problem, capillary columns have a number of advantages over packed column systems. Among these the most important ones are a high speed of analysis, a high separation efficiency and low residual surface activity. For these reasons the evaluatory study concentrated on capillary columns. The column of choice must provide adequate separation of the individual sulfur components of interest, *i.e.* it must not cause band broadening for high boiling compounds while simultaneously giving baseline separation for the H₂S/COS pair. Among the four capillary columns investigated the best results were obtained on an ultra-thick film non-polar 30 m \times 320 μ m \times 4 μ m SPBTM-1 SULFUR column.

Gas chromatography based analytical methods are relative techniques of determination. This means that they require calibration. The evaluation of different

calibration methods for GC-based analysis of sulfur components is the last topic described in **Chapter 3**. This study leads to the conclusion that for the preparation of concentrated calibration gas mixtures (higher ppm level), the use of cylinders with calibration gases is the best choice. When lower concentrations are required or if standards covering a fairly wide concentration range are needed, the use of permeation devices was found to be very attractive due to its accuracy, precision, ruggedness and simplicity.

On the basis of the optimized individual steps - sample enrichment, chromatographic separation and target component detection and quantitation - a new instrumental set-up for the sensitive, precise and accurate determination of sulfur components in natural gas was constructed and evaluated in **Chapter 4**. The newly designed instrument consists of a PTV injector employing a liner packed with Chromosorb 104 for selective sample enrichment, a non-polar ultra-thick film column for high resolution chromatographic separation and an SCD for sensitive and selective sulfur detection. A detection limit of $3 \mu\text{g S/m}^3$ for the individual sulfur compounds was obtained with a sample volume of 13 mL. Lower detection limits can be achieved by increasing the sample volume up to 500 mL using the direct sampling technique. The accuracy was found to be better than 10%. The precision of replicate measurements was in the range of 2-5%. The analysis time was around 30 to 35 min. The proposed procedure has been applied successfully in routine analysis in R&D laboratories of various companies.

As opposed to the development of an analytical procedure for laboratory use as described above, **Part Two** of this thesis, consisting of the Chapters 5 through 8, is dedicated to analytical systems for field applications. Real-time on-the-spot analytical results are more and more demanded in chemical industrial process control and emission monitoring. In this part of the thesis, vent stack gas monitoring and trace analysis of volatile organic compounds in air using a field-portable micro gas chromatograph are described.

Chapter 5, the first chapter of Part Two, serves as a general introduction into the process of developing gas chromatographs for on-line process control and/or field applications. The progress in high-speed narrow-bore capillary GC technology in this field is emphasized. An overview of the use of miniaturized field-portable GC instrumentation is given.

A commercially available standard field-portable micro-GC was evaluated and

optimized for vent-stack gas monitoring (**Chapter 6**). The work presented has addressed the problem of determining acetic acid as well as a wide range of polar and non-polar species widely differing in boiling points in a humid atmosphere. The micro-GC CP 2002 (Chrompack) was used. With two independent modules employing a thick-film FFAP column and a PoraPLOT Q column, respectively, the mixture involved could be adequately separated. Also another combination of columns, *i.e.* the combination of a PoraPLOT U and a CP Sil-8 CB column can be used for the analytical problem at hand. The latter column combination has shown higher robustness and can handle a larger number of components in a single chromatographic run. The detection limits achieved on this system are, however, somewhat poorer than those obtained with the PoraPLOT Q - FFAP system. It is demonstrated that the high water content of the samples has no adverse influence on the chromatographic performance of the system. For a field trial the PoraPLOT U - CP Sil-8 CB system was selected because of the fact that with this set of columns more components can be determined in a single run. The analytical results of the on-line at-site micro-GC measurements were in good agreement with those obtained using the (off-line/off-site) method currently in use. Detection limits of the components of interest are at the single-digit parts-per-million level, except for acetic acid which has a lowest detectable concentration of 30 ppm.

The detection limits in the low ppm level achievable with the standard micro GC hardly meet the sensitivity requirements needed for environmental applications of this instrument such as the analysis of organic micropollutants in the atmosphere. In order to improve the detection limits of high-speed field-portable GC instruments to the required parts-per-billion level, a preconcentration step is necessary. On-line coupling of a preconcentration device to a high-speed narrow-bore capillary GC instrument presents a tremendous challenge. The need for extremely narrow input bandwidths represents the most crucial criterium. This cannot be met without strict miniaturization of the trap if a preconcentration device based on an ATD technique is used. Here, another approach, however, is proposed, *i.e.* the equilibrium (ab)sorption technique developed in the present work.

Chapter 7 presents in detail the principles and theoretical aspects of the equilibrium (ab)sorption technique, a novel preconcentration method suited for on-line coupling to high-speed narrow-bore capillary gas chromatography in general and field-portable micro-GC in particular. Enrichment factors of at least 100 can be obtained rapidly without the use of complicated instrumentation. The new pre-

concentration technique is shown to have clear advantages over enrichment based on conventional ATD techniques. It can be carried out at ambient or higher trapping temperatures, gives uniform desorption profiles, reduces water effects, uses inert (ab)sorption materials and does not require a (cryogenic) refocusing step. Moreover, the new preconcentration technique allows the enrichment factors to be predicted from tabulated chromatographic data, thereby facilitating calibration.

Based on the theory described in Chapter 7, the on-line coupling of the new preconcentration technique with a field-portable micro-GC is realized. The results of this work are described in **Chapter 8**. The system was used for enrichment of standard *n*-alkane mixtures as well as for mixtures of volatile organic compounds (VOCs) from air. Using a non-polar trapping column, enrichment factors found for *n*-alkanes in the range of C₇ to C₁₀ ranged from 15 to 150 and agreed well with calculated values. No displacement effects were observed on this liquid phase even when large amounts of interfering components were present. Using highly retentive Thermocap A columns, enrichment factors in the range of 500 to 1000 could be achieved for VOCs. With the enrichment step the detection limits of these solutes could be improved to the low ppb level. The possibility of sampling at temperatures higher than ambient renders this stationary phase greatly flexible. The sampling time can, therefore, be shortened to an acceptable level of around 20 min. Unfortunately, displacement can occur when interfering components are present at high concentration levels restricting the applicability of the Thermocap A stationary phase to the analysis of components present at low (total) concentrations. When these conditions are not met a true liquid stationary phase must be used for enrichment.

As the use of this new preconcentration technique requires only minimum modification of the micro GC, the chromatographic performance of the instrument was not compromised by direct coupling to the preconcentration device. Analysis of a complex mixture of VOCs in air at ppb concentration level can be easily performed. Components with boiling points below 50°C will need a stationary phase with stronger retention, *e.g.* Thermocap C, PoraPLOT or ultra thick-film apolar columns.

The **Appendix** finally describes a procedure to predict chromatograms on the micro GC from thermodynamic data of the components of interest. These data can be collected from published sources, calculated from available retention indi-

ces or obtained from retention data measured in initial isothermal runs. The main intention of the model described in the appendix is to aid the operator in converting methods from standard GC instruments to the micro GC, a task that is complicated by the fact that peak broadening in the micro GC is difficult to predict.

SAMENVATTING

Een van de meest uitdagende taken voor de hedendaagse analytische chemie is het ontwerpen van analytische systemen voor de sporenanalyse van organische componenten in complexe monsters. De eisen gesteld aan de snelheid, gevoeligheid, specificiteit en nauwkeurigheid van de analyses worden steeds hoger. Met name geldt dit voor de milieuanalyse ten gevolge van de steeds strengere voorwaarden, die van overheidswege opgelegd worden aan emissies, water-, bodem- en luchtkwaliteit. Vergelijkbare vragen komen uit de chemische industrie, met name voor procesregeling. Hier bestaat de noodzaak om chemische processen steeds verder te optimaliseren voor wat betreft kwaliteit van de produkten, de efficiency van de reacties en het minimaliseren van de milieubelasting.

Om aan deze vraagstelling te voldoen moeten systemen ontwikkeld en geëvalueerd worden voor zowel laboratorium- als veldtoepassingen. Specifieke laboratorium-instrumentatie kan in principe complex zijn en als zodanig zeer flexibel. Dit type instrument kenmerkt zich veelal door een grote gevoeligheid en een hoge nauwkeurigheid van de analytische resultaten. Draagbare apparatuur voor veldtoepassingen heeft daarentegen het voordeel van de mogelijkheid van "real-time, on-the-spot" analyses.

In dit proefschrift worden twee voorbeelden voor het ontwerp van totaal-analysesystemen behandeld. Het eerste onderwerp is de bepaling van sporen zwavelhoudende componenten in aardgas met behulp van een laboratorium-opstelling. Het tweede onderwerp omvat de analyse van vluchtige organische componenten in procesemissies en voor het meten van luchtkwaliteit. Dit gedeelte is gebaseerd op een draagbaar chromatografiesysteem voor veldtoepassingen. Beide systemen zijn tengevolge van de aard van de monsters gebaseerd op gaschromatografie. Gezien het grote verschil in benodigde instrumentatie wordt de problematiek behandeld in twee aparte delen van het proefschrift.

Deel 1 (Hoofdstuk 1 tot 4) is getiteld: "ZWAVELANALYSE IN AARDGAS". Het belangrijkste doel van deze studie is de ontwikkeling van een op

gaschromatografie gebaseerd systeem voor gebruik in het laboratorium. De eisen voor wat betreft detecteerbaarheid van de individuele zwavelhoudende componenten in aardgas zijn zeer strikt (microgrammen zwavel per m³). Interferentie gedurende de scheiding en detectie veroorzaakt door de complexe matrix van aardgas, bemoeilijkt de analyse. Uiteindelijk bleek het noodzakelijk elk van de drie essentiële analysestappen te verbeteren: monstervoorbereiding, chromatografische scheiding en specifieke detectie van de zwavelhoudende componenten. Het uiteindelijke systeem omvat een 'Programmed Temperature' (PTV) injectiesysteem gepakt met Chromosorb 104 voor selectieve monster-concentrerend, een speciale capillaire kolom met extreem hoge filmdikte voor de scheiding en een (zwavel)chemiluminescentie detector voor zeer gevoelige en selectieve detectie. Het totale analytische systeem levert een detectielimiet van 3 µg S/m³ voor de individuele zwavelhoudende componenten. Dit bij behandeling van een aardgasmonster van 13 cm³. Lagere detectielimieten zijn mogelijk bij grotere monstervolumina.

Hoofdstuk 1 geeft een overzicht van de stand van zaken op het gebied van de analyse van zwavelhoudende componenten in uiteenlopende matrices zoals die was bij aanvang van het promotieonderzoek. Een duidelijke conclusie uit deze studie is dat de zeer strikte eisen die gesteld worden aan de nieuw te ontwikkelen methode voor zwavelbepaling slechts haalbaar zullen zijn indien elk van de eerder genoemde deelstappen uit de chromatografische procedure vergaand verbeterd kan worden. In hoofdstuk 2 worden de karakteristieken van een groot aantal al dan niet zwavel-specifieke detectoren in kaart gebracht. Op basis van gevoeligheid, selectiviteit, 'quenching-gedrag' en andere technische factoren, in combinatie met niet-technische aspecten zoals gebruiksgemak en kosten, wordt de keuze gemaakt voor toepassing van de zwavel chemiluminescentie detector. Met de keuze van de detector liggen de eisen waaraan de monstervoorbewerkings-techniek en de chromatografische scheiding zullen moeten voldoen vast. Hoofdstuk 3 beschrijft de zoektocht naar een adsorptiemateriaal dat geschikt is voor selectieve aanrijking van zwavelcomponenten uit aardgas. Niet alleen dient dit materiaal te beschikken over een hoge retentie voor de zeer vluchtige zwavelcomponenten waterstofsulfide en carbonylsulfide, het dient daarnaast geen interactie te vertonen met methaan, ethaan, propaan en bij voorkeur ook butaan. Een geschikt materiaal wordt gevonden in Chromosorb 104. In dit hoofdstuk komt verder ook de keuze van de meest geschikte chromatografische kolom aan de orde.

Dikke-film GLC kolommen blijken duidelijk de voorkeur te genieten boven kolommen van het PLOT-type. Dit door hun betere efficiëntie en inertie. Tot slot komt in hoofdstuk 3 ook de selectie van de meest geschikte calibratie-techniek aan de orde. Calibratie met gascilinders blijkt, door sterke adsorptie van de zwavelhoudende stoffen aan de cilinderwand in het zeer lage concentratie-bereik, niet langer mogelijk. Betere resultaten worden verkregen met dynamische calibratietechnieken die berusten op het gebruik van permeatie- of diffusiebuisjes. In hoofdstuk 4 wordt het uiteindelijke systeem geconstrueerd en geëvalueerd. Toepassing van het totale meetsysteem voor de analyse van een grote serie aardgasmonsters met lage zwavelconcentraties toont de bruikbaarheid op overtuigende wijze aan. Een aantal gasmonsters die in katalytische conversie-processen problemen veroorzaakten en waarin met de bestaande technieken geen zwavel aangetoond kon worden, blijken op laag niveau een scala aan zwavel-componenten te bevatten.

Deel 2: "EMISSIEMETING VAN VLUCHTIGE ORGANISCHE COMPONENTEN m.b.v. EEN DRAAGBARE GASCHROMATOOGRAAF". In dit deel (Hoofdstuk 5 tot 8) wordt het ontwerp van een totaalsysteem voor veldanalyses beschreven. "Real-time, on-the-spot" analyses zijn meer en meer gewenst voor procesregeling en emissie-toepassingen. De in dit proefschrift beschreven technieken zijn ontwikkeld voor metingen aan schoorsteengassen en sporenanalyses van vluchtige organische componenten in lucht. Uitgangspunt is een draagbaar micro-GC systeem met snelle, kleine diameter capillaire kolommen en warmtegeleidbaarheidsdetectie. Om aan de strenge eisen voor wat betreft detecteerbaarheid (ppb-niveau) te voldoen is een geheel nieuwe monster-concentreringstechniek ontwikkeld. Dit systeem, gebaseerd op evenwichts-absorptie verrijking is on-line gekoppeld met de micro-GC. Met behulp van deze techniek bleek het mogelijk de detectielimiet van de bestaande micro-GC te verbeteren van monsterconcentraties in de orde van ppm's naar het gewenste ppb-niveau. De resultaten van deze nieuwe methode worden vergeleken met de conventionele benadering: adsorptie-thermische desorptie.

Analoog aan deel 1 van dit proefschrift, begint ook deel 2 met een literatuurstudie. In deze studie, beschreven in hoofdstuk 5, wordt ingegaan op de huidige mogelijkheden voor GC analyses 'in het veld'. Hoewel on-line GC reeds relatief frequent toegepast wordt in de chemische procesindustrie, blijkt er hier duidelijk behoefte aan systemen die toepasbaar zijn voor complexere stromen. Voor milieutoepassingen worden draagbare GC systemen nog nauwelijks

toegepast. Dit is vooral een gevolg van de beperkte gevoeligheid van dit type meet-instrumentatie. Hoofdstuk 6 beschrijft de toepassing van de micro-GC voor emissie-monitoring in een industrieel fabricageproces. Door de grote hoeveelheid water, het brede vluchtigheids- en polariteitsbereik van de stoffen in deze stroom, alsmede door de sterk variërende concentraties van de diverse stoffen, was het tot nu toe onmogelijk de emissie continue te monitoren. Met het huidige meetsysteem gebaseerd op de Chrompack CP2002 micro-GC uitgerust met een PoraPLOT U en een CP SIL-8 CB kolom, kan de emissiestroom meerdere malen per uur gemeten worden. Dit brengt nieuwe methoden voor verbetering van de procesvoering binnen bereik. Het onderzoek beschreven in hoofdstuk 7 richt zich op het verbeteren van de gevoeligheid van de draagbare GC om de inzet van dit instrument voor 'in het veld' milieumetingen mogelijk te maken. In dit hoofdstuk wordt een nieuwe methode voor preconcentrerende van gasmonsters beschreven. Standaard technieken voor gasaanrijking kunnen niet gecombineerd worden met de draagbare GC. Dit omdat het gebruik van snelle, nauwe kolommen in dit instrument zeer strikte eisen stelt aan de injectiebandbreedte. De nieuwe methode, 'evenwichts absorptie aanrijking', levert een klein volume van een homogeen aangerijkt gas. On-line combinatie van deze methode met de micro-GC vereist geen aanpassing van de micro-GC. Aanrijdingsfactoren in het bereik van 500 tot 1000 zijn mogelijk zonder dat de efficiëntie van het micro-GC systeem daardoor negatief beïnvloed wordt. Dit hoofdstuk beschrijft de principes van de nieuwe methode en gaat in op de theoretische aspecten. Hoofdstuk 8 beschrijft de toepassing van de nieuwe methode voor de analyse van zeer lage concentraties vluchtige organische componenten in lucht. Met de nieuwe methode zijn detectiegrenzen in het lage ppb-bereik haalbaar, hetgeen de techniek direct toepasbaar maakt voor praktijkmetingen. Zonder voorconcentreringsmethode liggen de detectiegrenzen van de micro-GC in het ppm-gebied en daarmee boven het bereik waarin gemeten moet worden.

In de Appendix wordt een methode beschreven om uitgaande van retentie-gegevens verkregen op standaardapparatuur de scheidingscondities op de micro-gaschromatograaf te voorspellen. Deze methode is bedoeld als hulpmiddel bij het omzetten van laboratorium GC methoden naar veldtoepassingen.

ACKNOWLEDGEMENT

A Vietnamese proverb says "Forget not the one who planted the tree when you are savoring its fruits". In a similar thought, I would like to take this opportunity to acknowledge the help, support and encouragement of so many people who, either directly or indirectly, have "planted" a seed of knowledge in my intellectual life.

First of all I would like to thank my promotor, Carel Cramers, for giving me the chance to start, continue and successfully finish the Ph.D. study with invaluable guidance and support. My special thanks goes to my coach, Hans-Gerd Janssen. You have introduced to me the art of gas chromatography. Your innovative ideas, suggestions, comments are inseparable parts of my research.

I am greatly indebted to Jacques Rijks, Sr. Without his initial help I could not have started the study here in the first place. For the same reason and also for continuous support from the "home-ground" I owe gratitude to my mentors from Charles University in Prague, Karel Štulík, Vera Pacáková, Jirí Barek and Jirí Zima.

My study could not have come to a successful completion without the fruitful cooperation with experts from industry. For this I am obliged to André Smit, Ellen Kuiper-van Loo, Harm Vlap from N.V. Nederlandse Gasunie, Jürgen Lips, Philippe Mussche from Chrompack International B.V., and Alan Handley, Nigel Wilson from ICI Technology.

I am grateful to Piet Leclercq, Jan de Haan, Mark van Lieshout, Henry Snijders, Gerard Rutten, Denise Tjallema, Hans van Rijksewijk, Inge Vrijaldenhoven, Anja Huygen, Harrie Maathuis, Gius Rongen, Huub van Leuken, and Anton Bombbeck for their professional helps and advice. For a great working and social atmosphere I would like to thank my lab- and AIO-mates: Hans Mol, Xanwen Lou, Erik Baltussen, Patrick van Schijndel, Alex Scholten, Peter van Ysacker, Rico Derks, Roger Abels, and Cindy van den Boom.

Finally all my heart goes to my family: my Father, Mother and Sister Hà. I just hope that I can live up to the eternal love they always have for me.

CURRICULUM VITAE

The author of this thesis was born on the 6th August 1968 in Hanoi, Vietnam. From September 1987 till July 1993, he studied Analytical Chemistry at the Charles University in Prague, Czech Republic. His specialization was separation methods and electrochemical analytical techniques. He graduated (summa cum laude) with a research topic on the determination of trace amounts of carcinogenic nitroso- and azocompounds. In March 1993 he started the postgraduate study in the Laboratory of Instrumental Analysis, Eindhoven University of Technology, Eindhoven, The Netherlands.

LIST OF PUBLICATIONS

1. Hai Pham Tuan, Hans-Gerd Janssen, Carel A. Cramers, André L. C. Smit and Ellen M. van Loo: "*Determination of Sulfur Components in Natural Gas: A Review*", published in *J. High Resolut. Chromatogr.*, 17 (1994) 373-389.
2. Hai Pham Tuan, Hans-Gerd Janssen, Carel A. Cramers, Ellen M. Kuiper-van Loo and Harm Vlap: "*Evaluation of the Performance of Various Universal and Selective Detectors for Sulfur Determination in Natural Gas*", published in *J. High Resolut. Chromatogr.*, 18 (1995) 333-342.
3. Hai Pham Tuan, Hans-Gerd Janssen, Ellen M. Kuiper-van Loo and Harm Vlap: "*Improved Method for the Determination of Sulfur Components in Natural Gas*", published in *J. High Resolut. Chromatogr.*, 18 (1995) 525-534.
4. Hai Pham Tuan, Hans-Gerd Janssen and Carel A. Cramers: "*A Novel Pre-concentration Technique for On-line Coupling to High-Speed Narrow-Bore Capillary Gas Chromatography: Sample Enrichment by Equilibrium (Ab)sorption. Part 1: Principles and Theoretical Aspects*", published in *J. Chromatogr. A.*, 791 (1997) 177-185.
5. Hai Pham Tuan, Hans-Gerd Janssen, Carel A. Cramers, Phillippe Mussche, Jürgen Lips, Nigel Wilson and Alan Handley: "*A Novel Preconcentration Technique for On-line Coupling to High-Speed Narrow-Bore Capillary Gas Chromatography: Sample Enrichment by Equilibrium (Ab)sorption. Part 2: Coupling to a Portable Micro GC*", published in *J. Chromatogr. A.*, 791 (1997) 187-195.
6. Hai Pham Tuan, "*Determination of Sulfur Components in Natural Gas*", Eindhoven: Instituut Vervolgopleidingen, Eindhoven University of Technology. – III. Course Chemical Technology. – ISBN 90-5282-440-1.
7. Hai Pham Tuan, Hans-Gerd Janssen, Carel A. Cramers, Ellen M. van Loo, and Harm Vlap: "*Performance of Various Universal and Selective Detectors for Sulfur Determination in Natural Gas*", published in *Proceedings of*

the 16th International Symposium on Capillary Chromatography, Riva del Garda, Italy, September 27-30, 1994, p. 985-997.

8. Hai Pham Tuan, Hans-Gerd Janssen, Carel. A. Cramers, Phillippe Mussche, Jürgen Lips, and Nigel Wilson: "*Analysis of a Strongly Acidic Component in Very Humid Samples Containing Various Non-polar Components Using a Micro GC*", published in *Proceedings of the 18th Symposium on Capillary Chromatography*, Riva del Garda, Italy, May 20-24, 1996, p. 2213-2224.
9. Hai Pham Tuan, Hans-Gerd Janssen, Carel. A. Cramers, Phillippe Mussche, Jürgen Lips, Nigel Wilson and Alan Handley: "*Analysis of VOC's in Air Using a Portable Micro Gas Chromatograph in Conjunction with Preconcentration Techniques*" in *Proceedings of the 19th Symposium on Capillary Chromatography*, Wintergreen, Virginia, USA, May 18-22, 1997.
10. Mark van Lieshout, Hai Pham Tuan, Hans-Gerd Janssen and Carel Cramers: "*Trace Analysis of Sulfur Compounds in Natural Gas Using Large Volume Injection, Selective Enrichment and Sensitive SCD-Detection*" in *Proceedings of the 19th Symposium on Capillary Chromatography*, Wintergreen, Virginia, USA, May 18-22, 1997.

STELLINGEN

1. When the detector for a GC system is selected, the requirements that have to be met by the sample pretreatment step and the chromatographic separation are determined. *This thesis, Chapter 3.*
2. Small is beautiful, and this has always been true in separation science. *Smits, LC-GC International, January 1998, p. 12.*
3. Analytical instruments are moving from the function of generating just data into the domain of problem solving. *Overton et al., Field Anal. Chem. Technol., 1(2) (1996) 87.*
4. Although traditionally an engineering technique, micromachining has the potential to enable new analytical approaches. *Kovacs et al., Anal. Chem News & Features, July 1, 1996, p. 407A.*
5. Among the five steps common to any GC-based analytical procedure, sample collection and pretreatment are unarguably the most vulnerable steps. *This thesis, General Introduction and Scope.*
6. The statement by *Sacks et al.* that "The inlet bandwidths required to take full advantage of the resolving power of high-speed capillary separation columns cannot be achieved with conventional GC inlet systems" is not correct. *Sacks et al., Field Anal. Chem. Technol. 1(2) (1996) 97.*
7. For gas samples containing a wide range of components multi-segment adsorption traps are unavoidable. *Frank et al., Chromatographia 29 (1990) 571.*
8. The purpose of installing analyzers on-line is to obtain the analytical results with a speed of response that is comparable to process changes. *R. Villalobos, J. Chromatogr. Sci., 28 (1990) 341.*
9. The main reason that the column-on-chip is still not widely used in portable GC instruments is that etching and coating procedures for these columns are still in their infancy. *This thesis, chapter 5.*
10. The rate of acceptance of fast gas chromatography does not reflect the speed of the method.
11. While the Czechs are serious in joking, the Dutch talk jokingly about serious matters and the Vietnamese smile all the time.

Pham Tuan Hai
Eindhoven, 30 January 1998.